DEPARTMENT OF GEOLOGY, GEOGRAPHY AND ENVIRONMENTAL SCIENCE

UNIVERSITY OF STELLENBOSCH

Mineralogical characterisation of chromite in the UG2 Reef from Waterval Mine, Western Bushveld: Implications for minerals processing

By

S.D. Opoubou-Lando

Thesis presented in partial fulfilment of the requirements for the degree of

Master of Science

At Stellenbosch University

Supervisors: Dr Jodie Miller (University of Stellenbosch), Dr Megan Becker (University of Cape Town) and Professor Fanus Viljoen (University of Johannesburg)

March 2010

PLAGIARISM DECLARATION

I, Serge Opoubou-Lando declare that this work submitted for the degree of MSc at the University of Stellenbosch is the result of my own work and has not been previously submitted by me at another University for any degree. An effort to the best of my abilities is made to cite the contribution of others with due reference to the literature.

Signature: …….

Date: …….

ABSTRACT

The Bushveld Complex of South Africa contains three of the most important platinum deposits in the world namely the Merensky Reef, the Upper Group Two (UG2) chromitite reef and the Platreef. These three ore bodies are principally beneficiated by froth flotation. During the beneficiation of chromite hosted PGE's by froth flotation, chromite represents the principal gangue mineral. This is particularly true for the UG2 main seam. An excess of more than 3% in mass of chromite in the PGM concentrate is known to result in significant problems in the downstream processing and extraction of PGEs. The variability in texture and composition of chromite due to its primary crystallization and subsequent modification by the development of potholes or through IRUP intrusions are thought to influence the flotation behaviour of the UG2 main seam chromitite ore.

This study conducted at Waterval Mine investigated the role of mineralogical characteristics of chromites on the flotation performance of three different environments for the UG2 main seam: (1) "normal" UG2 main seam; (2) UG2 main seam affected by pothole formation; and (3) UG2 main seam affected by IRUP intrusion. This was achieved through an extensive petrographic investigation of the chromites from each environment, to individually characterise their primary textures. This was followed by compositional characterisation of the chromite from each environment. Finally the flotation performance of the ore from each environment was investigated, using small scale batch flotation experiments, to establish any linkage between the textures, the composition and the flotation performance of the chromite from different environments.

In this study it was found that the UG2 normal reef and the UG2 reef affected by pothole formation are both principally characterised by primary mineralogical features comprising mainly fine-grained chromite as the cumulate phase and orthopyroxene and plagioclase as intercumulate phases. These two reef types were also found to be identical in the composition of the chromites present. In addition, in both of these almost unaltered reef types it was found that chromite showed small recoveries by flotation. On the other hand, it was found that the UG2 affected by IRUP intrusion was affected by post-magmatic alteration that had overprinted primary textures and compositional features. This resulted in the replacement of primary minerals by secondary alteration assemblages. Orthopyroxene was

replaced by serpentine, chlorite, amphibole and talc, while plagioclase is replaced by sericitic alteration. Furthermore, this alteration also resulted in modification of the chromite compositions. The compositional change in the chromites from the IRUP reef type resulted in Fe and Ti enrichment of chromite with increasing magnetic properties, and Cr, Al and Mg depletion. The alteration also resulted in the coarsening of chromite in the IRUP affected main seam reef particularly at the bottom and the top of the main seam.

These compositional and textural modifications, principally the post-magmatic alteration of intercumulate orthopyroxene, resulted in a greater recovery of chromite by flotation in the concentrate from the IRUP affected ore compared to the two other two ore types where there was small amount of chromite recovered. The characterisation of the recovered chromite revealed that the principal reason for chromite flotation was caused by the mineral association of chromite with hydrophobic Si, Mg, Fe rich phases, principally altered orthopyroxene and associated serpentine, chlorite, amphibole and talc.

This investigation showed that the difference in mineralogical and flotation performances of chromite from the different UG2 main seam reef types was caused by the post-crystallisation alteration of cumulate and intercumulate phases due to the emplacement of IRUPs. Although IRUP affected UG2 main seam ore is not currently processed, it could be processed much more rapidly than the other two types of UG2 main seam ores because of its softer character resulting in shorter milling times. This is most likely a function of the presence of alteration phases and the presence of coarser chromite grains, as well as already brecciated chromite grains. Savings associated with the shorter milling time of this ore type are perhaps offset by the cost of the higher dosages of depressant required to suppress the floatable chromite in this ore type. However, given the energy cost of longer milling times, the cost of the depressant is likely to be insignificant. Moreover, the processing of the UG2 main seam ore affected by IRUP intrusion would also require a different approach to extraction of the ore to keep it separate from the normal reef ore.

ACKNOWLEDGEMENTS

I owe my deepest gratitude to Jodie Miller and Megan Becker, whose guidance, encouragements and support from the first till the last day of this project enabled me to develop an understanding of the subject. I would like also to thank Professor Fanus for the technical support and advises he provided me with. Thanks to Ronald Voordrow for his critical readings of the thesis. Thanks to Madeleine Frazenburg, Jenny Wiese, A/Prof Peter Harris, Gwinyai Chitiyo and the geology division at Waterval Mine for their technical supports.

This thesis would not have been possible without the financial and technical assistance that Anglo Platinum put at my disposal to make sure this project is a success. Particular thanks are addressed to Robert Schouwstra and Neville Plint for their assistance in the realization of this project. The Gabonese government is also to thank for the financial support it has been providing me with to make my stay possible in South Africa.

My deepest gratitude is presented to my family for their tireless love and support throughout my life. I am thankful to my father Lendoye Antoine, My uncle Mpoubou Firmin, My aunt Ebali Antoinette, My grand-father Mpoubou Antoine to whom I wanted to give a special present for the remaining days of his life. To the Mbazima family I would like to address my special thanks for all the support, care and love they offered me, particularly to Daisy Mbazima my future wife “I love you beautiful lady”. Additional thanks go to friends and brothers Elvis Mubamu Makady, Hans Eyeghe Bikong, Mfa Mezui Antoine Aime, Iningoue Aicha. To my mother Ndayele Claire to whom I dedicate my thesis to, without her all I have already realised on earth would just not be possible “this is your thesis mum”. You worked tirelessly and gave me the little you had to support me. You spare no effort to provide the best possible environment for me to grow up and attend school. You had never complained in spite of all the hardships in your life. I will forever remember your sufferings and love. I could not ask for more from you, let me simply say you have been perfect to me and for that I have no suitable word that can fully describe your everlasting love to me. I can just remember many sleepless nights that I put you through. Mother, I love you.

Last but not least, thanks to God for making my existence possible. You have completed my life with more joy. May your name be exalted, honoured, and glorified.

Table of Contents

Declaration ..... **i**

Abstract ..... **ii**

Acknowledgements ..... **iV**

Table of Contents ..... **V**

List of Figures ..... **X**

List of tables ..... **XV**

List of Abbreviations and Acronyms ..... **XVi**

List of Mineral Abbreviations ..... **XVii**

CHAPTER 1: INTRODUCTION **1**

1.1 Introduction 1

1.2 Mineralogy of Chromite 3

1.2.1 Composition 3

1.2.2 Texture 7

1.3 Mineral Processing of PGMs 9

1.3.1 Comminution 9

1.3.2 Classification 10

1.3.3 Separation via Froth Flotation 10

1.4 Process Mineralogy 12

1.5 Project Scope, Aim and Objectives 15

CHAPTER 2: REGIONAL GEOLOGY **17**

2.1 Overview of the Bushveld Complex 17

2.2 Stratigraphy of the Bushveld Complex 18

2.3 The UG2 Chromitite Layer in the Bushveld Complex 20

2.4 Modification of the UG2 chromitite layer 20

2.4.1 Potholes 21

2.4.2. IRUP Intrusion 22

2.5 The Rustenburg Section 23

2.5.1 Overview 23

2.6 Overview of Waterval Mine 23

CHAPTER 3: METHODOLOGY 29

3.1 Sample Collection and Preparation 29

3.1.1 Samples for Petrographic Studies 29

3.1.2 Samples for Batch Flotation Experiments 31

3.2 Ore Characterisation 32

3.2.1 Microscopy 32

3.2.2 Scanning Electron Microscopy (SEM) 32

3.2.3 Quantitative X-Ray Diffraction 33

3.2.4 Mineral Liberation Analysis (MLA) 34

3.3 Flotation Experiments 34

3.3.1 Flotation Apparatus 34

3.3.2 Milling 35

3.3.3 Flotation 36

3.3.4 Chemical Analysis 38

3.4 Floatable Gangue Calculation 40

CHAPTER 4: PETROGRAPHIC STUDIES 42

4.1 Overview 42

4.2 Textural Studies 42

4.2.1 UG2 normal reef 42

4.2.1.1 Hanging wall 43

4.2.1.2 UG2 Main Seam 44

4.2.1.3 UG2 Pegmatoidal Feldspathic Pyroxenite Footwall 47

4.2.2 UG2 Affected by Pothole Formation 48

4.2.2.1 Hanging Wall 48

4.2.2.2 UG2 Main Seam 49

4.2.2.3 UG2 Pegmatoidal Feldspathic Pyroxenite Footwall 51

4.2.3 UG2 Affected by IRUP Intrusion 52

4.2.3.1 Hanging Wall 54

4.2.3.2 UG2 Main Seam 55

4.2.3.3 UG2 Pegmatoidal Quartzo-Feldspathic Footwall 57

4.3 Compositional Analysis 58

4.3.1 UG2 Normal Reef 59

4.3.2 UG2 Affected by Pothole Formation 60

4.3.3 UG2 Affected by IRUP Intrusion 61

4.6 Summary 63

CHAPTER 5: BATCH FLOTATION ANALYSIS 65

5.1 Overview 65

5.2 Feed Characterisation 67

5.3 Mass Recovery Versus Water Recovery 68

5.4 Mineral Recovery 69

5.4.1 Mass Recovery of Major Minerals 69

5.4.2 Mass Recovery of Gangue Mineral Due to True Flotation 71

5.5 Characterisation of Floatable Gangue (MLA) 73

5.5.1 Modal Mineralogy of Floatable Gangue 73

5.5.2 Composition of Floatable Chromite 75

5.5.3 Texture of Floatable Chromite 77

4.2.2.1 Mineral Liberation 77

4.2.2.2 Mineral Association of Floatable Chromite 77

5.6 Summary 80

CHAPTER 6: DISCUSSION 81

6.1 Overview 81

6.2 Textural Variation of Chromite in the Three Reef Types 81

6.3 Compositional Variation of Chromite in the Three Reef Types 84

6.4 Influence of the Mineralogy on Flotation Performances 85

6.4.1 Ore Hardness 85

6.4.2 Flotation Performances 87

6.4.3 Floatable Chromite 89

6.5 Implications 90

CHAPTER 7: CONCLUSION AND Recommendations 92

7.1 Conclusions 92

7.2 Recommendations 93

REFERENCES 95

APPENDIX A. HAND SPECIMENS DESCRIPTIONS

APPENDIX B. SCANNING ELECTRON MICROSCOPY

Appendix B1. UG2 normal reef

Appendix B2. UG2 potholed reef

Appendix B3. UG2 IRUP reef

APPENDIX C. BATCH FLOTATION EXPERIMENTS

Appendix C1. UG2 normal reef

Appendix C2. UG2 potholed reef

Appendix C3. UG2 IRUP reef

APPENDIX D. COMPOSITIONAL ANALYSIS

APPENDIX E FLOATABLE GANGUE CALCULATION

APPENDIX F MINERAL LIBERATION ANALYSIS

Appendix F1. Modal Mineralogy

Appendix F1.1. UG2 normal reef

Appendix F1.2. UG2 potholed reef

Appendix F1.3. UG2 IRUP reef

Appendix F2. Mineral association

Appendix F2.1 UG2 normal reef

Appendix F2.2 UG2 potholed reef

Appendix F2.3. UG2 IRUP reef

List of figures

Figure 1.1: *Johnson spinel prism representing the compositional features of spinel minerals. Summits are represented by the six principal end-members. The two projection surfaces used to derive the prism are indicated on the left (adapted from Irvine, 1965)..... 5*

Figure 1.2*: Primary compositional variation of chromitite (n=104) from chromitite layers in the Bushveld Complex: (A) Cr^{3+}-Al^{3+}-Fe^{3+} and (B) Cr^{3+}-Al^{3+}-Mg^{2+}. Data from Cameron (1977), Eales and Reynolds (1986) and Engelbrecht (1985). 6*

Figure 1.3*: Conventional UG2 ore separation or processing flow sheet (Nel and Naude, 2005)*

..... 10

Figure 2.1: *Geological map of the Bushveld Complex, obtained from a compilation by Eales and Cawthorn (1996)..... 18*

Figure 2.2: *Stratigraphy of the major limbs of the Rustenburg Layered Suite. Taken and modified from Barnes et al. (2004), and based on Cawthorn and Walraven (1998) and White (1994). 19*

Figure.2.3: *Geological map showing the Western Limb of the Bushveld Complex and the subdivision of the Western Limb into two principal facieses as proposed by Wagner (1929). The northern Swartklip Facies and the southern Rustenburg Facies are separated by the Pilanesberg Complex. Location of some of the major platinum mines in the area is also shown (Adapted from Cawthorn and Barry, 1992; and Smith et al., 2003)..... 24*

Figure 2.4: *General stratigraphic column of the Upper Critical Zone revealed by mining activities in the Rustenburg Section area (Viljoen and Hieber, 1986)..... 25*

Figure 2.5: *Generalised stratigraphic column of Waterval Mine (Marlize Oosthuysen personal communication, 2008)..... 26*

Figure 2.6: *UG2 normal reef progressively deeping into the pothole depression. Note the progressive loss of the footwall. 27*

Figure 2.7: *IRUP intrusion relationship with both the UG2 main seam and its footwall; (A) passive replacement of the UG2 main seam and its footwall by the IRUP the footwall and (B) disruptive replacement of IRUP into the UG2 main seam, (photo B is a photo of the area of sampling taken by the sectional geologist Oosthuysen. Total length represents 4 to 5 meters (personal communication)..... 28*

Figure 3.1: *Sampling along the UG2 main seam in the three different reef types studied in this project. 30*

Figure 3.2: *location and numbering of each polished section prepared for petrographic studies..... 31*

Figure 3.3: *Correlation between calculated chemistry from XRD analysis and the actual chemical assay using major elements Cr, Si, Al, Fe and Mg from the three reef types. The dark blue dashed line represents a 1:1 compositional relationship of points 33*

Figure 3.4: *3L flotation apparatus separating particles base on their surface properties. The pulp is introduced from the top of the float cell and the bubble stream controlled by the impeller at the bottom of the float cell..... 35*

Figure 3.5*: Milling curves of different ore types 36*

Figure 3.6: *Example of graphs showing the calculation of truly floatable material based on the slope of experiments with depressant addition 41*

Figure 4.1: *Samples collected from the UG2 main seam normal reef at Waterval Mine. (A) contact between hanging wall and main sea; (B) UG2 main seam; and (C) transition between the bottom part of the UG2 main seam and its footwall. Note the coarse-grained aspect of the footwall. The coin is 2.5 cm in diameter..... 44*

Figure 4.2: *Textures of the UG2 main seam immediate hanging wall. (A) Subhedral orthopyroxene; (B) cumulate orthopyroxene with intercumulate plagioclase; (C) alteration development characterised by the progressive formation of chlorite due to orthopyroxene breakdown; (D) absence of chromite grains beyond the sharp contact between the hanging wall and the main seam. Note the anomalous colour of orthopyroxene resulting from the thickness of the thin section. Plane light (A, C, and D), and crossed polar (B)..... 45*

Figure 4.3: *Reflected light photomicrographs of: (A) fine-grained chromite; (B) chain-like texture, the dashed line is a path of grain connection; (C) coarser-grained area formed by aggregated chromite grains. Note the presence of 120^{o} triple junctions and the polygonal shape grain boundaries; (D) chromite lobate textures; (E) isolated rounded chromite grains present in orthopyroxene; and (F) inclusions of plagioclase in chromite grains..... 46*

Figure 4.4: *Textural features in the UG2 normal reef footwall. (A) Coarse grained cumulate orthopyroxene and intercumulate plagioclase; (B) Progressive replacement of orthopyroxene by phlogopite, (C) Fine to medium grained irregular chromite grains present as inclusions in orthopyroxene; and (D) phlogopite developing in orthopyroxene with small chromite inclusions in this orthopyroxene. Note the anomalous colour of orthopyroxene due to the thickness of the thin section 47*

Figure 4.5: *Samples collected from the UG2 main seam affected by pothole formation at Waterval Mine: (A) sample at the transition between the top part of the UG2 main seam and its hanging wal; (B) UG2 main seam; and (C) contact between the footwall and the main seam. Observe the coarse-grained aspect of the footwall. The coin is 2.5 cm..... 49*

Figure 4.6: *Photomicrographs of textural features in the hanging wall. (A) subhedral cumulate orthopyroxene grains; (B and C) progressive breakdown of*

orthopyroxene into talc; (D) rare fine-grained chromite in-between orthopyroxene, clinopyroxene and plagioclase. Transmitted light, crossed nicols (A, B and C) and plane polarized light (D). Note that orthopyroxene shows anomalous colours due to the thickness of the thin section 50

Figure 4.7: *Reflected light photomicrographs of textural features in the UG2 main seam. (A) fine-grained individual chromite grains; (B) chain texture, dashed lines are drawn to show the connection between grains; (C) aggregate of chromite grains characterised by 120^{o} triple junctions and polygonal shapes; (D) irregularly shaped chromite grains (SEM image); (E) plagioclase inclusions in chromite grains; and (F) remnants of sulphide minerals..... 51*

Figure 4.8: *Textures in the UG2 footwall. (A) chromite grains included in orthopyroxene being almost all rimmed by plagioclase; (B) location of chromite grains as inclusions and at the boundary of silicate phases; (C) orthopyroxene breaking down into talc; and (D) accessory phlogopite present in the footwall. Note the anomalous colour of orthopyroxene due to the thickness of the thin section. (Transmitted light, cross nicols)..... 52*

Figure 4.9: *Samples collected from the UG2 main seam affected by IRUP intrusion at Waterval Mine. (A) Transition between the top part of the UG2 main seam and its hanging wall; (B) UG2 main seam; and (C) contact between the footwall and the main seam. The footwall in this environment has a coarse-grained aspect and is characterized by a whitish color. The coin is 2.5 cm in diameter..... 53*

Figure 4.10: *(A) (A) UG2 hanging wall with orthopyroxene as the major component; (B) orthopyroxene alteration (serpentine and talc) observed under plan polarised light; (C) talc development within orthopyroxene; and (D) development of fine grained talc. The anomalous colour of orthopyroxene is caused by the thickness of the thin section. Plane polarized light (B) and crossed nicols (A, C and D). 54*

Figure 4.11: *(A) aggregated grains of chromite; (B) talc at the top contact of the UG2 main seam; (C) less aggregated grains with greater interstitial orthopyroxene, note the corrosive effect on chromite grains caused by circulating fluids; (D) fractures containing poorly sorted fine-grained brecciated chromite; (E) medium to coarse polygonal grains of chromite (up to 3 mm) and (F) fine grained chromite enclosed in a poikilitic orthopyroxene. (Reflected light)..... 56*

Figure 4.12: *Footwall alteration. (A) alteration of orthopyroxene into radial amphibole (probably tremolite); (B) calcite developing along fracture zones; (C) sericite forming as an alteration product of plagioclase; and (D) quartz crystallisation during alteration caused by IRUP intrusion. Amphibole shows high interference colours due to thin section thickness. (Transmitted light, crossed nicols)..... 58*

Figure 4.13*. Cr-spinel compositions from UG2 main seam normal reef from Waterval Mine: (A) Cr-Al-Fe^{3+}, (B) Cr-Al-Mg, (C) Mg-Ti-Fe^{2+}, and (D) Ti-(Fe^{3+} + Fe^{2+}). Fields represent the primary compositional domain of chromite grains..... 60*

Figure 4.14: *Cr-spinel compositions from UG2 main seam reef affected by pothole formation from Waterval Mine: (A) Cr-Al-Fe^{3+}, (B) Mg-Ti-Fe^{2+}, (C) Cr-Al-Fe^{3+}, and (D) Ti-(Fe^{3+} + Fe^{2+}). Fields characterise the primary compositional domain of chromite grains..*

..... 61

Figure 4.15: *Cr-spinel compositions in UG2 main seam reef affected by IRUP intrusion from Waterval Mine: (A) Cr-Al-Fe^{3+}, (B) Mg-Ti-Fe^{2+}, (C) Cr-Al-Fe^{3+}, and (D) Ti-(Fe^{3+} + Fe^{2+}). Fields characterise the primary compositional domain of chromite grains*

..... 62

Figure 5.1*: Mineralogical proportions of feed for each ore type. Serp (serpentine), Chl (chlorite), plag (plagioclase), opx (orthopyroxene) and chr (chromite).. ..... 67*

Figure 5.2: *Cumulative mass versus cumulative water recovery of the three ores with and without the addition of depressant. Error bars represent the 2σ standard deviation. 68*

Figure 5.3: *Mass versus water recovery of individual elements (Al, Cr, Mg, Ca, Si and Fe) in the three ore types. 70*

Figure 5.4: *Comparison of major elements (Al, Cr, Mg, CA, Si And Fe) distribution in three reef types for the two experimental conditions. (A) Al recovery, (B) Cr recovery, (C) Mg recovery, (D) Ca recovery, (E) Si recovery and (F) Fe recovery. 71*

Figure 5.5: *Mass of floatable gangue versus water recovery for the major elements of the three ore types. 72*

Figure 5.6: *Comparison of the modal mineralogy of the concentrates of the three ore types from the flotation tests with no depressant. 74*

Figure 5.7: *Mass recovery of chromite obtained in the final concentrate of each ore type in the with no depressant addition tests 75*

Figure 5.8: *Mass of chromite associated with different minerals recovered to the concentrate in batch flotation tests with no depressant addition for the three ore types. 78*

Figure 5.9: *Mineral association of chromite from the three ore types (A) UG2 normal reef ore, (B) UG2 affected by pothole reef ore, and (C) UG2 affected by IRUP intrusion ore 79*

List of Tables

Table 3.1: *Characterisation of sampling areas 30*

Table 3.2: *SEM standards for this project 33*

Table 3.3: *Particle count for different ore types 34*

Table 3.4: *Milling times and percentage passing conditions of different ore types 35*

Table 3.5: *Ions present in synthetic water (Wiese et al., 2005) 36*

Table 3.6: *Conditions with no depressant 37*

Table 3.7: *Conditions with depressant 37*

Table 3.8: *Condition of chemical analyses using inductively Coupled Plasma – Optical Emission Spectrometry techniques 39*

Table 4.1: *Representative analyses of chromite from the three reef types 59*

Table 5.1: *Summary of batch flotation experiments results. 66*

Table 5.2: *Classification of the composition of the different chromites analysed by MLA analysis of concentrates from batch flotation tests of each ore type... ..... 76*

Table 5.3: *Liberation proportion of chromite in the concentrates of the three ore types 77*

List of Abbreviations and Acronyms

- **GXMAP** - Grain-based X-ray mapping
- **ICP-OES** - Inductively Coupled Plasma – Optical Emission Spectrometry
- **IRUP** - Iron-Rich-Ultramafic-Pegmatoids
- **MLA** - Mineral Liberation Analyser/ Mineral Liberation Analysis
- **Oz**- Ounce
- **PAP**- Pouchou And Pouchoir Correction for Microprobe analyses
- **Pd**- Palladium
- **PGE** - Platinum Group Element
- **PGM** -Platinum Group Mineral
- **Pt**- Platinum
- **QEMSCAN** - Quantitative Evaluation of Minerals by Scanning Electron Microscope
- **RLS**- Rustenburg layered Suite
- **SEM** - Scanning Electron Microscope.
- **SIBX** - Sodium Isobutyl Xanthate
- **UG2** - Upper Group Chromitite layer.
- **XRD** - X-ray diffraction
- **XBSE** - Extended Back Scattered Electron
- **ZAF**- Stands for the three components of the matrix effects used for Microprobe Analyses Corrections; (Z) for atomic number, (A) for absorption and (F) fluorescence.

List of Mineral Abbreviations

- **Amph**- Amphibole
- **BMS**- Base metal Sulphide
- **Chl**- Chlorite
- **Chr**- Chromite
- **CPX**- Clinopyroxene
- **OPX**- Orthopyroxene
- **Phl**- Phlogopite
- **Plag**- Plagioclase
- **Serp**- Serpentine

CHAPTER 1: INTRODUCTION

1.1 Introduction

Platinum group elements or PGEs, which include Pt, Pd, Rh, Ru, Os and Ir, are found almost exclusively within chromitite layers in layered ultramafic complexes. Of the six PGEs, Pt and Pd are the most lucrative from an economic perspective and hence chromitite layers containing high concentrations of Pt and Pd have been the focus of most mining activity. The Bushveld Complex of South Africa contains three of the most important Pt and Pd deposits in the world, in the Merensky Reef, the Upper Group Two (UG2) chromitite and the Platreef (Cawthorn, 1999). Collectively these three deposits have been reported, based on proven and probable reserves, to contain in excess of 150 million oz of Pt and almost 70 million oz of Pd (Cawthorn, 1999). In these three reefs the PGEs are primarily hosted in platinum group minerals (PGMs) that form strong associations with base metal sulphides (especially chalcopyrite, pentlandite and pyrrhotite), and weaker associations with silicate minerals as well as with chromite (McLaren and De Villiers, 1982; Schouwstra *et al*., 2000). While the main minerals targeted for the beneficiation of PGEs are sulphides, chromite represents one of the principal gangue minerals in these ores, accounting for more than 26% to 50% of the mass of the ore in the UG2 for example (Mailula *et al*., 2003; Nel *et al*., 2005). Therefore, any beneficiation of the PGE ore must take into account the processing of chromite.

The presence of chromite in the PGE concentrate during the beneficiation process causes significant problems with downstream processing and extraction of PGEs. Most minerals processing plants are designed to accept a certain amount of chromite (around 3 modal %) in the PGM concentrate (Ekmekci *et al*., 2003; Nel and Naude, 2005). Where the amount of chromite exceeds 3%, the PGE grade in the flotation concentrate is reduced with significant consequences for the downstream processing. In particular, the stability of some chromite species at temperatures up to 2000˚C (Wesseldijk *et al*., 1999; McKenzie, 1996) can lead to

the build up of residual chrome spinel, resulting in a lack of optimal separation of matte and slag, that reduces the furnace efficiency and life time (Barnes *et al.*, 2004). Therefore, it is critical to understand the behaviour of chromite during the beneficiation process in order to minimise the amount of chromite present in the concentrate prior to smelting.

The beneficiation process involves three principal stages. These are: (1) liberation of the valuable minerals; (2) separation and concentration; and (3) disposal (Wills and Napier-Munn, 2006). In PGE processing operations, valuable PGMs are traditionally separated from gangue minerals (chromite) by flotation. The separation efficiency of chromite from base metal sulphides (and therefore PGMs) during froth flotation is thought to be influenced by the composition and the habit of chromite grains within the ore. Different compositions of chromite are believed to result in different surface properties which in turn alter the flotation properties of individual chromite grains (Gu and Wills, 1988). The habit of chromite refers to the different individual grain shapes and different grain shapes are known to attach differently to bubbles within the froth flotation cell (Yekeler *et al*., 2004; Ulusoy and Yekeler, 2005). Even prior to flotation, the habit of individual chromite grains can influence the breakage characteristics of the chromitite rock during crushing, milling and grinding (Tavares and das Neves, 2008). For these reasons, the efficiency of chromite separation is hypothesised to be influenced by the degree of compositional and textural heterogeneity of chromite grains.

Although the Merensky reef, the UG2 reef and the Platreef contain chromite hosted base-metal sulphides and PGMs (Hatton and Von Gruemewaldt, 1987; Holwell *et al*., 2007), the proportion of chromite associated with the UG2 is considerably greater than that of the Merensky and the Platreef. Hence, the need to understand the behaviour of chromite is more critical in the processing of UG2 ores. The UG2 has a complex stratigraphy with considerable lateral variation. In general though, the UG2 consists of a pegmatoidal feldspathic pyroxenite footwall, overlain by the UG2 main seam chromitite, overlain by feldspathic pyroxenite which contains the main leader and the triplet chromitite. In terms of mining activity, the main seam of the UG2 is always mined, but the mining of the leader chromitite depends on the thickness of feldspathic pyroxenite between it and the main seam. Therefore, attention has been focussed on the mineral processing properties of the

UG2 main seam chromitite. However, even within the main seam there are significant lateral variations in chromite composition and texture that are further compounded by the presence of potholes and Iron-Rich-Ultramafic-Pegmatoids (IRUP) intrusions.

The objective of this study is to investigate the influence of chromite compositional and textural variations in the UG2 main seam, at Waterval Mine on the western Bushveld, on the flotation behaviour of chromite. The study will investigate three different textural environments of the UG2 main seam: (1) "normal" UG2 main seam (defined as UG2 main seam with undisturbed and continuous footwall and hanging wall stratigraphy); (2) UG2 main seam affected by pothole formation; and (3) UG2 main seam affected by IRUP intrusion. Using these samples, the project will investigate the petrographic properties of chromites in each of these environments and then establish relationships between these factors and the flotation performance of chromite determined via laboratory-scale froth flotation experiments. This information can contribute to the refining of flotation procedures so that the amount of chromite in the final concentrate going through to the smelter is minimised, therefore helping to maximise the efficiency of PGE beneficiation.

1.2 Mineralogy of Chromite

1.2.1 Composition

Chromite is a member of the spinel group whose ideal formula is defined as $R^{2+}O.R^{3+}O_3$, where R^{2+} can accommodate Mg^{2+}, Fe^{2+}, Mn^{2+}, and Ni whereas R^{3+} can accommodate Cr^{3+}, Al^{3+}, and Fe^{3+} (Deer *et al*., 1992). The unit cell of chrome spinels is defined as sheets of oxygen anions roughly packed in a cubic shape containing 24 cations distributed between tetrahedral (A) and octahedral (B) sites (MacGregor and Charles, 1963). The distribution of cations between A and B sites in the unit cell determines the two structural types of spinel: (1) normal spinels where the eight tetrahedral sites are occupied by R^{2+} cations and the sixteen octahedral sites are occupied by R^{3+} cations; and (2) inverse spinels where the eight tetrahedral sites are occupied by R^{3+} cations and the sixteen octahedral sites are occupied by both R^{2+} and R^{3+} cations in a 1:1 ratio (Deer *et al*., 1992; Lumpkin, 2001).

Spinel minerals are divided into three principal series depending on which dominant cation occupies the octahedral site. The three principal series are: (1) the spinel series, in which the octahedral site is dominated by Al; (2) the chromite series, in which the octahedral site is dominated by Cr; and (3) the magnetite series, in which the octahedral site is dominated by Fe (Deer *et al*., 1992). The spinel series consists of four end-members which are spinel, hercynite, gahnite and galaxite. The chromite series consists of magnesiochromite and chromite while the magnetite series consists of magnesioferrite, magnetite, maghemite, ulvöspinel, franklinite, jacobsite and trevorite. The compositional relationship between these series is traditionally shown on a Johnson Spinel Prism. This prism shows spinels that either have Cr, Al or Fe^{3+} on the octahedral site and either Mg or Fe^{2+} on the tetrahedral site, giving six principle spinel end-members. The Johnson Spinel Prism therefore does not display relationships between Ti, Ni, Mn or Zn and other cations. Some of these relationships include the replacement of Mg by Zn to form gahnite, the substitution of Fe^{3+} and Mg by Mn^{3+} and Mn^{2+} to form jacobsite, the replacement Ni, Co and Zn for Fe^{2+} in magnetite, and Ti along with Fe^{2+} replacing Fe^{3+}(Deer *et al*., 1992)

At temperatures typical of basaltic magma (1050°-1250°C), there is an extensive solid solution between the six spinel end-members, with immiscibility gaps developing below these temperatures (Irvine, 1965). The composition of spinel that forms during cooling and development of this immiscibility gap is also a function of the co-existing cumulate phases. For example, chromites in orthopyroxenite have higher Cr/Al ratios than chromites in harzburgite (Hulbert and Von Gruenewaldt, 1985). This is thought to be related to the amount of Al accommodated by orthopyroxene in comparison to the amount accommodated by olivine. Similar studies on chromitite layers of the Upper Critical Zone showed that the UG1 chromitite layer, which is hosted by anorthosite, contains a higher Cr_2O_3 content than the UG2 which is hosted by orthopyroxenite (Eales and Reynolds, 1986). Even within individual chromitite layers there are compositional differences in relationship to stratigraphic height. In chromites of the UG1, there is a decrease in total Al cations as one progresses upward in the sequence leading to an increase in the Cr/Al ratio with increasing stratigraphic height. Similarly, there is an increase in Fe^{3+} and Ti cations and a decrease in the

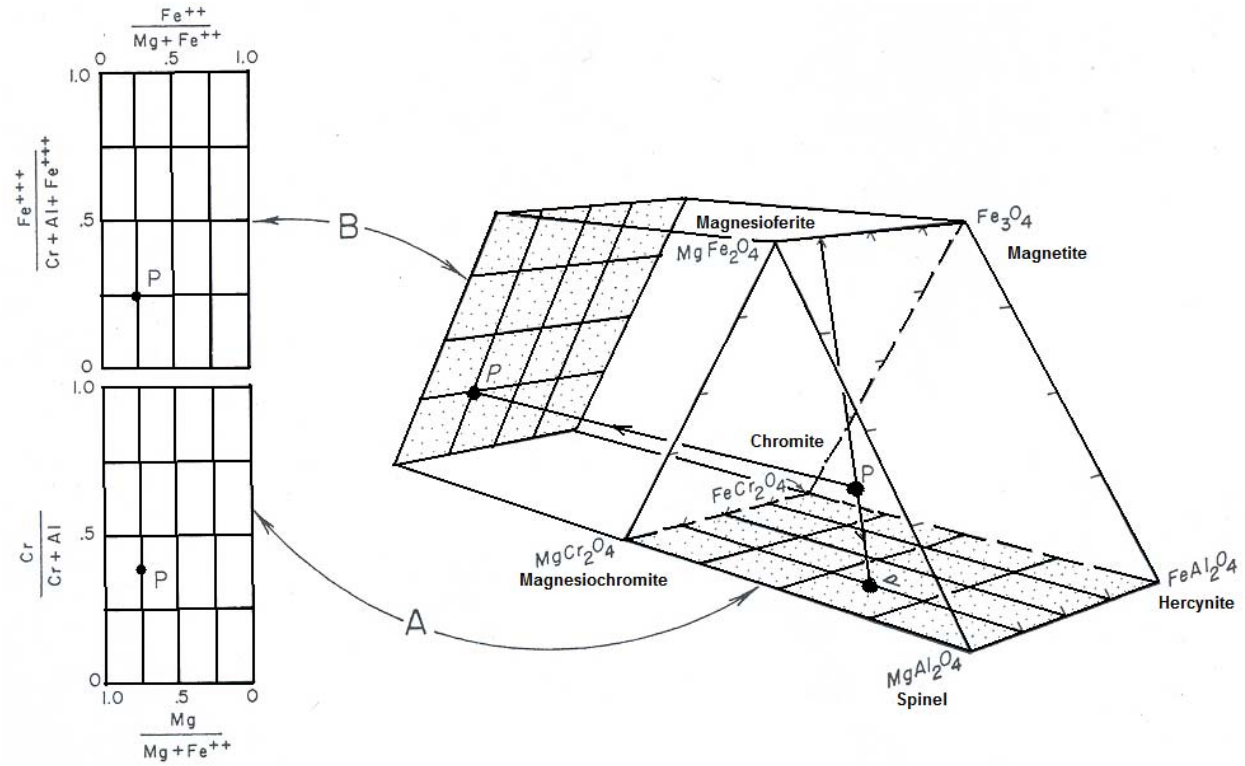

Figure 1.1: *Johnson spinel prism representing the composition features of spinel minerals. Summits are represented by the six principal end-members. The two projection surfaces use to derive the prism are indicated on the left (adapted from Irvine, 1965).*

Mg/(Mg + Fe^{2+}) ratio (Eales and Reynolds, 1986). The same study showed that the UG2 is characterised by the reverse compositional patterns in chromite with respect to stratigraphic height (Eales and Reynolds, 1986).

The study of the composition of the primary cumulate chromite by various authors, including Cameron (1977), Eales and Reynolds (1986) and Engelbrecht (1985), have shown that chromite in general portrays a restricted compositional variation. Figure 1.2 illustrates the primary composition of chromite in chromitite layers from the Bushveld Complex. Subsequently, in many places, these primary compositions have been affected by postcumulus requilibration in response to various processes such as IRUP intrusion, pothole formation, faulting and late-stage fluid activity. These processes collectively lead to important changes in chromite compositions which potentially have a direct impact on the floatability of the chromite grains.

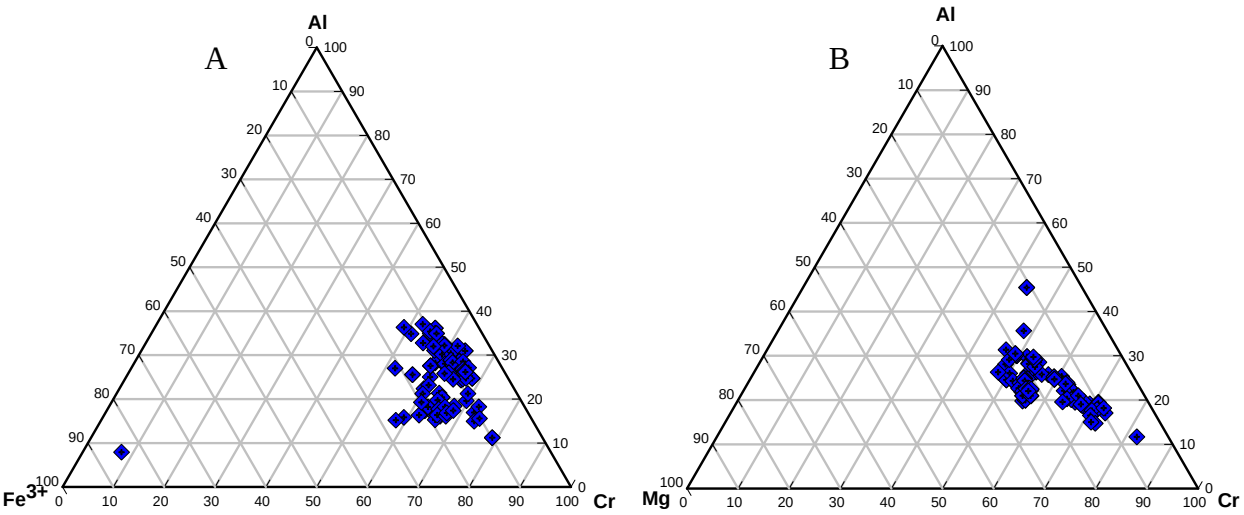

***Figure 1.2**: Primary compositional variation of chromitite (n=104) from chromitite layers in the Bushveld Complex: (A) Cr^{3+}-Al^{3+}-Fe^{3+} and (B) Cr^{3+}-Al^{3+}-Mg^{2+}. Data from Cameron (1977), Eales and Reynolds (1986) and Engelbrecht (1985).*

However, since the main driving forces for compositional change in the chromites are likely to be heat and fluids, significant impacts on chromite composition are likely to be related to IRUPs, faults and late-stage fluids rather than the development of potholes. Moreover, pothole formation is not well understood, particularly with respect to the relative timing of pothole formation and deposition of reef stratigraphy. Nevertheless, potholes are relatively common within particular layers in the Bushveld Complex, and therefore any link to compositional change would be significant. IRUP intrusions are thought to be of particular importance to postcumulus compositional alteration (Merkle, 1988). In the UG2 this is due to interactions between the pegmatoids and individual chromite grains near the contact zone with the basal part of the UG2 main seam resulting in metasomatic replacement followed by solid-state diffusion of cations causing Fe and Ti enrichment and Cr, Al and Mg depletion (Cameron and Glover, 1973).

Compositional change in chromite is also facilitated by the textural environment of the individual chromites. In particular, the surface area to volume ratio of chromite grains in contact with silicate grains is thought to be very important (Hatton and von Gruenewaldt, 1987). In fine grained areas of the UG2, because diffusion of elements across grain boundaries is encouraged by increases in temperature and pressure (Yamazaki *et al*., 2009), these areas are more susceptible to compositional modification during IRUP intrusion than coarse grained areas. Thus, compositional changes that can result in changing the flotation

behaviour of individual chromites (Gu and Wills, 1988) cannot necessarily be isolated from textural changes.

1.2.2 Texture

Chromite grains in layered intrusions tend to occur in one of two forms. The first is called "disseminated chromite" where chromite occurs as an accessory mineral, sparsely distributed, normally at the grain boundaries of cumulate phases, for example orthopyroxene and plagioclase in an orthopyroxenite. The second form is called "massive chromite" and is where chromite is the dominant phase and other phases such as orthopyroxene and plagioclase are post cumulus (Roach *et al*., 1998). In the UG2 main seam of the Bushveld Complex, chromite is present mostly in the massive form in chromitite layers. Just above and below the UG2 main seam, chromite grains occur in the disseminated form where grains are sparsely distributed along the boundaries of cumulate phases and are characterised by small grain sizes (0.05-0.3 mm) and sub-rounded to rounded shapes (Eales and Reynolds, 1986). Massive chromites on the other hand are characterised by larger anhedral aggregates of grains. Whereas the texture of disseminated chromites is relatively homogeneous and related only to primary crystallisation processes, the textures exhibited by massive chromites are the result not only of primary crystallisation processes but also secondary or post-cumulus processes as well (Hulbert and Von Gruenewaldt, 1985; Roach *et al*., 1998).

As a result, the range of textures in massive chromites is far greater than that exhibited by disseminated chromite and a complex terminology has been developed to describe these textures. The most common textures are sub-spherical, subhedral to euhedral grain shapes which are related to primary crystallisation of chromite grains (Eales and Reynold, 1986; Voordouw *et al*., 2009). The post-cumulus textures are dominated by sintering and annealing processes where compaction and densification of the hot cumulate pile results in sintering of the chromite grains to form welded aggregates of individual grains (Eales and Reynold, 1986). The latter are then annealed to remove internal grain boundaries, resulting in coarser irregular grain shapes. Since the sintering and annealing processes do not occur evenly, large variations in grain size and shape result and are clearly observable in the Bushveld Complex (Eales and Reynold, 1986).

In the Lower and Lower Critical Subzone in the Potgietersrus region, studies on chromitite layers have shown that there can be rapid and significant textural changes in chromite with stratigraphic height (Hulbert and Von Gruenewaldt, 1985). In this area, where chromitite directly overlies dunite, it has a massive texture made up of polygonal grains and is free of silicate inclusions (Hulbert and Von Gruenewaldt, 1985). After a few centimetres, this massive chromitite passes upward into a mottled type of chromitite, which, because of the higher proportion of silicate phases, has fewer polygonal chromite grains. This mottled chromitite is in turn overlain by another massive chromitite with polygonal grain shapes and rounded inclusions of olivine (Hulbert and Von Gruenewaldt, 1985). The top part of the chromitite contains fine to medium-grained chromite with irregular shapes, which in some cases mantle coarse and/or serpentinised olivine. Furthermore, it contains atoll textures in which chromite grains enclose other chromite grains, indicating two generations of chromite formation (Hulbert and Von Gruenewaldt, 1985). Chain texture, which is defined as the interconnectivity of individual grains of various shapes, was also identified in this region. These postcumulate changes are thought to be controlled not only by lattice strain energy and the grain boundary energy, but also by changes in temperature (Hulbert and Von Gruenewaldt, 1985).

In the Upper Critical Zone at Union Section Mine on the western limb, a study on the chromitites revealed that part of the area is characterised by variable chromite grain sizes varying from fine to coarse grains in an upward thickening section (Eales and Reynolds, 1986). The study also revealed the presence of dispersed chromite grains in silicate rocks, poikilitic pyroxene with fine-grained inclusions of chromite surrounded by coarse-grained chromite, and coarse-grained chromite positioned on top of one another within a poikilitic pyroxene. Some of these coarse-grained chromites also had a characteristic shape referred to as cuspate or lobate. On the far-western limb at Nietverdiend, the Lower Group chromitite layers, contain chromite grains with idiomorphous shapes as well as fractures leading to angular shapes separated by interstitial serpentine (Engelbrecht, 1985). Where these fractures are very extensive, they lead to microbrecciation (often patchily developed) of chromite.

The range of textural variations in massive chromite, discussed above, has the potential to affect the mineral processing of PGE-bearing chromite ores. The main processes that influence chromite textures and which might bear on minerals processing are sintering/annealing and fracturing. Both of these processes are potentially driven by the intrusion of IRUPs. The intrusion of IRUPs brings in heat, which drives sintering and annealing, and fluids, which drives fracturing, and therefore chromitites affected by IRUP intrusions often have different textures to those that are not (Cameron and Glover, 1973; Reid and Basson, 2002). Thus, these changes in chromite textures could be seen as potential factors influencing the flotation performance of the chromite grains during mineral processing of PGMs.

1.3 Mineral Processing of PGMs

Mineral processing is a complex process accomplished over several steps that can be grouped into two main phases: (1) liberation of the valuable mineral from the host mineral; and (2) separation and concentration of that valuable mineral (Wills, 1988). The liberation of the valuable mineral, also known as comminution, involves crushing and grinding, whereas the concentration of the valuable mineral is usually performed by froth flotation. An example of a UG2 beneficiation flowsheet illustrating the relationship between the various stages of mineral processing is shown in Figure 1.3.

1.3.1 Comminution

Comminution is a mechanical process where the raw material (i.e. ore) is put through a series of crushers and mills in order to reduce its particle size. This stage is important because it reduces the valuable minerals to a size suitable for separation from the waste material (gangue) by gradually exposing its surface and liberating it. Correct set up for comminution is critically important for the efficiency of froth separation as both under and over-grinding of material can result in poor recovery and low grade of valuable minerals from the flotation process.

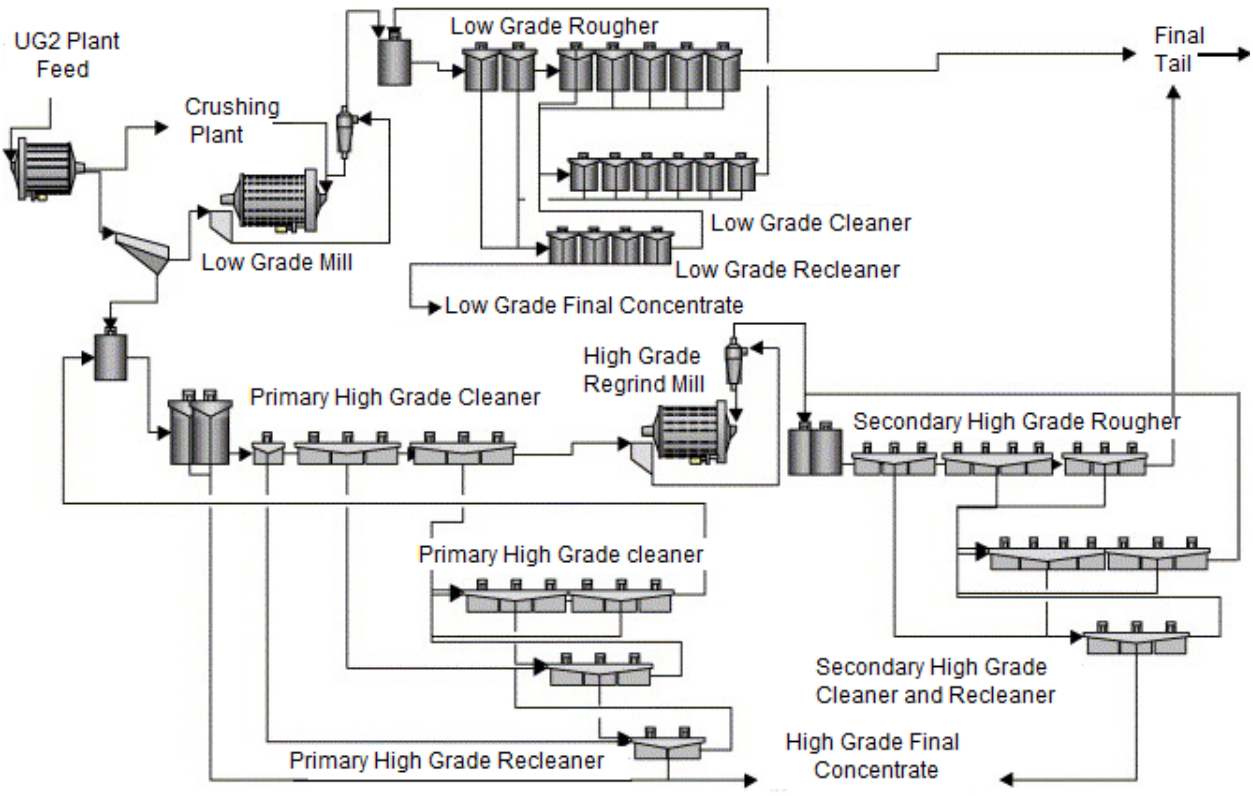

***Figure 1.3**: Conventional UG2 ore separation or processing flow sheet (Nel and Naude, 2005)*

1.3.2 Classification

Classification is the process during which fine particles are removed from coarser particles. The former (undersize) is removed from the grinding process and sent to the froth flotation circuit, whereas the latter (oversize) is sent back to the grinding circuit for further size reduction (Mainza *et al*., 2005). This separation is usually achieved with classifiers such as hydrocyclones or screens. Hydrocyclones rely on centrifugal and drag forces operating on particles through a water system (Mainza *et al*., 2005). This process separates particles based on their size, shape and density (Becker *et al*., 2008), whereas the use of screens is based entirely on the classification of particles by size and shape.

1.3.3 Separation via Froth Flotation

Froth separation involves the separation of particles by manipulating their physico-chemical properties through the addition of reagents to make valuable minerals attach to air bubbles which rise to the surface of the pulp and into the froth zone and are collected as concentrates. Not all valuable minerals have the natural ability to attach themselves to

bubbles so that they float. Hence, these minerals require the addition of reagents such as collectors and activators to render them hydrophobic. Conversely, some gangue minerals are naturally floatable and require the addition of depressants to form hydrophilic surfaces and prevent their flotation. Particles can report to concentrates via different mechanisms (Bradshaw *et al*., 2005; Savassi, 2005) that include:

- **True flotation:** a natural selective process referring only to particles with hydrophobic properties and constitutes the principal transporter of material recovered to the concentrate (Savassi *et al.,* 1998).
- **Recovery by entrainment:** a non selective recovery process in which all particles are mechanically transported to the froth phase due to the flow of water (Neethling and Cilliers, 2001). The review by Savassi *et al.* (1998) concluded that the principal factors affecting entrainment of all materials are water recovery, particle size, and percentage of solid in the pulp, froth structure, froth resident time and specific gravity of the mineral.
- **Recovery of composite particles** (middlings)**.** This is the process by which gangue particles are transported to the froth phase and are collected as concentrate products due to their association to hydrophobic minerals.

The presence of chromite in concentrates during froth flotation experiments has generally been attributed to entrainment or the presence of composite particles, since it is a naturally hydrophilic mineral (Welsseldjik *et al*., 1999; Ekmekçi *et al*., 2003). To understand why chromite reports to the concentrate various studies have investigated the behaviour of chromite in laboratory flotation experiments. An investigation of the addition of various types of collectors, including sodium isobutyl xanthate and dithiophosphate, on the flotation behaviour of chromite by Wesseldijk *et al*. (1999) found that these collectors alone had no significant effect on the flotation of chromite. However, when combined with the activator $CuS0_4$, the result was chromite recoveries above 60% in the concentrates.

Similarly, the flotation of chromite and serpentine was explored by Gallios *et al*. (2007). Their study aimed at investigating the outcomes of pH, collector concentration, modifier type and concentration on chromite flotation behaviour with the objective of establishing its

conditions of separation from serpentine. Based on their experiments, the authors concluded that medium quantities (20-30 mg/L) of sodium oleate as a collector at alkaline pH resulted in the strong activation of chromite. In addition, carboxymethyl cellulose used under alkaline pH conditions was found to be a strong depressant of chromite. On the other hand fluorosilicic acid, cyclodextrin and athylen diamine-tetraacetic acid were also found to be efficient activators at acidic and neutral pH. Thus, this study found that it is possible to selectively separate chromite from serpentine using various reagents.

The study of Ekmekci *et al*. (2003) examined the effects of frother type and frother height on the flotation behaviour of chromite from the UG2 ore. The findings of their different experiments showed that it was possible to obtain concentrates with less than 3% chromite when the height of the froth was increased. The effect of increasing froth height was to promote drainage of particles from the froth and minimise the amount of entrainment.

The incorporation of all the previously discussed aspects (mineralogy and the mineral processing) in this context related to chromite into one discipline called process mineralogy has proven positive for the beneficiation of an ore during mining activity (Baum *et al*., 2006). This discipline is discussed below.

1.4 Process Mineralogy

Process mineralogy, which is the combination of two disciplines that include mineral processing and mineralogy, has recently received considerable attention, first by Henley (1983) followed by the revision of Baum *et al*. (2006). The role of the process mineralogist is to provide information on aspects of the ore mineralogy and mill products so that metallurgical treatment can be improved (Henley, 1983). In his milestone paper, Henley (1983) depicts the importance of understanding the mineralogy of the ore from its exploration phase to its processing stage, and highlights the value of this information in developing and running concentrators that address specific characteristics of the ores. The understanding of ore mineralogy requires the involvement of various fields that comprise geology, mineralogy, engineering, sampling statistics, physics, mathematics, and chemistry (Henley, 1983; Lotter *et al*., 2002). This combination of different fields can provide important

information that can help to improve metallurgical treatments. Process mineralogy relies on information obtained by the mineralogist (including a description of the mineralogical assemblage, possible liberation size ranges, and identification of problematic minerals), being utilised by the minerals processing engineer in pilot plant testing to develop flowsheets, which will then help to refine specific metallurgical treatments (Baum *et al*., 2006). Improvements in the information provided by these different disciplines have been made possible by advances in analytical techniques.

Detailed textural factors such as the size of liberated minerals, their mineral association, the degree of liberation and modal mineralogy are important characteristics needed for modern digital mine planning, plant design and mineral processing operations (Fandrich *et al*., 2007). The determination of these characteristics using traditional tools, such as optical microscopy and/or semi-automated Scanning Electron Microscopy (SEM), are time consuming, user dependent and not necessarily statistically representative (Fandrich *et al*., 2007). Modern automated methods, despite being costly, are well equipped to produce a considerable amount of statistically reliable data in a relatively short period of time. In particular, these developments have focussed on the ability to perform statistically robust modal and liberation analyses that are then applied to mineral processing (Creelman and Ward, 1996; Lastra, 2007). These methods include the Quantitative Evaluation of Minerals by Scanning Electron Microscopy (QEMSCAN) and the Mineral Liberation Analyser (MLA) which are increasingly used to assist in improving metallurgical performance (Gu, 2003; Fandrich *et al*., 2007).

Different examples illustrating the importance of these modern analytical methods in the beneficiation of ores have been the subject of various publications. A practical example illustrating the importance of these modern analytical methods were surveys carried out at Raglan in Canada. The Raglan surveys of 1997 and 2000, dealt with ore types subdivided into end members comprising (1) massive sulphides, (2) net-textured sulphides and (3) disseminated sulphides (Lotter *et al*., 2002). During these surveys, the difference of nickel recovery between rougher and final concentrate of 5-7% was problematic to the plant recovery operation. This difference was found to be associated with the scavenger tailings (Lotter *et al.*, 2002). The use of QEMSCAN to investigate these losses revealed a lack of

particle liberation. On the basis of these results it was therefore decided that regrinding of the cleaner tailings before scavenger flotation for better liberation of the valuable mineral was necessary. This led to a sustainable recovery gain of the valuable minerals.

Another study showing the importance of modern analytical methods in mineralogical characterisation during ore beneficiation is the study by Rule and Anyimadu (2007) on different PGE ores (UG2, Merensky and Platreef). In this study the performance of flotation circuits at Anglo Platinum's concentrators in South Africa were continuously evaluated and monitored for flotation performance improvement with respect to the beneficiation of PGEs. During that study MLA analysis was used to measure and quantify mineral loss profiles across all reef types and operating plants within the Anglo Platinum group. This was done with the objective of redesigning the flotation circuit for recovery improvement. The study showed that the valuable mineral loss was related to poor liberation of PGMs in the +58 µm fraction (coarse fraction) and therefore required a redesigning of plants for finer grinding and finer flotation (Rule and Anyimadu, 2007).

Also looking at the mineral processing of the UG2 ore was the study by Nel *et al*. (2005). The principal goal of this study was to investigate the influence of open circuit regrind milling on UG2 ore composition and mineralogy at Impala's UG2 concentrator. The study used QEMSCAN to characterise particle textures in a flotation circuit. It was observed that the open circuit regrind resulted in a better liberation of PGMs in the concentrates, and that the liberation was accompanied by a redistribution of particle sizes in the circuit (Nel *et al*., 2005).

The importance of the characterisation of an ore prior to concentrator treatments done in relationship with laboratory experiments with the objective of optimally beneficiating the valuable minerals has proven to be a necessary step during mining operations (Baum *et al*., 2006). This project examines mineralogical characteristics of three selected reef types from the UG2 at Waterval Mine in order to understand the relationship between their mineralogical characteristics and their flotation performance.

1.5 Project Scope, Aim and Objectives

The central aim of this project is to determine the influence of chromite mineralogical characteristics on mineral processing of the UG2 main seam chromitite layer. The project was carried out using ore from Anglo Platinum's Waterval Mine on the western limb of the Bushveld Complex and examined three different types of UG2 main seam chromitite ore. These were: (1) UG2 normal reef; (2) UG2 reef associated with pothole formation; and (3) UG2 reef associated with the intrusion of IRUP's. Further details of the sampling and methodology are given in Chapter 3. In order to provide answers to the project aim, the following objectives have been identified.

Objective One

To determine whether there are textural differences in chromite grains in the UG2 main seam between: (1) normal reef, (2) reef affected by a pothole formation and (3) reef affected by IRUP intrusion.

a. What are the textural characteristics of the three different main seam environments?
b. Are the textural characteristics of three environments, related to primary or secondary processes?
c. If these textural characteristics are related to secondary processes does this also result in the development of new secondary silicate minerals

Objective Two

To determine whether there are compositional differences between chromites found in the UG2 main seam between: (1) normal reef, (2) reef affected by potholes formation and (3) reef affected by IRUP intrusion?

a. What are the compositional characteristics of chromites in the three main seam environments?
b. Are the compositional characteristics of the three environments related to primary or secondary processes?

c. If these compositional characteristics are related to secondary processes what are the geological driving features behind their generation and how did they affect chromite composition?

Objective Three

To determine how the composition and texture of chromites from the UG2 main seam influences the flotation behaviour of chromite?

a. What is the impact of textural differences on the flotation performance of these three main seam environments?

b. What is the impact of compositional variations from the three different environments on the flotation performance of chromite?

c. Does the presence of primary or secondary silicates influence the flotation behaviour of chromite from these three environments?

CHAPTER 2: REGIONAL GEOLOGY

2.1 Overview of the Bushveld Complex

The Bushveld Complex (Fig. 2.1) of South Africa, with an areal extent of 65000 km^2 and a thickness of 7 to 9 km, is a fabulous source of platinum group elements and a huge reserve of chromite (Eales and Cawthorn, 1996). The Bushveld Complex, which has been dated at 2.06 Ga (Walraven *et al*., 1990), is a layered igneous intrusion of variably mineralised mafic to ultramafic rocks associated with two felsic intrusive suites. Current day exposure of the Bushveld Complex indicates that there are five main limbs. These are the far western limb, the western limb, the northern limb (including both the Potgietersrus and Villa Nora sections), the eastern limb and the Bethal limb. The Bethal limb situated south of the complex is not exposed at the surface but has only been characterised using gravity and borehole information (Eales, 2001; Cawthorn *et al*., 2006). The connectivity of these limbs is not clear and certainly that of the eastern and western limbs below the surface has been a topic of debate amongst researchers.

Despite a wealth of information, the tectonic setting of the Bushveld Complex remains unclear (du Plessis and Walraven, 1989). Various settings have been proposed, including a stable cratonic environment (Crockett, 1969; Hunter, 1973a, 1975, 1976, Cawthorn and Walraven, 1998) and an extensive system related to an abyssal zone along which major mafic complexes and crustal materials are found (Jansen, 1982). In addition to the tectonic setting, the origin of the Bushveld Complex magmas is also controversial, in part because some of the tectonic settings, for example the stable cratonic setting, are incompatible with the formation of the large volumes of magma needed to create the Bushveld Complex (Eales and Cawthorn, 1996).

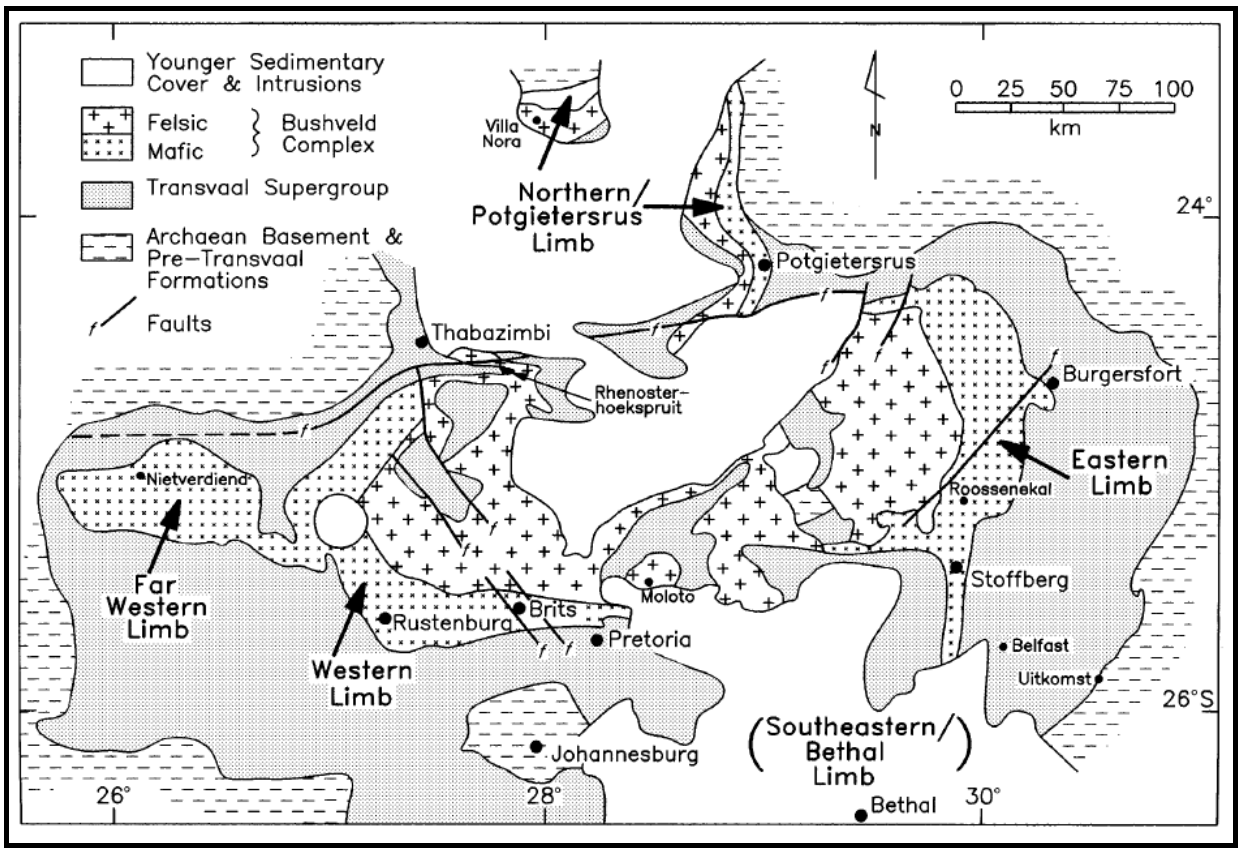

***Figure 2.1**: Geological map of the Bushveld Complex, obtained from a compilation by Eales and Cawthorn (1996).*

2.2 Stratigraphy of the Bushveld Complex

The Bushveld Complex represents a multi-faceted association of intrusive rocks principally divided into three suites. These are the Rustenburg Layered Suite (RLS) principally composed of mafic to ultramafic rocks, which are host to the mineralisation, and the Lebowa Granite and Rashoop Granophyre Suites, both of which are younger than the RLS (Vermaak and Von Gruenewaldt, 1986). The UG2 chromitite layer studied in this project is part of the RLS, and is therefore the only suite for which a stratigraphic description is given below. Some parts of the RLS stratigraphy, including the UG2 chromitite layer, have been disrupted by processes such as the formation of potholes and the intrusion of IRUPs. The presence of potholing and IRUPs is known to modify the texture and composition of minerals within affected layers. For this reason, these post-magmatic features will be discussed under separate sections in subsequent sections.

The RLS is divided into five zones referred to as the Marginal Zone (mainly norites), the Lower Zone (cyclical harzburgites and pyroxenites), the Critical Zone (interlayered

chromitite, pyroxenite and norite), the Main Zone (cyclical norites, gabbronorites and anorthosites) and the Upper Zone (cyclical units of magnetites, gabbronorites, anorthosites, and diorites). Some of these zones are further subdivided into sub-zones. The Critical Zone (CZ) is divided into two separate sub-zones, the Lower Critical Sub-zone (LCSZ) and the Upper Critical Sub-zone (UCSZ), both of which contain chromitite layers. The UG2 chromitite is hosted by the Upper Critical Sub-zone (Fig. 2.2). The subdivision in Figure 2.2 was characterised according to the appearance of different cumulate phases (SACS, 1980).

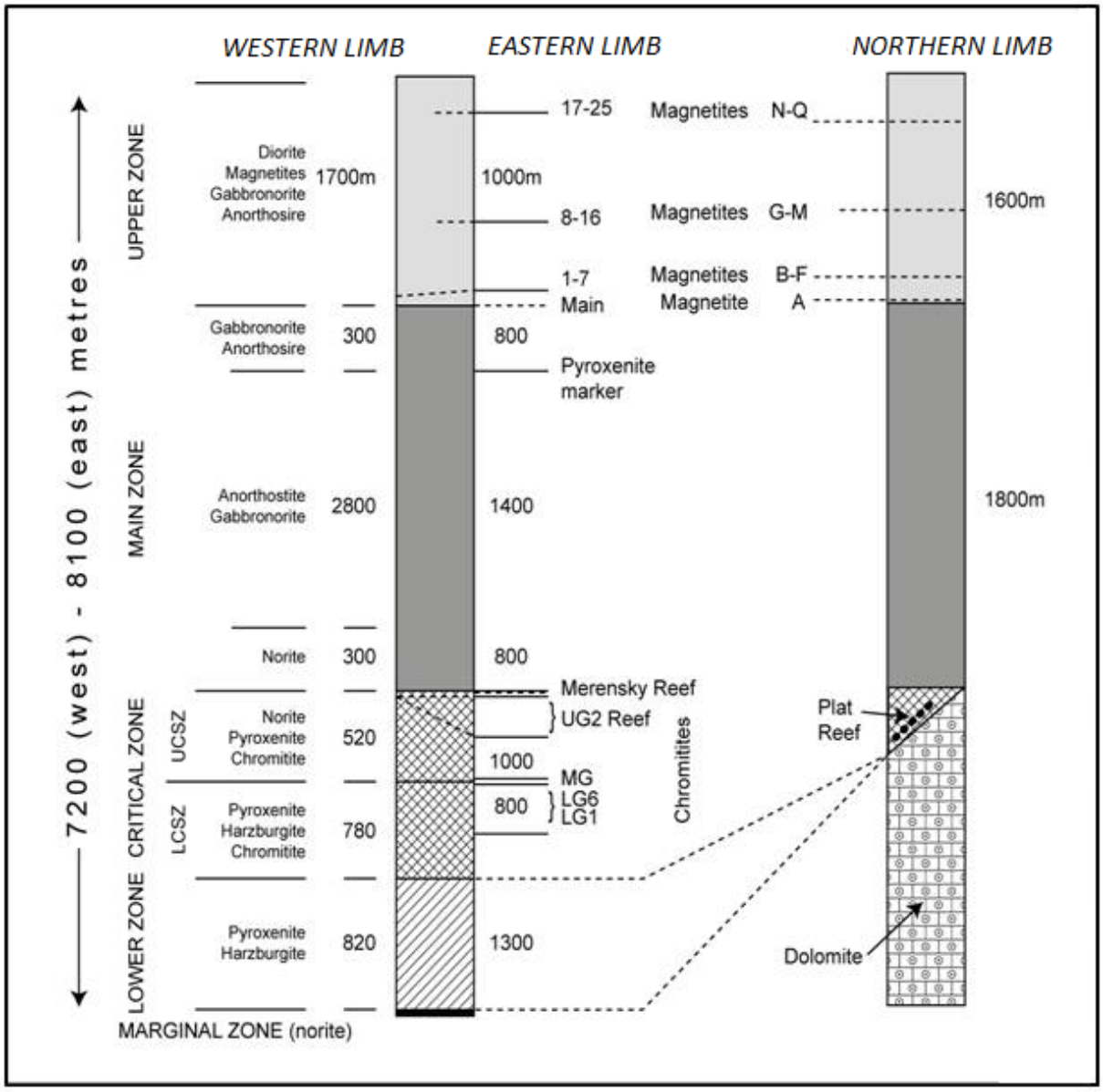

Figure 2.2: *Stratigraphy of the major limbs of the Rustenburg Layered Suite. Taken and modified from Barnes et al (2004), and based on Cawthorn and Walraven (1998) and White (1994).*

2.3 The UG2 Chromitite Layer in the Bushveld Complex

Chromitite layers in the Bushveld Complex are localised in the Critical Zone (Mondal and Mathez, 2007), where they are subdivided into three groups (Lower (LG), Middle (MG) and Upper (UG) Group) on the basis of their height in the Critical Zone (Eales, 2001). The UG2 chromitite layer therefore represents the second layer of the Upper Group and lies between 20 m to 400 m beneath the Merensky reef (Schouwstra *et al*, 2000). This chromitite layer is enclosed within a ~25 m thick pyroxenite termed the UG2 pyroxenite (Mondal and Mathez, 2007). The thickness of the UG2 varies throughout the RLS, ranging between 40 cm and 2.5 m, and averaging ~ 1 m thick (Schouwstra *et al*., 2000). The reef dips at angles between 5° and 70° toward the central part of the RLS (McLaren and De Villiers, 1982). The UG2 chromitite consist of a main chromite seam, which is on average 60 to 70 cm thick, and two or three leader seams which are much thinner (Viljoen and Hieber, 1986).

The mineralogical composition of the UG2 main seam chromitite layer is principally chromite (60-90 modal %), orthopyroxene (5-25 modal %) and plagioclase (5-15 modal %) (McLaren and De Villiers, 1982). The accessory phases are mainly clinopyroxene, base metal sulphides (BMS), ilmenite, magnetite and rutile. PGEs are known to occur in association with chromite and BMS (Eales and Reynolds, 1986; Schouwstra *et al*., 2000; Godel *et al*., 2007, Penberthy *et al*., 2000).

2.4. Modification of UG2 Chromitite Layer

There are several ways in which the primary characteristics of the UG2, in terms of composition and texture of chromite grains, may be modified. The most significant of these include faults, dykes, potholes and IRUP intrusions (van Schoor, 2005). Weathering is an additional factor affecting the primary mineralogy of the UG2 layer. Weathering of the UG2 has been documented (Hey, 1999) on a borehole running through the UG2 reef at Union Section mine (in the north-western Bushveld Complex) and the following observations recorded:

- Weathering causes the outer part of chromite to fracture and become slightly enriched in chromium while it gets depleted in iron.

- Weathering results in the dissolution of base metal sulphides (BMS)
- PGMs have undergone different degrees of weathering.

In addition, various alteration processes (other than weathering such as metasomatism) have led to the breakdown of primary minerals and the formation of numerous secondary silicates such as amphiboles, epidotes and quartz (Li *et al.,* 2004).

Of the different processes affecting primary features resulting from the crystallisation of the UG2 chromitite layer, potholes and IRUPs sampled as part of this project will be the only post-magmatic features discussed below.

2.4.1 Potholes

In the Bushveld Complex a pothole is a zone where the localised absence of sections of the stratigraphy result in, in the case of both the Merensky and the UG2 reefs, transgression of the chromitite layers down through the footwall units. The formation of these potholes has been the subject of ongoing debate and numerous models have been put forward including amongst others: (1) erosion of the cumulate pile (Viljoen and Hieber, 1986; Viring and Cowell, 1999); (2) density and viscosity contrasts during compaction and fluid loss (Lee, 1981; Ballhaus, 1988); and (3) sites of concentrated fluxing by reducing fluids (Buntin *et al*., 1985; Kinloch and Peyerl, 1990). A detailed assessment of these models is beyond the scope of this study. However, studies on the effects of pothole formation on chromite composition have shown variable compositional modifications.

An investigation of the effect of pothole formation on the Merensky Reef conducted at Rustenburg, Impala and Union Mines concluded that although the composition of individual chromite grains was fairly homogeneous in a given locality, there was a variation in composition at a regional scale (Buntin *et al*., 1985). This range in composition was characterised by an increase in total Fe and a decrease in Cr and Al from potholed to normal Merensky Reef for Rustenburg and Impala Mines, and an increase in total Fe and a decrease in Cr, Al and Mg from the potholed to normal Merensky Reef for Union Mine. According to Buntin *et al.*, (1985) this compositional change was associated with the phenomena of isothermal injection of hot fluids into the normal Merensky Reef related to the formation of potholes.

The relationship between pothole formation and mineralogical modification of stratigraphic layers has also been investigated in the Merensky Reef at Brakspruit Shaft of Rustenburg Platinum Mines (Ballhaus, 1988). The study examined three different environments: (1) an undisturbed Merensky Reef stratigraphy; (2) the Merensky Reef toward the centre of the pothole; and (3) the Merensky Reef in the centre of the pothole. Petrographic characterisation of these environments found that the Merensky Reef is generally a fine-grained feldspathic pyroxenite rock type but with increasing proximity to the centre of the pothole turns into a much coarser-grained gabbro pegmatite in which graphite is a major component and sulphide minerals occur as interstitial phases. The presence of graphite is associated with the activity of C-H-O-S volatiles evolving from a late-stage crystallising magma.

2.4.2. IRUP Intrusion

Layered rocks of the Bushveld Complex may be transgressed by numerous discordant bodies of ultramafic rocks (Viljoen and Scoon, 1985). These discordant ultramafic bodies show a variation in composition ranging from magnesian dunite, iron-rich dunite, wehrlite and clinopyroxenite to iron oxide dominated (Cawthorn *et al.*, 2000). They may be up to hundreds of meters in vertical extent with diameters less than 200 m and in exceptional cases, the largest pipes have diameters reaching 2 km. In the Bushveld Complex, IRUPs are in general associated with anorthosite layers, which are most abundant in the Upper Critical Zone Sub-zone, and are also associated with disturbed areas characterised by faults and dykes of post Bushveld age (Viljoen and Scoon, 1985). Viljoen and Scoon (1985) also indicated that the mineralogy of IRUPs is related to the stratigraphic height, and so defined two sub-divisions: (1) the silicate dominated group found in the Critical Zone and (2) the Fe-Ti oxide dominated group found in the Upper Zone. Both of these groups are present at intermediate levels (Main Zone and Lower Upper Sub-zone).

An investigation on the influence of IRUP intrusions on the variation in chromite composition using samples from the Farm Annex Grooteboom, Tweetfontein, and De Grooteboom revealed that the composition of chromite near the contact with pegmatoids developed a range of compositions from chromite to titanomagnetite toward to the contact zone (Cameron and Glover, 1973). Cameron and Glover (1973) also observed that these

compositional modifications to chromite were accompanied by textural modifications such as the development of large polygonal grains. These modifications are associated with solid solution diffusion reactions with the intruded IRUP.

Other studies conducted separately at Northam Platinum and at Amandelbult Platinum Mines in the northwestern part of the Bushveld Complex also looked at the effects of IRUP intrusions on chromitite layers. These studies concluded that the IRUP intrusions result in the preferential replacement of intercumulate plagioclase and resulted in compositional and textural modification of chromite grains due to interaction of pegmatite melts with pre-existing chrome spinel phases (Reid and Basson, 2002; Scoon and Eales, 2002).

2.5. The Rustenburg Section

2.5.1 Overview

The Rustenburg Section is one of the Anglo Platinum lease properties and contains Waterval Mine (Fig. 2.3) which is the sampling area for this project. Rustenburg Section is situated south of the Pilanesberg Alkaline Complex along an east-west strike line running from Brakspruit to Boschfontein and is 29 km long with an approximate width of 7 km in its central part (Viljoen and Hieber, 1986). It forms part of Rustenburg Platinum Mines Limited (RPM) together with Amandelbult, Union Mine and Bafokeng-Rasimone Platinum Mine (BRPM). The first two mines are situated north of the Pilansberg Complex (Fig.2.4) whereas the latter occurs south of the Pilansberg Alkaline Complex.

The stratigraphic section at Rustenburg Section (Fig. 2.4) with its multitude of stratigraphic layers of high economic value, including the UG2 and the Merensky Reef is floored by pre-existing Transvaal rocks (Viljoen and Hieber, 1986).

2.6 Overview of Waterval Mine

Waterval is one of the underground operational mines in Rustenburg Section and is the location where samples for this project were collected. It is situated in the south-western

part of the Rustenburg Section lease area (Fig. 2.3). In this section, only a small portion of the entire UCZ stratigraphy has been exposed by mining activity. The exposed

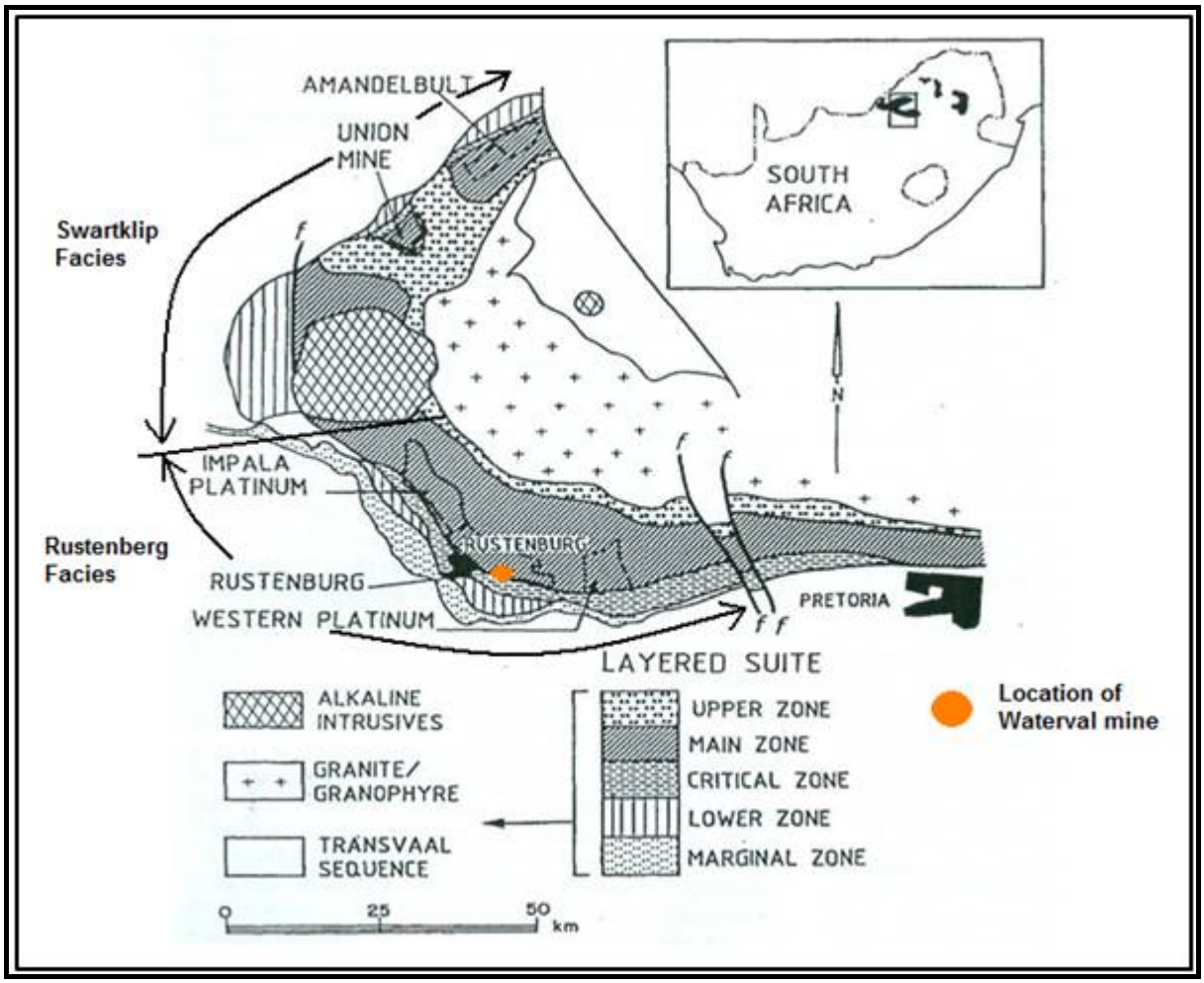

Figure.2.3: *Geological map showing the Western Limb of the Bushveld Complex and the subdivision of the Western Limb into two principal facieses as proposed by Wagner (1929). The northern Swartklip Facies and the southern Rustenburg Facies are separated by the Pilanesberg Complex. Location of some of the major platinum mines in the area is also shown (Adapted from Cawthorn and Barry, 1992; and Smith et al., 2003).*

stratigraphy is illustrated in Figure 2.5. The base of the section starts with a norite overlain by a medium to coarse grained pegmatoidal feldspathic pyroxenite footwall (FW). The contact between the footwall and the UG2 main seam chromitite is generally sharp although it may be sinuous on a centimetre scale. Towards the top of the main seam chromitite is a fine-grained feldspathic pyroxenite layer called the Main Seam Parting (UG2MSP). This layer is on average between 3 and 7 cm in thickness and is usually within 15 cm of a feldspathic pyroxenite overlying the main seam chromitite, that constitutes the immediate main seam chromitite hanging wall which is approximately 1.4 m in thickness. This pyroxenite

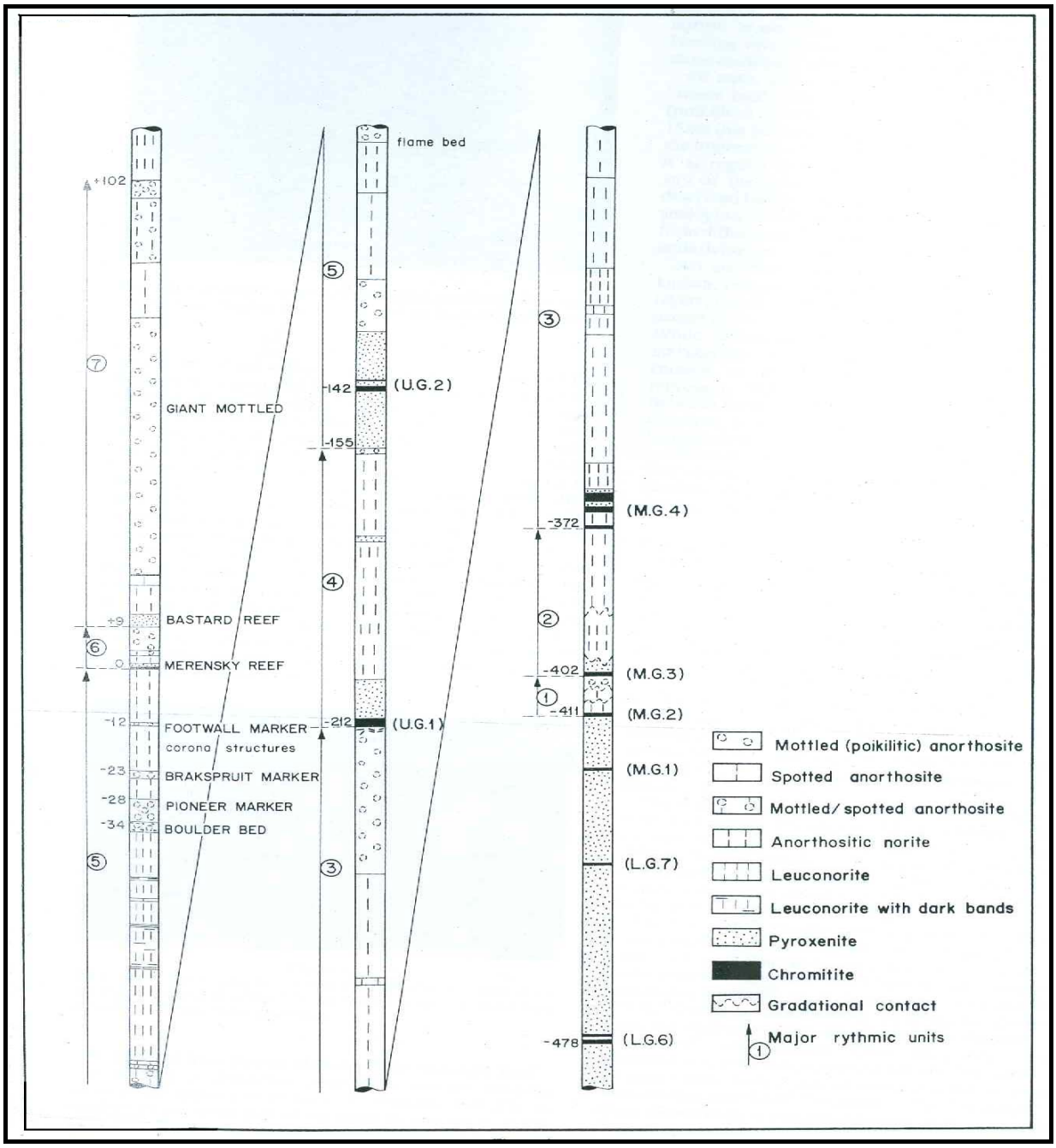

Figure 2.4: *General stratigraphic column of the Upper Critical Zone revealed by mining activities in the Rustenburg Section area (Viljoen and Hieber, 1986).*

hosts a chromitite stringer 1-2 mm thick, referred to as the UG2LT, that is located at variable distances above the UG2 main seam. The UG2 main seam chromitite immediate HW pyroxenite is overlain by another chromitite layer named the main leader seam and referred to as UG2L. This seam is not always mined, and reaches a thickness of up to 30 cm. The

vertical distance between the UG2 and the UG2L is variable and determines if both chromitite layers should be mined or not. At Waterval both the UG2 main seam and UG2L are mined if the distance between them is less than 1.4 m. Above that distance only the UG2 main seam is mined. The UG2L is overlain by an approximately 7 to 8 m of feldspathic pyroxenite that hosts three thin chromitite layers known as the chromitite triplets (UG2T). From bottom to top these triplets are named T1, T2 and T3. The top most part of the stratigraphic column at Waterval mine is terminated by a poikilitic anorthosite (UG2A), which marks the upper-most extent of the stratigraphic section that is under investigation.

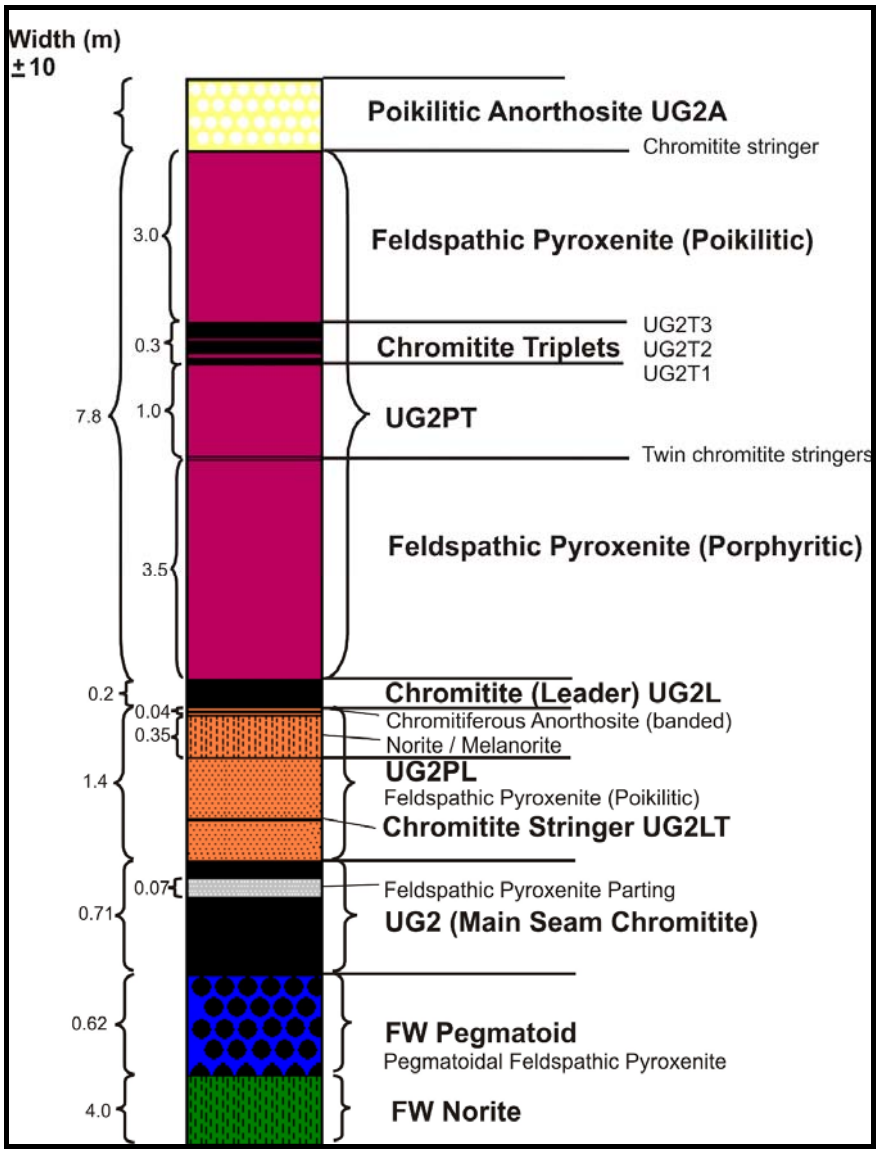

Figure 2.5 *Generalised stratigraphic column of Waterval Mine (M Oosthuysen personal communication, 2008)*

Waterval Mine, like the rest of the Bushveld Complex, contains an abundance of potholes and IRUPs that have affected the geology at different scales and stratigraphic levels, producing various modifications of the UG2 chromitite and its enclosing silicate rocks. The pothole sampled as part of this study was only partly observed because it represents an unmined reef and therefore an area where the reef is not fully exposed by mining activity (Fig. 2.6). This pothole occurred over a short distance of approximately 6 to 8 m and showed very little change in the thickness of the UG2 main seam inside and outside of the pothole, compared to what has been observed by Ballhaus (1988) where the chromitite reef thins toward the pothole depression. The sampled IRUP at Waterval Mine showed a volume for volume replacement with the pegmatoidal feldspathic pyroxenite footwall to the UG2 main seam. (Fig 2.6). Unlike typical IRUP intrusions which are dominantly composed of clinopyroxene and olivine (e.g. Reid and Basson, 2002), the IRUP at Waterval is extremely felsic, composed of altered plagioclase and quartz, but exhibits all the other aspects of an IRUP intrusion. These IRUPs at Waterval Mine have been described by the sectional geologist to be pipe-like shaped, discordant, concordant or irregularly shaped (per. comm. M. Oosthuysen, 2007).

Figure 2.6: *UG2 normal reef progressively deeping into the pothole depression. Note the progressive loss of the footwall.*

These IRUPs show a dual relationship with the UG2 main seam as in some places they are clearly cross-cutting the UG2 main seam and in some other places they are not (Fig.2.7).

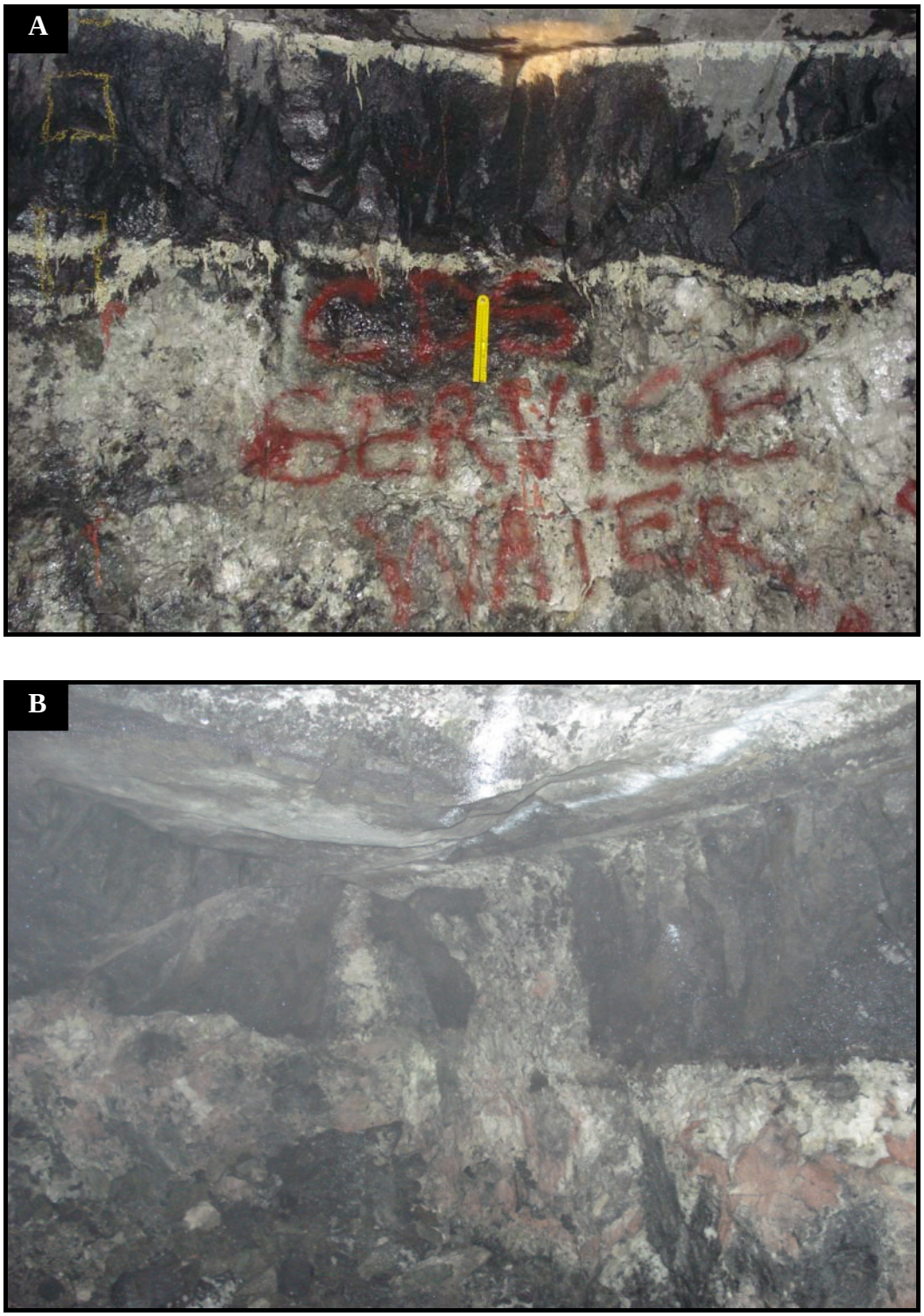

Figure 2.7: *IRUP intrusive relationships with both the UG2 main seam and its footwall; (A) ponding of the IRUP below the UG2 main seam and (B) IRUP cross-cutting the UG2 main seam from sampled area (photo courtesy of M. Oosthuysen: photo field of view is ~4 to 5 m).*

CHAPTER 3: METHODOLOGY

3.1 Sample Collection and Preparation

3.1.1 Samples for Petrographic Studies

Three different UG2 reef types were selected for this study: (1) UG2 normal reef (undisturbed UG2 stratigraphy); (2) UG2 reef affected by pothole formation; and (3) UG2 reef affected by IRUP intrusion. For each of the reef types, the UG2 main seam was selected for sampling. For each section of the UG2 main seam sampled, a series of samples through the seam were collected from four different locations labeled A, B, C and D (Fig. 3.1). Although each of the four sample locations came from the same vicinity, the exact distance between each of the four locations is variable across the different reef types because of differences in exposure of the reef at each section. The location and characteristics of the reef face sampled for each reef type are given in Table 3.1. Three of these locations (A, B and C) represented samples used to make polished blocks for petrographic studies and the last location (D) represented the location where samples for batch flotation experiments were collected (Fig. 3.1). The preparation and processing of samples from location D are discussed further in Section 3.1.2. For each reef type, petrographic samples were taken from three locations (A, B and C) to assess potential compositional and textural heterogeneities in each reef type. For each of these location, samples were taken from three different stratigraphic positions corresponding to the upper contact (samples labeled 1, 4, 7), middle zone (samples labeled 2, 5, 8) and the bottom contact (samples labeled 3, 6, 9) of the UG2 main seam (Fig. 3.2). A photo and description of each of these samples is given in Appendix A. From each of these stratigraphic positions, each sample was further divided into another three stratigraphic sub-positions (a, b and c) from each of which a section was cut to make a polished block (Fig. 3.2).

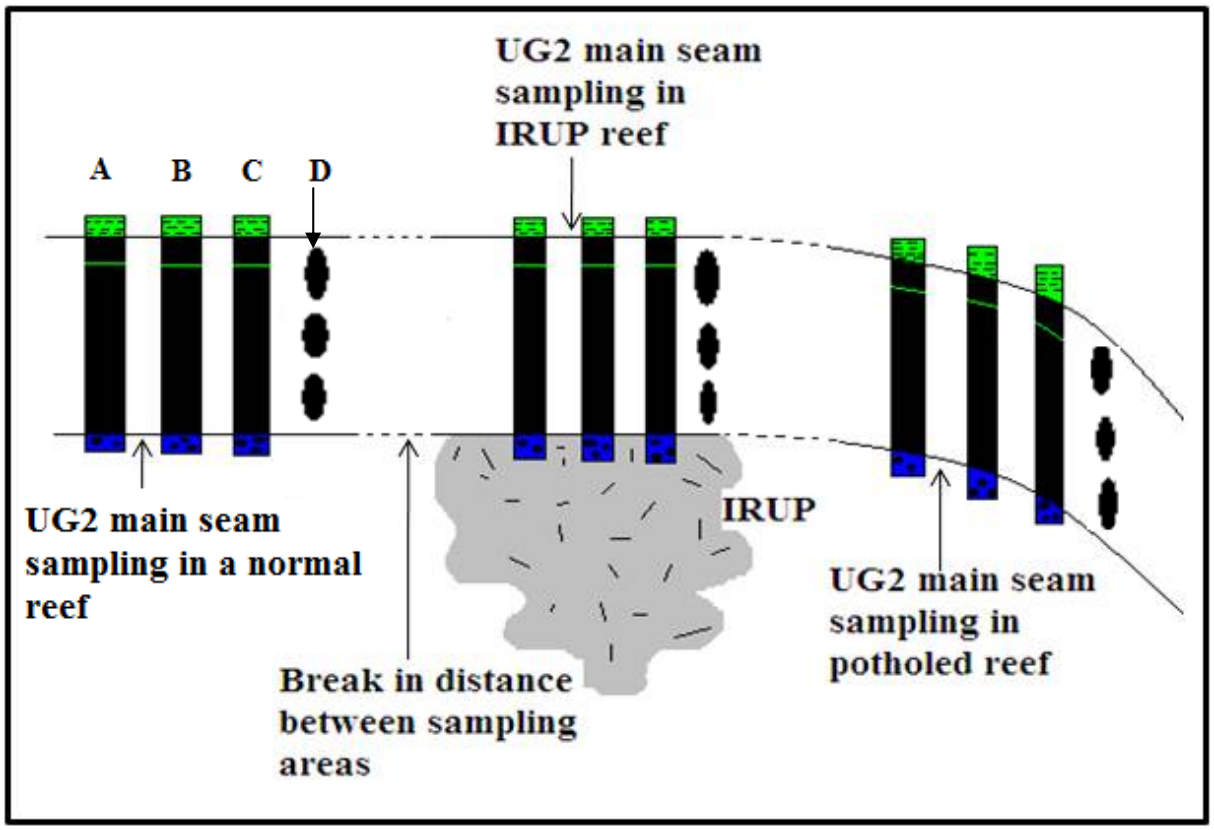

Figure 3.1: *Sampling along the UG2 main seam in the three different reef types studied in this project.*

Therefore, each sampling location (A,B and C) for each reef type had a total of 9 polished blocks made and a total of 27 polished blocks per reef type.

Table 3.1: *Characterisation of sampling areas*

Reef type	Location	Main Seam height	Sample weight	length of the sampling face
UG2 normal reef	3 West, Waterval Central Shaft, Panel 10, BLT 0859	0.7m	13kg	18m
UG2 potholed	West Shaft Capital development (WC-CDS), road way 2, peg. no 3438	0.75m	13kg	3m
UG2 IRUP	West Shaft Capital development (WC-CDS), road way 1, peg no 3462	0.61m	13kg	10m

Sample blocks were cut perpendicular to stratigraphy at the University of Stellenbosch and sent to Anglo Research Laboratories for polishing. Approximately 7 to 10 cm of the footwall and hanging wall was also collected from each reef type. This was done to examine the petrographic characteristics of interstitial chromite immediately above and below the main seam reef. In total 12 thin-sections, four per reef type, two representing the footwall and two the hanging wall were made. These thin-sections were made at the Department of Geological Sciences at the University of Cape Town (UCT).

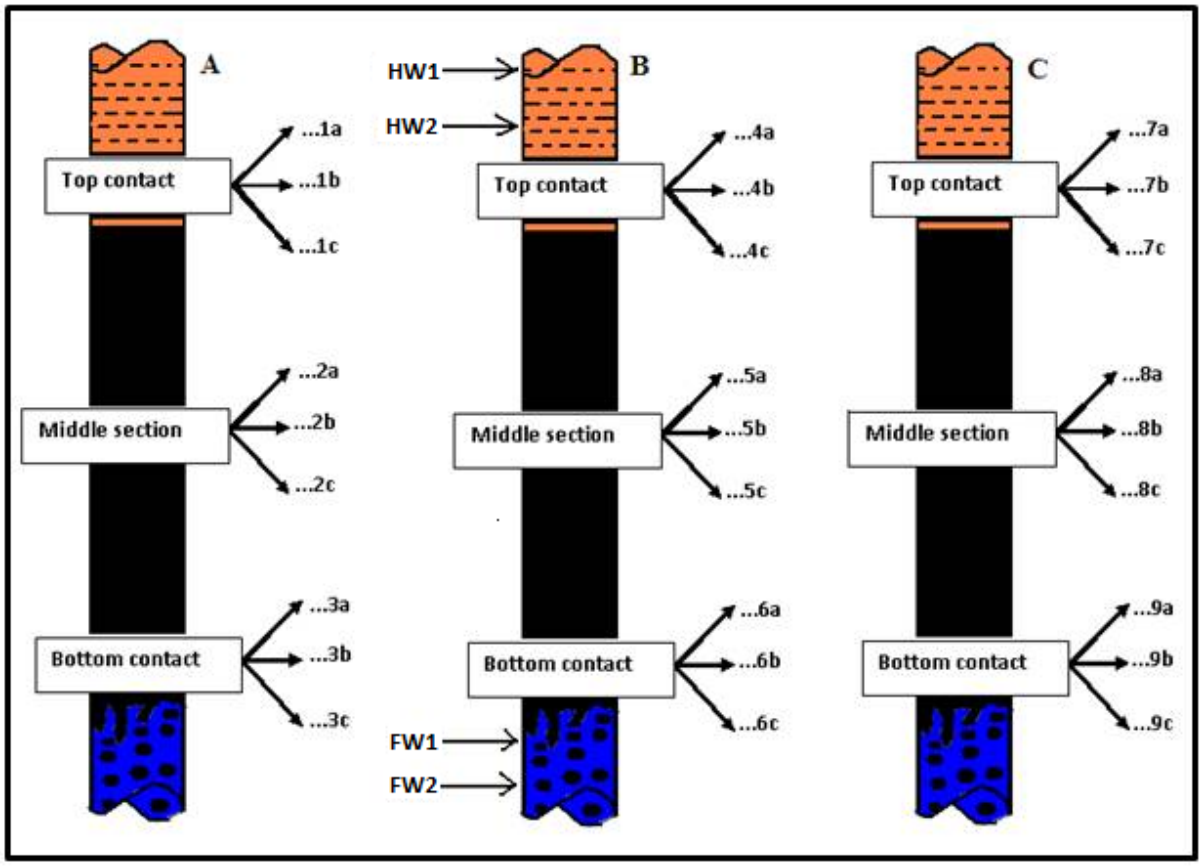

Figure 3.2: *Location and numbering of each polished section prepared for petrographic studies.*

3.1.2 Samples for Batch Flotation Experiments

Approximately 13kg of UG2 main seam material was collected from each of the normal, pothole and IRUP reef types for batch flotation experiments. Note that in the flotation sections these three reef types are referred to as ore types. For each reef type this material came from location D (Fig. 3.1) where three samples were taken, corresponding to the top, middle and bottom of the UG2 main seam. No hanging wall or footwall material was

collected with these samples. For each reef type, the position of the D location was chosen on the basis of representativeness of the UG2 main seam for that reef type. Each reef type was crushed using a stainless steel jaw crusher in the Geology Department at the University of Cape Town. The crushed ore was screened at 4000µm and the three samples of each reef type were mixed to ensure sample homogeneity. The homogeneity was realised using three buckets of 10 to 15l each in which the crushed ore was alternatively transfered for over 12 times. The screened and mixed ore was then split using a rotary splitter into ten 1.3 kg bags. Four of these bags were used for the establishment of milling curves for each ore type and the other six for batch flotation experiments.

3.2 Ore Characterisation

In this section the different techniques used to investigate the UG2 samples collected for this project are described.

3.2.1 Microscopy

The thin sections and polished blocks were studied using a Leitz Laborlux 12 Pol microscope, connected to a Nikon Coolpix 4500 camera for textural identification and photography.

3.2.2 Scanning Electron Microscopy (SEM)

The major element composition of chromite (Appendix B) was determined using a LEO Scanning Electron Microscope (SEM) connected to an Oxford Instrument Energy Dispersive Spectrometer (EDS) housed in the Central Analytical Facility at Stellenbosch University. Prior to analysis, the surfaces of the thin sections and polished blocks studied were coated with a 15µm layer of carbon. The working distance was 13mm, with an accelerating voltage of 20 kV, a 4.00 nA beam current and an acquisition time of 50s. Raw data were processed with the online INCA programs using Astimex standards presented in Table 3.2. Based on the pre-set analytical conditions, a range of analysis results between 97 and 101 weight % total was considered to represent an acceptable analysis. Fe was the only element with dual valency and Fe^{3+} and Fe^{2+} were recalculated assuming ideal spinel stoichiometry based on 32 oxygens following the method of Droop (1987). The error margin of the SEM stoichiometry was 0.05 cation units.

Table 3.2: *SEM standards for this project*

Standards	Chromite	Ilmenite	Pyrope Garnet	Rhodonite	Biotite	Magnetite	Albite	Olivine
Elements	Cr	Ti	Al, Mg	Mn	K	Fe	Si, Ca, Na	Ni

3.2.3 Quantitative X-Ray Diffraction

Prior to X-Ray Diffraction (XRD) analysis, a feed sample of each ore type was representatively split using a rotary micro riffler to obtain 3.5g. Each 3.5g feed was pulverised for 10 min using a Micronising Mill. This was done to minimise particle size effects during QXRD analysis. The micronised ores were sent to the University of Pretoria for XRD analysis using a Panalytical X'Pert Pro Multi Purpose Diffractometer (X'Pert Pro MPD). The instrument used an automatic divergent slit with cobalt K_α radiation. The measurements were done between 3 and 80° 2θ using a 0.001° step size. The quantification of mineralogical phases was performed at UCT using the Autoquan Rietveld software. Chemical analyses were calculated from the XRD analysis in order to validate them against the actual chemical analysis of the feed samples. Good correlation was obtained between the actual and calculated chemical assays for the major elements (Al, Cr, Mg, Ca, Si and Fe) for all three reef types (Fig. 3.3).

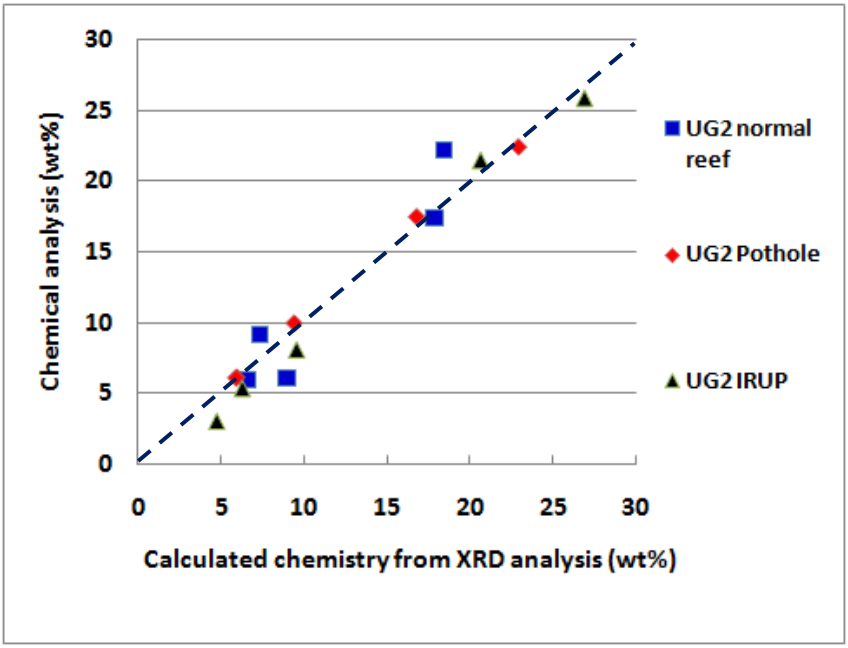

Figure 3.3: *Correlation between calculated chemistry from XRD analysis and the actual chemical assay using major elements Cr, Si, Al, Fe and Mg from the three reef types. The dark blue dashed line represents a 1:1 compositional relationship of points.*

3.2.4 Mineral Liberation Analysis (MLA)

Subsequent to batch flotation experiments, selected flotation concentrates samples were chosen for analysis using MLA. A total of 6 samples per reef type was selected and wet screened to obtain one fraction size (38-75µm) to ensure that only particles recovered by flotation and not entrainment were examined. The obtained samples were sent to the University of Johannesburg for MLA analysis. Prior to analysis, samples were mounted into 30 mm diameter grain mounts that were then carbon coated. Samples were analysed on a FEI Field Emission Quanta 600F MLA with a detection limit of 100 pixels on a 400x magnification which calculates out as a 15 micron-sized particle. The analyses were done using a 6.6 µm beam spot size, with a 25 kV acceleration voltage, a 206 µA emission current, and a Cu standard grey level of 134. In addition, for each grey level region identified, a minimum of 2200 counts per second (CPS) were required for determination of the phase. Samples were analysed using Extended Back Scattered Electron liberation analysis with automated standards collection (XBSE_STD) for mineralogical phase determination in different ores based on their grey level. In addition a grain-based X-ray mapping procedure (GXMAP) was done on chromite. The number of particles analysed is given in Table 3.3.

Table 3.3: *Particle count for different ore types*

	Normal Reef	**Pothole Reef**	**IRUP Reef**
Total Particles	101462	175083	84485
Total Chromite	4399	5608	24429
% chromite	4.34	3.20	28.92

3.3 Flotation Experiments

3.3.1 Flotation Apparatus

Batch flotation experiments were conducted using a 3L modified Leeds flotation cell in the mineral processing laboratory at the University of Cape Town (UCT) (Fig. 3.4).

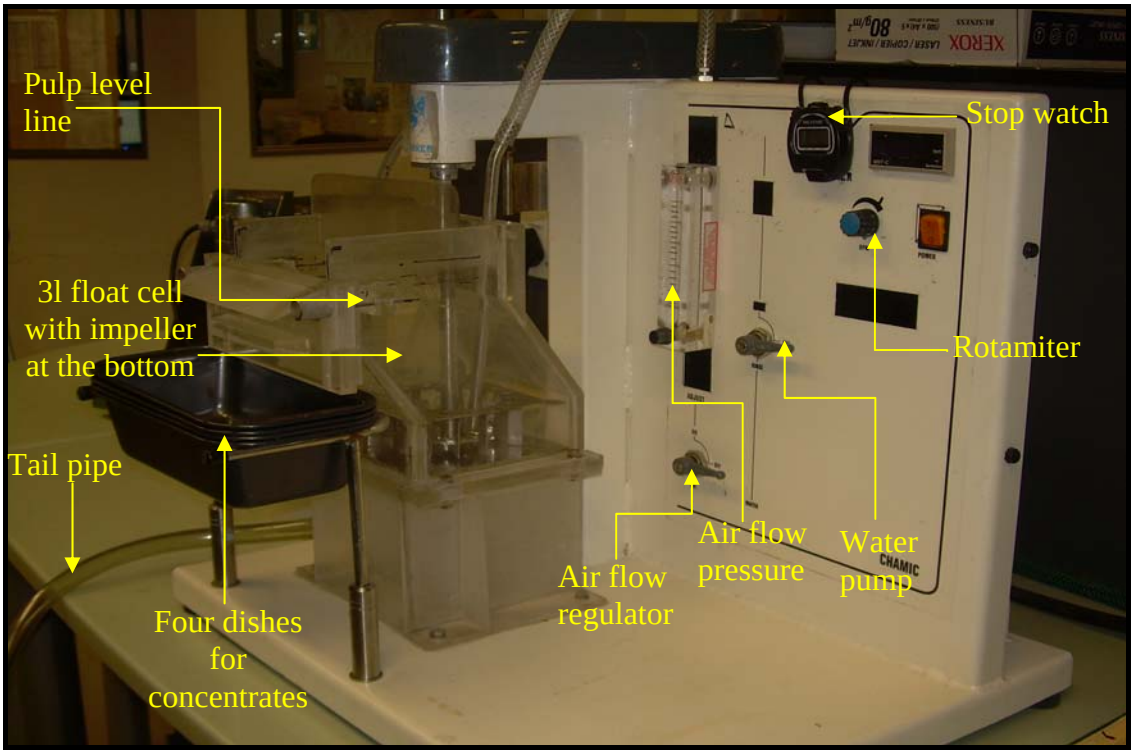

Figure 3.4: *3L flotation apparatus separating particles base on their surface properties. The pulp is introduced from the top of the float cell and the bubble stream controlled by the impeller at the bottom of the float cell.*

3.3.2. Milling

For the flotation experiments in this project, the milled ore going into the flotation cell was milled to 60% of material passing 75µm. In order to determine how long each ore type needed to be milled to meet these conditions, milling curves were established for each ore type. This was achieved by first milling 1.3kg of UG2 crushed ore in the presence of a rod mill containing 20 rods of different sizes and 500ml of tap water. The rod mill rotation speed was set at 90 rotations/min. The milling conditions and results are shown in Table 3.4 and Figure 3.5.

Table 3.4*: Milling times and percentage passing conditions of the three ore types*

UG2 Normal Reef		UG2 Affected by a Pothole		UG2 Affected by an IRUP	
Time	**% Passing**	**Time**	**% Passing**	**Time**	**% Passing**
15	32.92	15	39.25	10	58.78
20	40.33	20	47.07	20	89.63
30	54.37	25	57.27	30	98.19
35	62.39	33.3	71.57		-

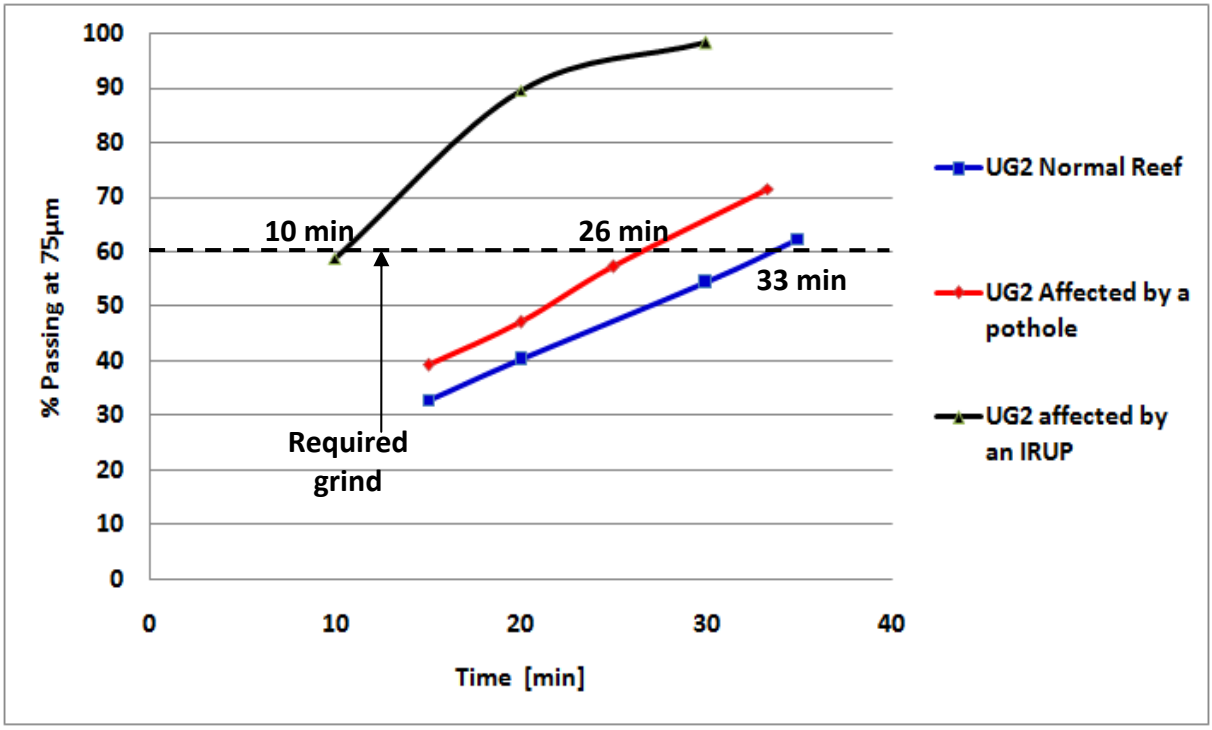

***Figure 3.5**: Milling curves of three ore types.*

3.3.3 Flotation

Six 1.3 kg bags of each ore type were used for batch flotation experiments: The batch flotation was conducted in triplicate for two different conditions. The first condition was with no addition of depressant (three 1.3 kg bags) and the second condition was with depressant added (three 1.3 kg bags). Subsequent to milling the ore, the slurry was transferred to a 3L modified Leeds flotation cell. Synthetic plant water (Table 3.5) was used to make the slurry/pulp up to a volume of 3 litres.

***Table 3.5:** Ions present in synthetic water (Wiese et al., 2005).*

Ions	Ca^{2+}	Mg^{2+}	Na^{+}	Cl^{-}	SO_4^{2-}	NO_3^{-}	NO_2^{-}	CO_3^{2-}	TDS
Synthetic water	80	70	153	287	240	176	-	17	1023

The pulp level was manually controlled by addition of synthetic plant water. The impeller speed was set at 1200 rpm. The air supply used to create a bubble stream in the flotation cell was maintained at a flow rate of 7 L/min in all tests and the froth height was kept constant at 3 cm throughout. Times for key steps in the two sets of experiments are shown

in Tables 3.6 and 3.7. Four concentrates (C1, C2, C3, and C4) were obtained by scraping the froth into four dishes at four different time intervals (see Tables 3.6 and 3.7). In each time interval, the froth was scraped every 15 seconds.

Table 3.6: *Conditions with no depressant*

Operation	Reagent	Characteristic	Quantity	Addition point	Time (min)
Conditioning	SIBX	Collector	100g/t	Float cell	0
	DOW200	Frother	40g/t	Float cell	2
Air flow	-	-	7l/min	-	3
Flotation	C1	-	-	-	5
	C2	-	-	-	7
	C3	-	-	-	13
	C4	-	-	-	21

Table 3.7: *Conditions with depressant*

Operation	Reagent	Characteristic	Quantity	Addition point	Time (mn)
Conditioning	SIBX	Collector	100g/t	Float cell	0
	Stypress 504	Depressant	400g/t	Float cell	2
	DOW200	Frother	40g/t	Float cell	4
Air flow	-	-	7l/min	-	5
Flotation	C1	-	-	-	7
	C2	-	-	-	11
	C3	-	-	-	17
	C4	-	-	-	25

Prior to each batch flotation experiment, a feed was taken for mineralogical phase characterisation of the pulp using the X-ray diffraction analyses, at the end of each test two tails (T2 and T3) were directly taken from the pulp for analysis of initial and final conditions. T1, not discussed here, is the remaining pulp after completion of the experiment, and used only for mass balancing. Water recoveries were measured for each test. Feeds, concentrates and tails were filtered, dried and individually weighed in preparation for subsequent analysis.

3.3.4 Chemical Analysis

Subsequent to the batch flotation experiments, the obtained concentrates of each batch flotation experiment were individually weighed and screened at +38μm. The lack of sufficient mass from the screened materials for chemical analysis required the combination of individual concentrates C1, C2, C3 and C4 from the two experimental conditions, feeds from one of the experimental conditions (since the feeds of both experimental conditions are identical), and tails T2 and T3 to obtain single samples of C1, C2, C3, C4, feed, T2 and T3 for each ore type for each experimental condition. The combined samples were then split to obtain the 1g samples that were bused for analysis. This combining of samples prior to geochemical analysis, has a positive effect on the analyses in the sense that analyzing the average concentrate will only reduce the influence of experimental errors. The combination of the triplicate materials for each experimental condition took into account ore properties such as host rock, ore mineralization, ore texture, degree of alteration, hardness, grade and recovery performance (Fragomeni *et al.*, 2006). In addition, a comparative analysis done as part of this study on the reproducibility of individual triplicates done at 95% confidence showed very little variation, allowing for the confident mixing of the triplicates. All samples were analysed for Al, Fe, Cr, Mg, Mn, Si, Ca, Co, Cu, Ti, Ni, V, Pb and Zn using ICP-OES (Appendix D). Analyses were conducted by International Genalysis Laboratory Services in Australia. The experimental conditions of the geochemical analyses are summarized in Table 3.8.

ELEMENTS	Al	Ca	Co	Cr	Cu	Fe	Mg	Mn	Ni	Pb	Si	Ti	V	Zn
Units	%	%	ppm	ppm	ppm	%	%	ppm	ppm	ppm	%	%	ppm	ppm
Detection	0.02	0.2	20	50	20	0.01	0.01	20	20	50	0.1	0.01	50	20
Method	D/OES	D/OES	D/OES	D/OES	D/OES	D/OES	D/OES	D/OES	D/OES	D/OES	D/OES	D/OES	D/OES	D/OES
Checks														
Normal reef C1 blank float	7.52	3.5	395	99082	5323	11.09	7.03	1044	12945	X	13.7	0.35	673	302
Pothole T3 float	8.7	1.6	218	219036	63	17.28	5.87	1566	1223	X	5.6	0.39	1587	630
IRUP T3 float + Sty 504	7.75	0.9	247	249043	X	20.72	5.06	1807	1282	X	2.7	0.68	1755	846
Standards														
MPL-2	4.37	0.8	234	1335	1926	2.48	0.82	1758	1808	1981	33.7	0.02	161	1327
SARM5	2.11	2	104	24059	X	8.81	15.04	1634	575	X	24.5	0.11	266	124
AMIS0010	7.19	2.1	1040	151650	755	14.39	7.41	5214	1151	X	11.1	0.36	1091	437
SARM7.2	7.89	1.4	217	204856	366	17.42	6.71	1507	1728	X	6.6	0.41	1408	562
BLANKS														
Control Blank	X	X	X	X	X	0.03	X	X	X	X	X	X	X	X
Control Blank	X	X	X	74	X	0.01	X	X	X	X	X	X	X	33
Acid Blank	X	X	X	X	X	X	X	X	X	X	X	X	X	X

Table 3.8: *Conditions of chemical analyses using inductively Coupled Plasma – Optical Emission Spectrometry techniques*

3.4 Floatable Gangue Calculation

From the chemical assay results, Al, Cr, Mg, Ca, Si and Fe were chosen based on their abundances in the crystal lattice of the main mineral phases in this project, to represent the behavior of those minerals. Cr and Fe were used as a proxy for chromite, Si, Al and Ca as a proxy for plagioclase and Si, Fe and Mg as a proxy for orthopyroxene. Using these proxies, cumulative masses and cumulative water recoveries of these elements in each concentrate were used to plot mass versus water recovery graphs for each element. Details of these calculations are given in Appendix E. An example of a mass versus water graph is given in Figure 3.6, the actual six graphs plotting mass versus water recovery are given in chapter 5. From this graph it can be observed that recovered masses in the experiment with no depressant addition are characterised by straight lines. This is indicative of the recovery process taking place through entrainment (Neethling and Cilliers, 2002; Engelbrecht and Woodburn, 1975). Gradients of straight lines characterising the relationship between mass and water recovery in the experiment with the addition of the depressant were used to infer the amount of entrained gangue. This was done by multiplying the slope of each ore by its corresponding water recovery. As defined by Wiese (2009), the total mass represents the mass of material recovered in the experiment with no depressant addition and in which all the potentially floatable material was recovered. The total mass therefore contains valuable minerals, floatable gangue and entrained gangue. The assumption that the mass of valuable minerals (PGMs) is negligible is justified because of the low grade associated with platinum mining. Therefore, the total mass recovered is composed almost entirely of floatable gangue and entrained gangue. The mass of floatable gangue is obtained by subtracting the calculated entrained gangue from the total mass (floatable gangue) obtained in the experiment with no depressant addition (Wiese, 2009).

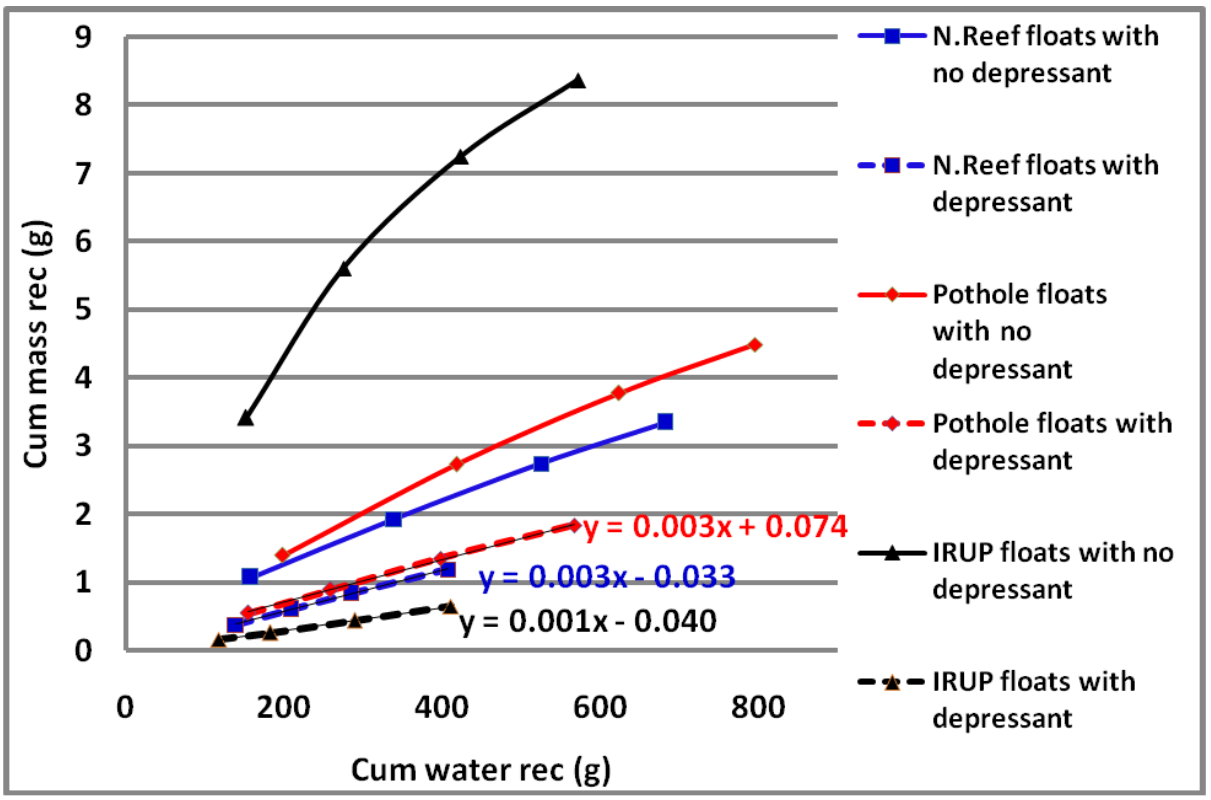

Figure 3.6: *Example of graphs showing the calculation of truly floatable material based on the slope of experiments with depressant addition.*

CHAPTER 4: PETROGRAPHIC STUDIES

4.1 Overview

This chapter examines and compares textural and compositional characteristics of chromite from three environments of the UG2 main seam (UG2 normal reef, UG2 reef affected by pothole formation and UG2 reef affected by IRUP intrusion). The textural investigation primarily examines hand specimens of the different reef types, and subsequently presents the petrographic study of those samples. For each reef type an overview of the stratigraphic section where the samples were taken is provided followed, by detailed petrographic information on the hanging wall, main seam and footwall for each reef type. This information is followed by compositional data for chromites from each main seam environment and the spatial variation in chromite composition determined.

4.2 Textural Studies

4.2.1 UG2 Normal Reef

The hanging wall to the UG2 main seam in the normal reef is a feldspathic pyroxenite also called melanorite. It is a fine-grained, equigranular rock comprising cumulate orthopyroxene that is dominant over plagioclase which represents the most important interstitial phase. In this hanging wall, chromite is virtually absent outside the contact zone with the sharp and linear top margin of the UG2 main seam (Fig. 4.1A).

The UG2 main seam underneath the feldspathic pyroxenite hanging wall comprises two chromite seams that are separated by the UG2 Main Seam Parting (UG2MSP) that has an average width of 3cm (Fig. 4.1A). While the UG2MSP shows similar characteristics to the feldspathic pyroxenite hanging wall, the two chromitite horizons of the UG2 main seam exhibit similar mineralogies and textures to one another, and will therefore be discussed as

one unit. These two chromitite seams are composed dominantly of fine-grained chromite and have an equigranular texture with a friable aspect. Chromite grains in some areas tend to cluster together to form agglomerates of coarser grains giving the rock a darker colour due to the reduced amount of interspersed orthopyroxene and plagioclase. The proportion of these clustered grains represents only a small fraction (approximately 3%) compared to the dominant fine-grained chromite (Fig. 4.1B)

The footwall underlying the main seam in the UG2 normal reef is a medium- to coarse-grained pegmatoidal feldspathic pyroxenite. This footwall is mainly composed of orthopyroxene and plagioclase. Chromite is almost absent in the footwall with the exception of a few grains trapped between plagioclase and orthopyroxene. The contact of this pegmatoidal feldspathic pyroxenite footwall with the overlying UG2 main seam is a sharp and sinuous contact (Fig. 4.1C). Hand samples of this reef type rarely show alteration effects.

4.2.1.1 Hanging Wall

The feldspathic pyroxenite hanging wall is defined by a granular texture and dominated by silicate minerals, principally cumulate orthopyroxene (80 modal %). The shape of orthopyroxene grains is mostly subhedral and their grain sizes vary from ~ 0.4 mm to approximately 2.5 mm (Fig 4.2A). Plagioclase represents the main intercumulate phase making up approximately ~17% of the modal mineralogy (Fig. 4.2B). Chlorite, which is present in minor amounts, develops mostly as a fine-grained alteration product of orthopyroxene (Fig. 4.2C). Clinopyroxene, which is an accessory phase, forms large poikilitic grains that, in some instances, enclose orthopyroxene and chromite. Chromite, which is also an accessory phase, is characterised by grain sizes of less than 0.2 mm in diameter and sub-equant anhedral shapes. It occurs mostly as inclusions in, or at the boundary of, clinopyroxene, orthopyroxene and plagioclase. The distribution of chromite in the feldspathic pyroxenite hanging wall immediately above the UG2 main seam, generally shows a rapid disappearance with increasing distance from the UG2 main seam but can in places cease very abruptly (Fig. 4.2D).

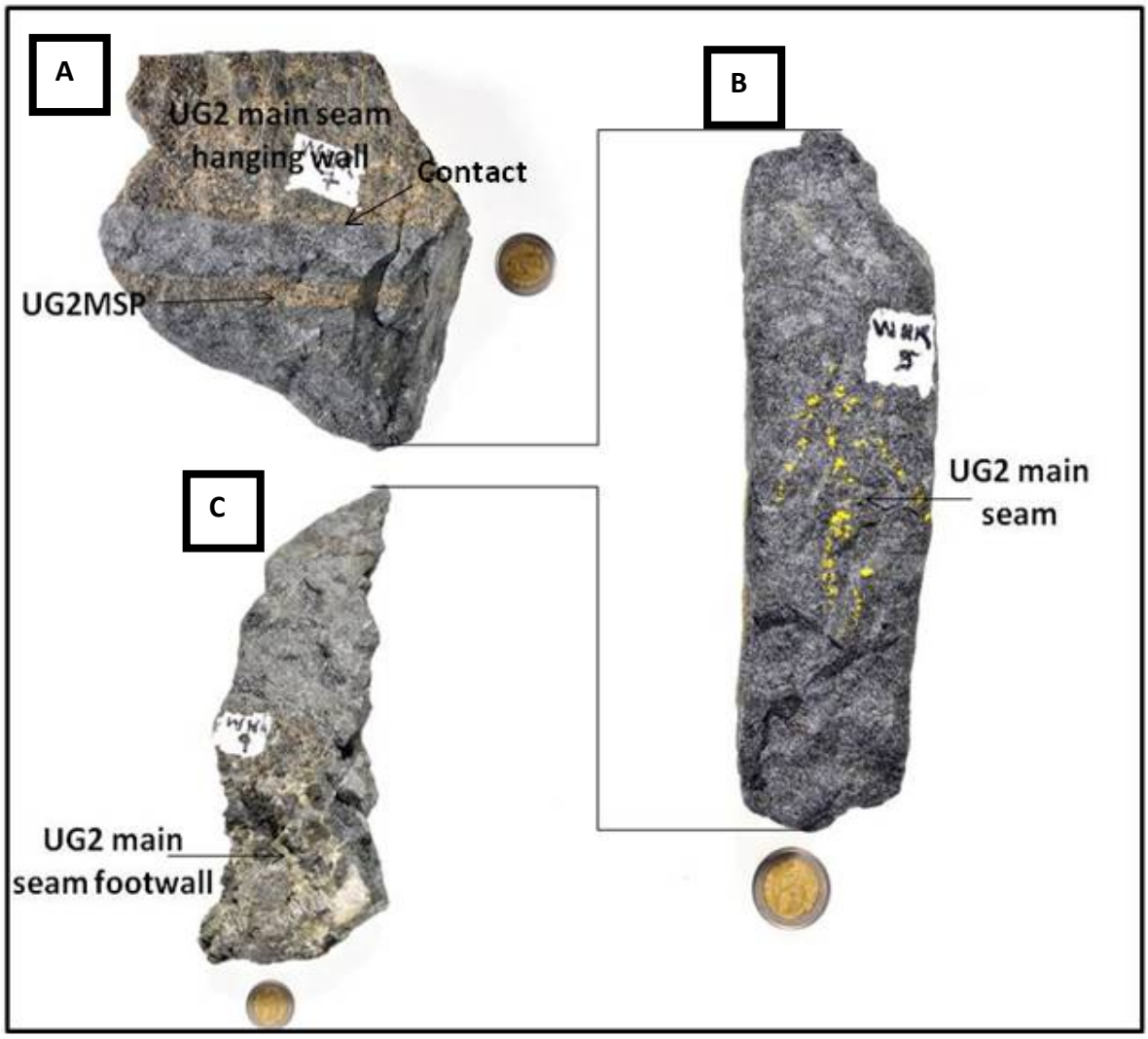

Figure 4.1: *Samples collected from the UG2 main seam normal reef at Waterval Mine. (A) contact between hanging wall and main seam; (B) UG2 main seam; and (C) transition between the bottom part of the UG2 main seam and its footwall. Note the coarse-grained aspect of the footwall. The coin is 2.5 cm in diameter.*

4.2.1.2 The UG2 Main Seam

The principal component of the UG2 main seam is fine-grained chromite, characterised by sub-equant anhedral shapes, that represents approximately 75-80 modal % of the main seam (Fig. 4.3A). Interconnectivity of chromite grains to form irregular networks defining chain-like textures are common (Fig. 4.3B). Locally, chromite grains have clustered together. In these patches their grain sizes have increased (from ~0.2 mm to an average of 0.7 mm) and the grain shapes are polygonal with 120° triple junctions at their boundaries (Fig. 4.3C).

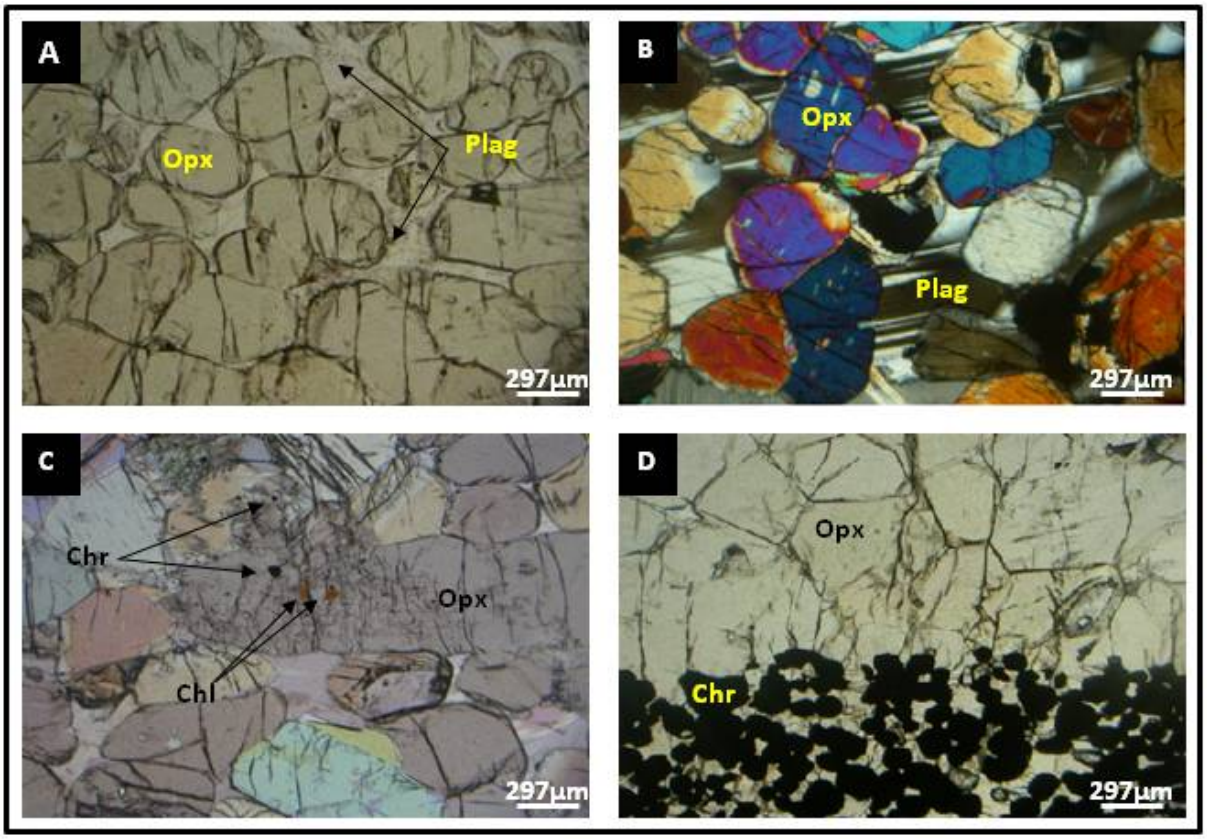

Figure 4.2: *Textures of the UG2 main seam immediate hanging wall. (A) Subhedral orthopyroxene; (B) cumulate orthopyroxene with intercumulate plagioclase; (C) alteration development characterised by the progressive formation of chlorite due to orthopyroxene breakdown; (D) absence of chromite grains beyond the sharp contact between the hanging wall and the main seam. Note the anomalous colour of orthopyroxene resulting from the thickness of the thin section. Plane light (A, C, and D), and crossed polar (B).*

In these coarser patches, lobate shapes are also likely to be found (Fig. 4.3D). In general, the proportion of clustered grains is greater near the contact between the UG2 main seam and the footwall, with finer grain sizes found higher within the main seam. This has resulted in the development of an apparent upward fining sequence. In conjunction with the variation in chromite grain sizes and shapes, are variations in the proportion and distribution of intercumulate orthopyroxene and plagioclase. Generally, orthopyroxene and plagioclase are both intercumulate with respect to the chromite. However, locally, orthopyroxene and plagioclase can both become the dominant mineral phase. In these areas, chromite occurs as small rounded inclusions within the silicate phases (Fig. 4.3E). The patches of clustered coarser chromite are characterised by the presence of plagioclase and orthopyroxene

trapped as inclusions (Fig. 4.3F). Remnants of accessory sulphide minerals, principally chalcopyrite and pyrrhotite are sparsely distributed. Phlogopite is present in trace amounts.

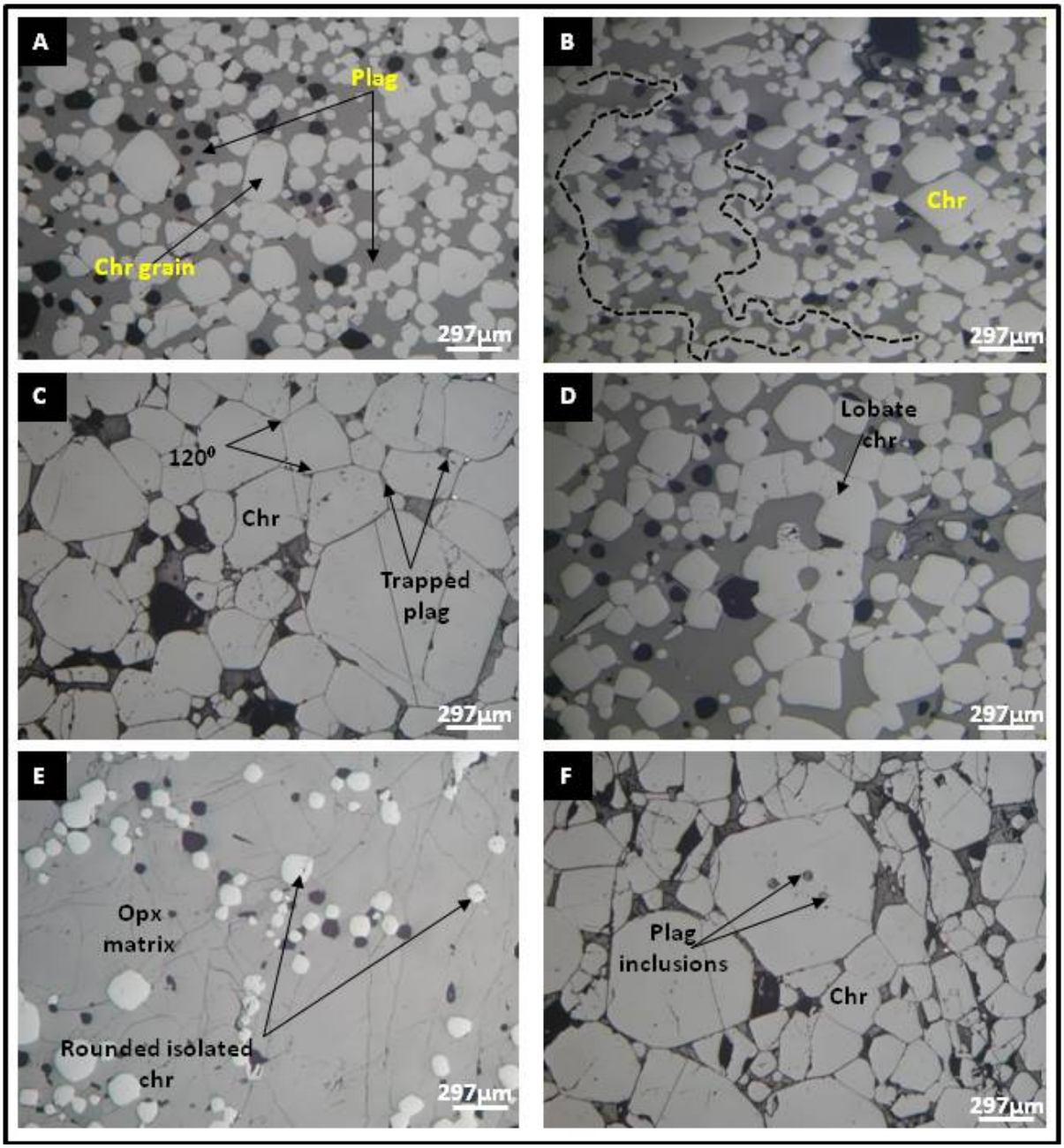

Figure 4.3: *Reflected light photomicrographs of: (A) fine-grained chromite; (B) chain-like texture, the dashed line is a path of grain connection; (C) coarser-grained area formed by aggregated chromite grains. Note the presence of 120^o triple junctions and the polygonal shape grain boundaries; (D) chromite lobate textures; (E) isolated rounded chromite grains present in orthopyroxene; and (F) inclusions of plagioclase in chromite grains.*

4.2.1.3 Pegmatoidal Feldspathic Pyroxenite Footwall

The principal mineralogical phases of the footwall are cumulate orthopyroxene (~75-85 modal %) and intercumulate plagioclase (~10-15 modal %). Orthopyroxene exhibits grain sizes between 1 and 3 cm in diameter and has anhedral to subhedral grain shapes (Fig. 4.4A). Accessory phases randomly distributed in between cumulate phases are principally biotite, chlorite and chromite. Biotite is associated with areas of orthopyroxene alteration (Fig. 4.4B and 4.4C), whereas small grains of chromite occur as inclusions in coarse orthopyroxene and plagioclase (Fig. 4.4D).

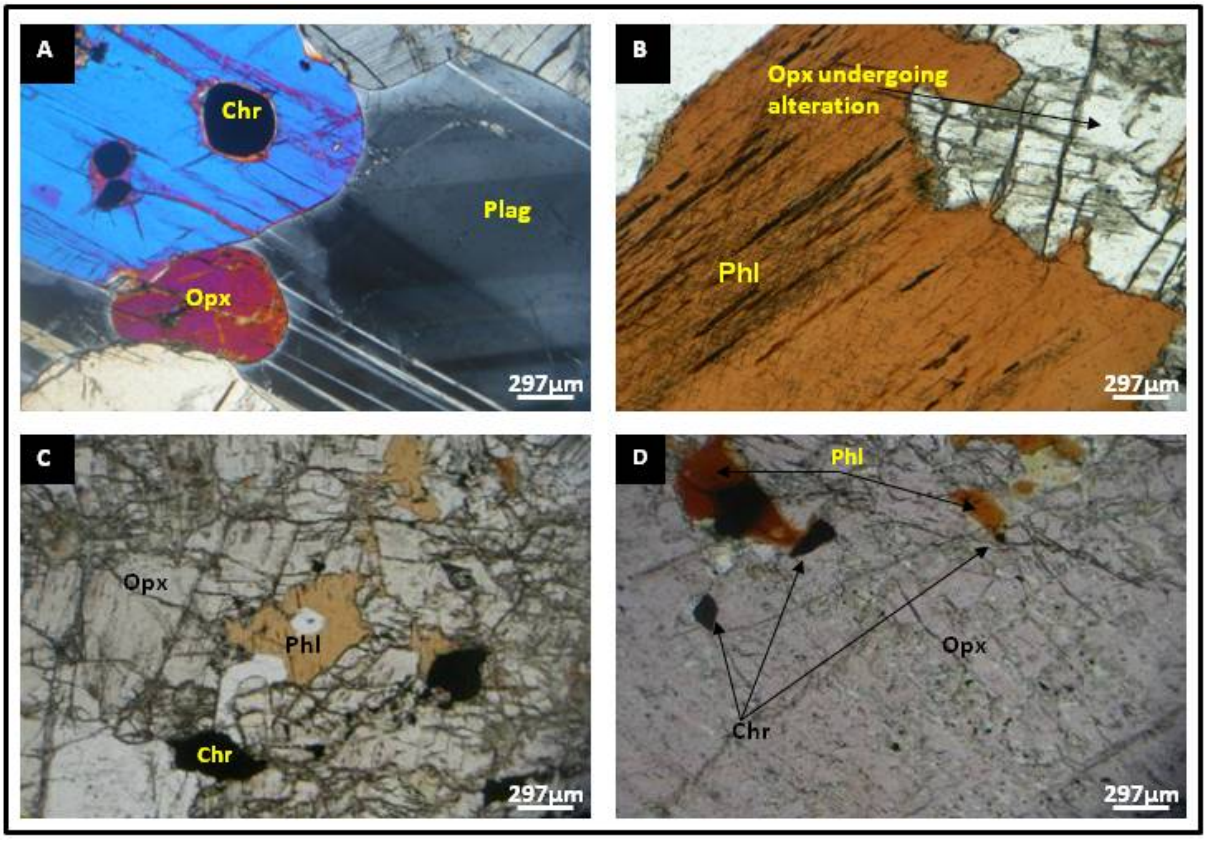

Figure 4.4: *Textural features in the UG2 normal reef footwall. (A) Coarse grained cumulate orthopyroxene and intercumulate plagioclase; (B) Progressive replacement of orthopyroxene by phlogopite, (C) Fine to medium grained irregular chromite grains present as inclusions in orthopyroxene; and (D) phlogopite developing in orthopyroxene with small chromite inclusions in this orthopyroxene. Note the anomalous colour of orthopyroxene due to the thickness of the thin section.*

4.2.2 UG2 Reef Affected by Pothole Formation

The UG2 reef affected by pothole formation in this study is a three component stratigraphic section at the top of which is the UG2 feldspathic pyroxenite hanging wall (Fig. 4.5A). This hanging wall is equigranular with orthopyroxene as its dominant mineral and is separated from the UG2 main seam by a sharp and concave curved contact directed toward the pothole depression.

The UG2 main seam underlies the feldspathic pyroxenite hanging wall and is principally composed of chromite grains that give the hand samples a dark greyish appearance. As described previously, the UG2MSP, with a variable thickness, separates the two parts of the UG2 main seam. The two chromitite seams are mainly composed of chromite with subsidiary plagioclase and orthopyroxene (Fig. 4.5B). The overall texture is generally granular.

The pegmatoidal feldspathic pyroxenite footwall (Fig. 4.5C) is principally composed of orthopyroxene, plagioclase, and accessory chromite. Individual grain sizes of orthopyroxene and plagioclase are variable but may reach 3 cm. The footwall is separated from the UG2 main seam by a sharp but irregular contact.

4.2.2.1 Hanging Wall

The mineralogy of the hanging wall is dominated by fine-grained cumulate orthopyroxene and intercumulate plagioclase. Orthopyroxene, which makes up in excess of 80 modal % of the hanging wall is characterised by subhedral grain shapes that define an overall granular texture (Fig. 4.6A). The size of orthopyroxene grains reaches approximately 1.6 mm. Fine-grained talc and chlorite are present as alteration products of orthopyroxene (Fig. 4.6B and 4.6C). The main intercumulate mineral phase is plagioclase (Fig. 4.6B), but large irregularly shaped grains of clinopyroxene are also present as an intercumulate phase and surround isolated grains of cumulate orthopyroxene (Fig. 4.6D). This association in which intercumulate clinopyroxene has crystallised around cumulate orthopyroxene shows that clinopyroxene post-dates orthopyroxene. Chromite is only present as rare small, disseminated grains with sub-equant anhedral shapes. These chromite grains are mostly found at the boundary of, but also as inclusions in, plagioclase, orthopyroxene and clinopyroxene (Fig. 4.6A and 4.6D).

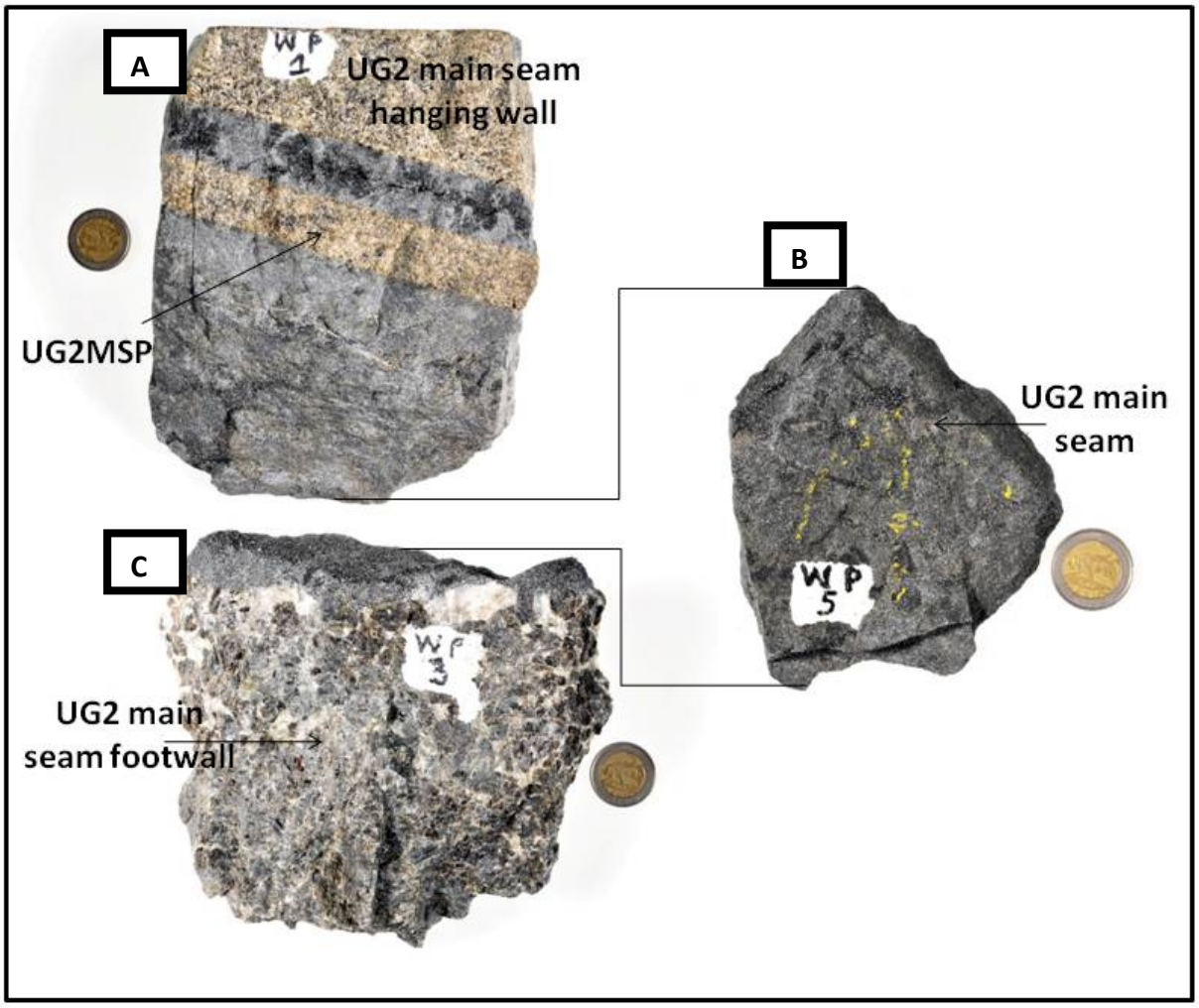

Figure 4.5: *Samples collected from the UG2 main seam affected by pothole formation at Waterval Mine: (A) sample at the transition between the top part of the UG2 main seam and its hanging wall; (B) UG2 main seam; and (C) contact between the footwall and the main seam. Observe the coarse-grained aspect of the footwall. The coin is 2.5 cm.*

4.2.2.2 UG2 Main Seam

The mineralogy of the main seam for this reef type is dominated by fine-grained chromite (~0.2 mm on average) that makes up approximately 75-80 modal % of the reef (Fig. 4.7A). This fine-grained chromite generally exhibits sub-equant anhedral grain shapes but may also display the development of chain textures (Fig. 4.7B). Like the UG2 normal reef main seam, locally chromite grains have clustered together and in these patches the grain size has increased to approximately 0.6 mm (Fig. 4.7C). However, unique to the UG2 potholed reef main seam is the presence of highly irregular chromite grain shapes reminiscent of corroded and embayed structures (Fig. 4.7D).

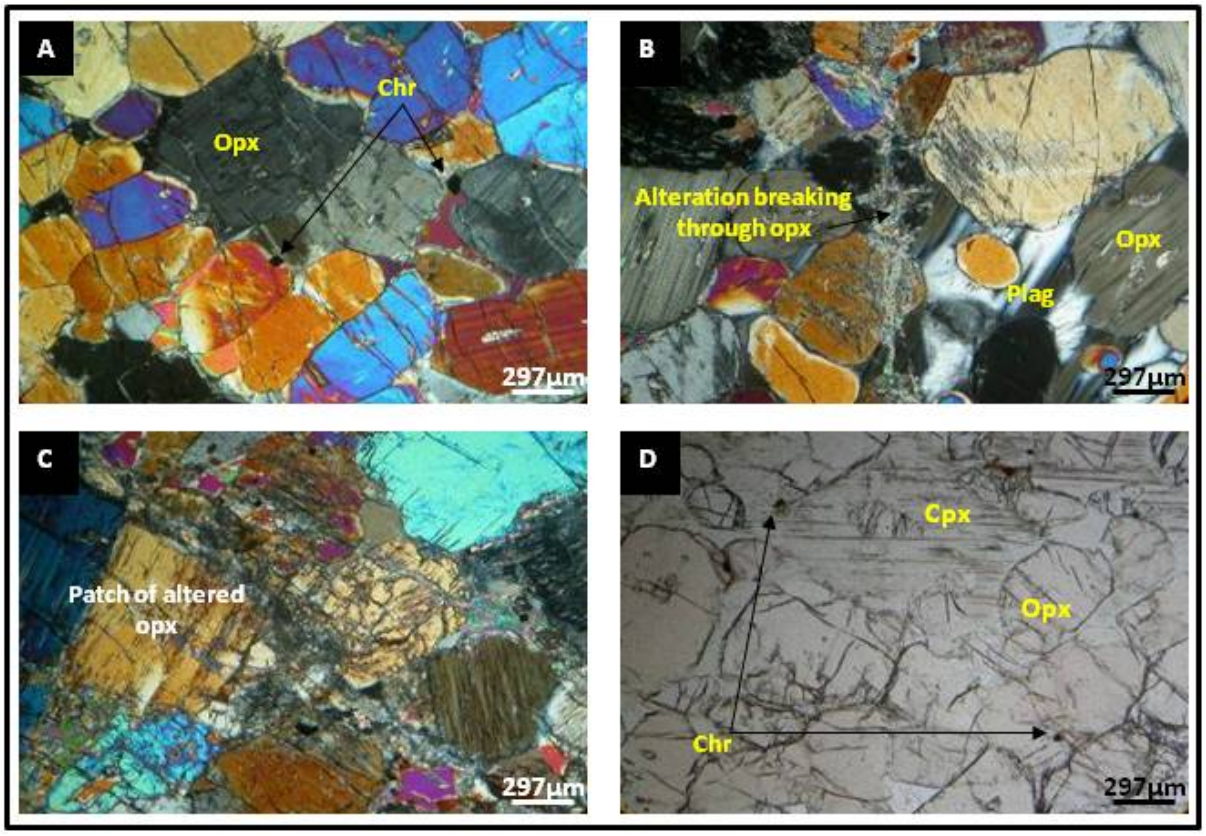

Figure 4.6: *Photomicrographs of textural features in the hanging wall. (A) subhedral cumulate orthopyroxene grains; (B and C) progressive breakdown of orthopyroxene into talc; (D) rare fine-grained chromite in-between orthopyroxene, clinopyroxene and plagioclase. Transmitted light, crossed nicols (A, B and C) and plane polarized light (D). Note that orthopyroxene shows anomalous colours due to the thickness of the thin section.*

These highly irregular chromite shapes have no particular stratigraphic association. The origin of this type of texture remains unclear and is beyond the scope of this project. However, they may be the result of resorption due to late stage magmatic pockets. Plagioclase (15 modal %) and orthopyroxene (10 modal %) represent the intercumulate phases and in some instances are seen as inclusions in coarse chromite grains (Fig. 4.7E). Remnants of accessory sulphide minerals, principally chalcopyrite and pyrrhotite, are randomly distributed (Fig. 4.7F).

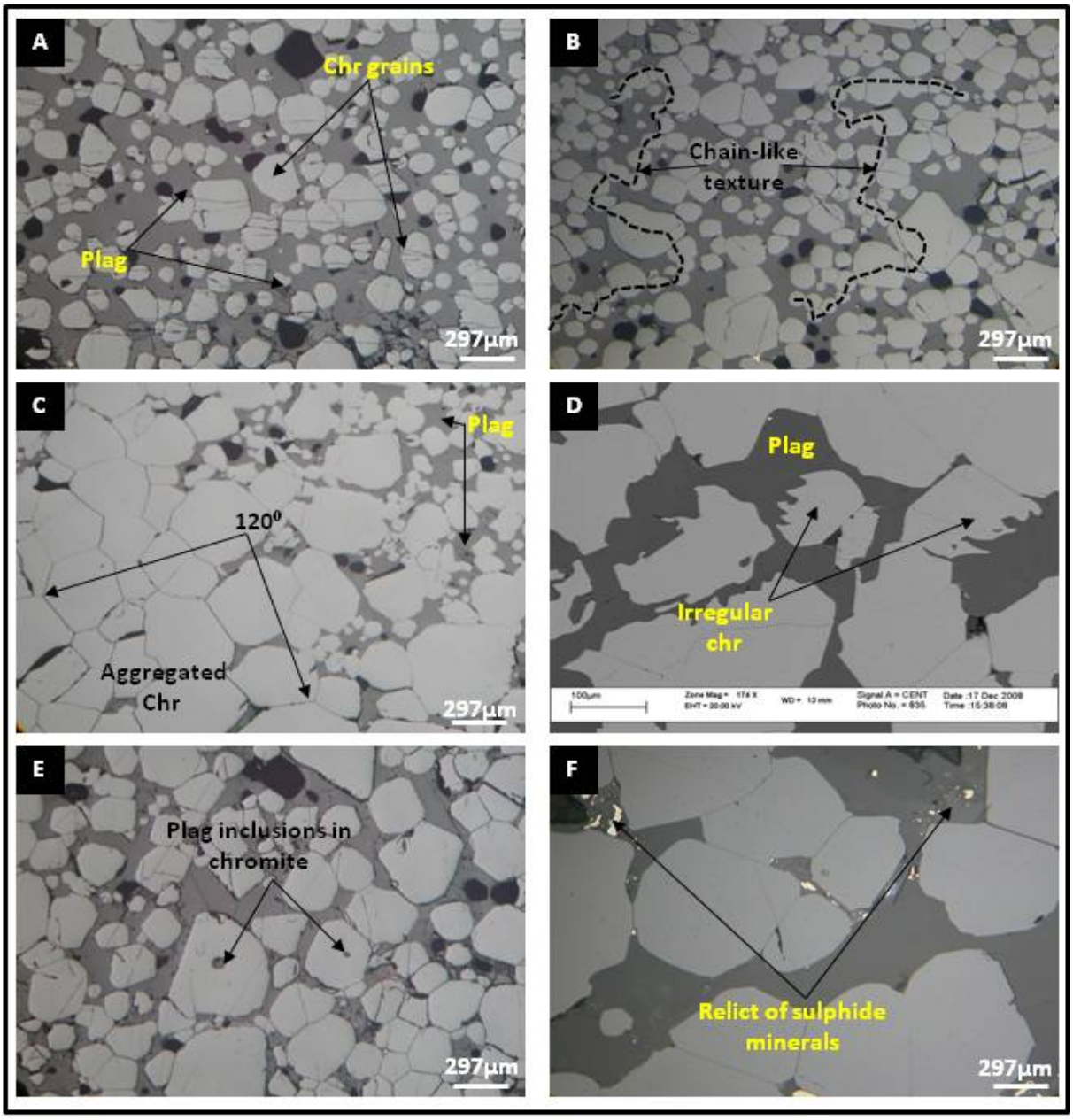

Figure 4.7: *Reflected light photomicrographs of textural features in the UG2 main seam. (A) fine-grained individual chromite grains; (B) chain texture, dashed lines are drawn to show the connection between grains; (C) aggregate of chromite grains characterised by 120^o triple junctions and polygonal shapes; (D) irregularly shaped chromite grains (SEM image); (E) plagioclase inclusions in chromite grains; and (F) remnants of sulphide minerals.*

4.2.2.3 UG2 Pegmatoidal Feldspathic Pyroxenite Footwall

Coarse-grained orthopyroxene (85 modal %) and plagioclase (14 modal %) represent the main mineral phases in the footwall. The size of orthopyroxene and plagioclase reach 3 cm and their shapes are mostly subhedral. Phlogopite, talc and chromite represent accessory phases. Features such as chromite rimmed by plagioclase, both of which are contained in

orthopyroxene are also observed (Fig. 4.8A). Chromite in the footwall is present as inclusions and at the boundaries of orthopyroxene and plagioclase (Fig. 4.8B).

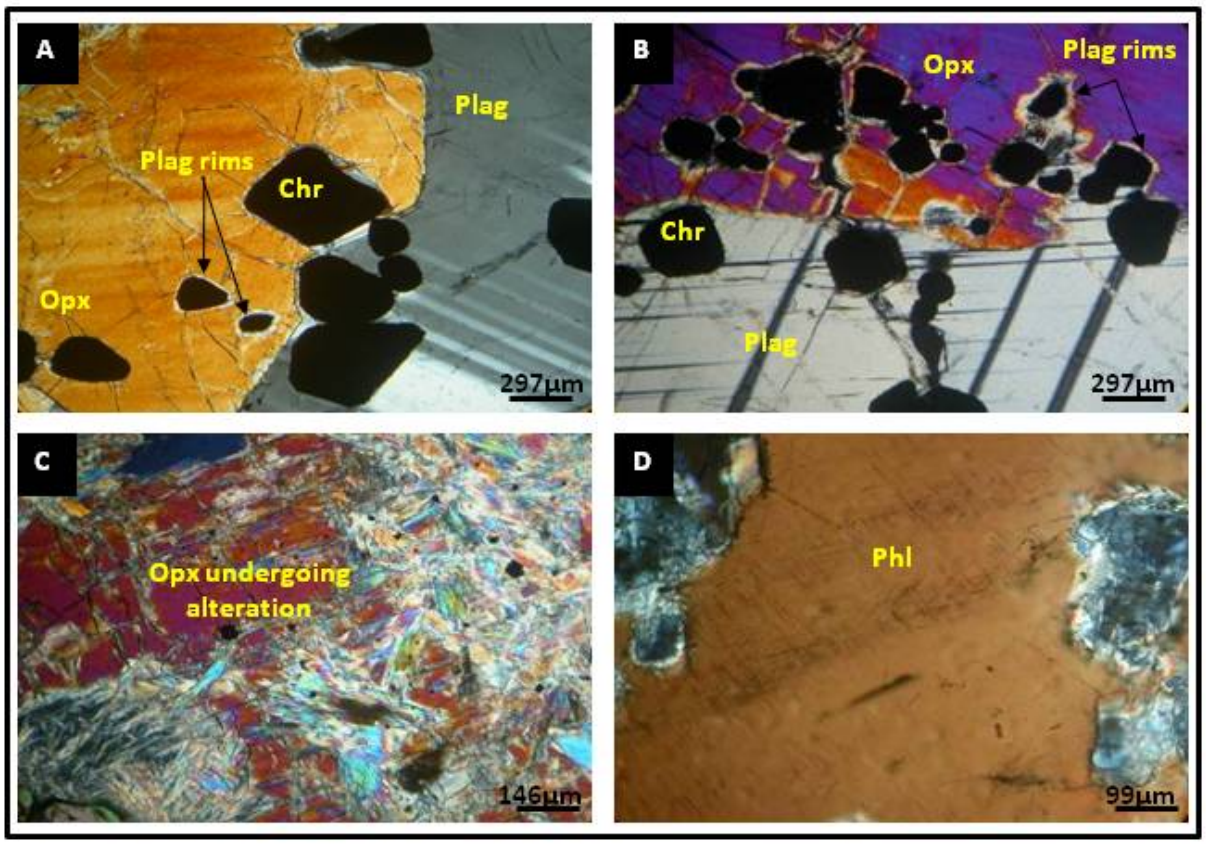

Figure 4.8: *Textures in the UG2 footwall. (A) chromite grains included in orthopyroxene being almost all rimmed by plagioclase; (B) location of chromite grains as inclusions and at the boundary of silicate phases; (C) orthopyroxene breaking down into talc; and (D) accessory phlogopite present in the footwall. Note the anomalous colour of orthopyroxene due to the thickness of the thin section. (Transmitted light, cross nicols).*

Talc has developed within orthopyroxene as an alteration phase and is characterised by randomly-oriented fine, fibrous grains (Fig. 4.8C). Phlogopite is also observed as an alteration product forming due to the progressive breakdown of orthopyroxene (Fig. 4.8D).

4.2.3 UG2 Reef Affected by IRUP Intrusion

The hanging wall of the UG2 affected by IRUP intrusion is a feldspathic pyroxenite rock principally composed of orthopyroxene. Plagioclase is the dominant intercumulate mineral. Alteration of the hanging wall is observed through the change in colour from dark greyish in the normal and pothole reef to light greyish in the IRUP affected reef (Fig. 4.9A).

The UG2 main seam in this reef type is separated from the hanging wall by a sharp and linear contact and from the footwall by an irregular contact along which there is a concentration of phlogopite (Fig. 4.9B). Just above the phlogopite line, the UG2 main seam is composed of two chromite horizons separated by the UG2MSP. The UG2 chromitite horizon below the UG2MSP exhibits coarse-grained chromite that is well developed at the bottom of the UG2 main seam near the contact with the footwall (Fig. 4.9C) and in this zone the main seam has developed magnetic properties. Serpentine alteration characterised by a greenish colour and soapy lustre is unique to this reef type.

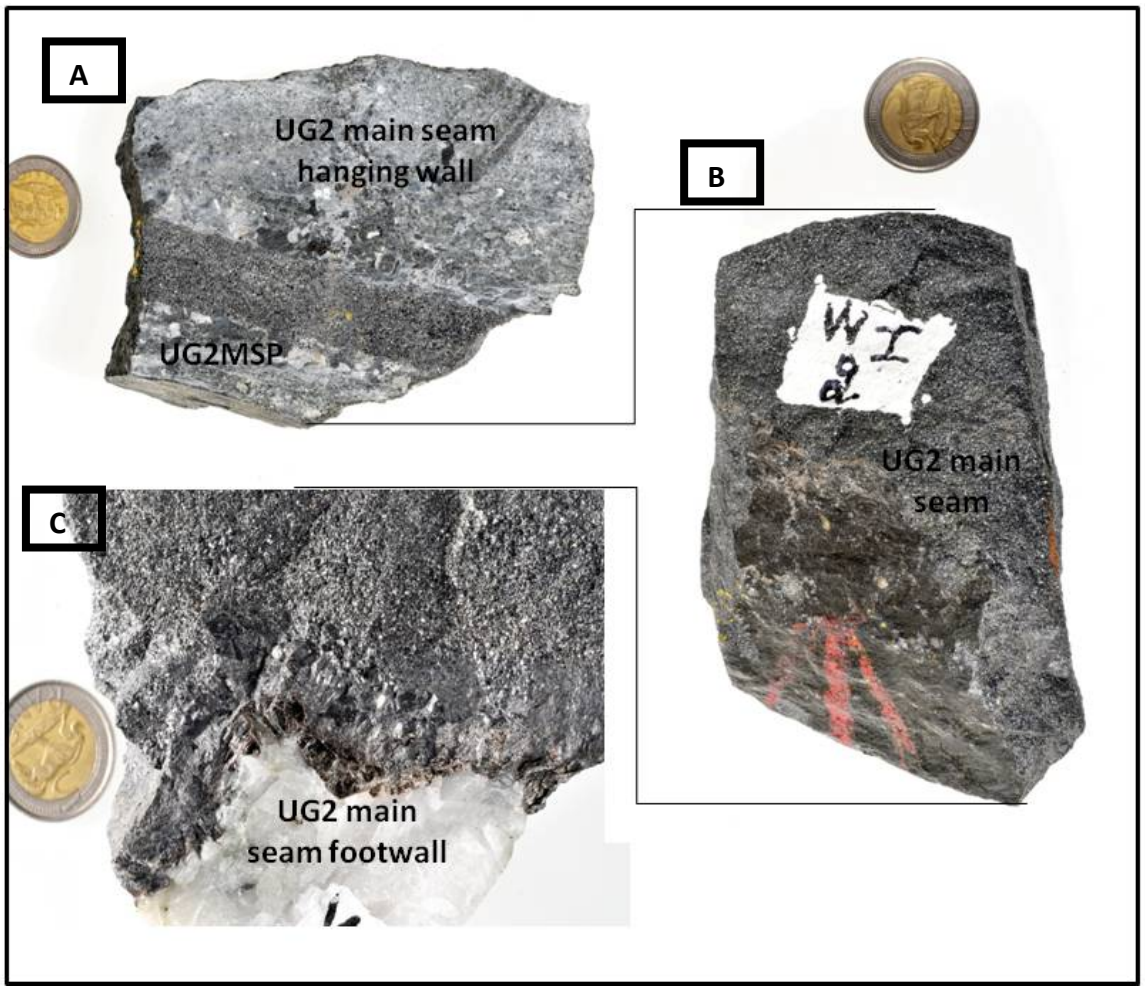

Figure 4.9: *Samples collected from the UG2 main seam affected by IRUP intrusion at Waterval Mine. (A) Transition between the top part of the UG2 main seam and its hanging wall; (B) UG2 main seam; and (C) contact between the footwall and the main seam. The footwall in this environment has a coarse-grained aspect and is characterized by a whitish color. The coin is 2.5 cm in diameter.*

The footwall of this reef type is coarse-grained and consists principally of two minerals, plagioclase and quartz (Fig.4.9C). Chromite occurs as an accessory mineral that is mainly associated with plagioclase and, very seldom, with quartz. Chalcopyrite, pentlandite and pyrrhotite are also accessory and principally localized along sub-vertical fractures. The presence of serpentine is shown by the soapy and greenish colour present on some samples.

4.2.3.1 Hanging Wall

Medium-grained cumulate orthopyroxene (75-85 modal %) is the dominant phase in the hanging wall (Fig. 4.10A) and is variably altered to talc (Fig. 4.10B and 4.10C). The shape of orthopyroxene is mostly subhedral and its grain size can be up to 4.5 mm. Plagioclase represents the most important intercumulate phase and make up approximately 7 modal %.

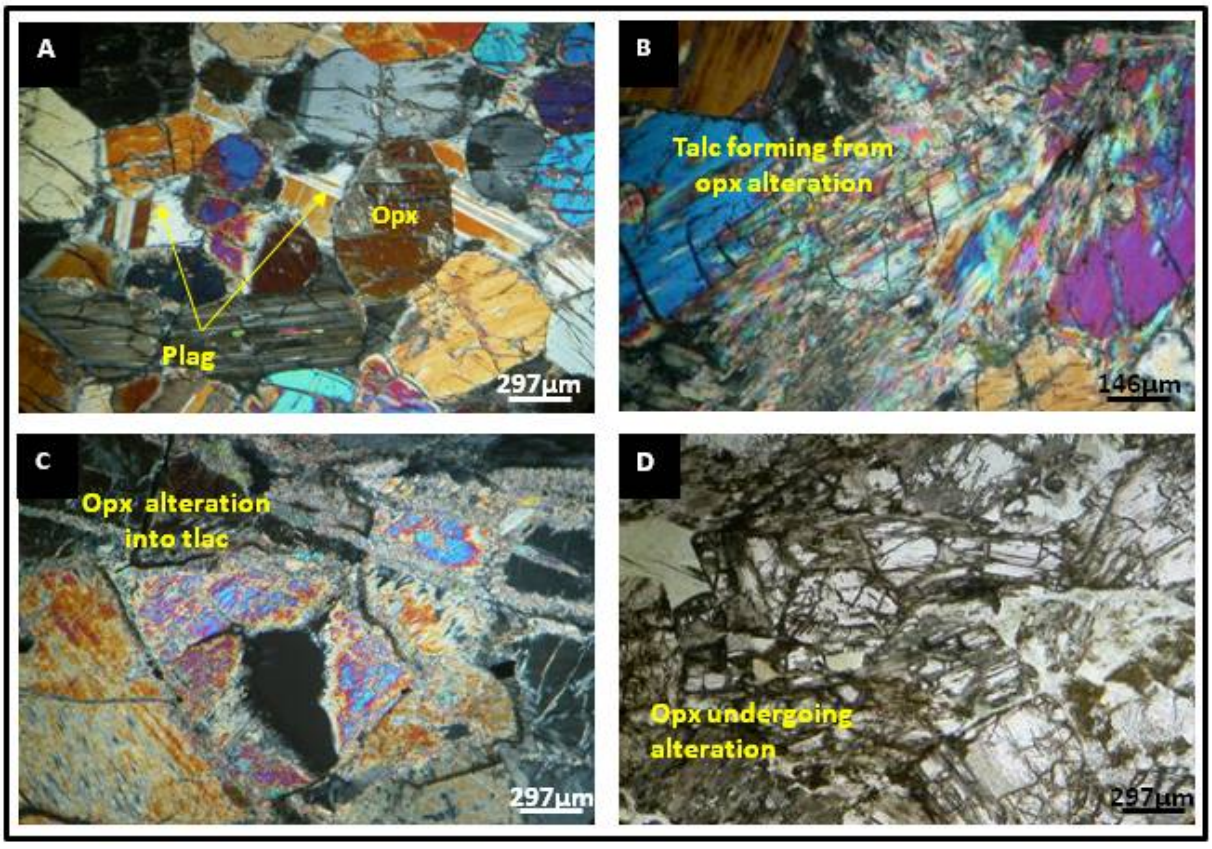

Figure 4.10: *(A) UG2 hanging wall with orthopyroxene as the major component; (B) orthopyroxene alteration (serpentine and talc) observed under cross polars; (C) talc development within orthopyroxene; and (D) development of fine grained talc. The anomalous colour of orthopyroxene is caused by the thickness of the thin section. Plane polarized light (B) and crossed nicols (A, C and D).*

Chromite grains above the contact with the UG2 main seam represent an accessory phase accounting for less than 1 modal % with grain sizes of less than 0.2 mm and sub-equant anhedral shapes. Although generally colourless, the development of talc results in a dirty brown-green colour in thin-section (Fig. 4.10D) and may be associated with serpentine development.

4.2.3.2 UG2 Main Seam

Chromite represents the principal component of this UG2 main seam and makes up in excess of 90 modal %. Orthopyroxene is the dominant intercumulate phase, but generally makes up less than 6 modal % and is mostly altered to talc and serpentine (Fig. 4.11B). Unlike the UG2 main seam for the normal and potholed reef types, the main seam in the IRUP reef type displays a pronounced stratigraphy with respect to both shape and size of chromite grains. A significant difference between this main seam and that of the other two reef types is the almost complete absence of plagioclase in this main seam.

The top part of the UG2 main seam in this reef type is dominated by clustered grains of chromite with grain sizes on average around 0.7 mm in diameter and characterised by smooth boundaries and polygonal grain shapes (Fig. 4.11A). The interstices of these polygonal grains are locally filled with sulphide minerals (chalcopyrite and pyrrhotite) (Fig. 4.11A) as well as orthopyroxene and its alteration products (Fig. 4.11B). Sulphides in this part of the reef are generally coarser (>0.2mm) than sulphides recorded in the main seams from the other two reef types.

The middle section of the UG2 main seam in this reef type is dominated by chromite grains that have diameters averaging 0.5 mm with angular grain shapes and rough boundaries (note that these textures are dissimilar to those observed in the potholed reef type, see Section 4.2.2.2) (Fig. 4.11C). This middle section also exhibits fractured to brecciated, small, and poorly sorted chromite grains localised along fractures where it defines a cataclastic texture (Fig. 4.11D). Fluids circulating along these fractures have driven alteration of the intercumulate orthopyroxene to talc and serpentine.

The base of the main seam overlying the footwall is characterised by a recrystallised horizon. This horizon is only observed in the UG2 main seam bottom (2–3 cm thick) that is separated from the footwall by a thin continuous layer of phlogopite. The recrystallised horizon displays magnetite properties and could therefore be called massive magnetite.

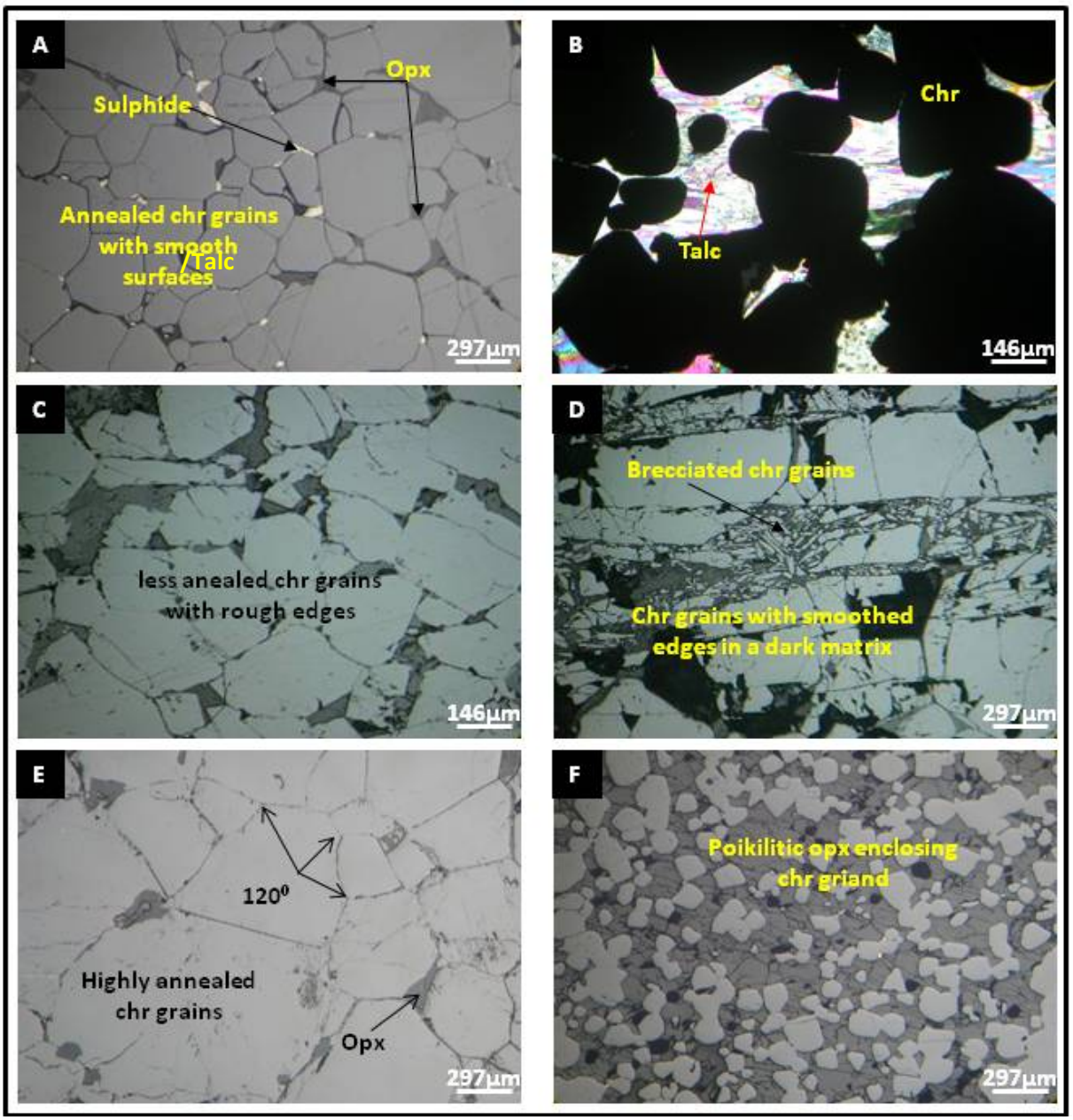

Figure 4.11: *(A) aggregated grains of chromite; (B) talc at the top contact of the UG2 main seam; (C) less aggregated grains with greater interstitial orthopyroxene, note the corrosive effect on chromite grains caused by circulating fluids; (D) fractures containing poorly sorted fine-grained brecciated chromite; (E) medium to coarse polygonal grains of chromite (up to 3 mm) and (F) fine grained chromite enclosed in a poikilitic orthopyroxene. (Reflected light).*

The massive magnetite is composed of coarse-grained recrystallised polygonal chromite and magnetite which sometimes coexist in some locations and can reach 3 to 4 mm in diameter with 120° triple junctions between grains (Fig. 4.11E). The coarse and polygonal aspects of chromite and magnetite are better developed near the contact with the footwall where the absence of intercumulate orthopyroxene and plagioclase is most noticeable. In this area, orthopyroxene is only present as rare inclusions in recrystallised chromite and magnetite (Fig. 4.11E). Immediately above the recrystallised magnetite horizon, chromite grains show a continuous textural variation from massive chromite to disseminated grains where intercumulate orthopyroxene gradually increases in modal % (3 to 5 cm further up in the stratigraphy). This increase in orthopyroxene modal % coincides with the decrease in chromite and magnetite grain sizes (Fig. 4.11F).

4.2.3.3 The UG2 Feldspathic Pyroxenite Footwall

The footwall to the UG2 main seam affected by IRUP intrusion is composed of a highly altered chaotic textural agglomeration of minerals comprising sericite (60 modal %) quartz (20 modal %), tremolite (18 modal %) and calcite (2 modal %). The chaotic relationship of these minerals developed during the intrusion of the IRUP that resulted in the preferential replacement of the orthopyroxene and plagioclase-rich footwall. Orthopyroxene has been altered to serpentine, tremolite and talc, while plagioclase has been altered to sericite (Fig. 4.12A to D). Quartz is probably derived from the felsic IRUP intusions which underlie the footwall in this location.

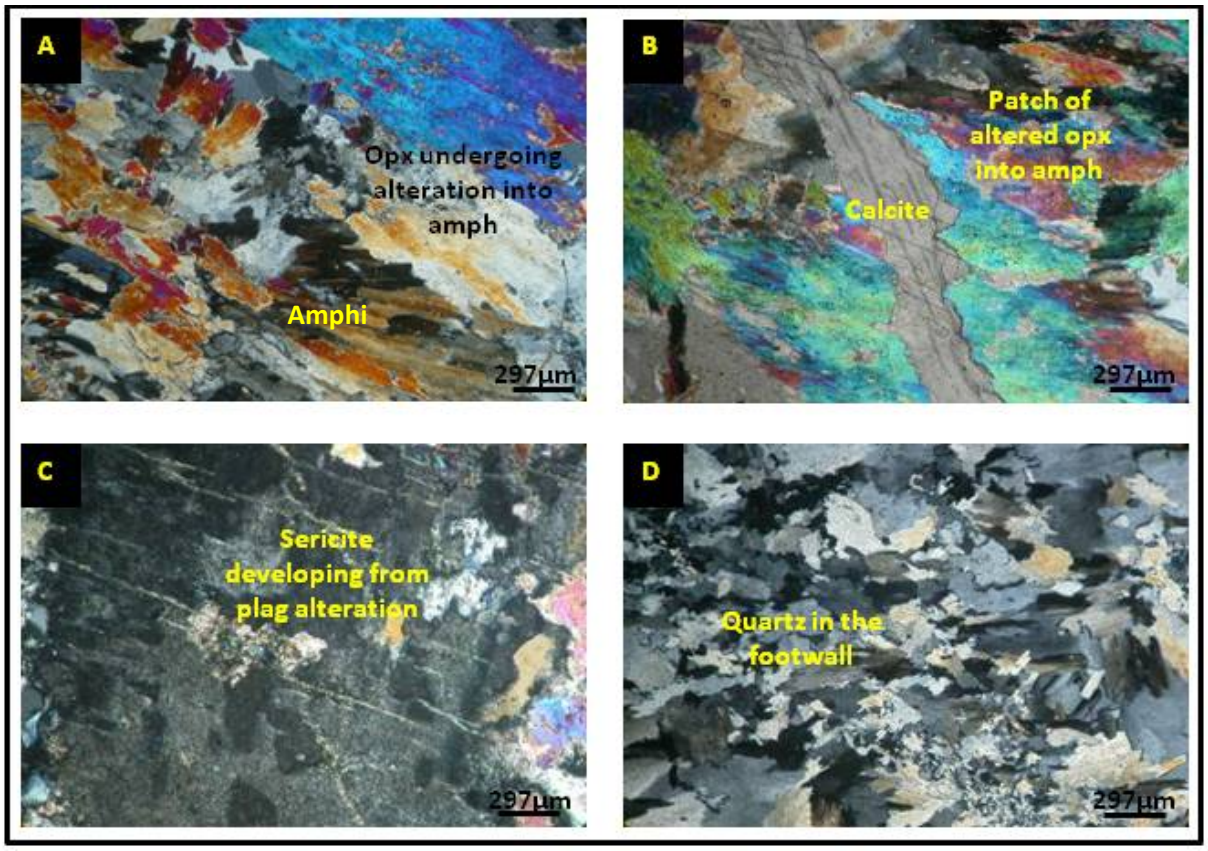

Figure 4.12: *Footwall alteration. (A) alteration of orthopyroxene into radial amphibole (probably tremolite); (B) calcite developing along fracture zones; (C) sericite forming as an alteration product of plagioclase; and (D) quartz crystallisation during alteration caused by IRUP intrusion. Amphibole shows high interference colours due to thin section thickness. (Transmitted light, crossed nicols).*

4.3 Compositional Analysis

The composition of over 270 chromites from the three different UG2 main seam reef types (normal reef, potholed reef and the IRUP reef) was undertaken using an SEM connected to an EDS system. Table 4.1 is a representative summary of the chromite compositions from these three reef types. The full set of data are given in Appendix B.

***Table 4.1**: Representative analyses of chromite from the three reef types*

	UG2 normal reef		UG2 pothole		UG2 IRUP reef				
	1	2	3	4	5	6	7	8	9
Cr_2O_3	44.10	45.30	43.89	42.75	43.68	43.94	23.80	19.72	9.53
Al_2O_3	15.62	15.60	16.20	16.43	18.88	18.35	5.13	4.66	4.70
TiO_2	0.97	1.08	1.28	1.13	1.00	1.08	8.09	8.37	13.15
FeO	28.61	28.87	29.86	28.69	28.57	28.91	61.79	65.58	69.01
MgO	8.44	8.58	8.89	8.54	7.99	7.97	0.18	0.10	0.18
MnO	0.66	0.60	0.56	0.61	0.55	0.51	1.15	0.97	0.60
NiO	0.22	0.14	0.26	0.16	0.15	0.14	0.03	0.11	0.06
Total	98.61	100.17	100.95	98.31	100.82	100.90	100.17	99.51	97.21
MnO corrected*	0.48	0.42	0.39	0.44	0.37	0.33	1.05	0.89	0.56
Total	98.43	99.99	100.78	98.14	100.64	100.72	100.07	99.43	97.18
	Cation based on 32 oxygens and Fe^{2+}/Fe^{3+} assuming full site occupancy								
Cr	9.19	9.30	8.90	8.89	8.84	8.90	5.39	4.50	2.22
Al	4.85	4.78	4.90	5.10	5.70	5.54	1.73	1.59	1.63
Ti	0.19	0.21	0.25	0.22	0.19	0.21	1.74	1.82	2.91
Fe^{3+}	1.54	1.47	1.65	1.53	1.06	1.11	4.94	5.67	5.70
Fe^{2+}	4.77	4.80	4.75	4.78	5.05	5.08	9.85	10.16	11.30
Mg	3.31	3.32	3.40	3.35	3.05	3.05	0.08	0.04	0.08
Mn	0.11	0.09	0.08	0.10	0.08	0.07	0.25	0.22	0.14
Ni	0.05	0.03	0.05	0.03	0.03	0.03	0.01	0.01	0.02
Total	24	24	24	24	24	24	24	24	24

*****MnO corrected equals wt% MnO – 0.004*wt% Cr_2O_3 and is done to correct for a strong spectral interference between Mn and Cr*

4.3.1. UG2 Normal Reef

Chromite in this reef type is dominantly a Cr + Fe spinel and is according to the classification of the Johnson Spinel Prism a chromite (Fe > Mg) with some variation towards magnesiochromite. Cr^{3+} cations vary between 8.46 and 9.31, Fe^{2+} cation vary between 4.45 and 5.52 and Mg cations vary between 2.50 to 3.60 cations on the basis of 32 oxygen per formula unit (pfu). Fe^{3+} is typically low with a maximum of 2.89 calculated cations pfu, and Al^{3+} has a maximum of 5.30 cations pfu. Both Fe^{3+} and Al^{3+} can substitute for Cr in the chromite structure and in part reflect the solid solution that exists between chromite and hercynite spinels. In the chromites from this reef type, this is seen by the complimentary behaviour of the trivalent cations, where Fe^{3+} and Al^{3+} cations vary in relation to one another but at a constant Cr cation content (Fig. 4.13A). In comparison, Mg^{2+} substitutes for Fe^{2+} and therefore shows no variation with Al^{3+} or Cr (Fig. 4.13B). In these chromites, Ti cations are in very low abundance with a maximum of 0.48 cations pfu. Ti does not appear to vary

significantly with Fe^{2+} or Mg (Fig. 4.13C) but when plotted against Fe^{2+}+ Fe^{3+} there is a clear positive relationship (Fig. 4.13D) but this is most likely tied to Fe^{3+}. Overall, the chromite compositions for the UG2 main seam in normal reef are relatively homogeneous.

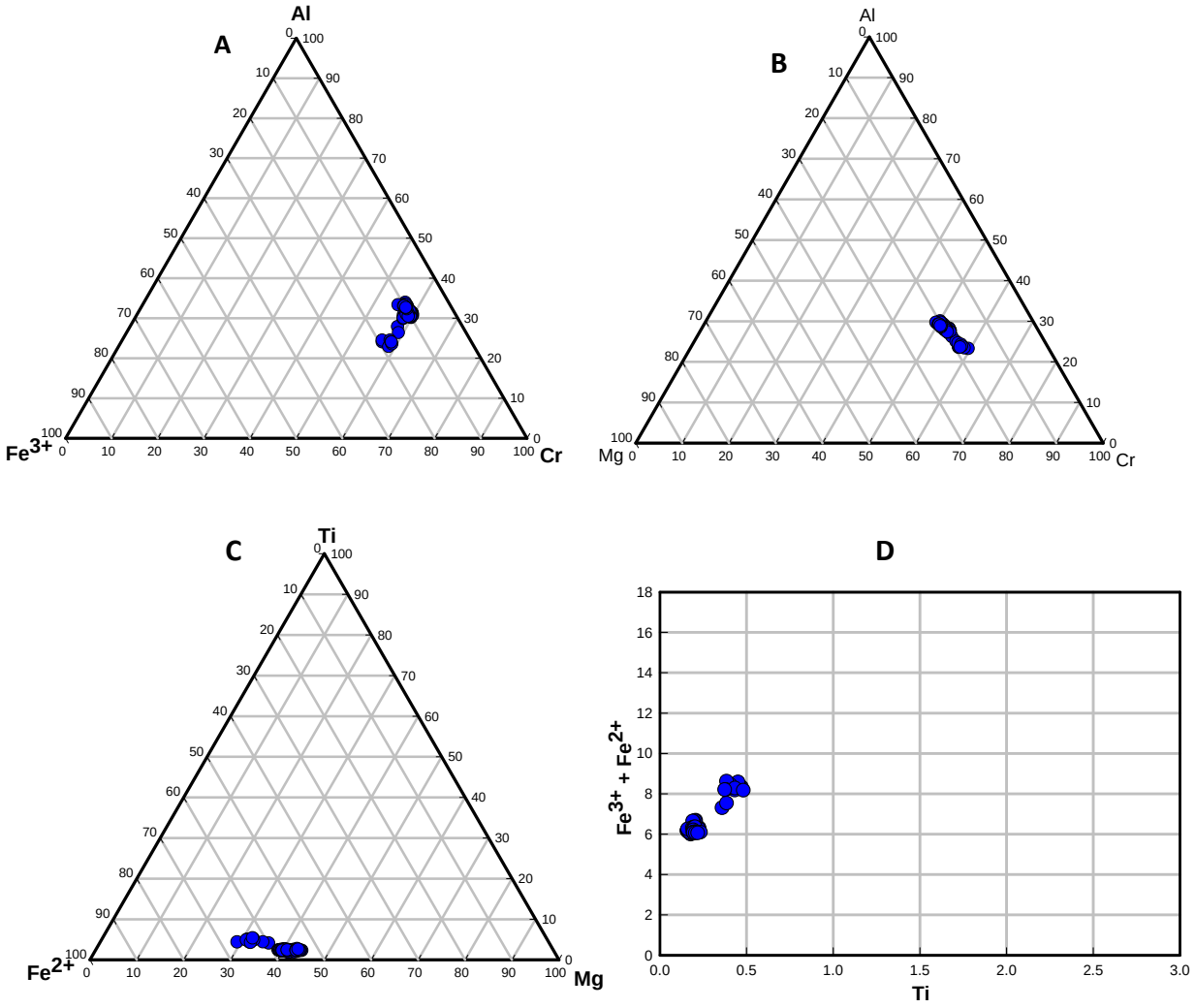

***Figure 4.13**: Cr-spinel compositions from UG2 main seam normal reef from Waterval Mine: (A) Cr-Al-Fe^{3+}, (B) Cr-Al-Mg, (C) Mg-Ti-Fe^{2+}, and (D) Ti-(Fe^{3+} + Fe^{2+}). Fields represent the primary compositional domain of chromite grains.*

4.3.2 UG2 Affected by Pothole Formation

Compositional analyses of chromite in the UG2 reef affected by potholing are similar to the UG2 normal reef and show the presence of chromite (Fe^{2+} > Mg) with variable amounts of Al^{3+} and Fe^{3+}. However, chromites in the UG2 main seam potholed reef are defined by a

more restricted compositional range than in the normal reef. Cr^{3+} cations average 8.95 pfu with a standard deviation of 0.12 cations pfu. Al^{3+} varies slightly between 4.74 and 5.50 cations pfu and Fe^{3+} varies even less, between 1.38 and 1.69 cations pfu. There is no obvious variable correlation between these trivalent cations (Fig. 4.14A). The variation is even less between Mg (cations between 3.21 and 3.67 pfu) and Fe^{2+} (Fig. 4.14B) and the amount of Mg does not vary in any way with Al^{3+} and Cr (Fig. 4.14C). The amount of Ti present is almost negligible with less than 0.2 cations pfu with minimal variation with Fe^{2+} + Fe^{3+} (Fig. 4.14D).

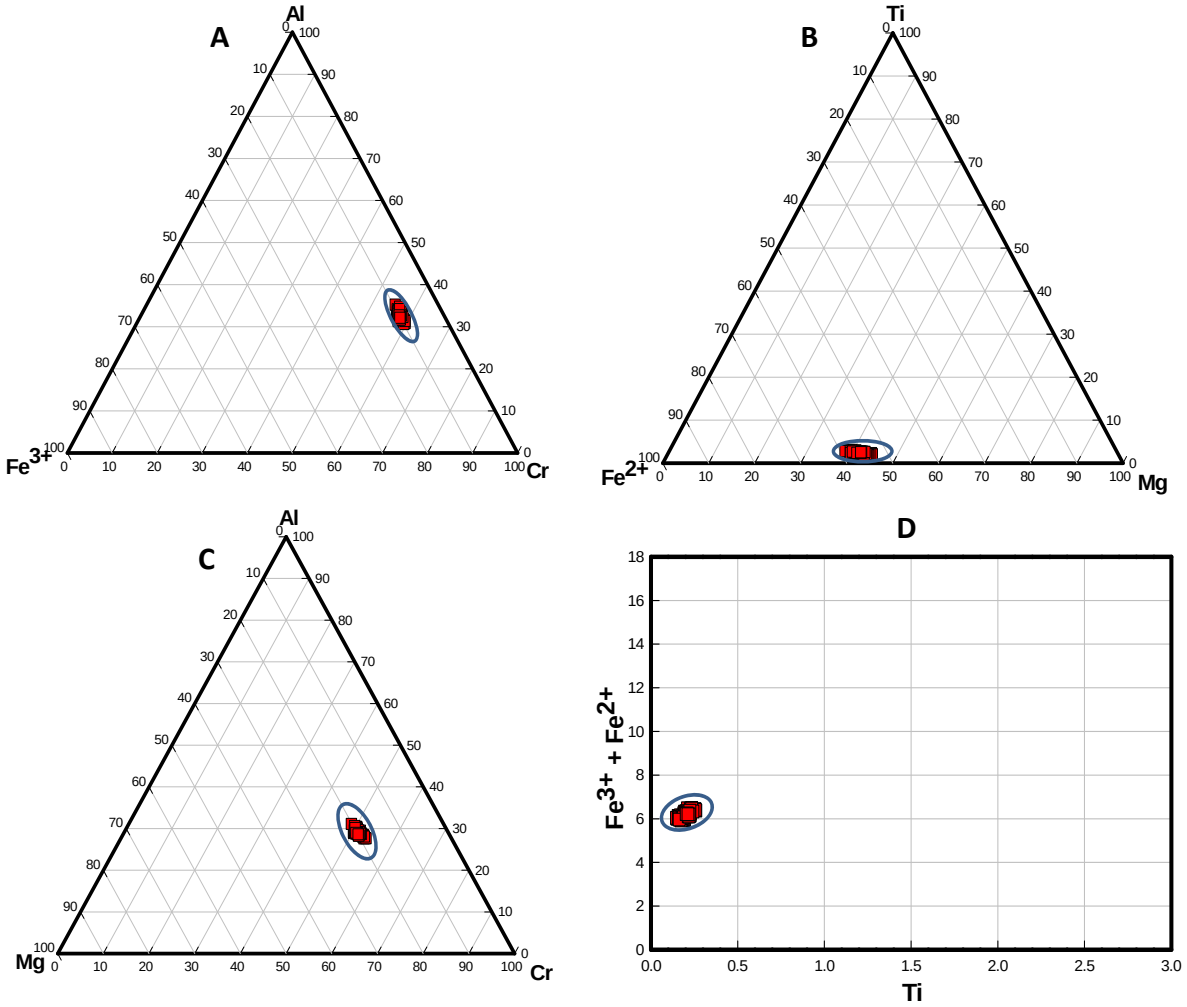

Figure 4.14: *Cr-spinel compositions from UG2 main seam reef affected by pothole formation from Waterval Mine: (A) Cr-Al-Fe^{3+}, (B) Mg-Ti-Fe^{2+}, (C) Cr-Al-Fe^{3+}, and (D) Ti-(Fe^{3+} + Fe^{2+}). Fields characterise the primary compositional domain of chromite grains.*

4.3.3 UG2 Affected by IRUP Intrusion

The composition of chromite in this reef represents a heterogeneous dataset that is defined by a compositional gap which divides the chromite population into two groups. One group

shows a restricted composition and the second group shows a much broader range in composition (Fig. 4.15). The chromite population with a restricted composition is almost identical to chromite compositions from the UG2 normal reef and the UG2 potholed reef. This is a Cr-Fe^{2+} rich composition with minor amounts of Fe^{3+}, Al^{3+} and Mg cations which vary in a manner most similar to that in the UG2 potholed reef (Fig. 4.15A-D). Compared to this chromite composition, the second chromite composition associated with the recrystallised bottom 2-3 cm of the UG2 main seam shows a significantly broader range of compositions and in particular a pronounced trend between Fe^{3+} and Ti cations in association with Cr cations. Figure 4.15 illustrates these two compositional groups clearly.

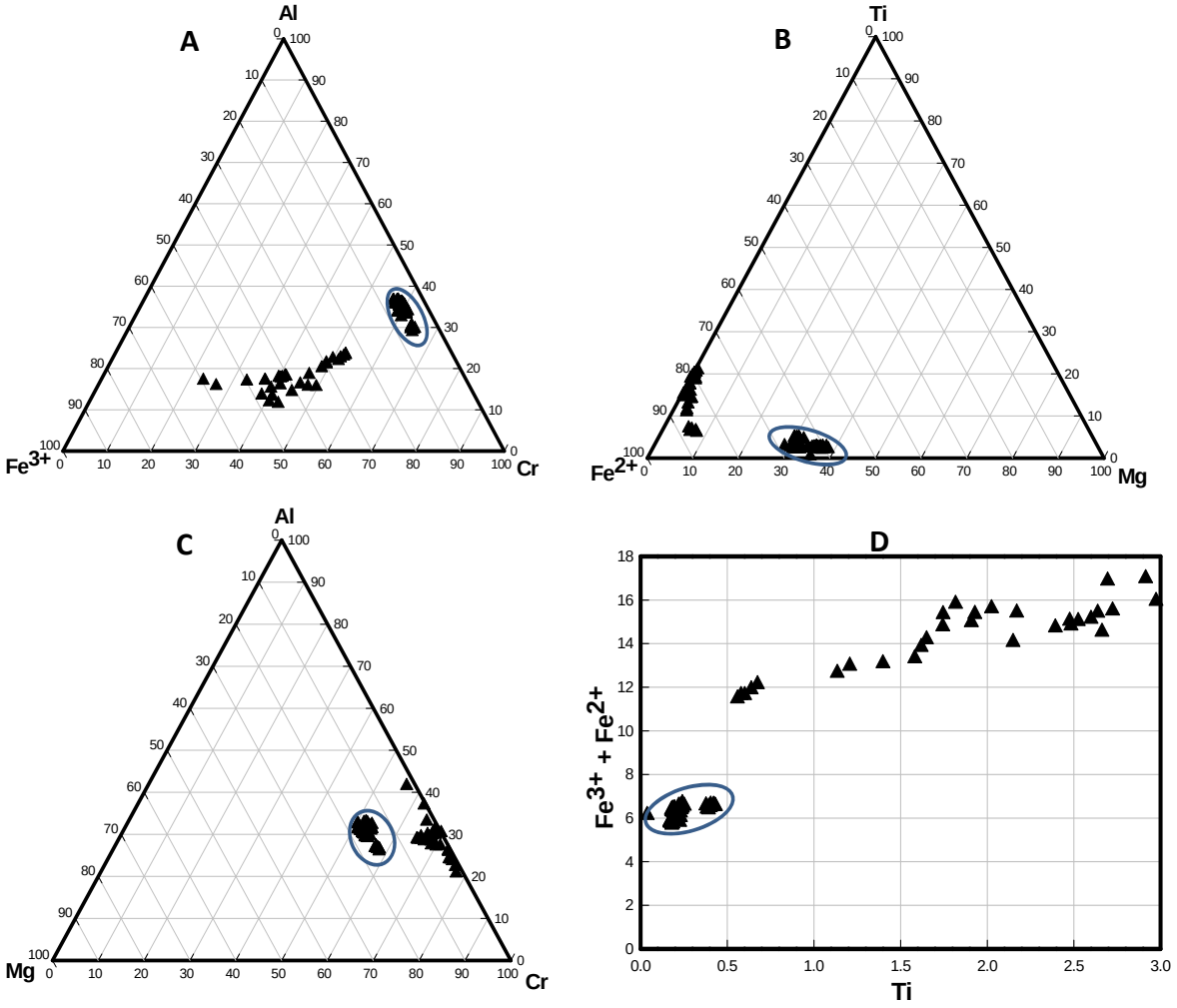

Figure 4.15: *Cr-spinel compositions in UG2 main seam reef affected by IRUP intrusion from Waterval Mine: (A) Cr-Al-Fe^{3+}, (B) Mg-Ti-Fe^{2+}, (C) Cr-Al-Fe^{3+}, and (D) Ti-(Fe^{3+} + Fe^{2+}). Fields characterise the primary compositional domain of chromite grains.*

Whereas, the variation in trivalent cations in the normal reef was due to coupled substitution of Fe^{3+} and Al^{3+} for Cr, in the IRUP reef, the variation in the trivalent cations for the second group appears to be a coupled substitution of Fe^{3+} and Ti for Al^{3+} and Cr (Fig. 4.15A-D). The two groups have different proportions of Mg cations but the variation within each group is not very significant (Fig. 4.15B and 4.15C). The higher Fe^{3+} and Ti cation proportions indicates that this chromite is more strictly defined as a magnetite and this would explain the magnetic properties of the bottom part (3cm bottom part) of the UG2 main seam for this reef type. The Ti substitution indicates that the magnetite may be transitional to ulvöspinel which would account for the poor 2:1 ratio of the trivalent and divalent cations in this reef type, which may be up to 11.3 R^{2+} / 12.6 R^{3+}.

4.4 Summary

From this study the following points can be presented as key findings:

- Texturally the UG2 main seams in the normal reef and reef affected by pothole formation are identical and dominated by chromite with sub-equant anhedral grain shapes. The UG2 affected by IRUP intrusion differs from these two reef types by being dominated by the presence of coarser grains with polygonal shapes and also the presence of fractured and brecciated grains.

- Mineralogically, the three reef types show differences between each other, but these difference are negligible between the UG2 normal reef and the UG2 reef affected by pothole formation. In both these reef types the main phases are in order of decreasing abundance chromite, plagioclase and orthopyroxene. The only difference is the presence of chlorite in the UG2 normal reef which is not present in the potholed reef. In comparison, the UG2 reef affected by IRUP intrusion lacks plagioclase and the orthopyroxene is typically altered.

- Alteration of primary magmatic minerals orthopyroxene and plagioclase, which can be both cumulate and intercumulate phases, to secondary minerals sericite, quartz, amphibole (tremolite), serpentine and talc is more prevalent in the UG2 reef affected by IRUP intrusion and lesser in the two other reef types.

- Compositionally, the UG2 normal reef and the UG2 reef affected by pothole formation are dominated by chromite grains with Cr-rich compositions and Fe, Al and Mg as the other principal elements. The UG2 reef affected by IRUP intrusion is composed of two spinel compositions; (1) Fe^{2+}-rich chromite with a composition similar to the normal and potholed reef types where $Cr/Fe^{2+}>1$; and (2) an Fe^{3+}+Ti-rich chromite (magnetite transitional to ulvöspinel) composition where $Cr/Fe^{2+}<1$. The magnetite compositions are only observed at the bottom (lowermost 3-4 cm) of the UG2 main seam reef affected by IRUP intrusion.

CHAPTER 5: BATCH FLOTATION ANALYSIS

5.1 Overview

The purpose of this section is to investigate the influence of the mineralogical characteristics of chromite from the main seam in a UG2 normal reef, a UG2 reef affected by pothole formation and a UG2 reef affected by IRUP intrusion (chapter 4), on the flotation performance of these different reef types. In order to do this, two experimental conditions were chosen for batch flotation tests; (1) no depressant addition, and (2) with depressant addition. The objective of the first condition was to allow for the recovery of all naturally floating gangue. The objective of the second condition was to prevent naturally floatable gangue from being recovered by the addition of a high depressant dosage (400 g/t). Therefore, the only material recovered during flotation at a high depressant dosage is through entrainment. Once the entrainment is accounted for, the mineralogy of the naturally floatable gangue can be investigated (Wiese, 2009). Subsequently, it can be determined if chromite constitutes naturally floatable gangue and the mineralogical characteristics of naturally floating chromite can be further investigated using MLA. Table 5.1 presents a summary of the results of the batch flotation tests and gives milling times, average cumulative mass recovery, average cumulative water recovery, and mass of floatable gangue for various elements (Al, Cr, Mg, Ca, Si and Fe). The full set of results is given in Appendix C.

Reef Type	Milling time	Samples	Time (min)	Depres-sant Addition	Ave. Cum. Mass Recovery (g)	Ave. Cum. Water Recovery (g)	Al rec %	Cr rec %	Mg rec %	Ca rec %	Si rec %	Fe rec %	Final Floatable Al (g)	Final Floatable Cr (g)	Final Floatable Mg (g)	Final Floatable Ca (g)	Final Floatable Si (g)	Final Floatable Fe (g)
UG2 Normal Reef Ore	33 min	C1	3	0g/t	7.86	158.14	1.50	0.68	2.29	3.50	4.38	0.98	0.23	0.60	0.73	0.19	1.29	0.15
		C2	5		13.01	340.07												
		C3	9		17.93	524.94												
		C4	15		21.77	681.72												
		C1	5	400g/t	3.57	139.71	0.80	0.47	0.82	1.75	1.69	0.59						
		C2	7		5.35	208.41												
		C3	11		7.27	284.59												
		C4	17		10.09	407.56												
UG2 Pothole Reef Ore	26 min	C1	3	0g/t	11.4	198.48	1.81	0.90	3.35	4.58	6.2	1.81	0.17	0.23	0.34	0.06	2.03	1.27
		C2	5		19.55	418.36												
		C3	9		26.14	623.9												
		C4	15		30.84	796.06												
		C1	5	400g/t	7.11	154.94	1.17	0.62	0.98	2.91	2.41	1.33						
		C2	7		10.24	259.06												
		C3	11		13.79	397.8												
		C4	17		17.53	567.34												
UG2 IRUP Reef Ore	10 min	C1	3	0g/t	20.81	152.02	2.81	2.17	9.13	9.94	23.25	3.38	2.02	5.03	5.10	0.95	7.39	5.31
		C2	5		35.22	275.65												
		C3	9		47.3	423.48												
		C4	15		50.55	571.57												
		C1	5	400g/t	2.42	118.1	0.51	0.44	0.91	1.10	1.78	0.71						
		C2	7		3.78	183.25												
		C3	11		5.97	289.41												
		C4	17		8.37	411.01												

Table 5.1: *Summary of batch flotation experimental results*

5.2 Feed Characterisation

Quantitative X-Ray Diffraction (QXRD) analyses were conducted on feed samples from the three different ore types of the main seam studied in this project. This was done to mineralogically characterise the feeds within these three different ore types prior to batch flotation experiments. Results of these analyses are summarized in Figure 5.1.

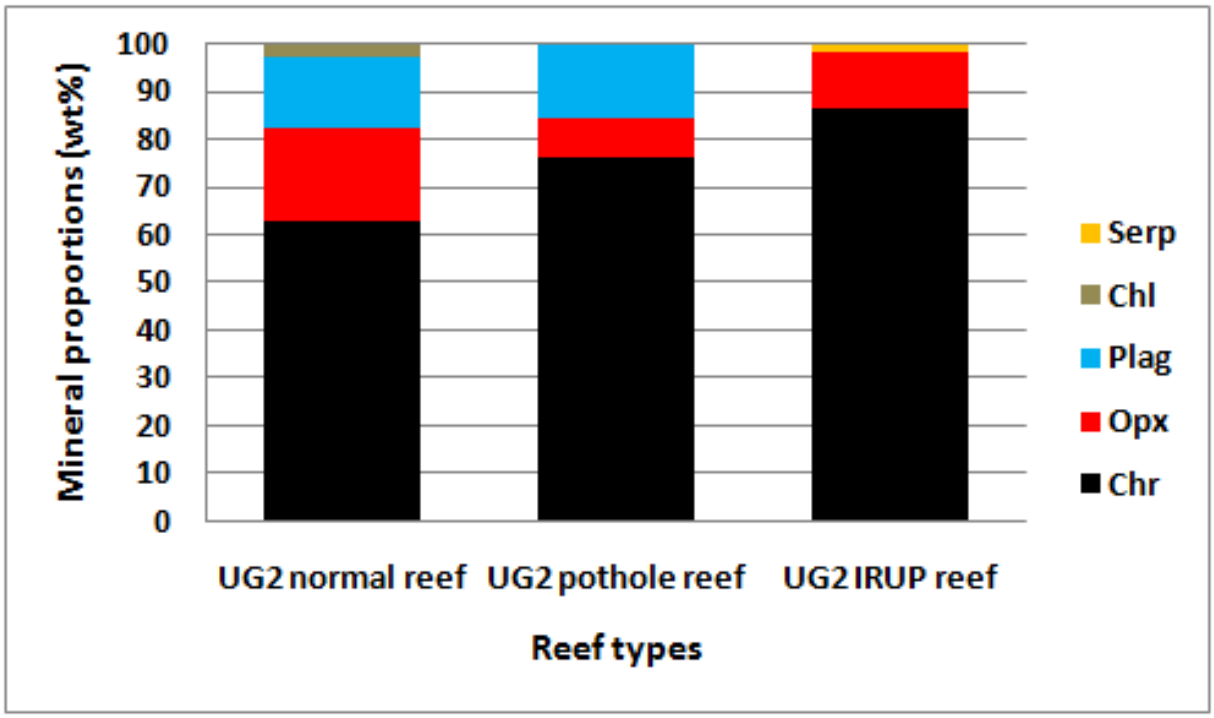

***Figure 5.1**: Mineralogical proportions of feed for each ore type. Serp (serpentine), Chl (chlorite), plag (plagioclase), opx (orthopyroxene) and chr (chromite).*

In the UG2 normal reef ore feed, chromite is the principal phase (63 wt %) and orthopyoroxene and plagioclase make up 19 wt % and 15 wt % of the feed respectively. Minor chlorite is also present (3 wt %). The ore feed of the UG2 affected by pothole formation consists of 76 wt % chromite, 16 wt % plagioclase, and 8 wt % orthopyroxene. The ore feed of the UG2 reef affected by IRUP intrusion consists of 86 wt % chromite, 12 wt % orthopyroxene and 2 wt % serpentine.

5.3 Mass Recovery Versus Water Recovery

Mass and water recoveries from batch flotation tests of the three ore types are shown in Fig. 5.2 for both conditions investigated.

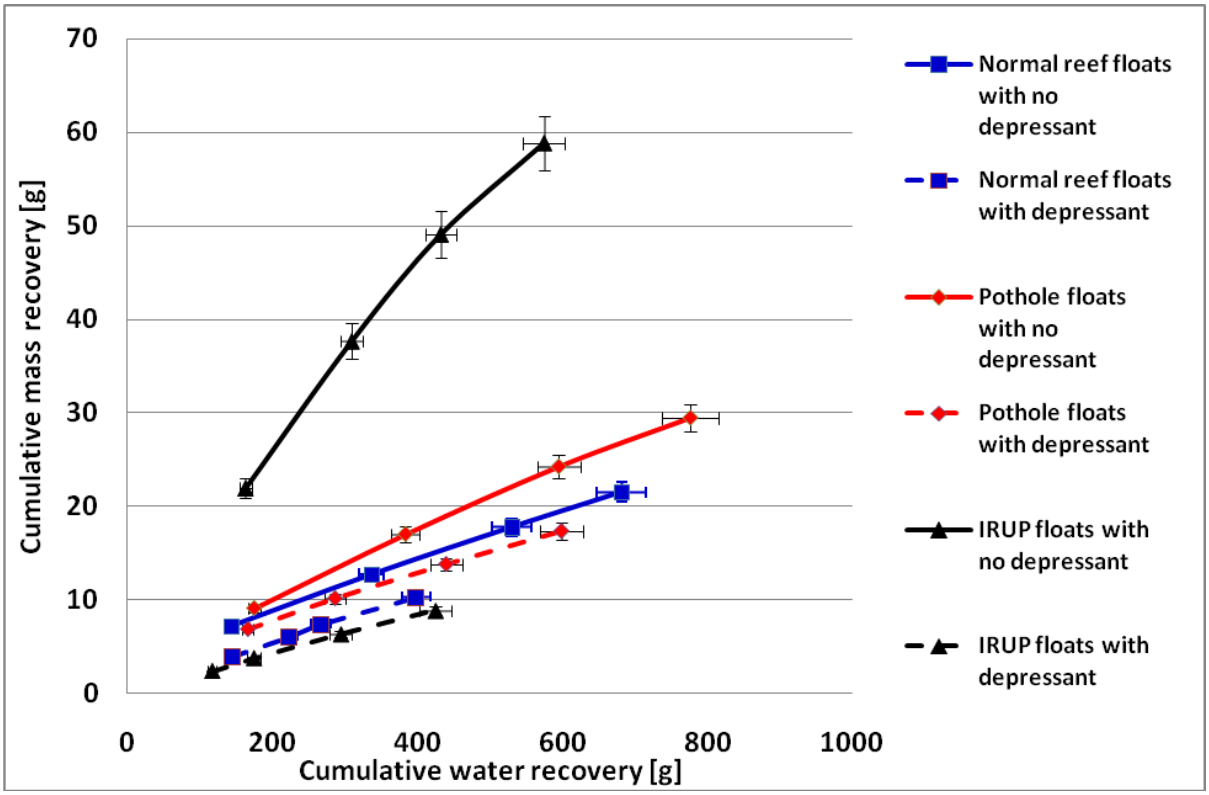

Figure 5.2: *Cumulative mass versus cumulative water recovery of the three ores with and without the addition of depressant. Error bars represent the 2σ standard deviation.*

For the tests with no depressant addition, there is far greater solid mass recovered in the UG2 affected by IRUP ore than the amount of mass recovered in the UG2 normal and UG2 affected by pothole formation ores (Fig. 5.2). The UG2 pothole ore on the other hand shows slightly more water and mass recovery than the UG2 normal ore. With the addition of depressant, the smallest amount of water and mass recovered is in the UG2 IRUP ore. The addition of depressant only caused a small reduction in the amount of water and mass recovered in the other two ore types. Furthermore, it can be observed that, the mass-water recovery relationship is linear for the tests with depressant addition, particularly for the UG2 normal and pothole ores and therefore confirms that mass recovery is only taking place through entrainment (i.e. no floating gangue is recovered).

5.4 Mineral Recovery

5.4.1 Mass Recovery of the Major Minerals

In order to investigate the recovery of the dominant gangue minerals, a comparison of major elements recovered during batch flotation experiments can be made. XRD results and the petrography study presented in Chapter 4 showed that the main minerals present in the UG2 ore are chromite, orthopyroxene and plagioclase. These minerals are principally composed of Cr, Al, Si, Fe, Mg and Ca and these elements will be used as proxies for the recovery of chromite (Cr and Fe), orthopyroxene (Si, Mg and Fe), and plagioclase (Si, Al, and Ca).

Figure 5.3 and 5.4 show the difference in mass of the different elements recovered during batch flotation experiments of the three ore types. The most noticeable feature is the amount of material recovered in the UG2 ore affected by IRUP with no depressant addition compared to the other two ore types. The effect of depressant addition is greater for the UG2 IRUP ore than for the other two ore types and caused a significant reduction in Cr, Mg, Si and Fe. This indicates flotation of Si, Cr, Fe and Mg bearing phases, which in the context of this study are orthopyroxene and chromite. Very low mass recovery of Al and Ca was noted for all three ore types, for both sets of flotation conditions and indicate the recovery of only minor plagioclase.

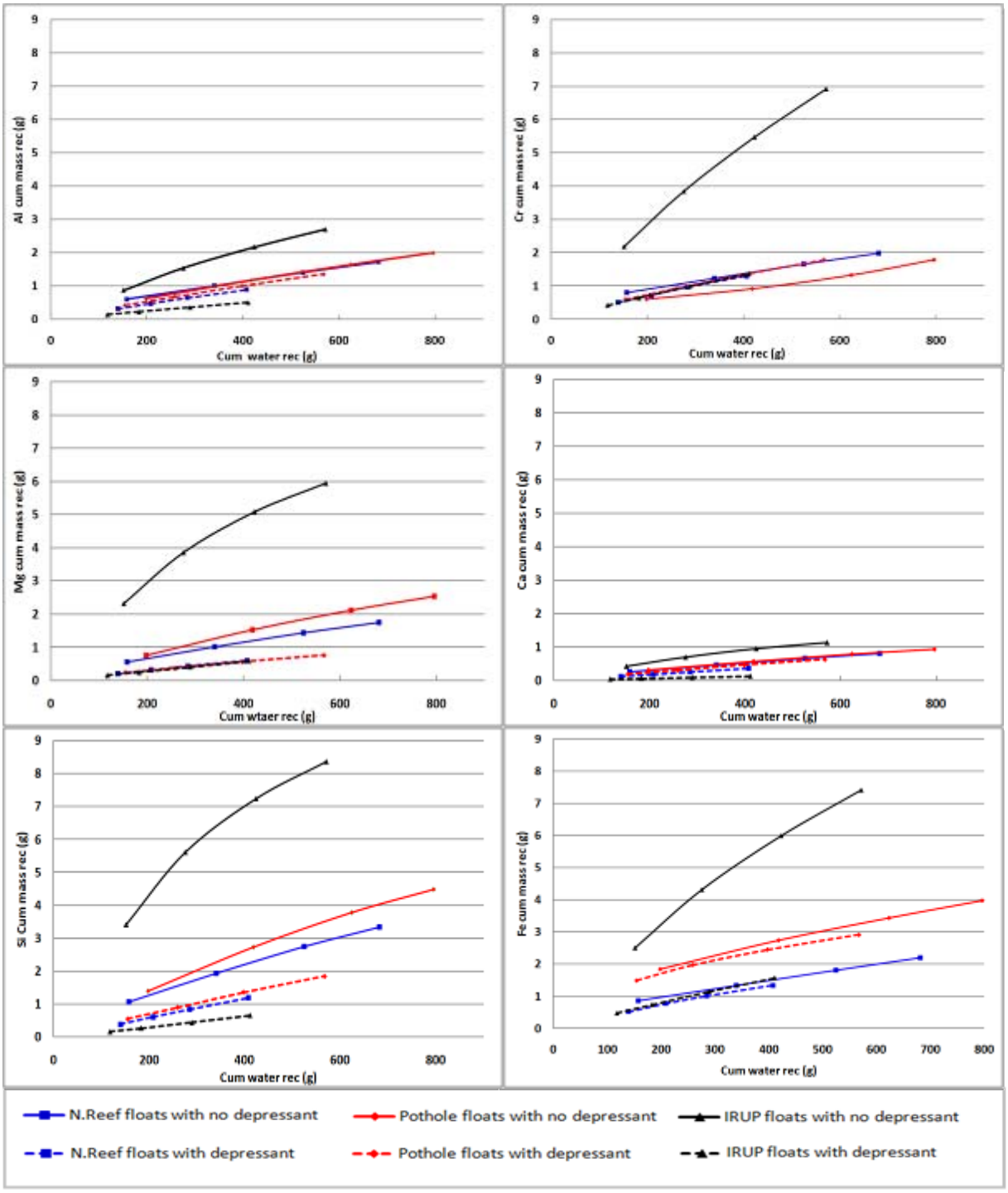

Figure 5.3: *Mass versus water recovery of individual elements (Al, Cr, Mg, Ca, Si and Fe) in the three ore types.*

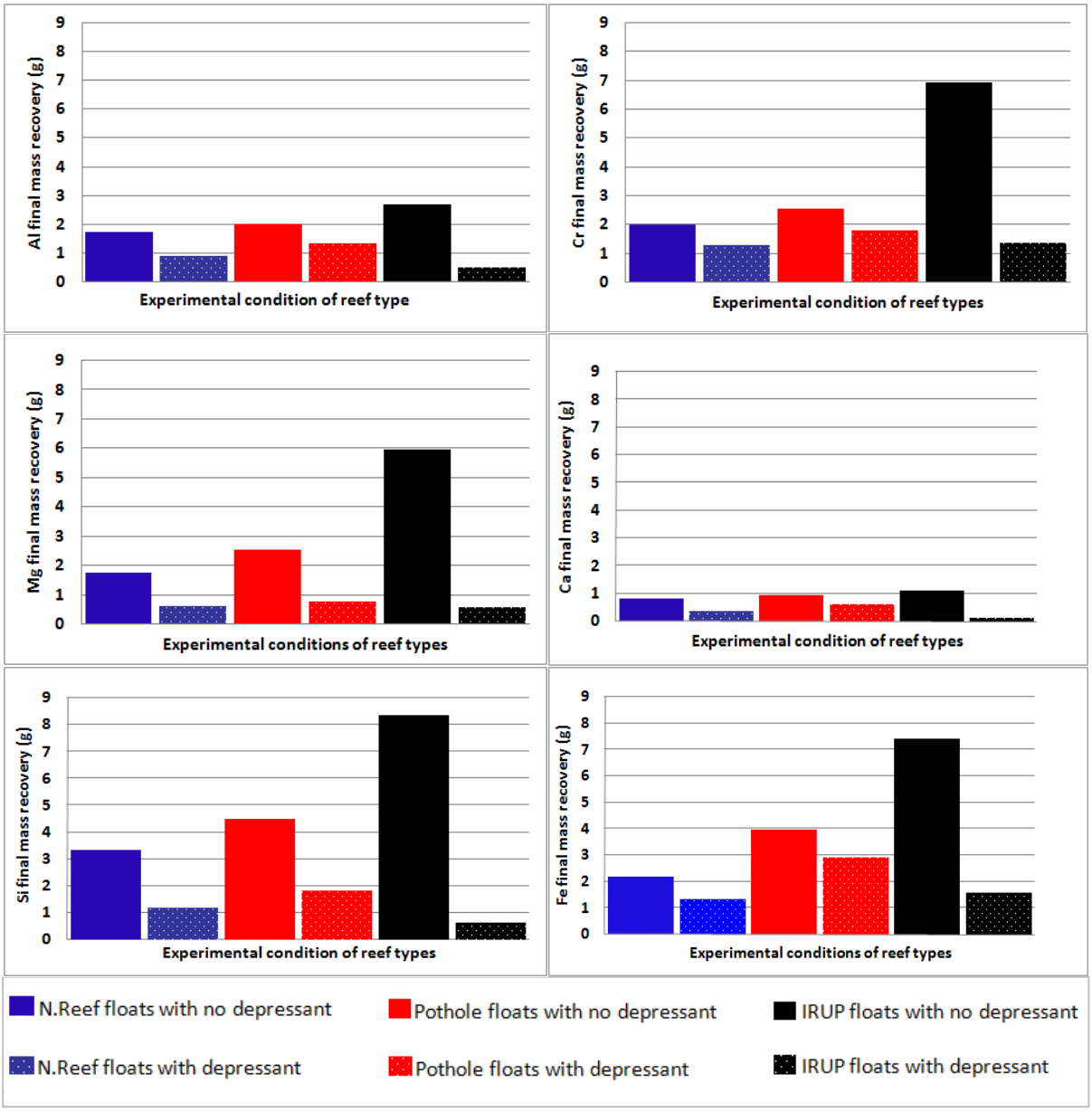

Figure 5.4: *Comparison of the major element (Al, Cr, Mg, CA, Si And Fe) distribution in the three ore types for the two experimental conditions. (A) Al recovery, (B) Cr recovery, (C) Mg recovery, (D) Ca recovery, (E) Si recovery and (F) Fe recovery.*

5.4.2 Mass Recovery of Gangue Minerals Due to True Flotation

In order to determine the amount of floatable gangue recovered in batch flotation tests, the amount of material recovered by entrainment first needs to be accounted for. This is done using the methodology of Wiese (2009), as explained in Section 3.5. The basis of this methodology is that the contribution of the valuable PGM minerals is negligible to the mass

recovery, and that the amount of material recovered by entrainment can be calculated and removed from the total mass recovered when the entrainability factor is known. Figure 5.5 shows the calculated mass versus water recovery for floatable gangue shown for various major elements for the three different ore types. Detailed calculations are given in Appendix C.

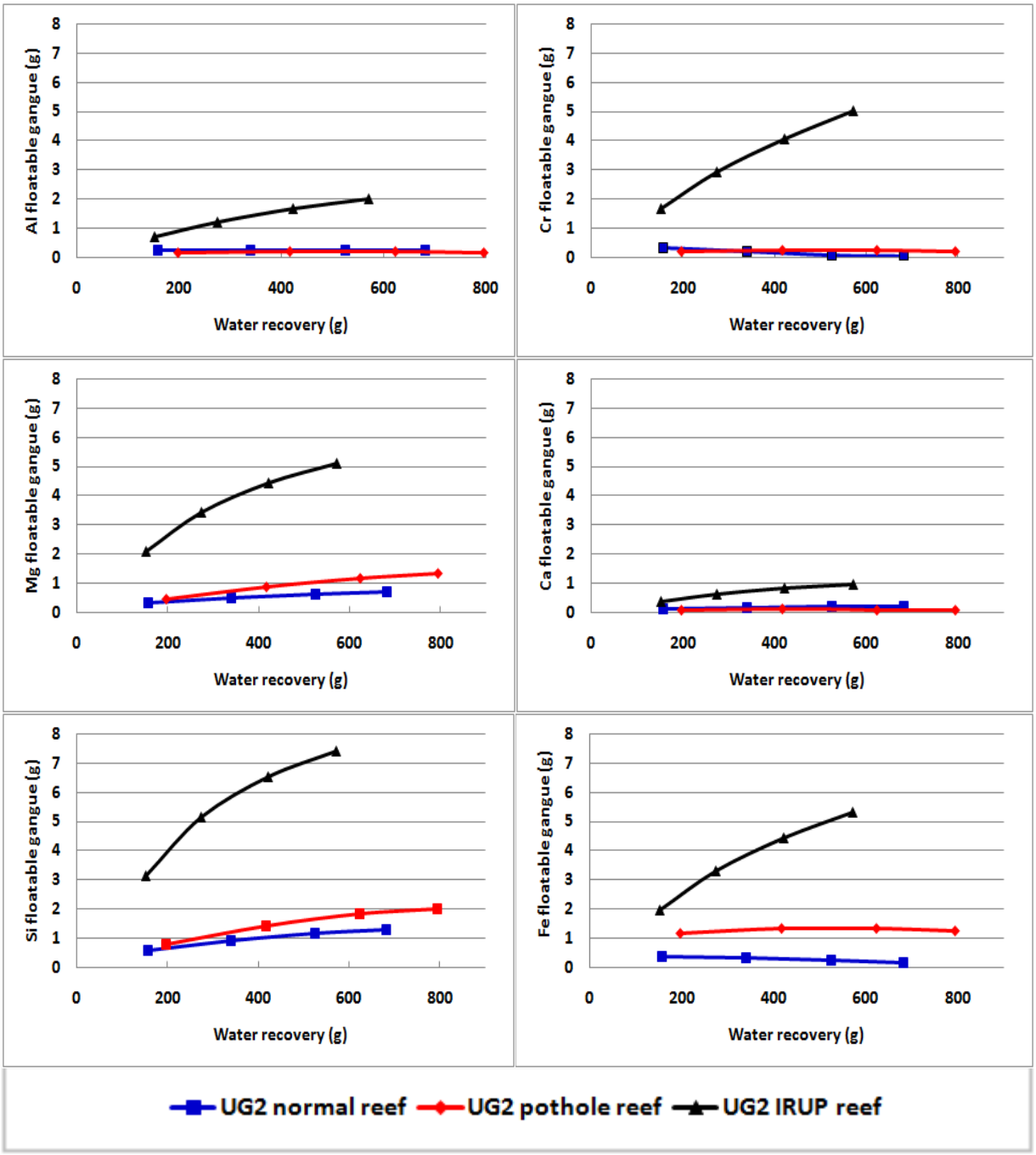

Figure 5.5: *Mass of floatable gangue versus water recovery for the major elements of the three ore types.*

Figure 5.5 shows that Cr, Mg, Si and Fe are the main elements recovered and represent the recovery of chromite and orthopyroxene. This indicates that these two minerals constitute naturally floating gangue. The greatest recovery of orthopyroxene and chromite occurred in the UG2 affected by IRUP ore. The ores of the UG2 normal reef and UG2 reef affected by pothole formation only show a small amount of floatable orthopyroxene and chromite. Orthopyroxene and chromite are not considered to be naturally floatable (Mailula *et al*., 2003; Ekmekçi *et al*., 2003), and therefore it is necessary to further investigate any mineralogical phenomena that can cause its floatability.

5.5 Characterisation of Floatable Gangue (MLA)

MLA analyses were conducted on concentrates from the batch flotation tests with no depressant addition in order to investigate the mineralogy of the naturally floating chromite. MLA analyses were only conducted on the +38-75µm size fraction in order to eliminate the effect of entrainment of fine particles. The goal of these analyses was to investigate the composition, liberation and mineralogical association of chromite in the UG2 IRUP ore compared to the UG2 normal ore and UG2 potholed ore to determine which mineralogical factors were responsible for its natural floatability.

5.5.1 Modal Mineralogy of Floatable Gangue

The quantitative evaluation of the mineralogy of the concentrates collected during flotation of the three ore types using MLA revealed that the modal mineralogy of these ores is variable. Figure 5.6 is a simplified list of these minerals. Detailed tables of the modal mineralogy of each ore type are given in Appendix F1.

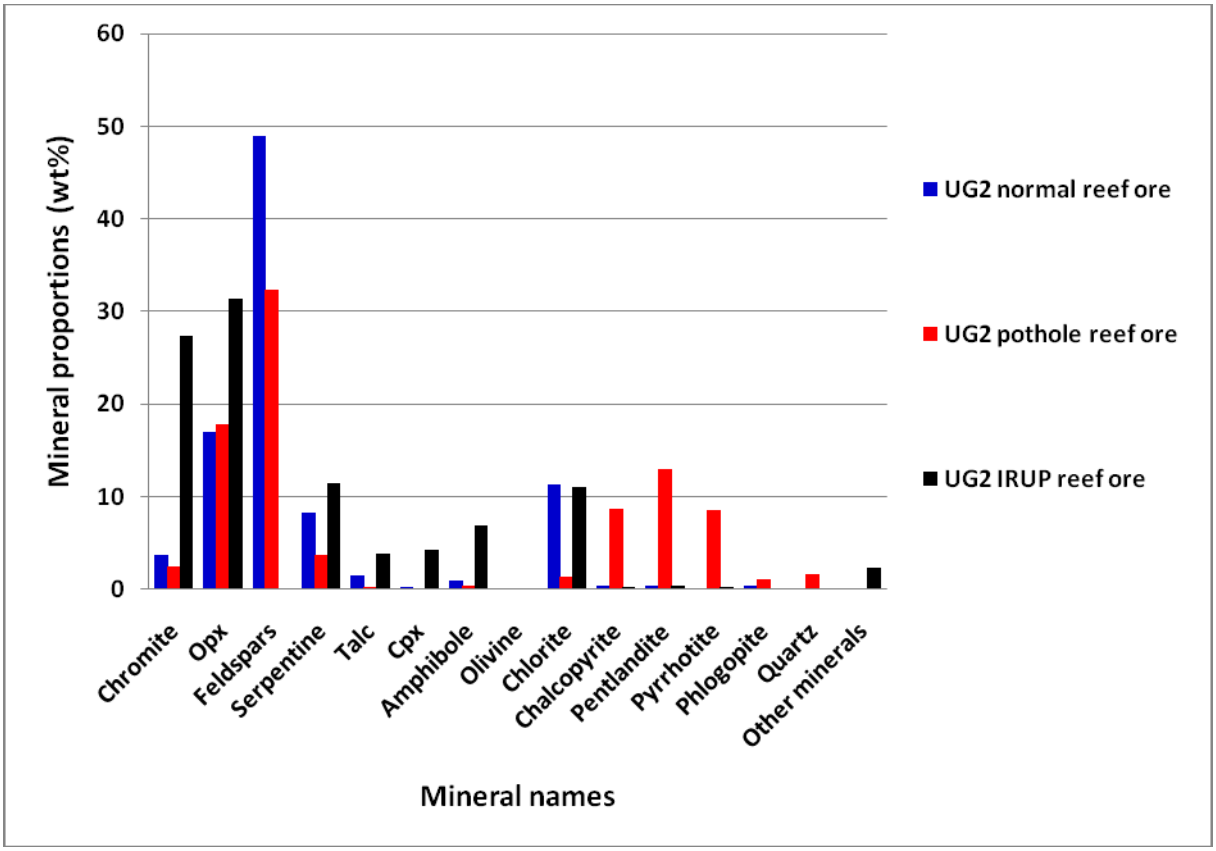

Figure 5.6: *Comparison of the modal mineralogy of the concentrates of the three ore types from the flotation tests with no depressant.*

The dominant features observed in Figure 5.6 are the differences in the relative mineral abundances of these three ore types. The UG2 affected by IRUP ore has the greatest amount of chromite (27 wt %), orthopyroxene (31 wt %), serpentine (11.5 wt %) and talc (3.9 wt %) relative to the other ores (Fig. 5.6). Compared to the UG2 affected by IRUP ore, the UG2 normal reef and pothole ores are characterised by high proportions of feldspars (49 wt % and 32 wt %, respectively) and small proportions of chromite (less than 4 wt % for each ore type) and orthopyroxene (less than 18 wt % for each ore type). The UG2 IRUP ore and the UG2 normal reef ore show similar abundances of chlorite (10 wt %). Sulphide minerals (chalcopyrite, pentlandite and pyrrhotite) on the other hand are particularly abundant in the UG2 affected by pothole reef ore (Fig. 5.6).

Since chromite is the mineral of interest in this study, the mass recovery of chromite to the concentrate from the batch flotation tests is shown for each ore type in Figure 5.7.

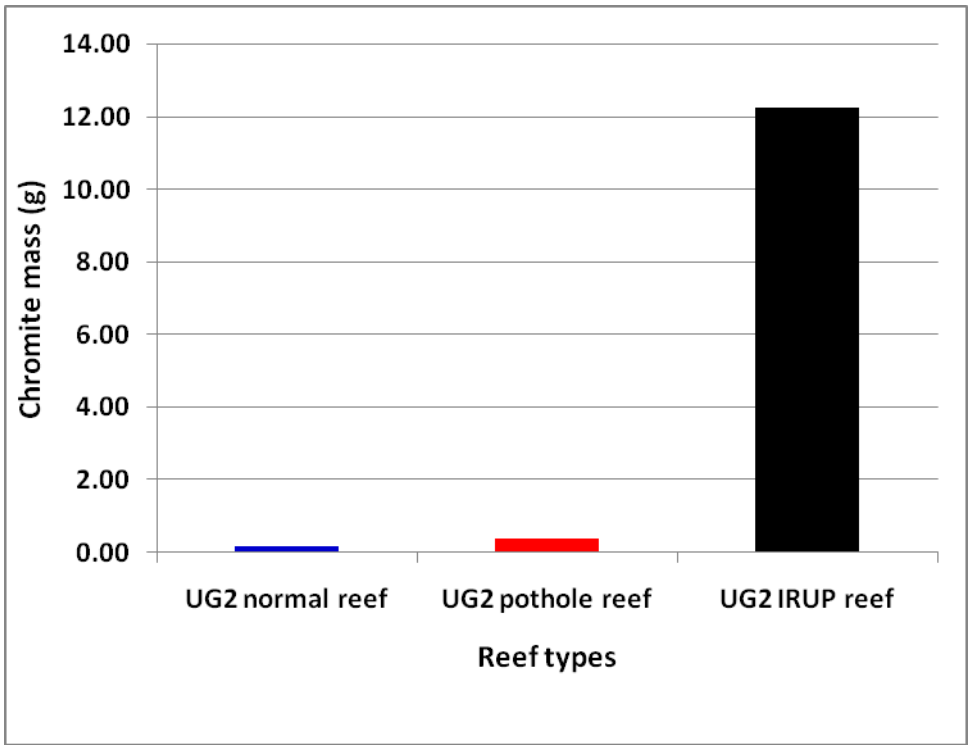

Figure 5.7: *Mass recovery of chromite obtained in the final concentrate of each ore type in the with no depressant addition tests.*

The greatest chromite mass recovery was obtained in the UG2 affected by IRUP reef ore (12.2g), followed by the UG2 pothole reef ore (0.38g) and the UG2 normal reef ore (0.18g) (Fig. 5.7). This significant recovery of chromite in the UG2 affected by IRUP ore, compared to the other two ore types illustrates the extent to which floatable chromite can be a problem and led to the investigation of the mineralogical characteristics of floatable chromite in order to understand the reason for its natural floatability.

5.5.2 Composition of Floatable Chromite

The composition of floatable chromite from the UG2 affected by IRUP intrusion was further investigated to find out if there were any differences in the composition of naturally floating chromite in the UG2 IRUP ore relative to the non floating chromite in the UG2 normal and pothole ores. In the preliminary mineralogical characterisation (Chapter 4), two populations of chromite composition were found: (1) a population with $Cr/Fe^{2+}>1$ (chromite); and (2) population of chromite with $Cr/Fe^{2+}<1$ (magnetite to ulvöspinel formed in response to IRUP

intrusion) (see Chapter 4). MLA analyses resulted in the identification of different groups of chromite compositions also named "chromite bins". These bins are defined based on their different raw peak intensities (Table 5.2). Bins 1 to 4 are the composition of chromite corresponding to composition of chromite pre-existing in the MLA software library, and bins A to F compositions of chromite identified in this project and different from the pre-existing chromite compositions. However, the raw peak intensities, are not directly comparable to the compositional analyses presented in Chapter 4 since no corrections, e.g. PAP and ZAF, (Pouchou and Pichoir, 1991; Goldstein *et al*., 2003) have been applied to them. However, Table 5.2 shows that the most commonly determined chromite compositions from each ore type correspond to chromite in bins D (~ 10%), E (~12%), and F (~61 %).

As the UG2 normal and the UG2 affected by pothole ores are composed of chromite with a fairly homogeneous composition (Section 4.5), it can be concluded that the composition of chromite in bins D, E, and F most likely corresponds with the $Cr/Fe^{2+}>1$ chromite composition. This composition is interpreted to be the primary composition of chromite unaffected by the Fe-rich fluids associated with the emplacement of the IRUPs. Thus, it can be concluded that the naturally floating chromite in the UG2 affected by IRUP ore is also of primary origin and that compositional changes of chromite due to IRUP intrusion did not affect the flotation behaviour of chromite.

Table 5.2: *Classification of the composition of the different chromites analysed by MLA analysis of concentrates from batch flotation tests of each ore type.*

Mineral	Normal reef ore (%)	Pothole reef ore (%)	IRUP reef ore (%)
Chromite_1	0.10	0.15	1.32
Chromite_2	1.16	1.02	2.54
Chromite_3	1.94	3.07	4.74
Chromite_4	0.00	0.15	0.02
Chromite_A	0.87	0.88	3.14
Chromite_B	2.61	4.83	6.50
Chromite_C	1.36	2.64	4.74
Chromite_D	15.00	10.54	7.25
Chromite_E	11.23	14.49	12.95
Chromite_F	65.73	62.23	56.79

5.5.3 Texture of Floatable Chromite

5.5.3.1 Mineral Liberation

This section investigates whether the difference in chromite liberation is responsible for rendering chromite naturally floatable. Liberation in this project is evaluated on the basis of the free surface measurement (surface association to background) obtained from the MLA that is used as a proxy for mineral liberation (Table 5.3).

Table 5.3: *Liberation proportion of chromite in the concentrates of the three ore types.*

	UG2 normal ore	**UG2 pothole ore**	**UG2 IRUP ore**
Free surface (%)	93	92	89

The free surface of chromite was greater in the UG2 normal reef ore (93 %) compared to the free surface of chromite in the UG2 affected by pothole formation ore (92 %), which in turn was greater than the free surface of chromite in the UG2 affected by IRUP intrusion (89 %). Therefore, the UG2 affected by IRUP ore is slightly less liberated than the UG2 pothole and normal ore types. The differences in liberation are most likely not significantly different from one another.

5.5.3.2 Mineral Association of Floatable Chromite

The complete list of minerals obtained from the MLA analysis of concentrates of the three ore types (Appendix F2) was recombined and simplified in order to examine the mineral associations. The following mineral groupings were applied: base metal sulphides (chalcopyrite, pyrrhotite, pyrite, and pentlandite), pyroxenes (orthopyroxene and clinopyroxene), feldspars (plagioclase and orthoclase and epidote), serpentine, talc, chlorite, amphibole, and others minerals (all remaining minerals). The mass of chromite associated with these different minerals from the three ore types is summarised in Figure 5.8.

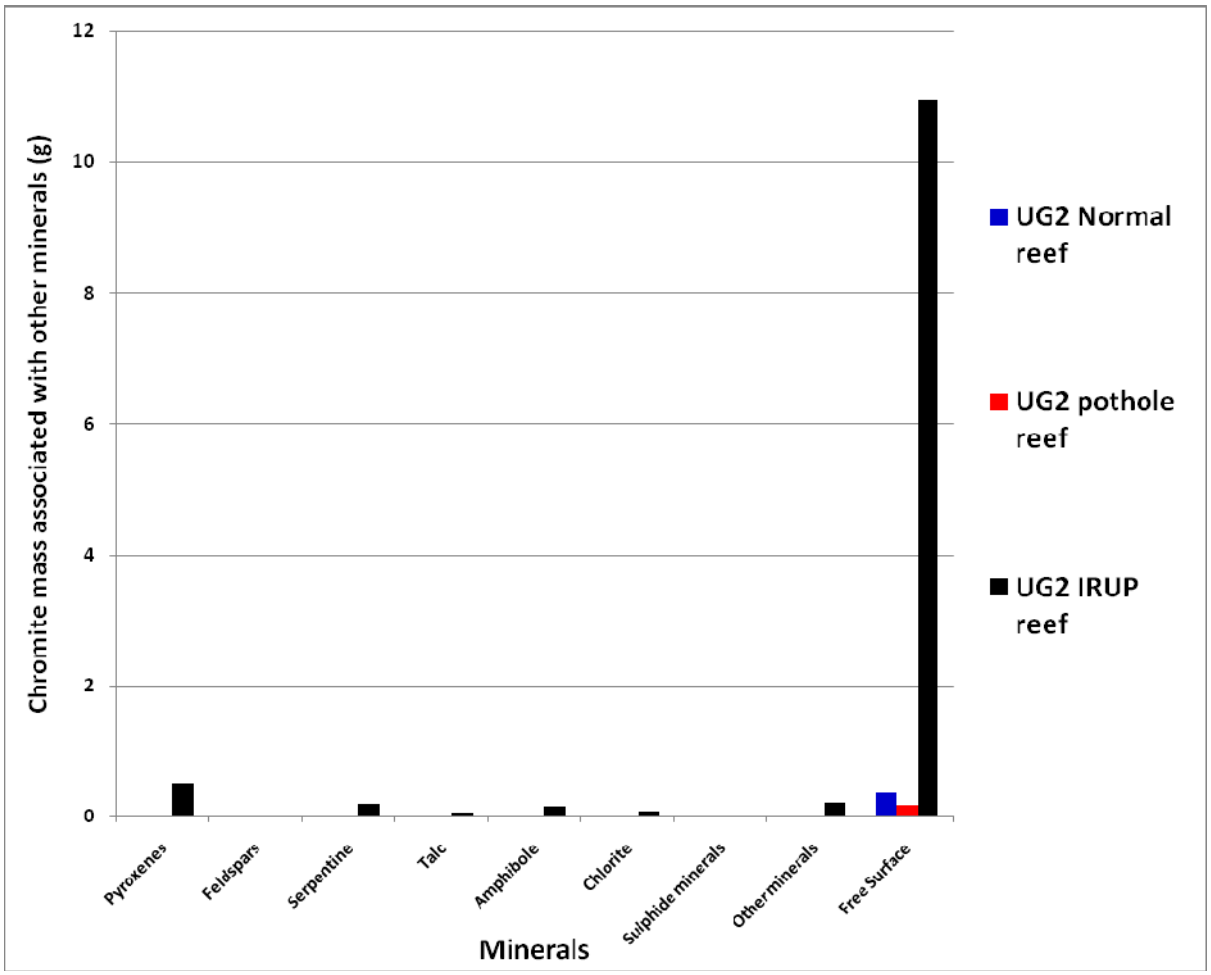

Figure 5.8: *Mass of chromite associated with different minerals recovered to the concentrate in batch flotation tests with no depressant addition for the three ore types.*

In both the UG2 normal reef ore and UG2 pothole reef ore, chromite is mainly associated with background (i.e. liberated chromite, 0.35g and 0.17g respectively) (Fig. 5.8). In the UG2 affected by IRUP ore, chromite is dominantly associated with free surface (i.e. liberated chromite, 11g), but is also associated with pyroxenes (0.5g), serpentine (0.19g), amphibole (0.17g), chlorite, talc and other minerals. A representation of the chromite particles associated with pyroxene, serpentine, talc, feldspars, chlorite, amphibole, sulphide minerals and other minerals in the UG2 IRUP ore type is given in Figure 5.9.

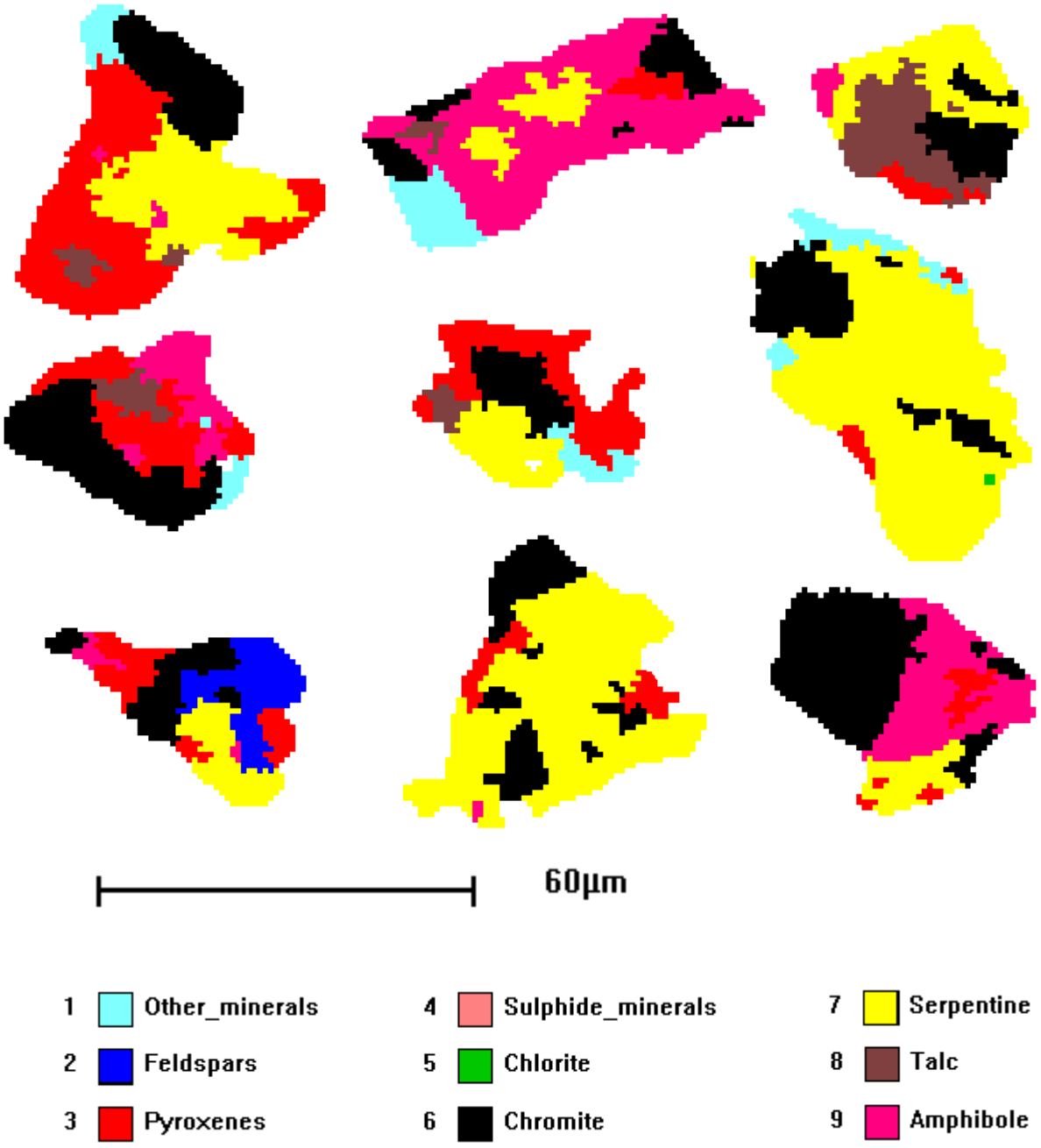

***Figure 5.9**: Examples of the types of chromite particles and their mineral associations recovered during batch flotation tests of the UG2 affected by IRUP ore.*

5.6 Summary

From this study the following points can be presented as key findings:

- Feed characterisation showed that the main seam ores from the UG2 normal reef and the UG2 reef affected by pothole formation are similar (UG2 normal reef: 63 wt % chromite, 19 wt % plagioclase and 15 wt % orthopyroxene; UG2 affected by pothole: 64 wt % chromite, 16 wt % plagioclase and 8 wt % orthopyroxene). The main seam ore from the UG2 affected by IRUP intrusion consists of 86 wt % chromite, 12 wt % orthopyroxene and 2 wt % serpentine.
- Mass recoveries from batch flotation tests showed that the UG2 main seam ores from normal reef and the reef affected by pothole formation are in general characterised by similar mass recoveries, whereas the UG2 main seam ore affected by IRUP intrusion shows the greatest amount of recovered material in the experiment with no depressant addition and the least amount of recovered material in the with depressant condition.
- The UG2 affected by IRUP ore showed floatable chromite estimated at 27.32 wt % that represents a mass of 12.24g, that is different from floatable chromite in normal reef ore (3.70 wt % representing a mass of 0.18g) and pothole reef ore (2.42 wt % representing a mass of 0.38g).
- The composition of naturally floating chromite in the UG2 reef affected by IRUP intrusion ore was determined to be similar to that of the UG2 normal reef ore and the UG2 pothole reef ore and is therefore of primary composition ($Cr/Fe^{2+}>1$).
- Chromite from the three ore types showed good liberation, but to different extents, with the UG2 IRUP ore being slightly less liberated than the UG2 pothole reef ore which in turn had less liberated particles than the UG2 normal reef ore.
- Chromite in the UG2 normal reef and the UG2 affected by pothole formation is mainly associated with feldspars 2.71 % and 2.53 % respectively. Comparatively, chromite in the UG2 affected by IRUP intrusion is dominantly associated with pyroxenes that represent 4.07% and its alteration minerals, particularly serpentine (1.54%) talc (0.46%) and amphibole (1.37%).

Chapter 6: Discussion

6.1 Overview

This chapter examines the relationship between the mineralogy of chromite from the UG2 normal reef main seam, the UG2 pothole reef main seam and the UG2 IRUP reef main seam (chapter 4), and its flotation performance in those three reef types (Chapter 5). This chapter is divided into three sections which address each of the three key questions identified in Section 1.5.

6.2. Textural Variation of Chromite in the Three Reef Types

This study has grouped textures from the three studied reef types into two main groups of textures. The first group comprises textures from the UG2 normal reef and the UG2 reef affected by pothole formation. Despite slight textural variations between these two reefs, they are dominated by identical primary mineralogies of cumulate chromite and intercumulate silicates (orthopyroxene and plagioclase) as well as an accessory mineral assemblage consisting of clinopyroxene, phlogopite, chlorite and sulphide minerals.

The main seam in these two environments is characterised by the presence of fine-grained sub-equant anhedral cumulate chromite grains. The texture of this chromite is considered to be of primary origin because it is associated with unaltered intercumulate orthopyroxene and plagioclase. Locally this chromite shows the development of chain-like textures that are the result of the interconnectivity of chromite grains. However, a coarsening of these chromite grains toward the bottom of the UG2 main seam is observed in both environments. In these regions, chromite is dominated by annealed polygonal grains that contain rounded inclusions of plagioclase. These inclusions probably represent remnants of the intercumulate

phase trapped at the junction of polygonal grains (ie at triple point), the boundaries of which have subsequently been removed via the annealing process leaving the isolated silicate grain. The annealing process is thought to have been caused by sintering of grains due to compaction of the overlying stratigraphic pile. However annealed grains are a minor component (less than 5%) of these environments compared to the fine sub-equant anhedral chromite grains.

The intercumulate silicates in the main seam are orthopyroxene and plagioclase but their proportions differ between the two reefs. In the UG2 normal reef main seam, orthopyroxene is dominant over plagioclase whereas in the UG2 potholed reef main seam plagioclase is dominant over orthopyroxene. However, neither orthopyroxene nor plagioclase shows significant alteration in either main seam environment. The hanging wall and footwall of both environments are principally composed of cumulate orthopyroxene and variable but lower amounts of intercumulate plagioclase. The hanging walls are fine-grained and the footwalls are coarse-grained. The contact between both the footwall and hanging wall and the main seam chromitite is sharp, and therefore in the footwall and hanging wall of both environments there are only trace amounts of chromite. In addition, the hanging walls and footwalls are affected by minor alteration in which chlorite and talc can be seen replacing orthopyroxene.

In comparison, chromite from the UG2 main seam affected by IRUP intrusion represents the second textural group. In this reef type a clear modification of primary minerals (chromite orthopyroxene and plagioclase) as a result of IRUP intrusion has occurred. These modifications have manifested in two main ways: (1) enlargement of chromite grains; and (2) pronounced alteration of primary silicate phases. The principal chromite textural features present in the UG2 main seam affected by IRUP are: (1) the development of medium to coarse polygonal grains with well formed 120^{o} triple junction grain boundaries; (2) irregular chromite shapes with transitional shapes between annealed polygonal grains and the primary fine-grained sub-equant anhedral chromite grains; and (3) localised regions of fractured to highly brecciated chromite grains.

The high proportion of annealed chromite grains present at the top and bottom of the main seam is thought to have developed due to the high heat from the emplacement of the IRUP. At the site of sampling, an IRUP body can be seen totally replacing the footwall and also truncating the UG2 main seam and spreading laterally along the top of the UG2 main seam. This explains the presence of highly annealed chromite grains at the top and bottom but not in the middle of the main seam. However, ponding of the IRUP below the main seam chromitite has generated more extensive annealing of chromite at the base of the main seam resulting in the formation of the coarsest chromite observed. This very coarse chromite is in the bottom 3 cm of the main seam and is also the location of modified chromite compositions (see Section 6.3 below). Rare patches of original fine-grained sub-equant anhedral chromite are only preserved where unaltered intercumulate orthopyroxene still exists and has affectively shielded the chromite from annealing.

The intrusion of the IRUP also generated hot fluids. These fluids have resulted in the localised development of brecciated chromite grains, presumably along microfractures. The brecciation is mostly confined to the middle of the main seam and may therefore be related to the zones where the IRUP is truncating the main seam. However, this study does not have enough spatial information to quantify this. The high proportion of altered silicate in this reef type is probably also related to the presence of these fluids which caused the breakdown of orthopyroxene to form serpentine, talc chlorite and amphibole and breakdown of plagioclase to form sericite. These alteration minerals are randomly distributed amongst the chromite grains and are sometimes present as inclusions. Similarly, both the hanging wall and the footwall show extensive alteration to the same secondary mineralogy as well as the development of quartz and calcite.

In summary, in the context of this study, no clear textural variation was found between the potholed reef main seam chromitite and the normal reef main seam chromitite. This may have been because of the nature of the pothole sampled where there was no obvious thinning of the reef into the pothole as has been observed elsewhere. In addition, the absence of pronounced textural variations in chromite with stratigraphic height within the UG2 normal reef main seam chromitite may suggest that the location sampled as part of this

study was not entirely representative. Further studies should be undertaken to assess the degree of textural variation at this location. Similarly, the sampling of additional pothole structures at Waterval would help in determining how representative the sampled pothole really is. What is clear is that the UG2 main seam chromitite affected by IRUP intrusion has clear and pronounced textural differences to the normal and potholed reefs. This has been seen previously (e.g. Reid and Basson, 2002) but it is perhaps worth investigating the textural variation associated with other IRUP bodies, given the unusual nature of the IRUP examined as part of this study.

6.3. Compositional Variation of Chromite in the Three Reef Types

Compositional studies of chromite from the UG2 chromitite main seam sampled in the three different environments has led to the identification of two distinctive groups. The first group comprises chromite compositions from the UG2 normal main seam, the UG2 main seam affected by pothole formation and some chromites from the UG2 main seam affected by IRUP intrusion. This chromite composition is characterised by Fe^{2+}-rich chromite where $Cr/Fe^{2+}>1$. The group has very little compositional variation and this is mostly characterised by substitutions in the R^{3+} cation site, principally Al^{3+} and Fe^{3+} substituting for Cr and probably mostly reflects the solid solution that exists between chromite and hercynite. Some substitution between Fe^{2+} and Mg^{2+} is also seen and this would reflect the complete solid solution between chromite and magnesiochromite. This composition is interpreted to be characteristic of primary chromite with no or very little postcumulate compositional change.

The second chromite compositional group is present only in the UG2 main seam affected by IRUP intrusion. This second group of compositions is characterised by Fe^{3+}+Ti-rich chromite composition where $Cr/Fe^{2+}<1$. This composition is identified as a magnetite rather than chromite and is probably transitional to ulvöspinel because of the high Ti content. Chromite grains displaying this composition are associated with texturally recrystallised massive chromite characterised by coarse annealed polygonal grains found near the contact between the footwall and the base of the UG2 main seam and is where magnetic properties are noticed. Compositional changes in the UG2 IRUP have usually been attributed to solid state

diffusion of cations due to interaction between Cr-Al rich chromite grains and Fe-Ti rich fluid introduced during IRUP intrusion (Scoon and Eales, 2002), that result in Cr and Al depletion and Fe-Ti enrichment of chromite. During this process, the most affected parts of layers are usually those more exposed to IRUP contact, whereas the less exposed grains within the layer retain their primary composition, resulting in the double chromite composition observed. This is clearly the case here, because of the ponding of the IRUP beneath the UG2 main seam chromitite and the concentration of these magnetite compositions in contact with this ponded IRUP.

6.4 Influence of Mineralogy on Flotation Performances

6.4.1 Ore Hardness

The different mineralogical characteristics of the three reefs discussed above have resulted in differences in the milling times of the three different ores. The UG2 main seam ore affected by IRUP intrusion had the shortest grinding time (10 min), followed the UG2 main seam ore affected by pothole formation (26 min) and the longest grinding time was for the UG2 normal reef main seam ore (33 min). This implies that the UG2 main seam affected by IRUP intrusion is the softest ore, while the UG2 normal reef main seam is the hardest ore. The milling times for the UG2 normal reef main seam and the UG2 main seam affected by pothole formation are considered to be very similar. Comparatively, the UG2 main seam affected by IRUP intrusion is distinguished by a milling time approximately half of the two other reef types. This reduction in milling time is most likely related to: (1) the different grain sizes in this reef type; and (2) the presence of altered silicate phases.

Investigation of particle sizes on the behavior of a rock during milling and grinding has shown that for rocks of the same nature, coarser-grained versions will break more easily compared to finer-grained versions (Tavares and Neves, 2008). This is because a mineral's resistance to fragmentation during milling and crushing is related to the size of the perimeter of that mineral. Greater surface exposure of a grain will result in greater phase contact where cracks can initiate (Tavares and Neves, 2008). Chromite grains from the UG2 main seam affected by

IRUP intrusion have undergone major grain size changes in response to the intrusion of the IRUP. These textural changes, which are more prominent at the top and bottom of the UG2 main seam, are characterised by significantly coarser chromite grains. UG2 normal reef and pothole reef ore is typically characterized by grain sizes of around 0.2mm diammeter. In comparison, the IRUP affected reef ore is characterized by grain sizes between 3 and 20 times this size, with a maximum grain size of around 4mm. This coarser-grained chromite from the UG2 main seam affected by IRUP is therefore likely to be a key component of its softness that resulted in the reduction of its milling time.

Additionally, it has been shown that the connectivity (which is partly a function of grain shape) of grains is an important parameter in controlling the mechanical response of a mineral during fracturing and crushing (Tavares and Neves, 2008). Chromite grains in the UG2 reef affected by IRUP intrusion are dominated by a pattern made up of polygonal grains that are in continuous contact on almost all their boundaries with other chromite grains. This closely packed pattern is more likely to favour continuous crack propagation from the point of crack initation. This process can in part be seen preserved in the main seam of the IRUP affected reef in the sections where brecciated grains are present. These brecciated grains probably represent zones where microcrack development (possible in response to hot fluids derived from the intruding IRUP; see Section 6.2 above) generated zones of shattered chromite. In contrast, the fine-grained chromite grains which have fewer points of contact, ie less connectivitiy, will favour discontinuous crack propagation because there is not a continuous medium through which the crack can propagate. Therefore, fine grained chromite often acts as a barrier to cracking. This is also true of the intercumulate minerals which are less rigid and will therefore tend to respond plastically to initial compression during crushing which also inhibits crack propagation (Tavares and Neves, 2008). Thus, the shorter milling time for the IRUP affected ore is also a function of the chromite grain shape and connectivity in this reef compared to the other two reef types.

Alteration is probably also an important component that contributes to the specific response of an ore during milling or crushing. Mineralogical studies of the UG2 main seam ore from

the three environments studied in this project show no visible alteration of cumulate chromite. On the other hand, the intercumulate minerals (orthpyroxene and plagioclase) do show the development of alteration, particularly in the case of the UG2 reef affected by IRUP intrusion where extensive development of secondary minerals such as serpentine, talc, chlorite, and amphibole. These secondary minerals progressively form from the continual breakdown of orthopyroxene preferentially along cleavage planes. This process results in the continual weakening of the internal structure (relationship between the cumulate and intercumulate components) of the UG2 main seam reef. In the case of the UG2 main seam ore affected by IRUP intrusion the intercumulate phase is mainly orthopyroxene which has altered to the above mentioned secondary minerals. This weakening process probably made a very significant contribution to the fast size reduction of the UG2 main seam ore for the IRUP affected reef by simply breaking along the highly altered and weakened orthopyroxene.

6.4.2 Flotation Performances

Investigation of the mineralogy of the three ore types of the UG2 main seam for this project revealed that the UG2 main seam normal ore and the UG2 main seam affected by pothole formation ore are quite similar. These two ore types are composed of chromite, plagioclase and orthopyroxene, with the normal reef ore containing additional chlorite as a secondary phase. Comparatively the UG2 main seam affected by IRUP intrusion ore comprises chromite, orthopyroxene and serpentine. Analysis of the flotation performance of these three ore types showed that the UG2 main seam ore affected by IRUP intrusion is characterised by a greater recovery of mass and water with no depressant addition, compared to the UG2 main seam normal reef ore and the UG2 main seam ore affected by pothole formation. When depressant is added, the amount of material and water recovered from the UG2 ore affected by IRUP reef is less than the amount of material recovered in the UG2 main seam normal and the UG2 affected by potholed formation ores which both showing similar mass recoveries. The decrease in the amount of recovered material from the UG2 main seam ore affected by IRUP intrusion is indicative of the recovery process of material taking place not only by entrainment but also by mineral association to naturally floatable minerals.

Mass recovery characterisation of these ores (see Section 5.4.1) revealed the presence of Si, Mg, Cr and Fe rich minerals in varying proportions. These minerals, in all three ores types, were inferred to be orthopyroxene, its alteration products and chromite, with significantly higher masses of chromite present in the IRUP ore. The apparent association of chromite with naturally floatable minerals is only observed in the UG2 ore affected by IRUP intrusion. The reason for this association particular to the UG2 ore affected by IRUP intrusion can be found in the coarse-grained polygonal, brecciated and altered textural aspect of chromite from this ore type. These textural features, discussed in Section 6.2, probably resulted in the profound weakening and rapid disaggregation of the UG2 ore affected by IRUP intrusion as reflected in the shorter milling time for this ore. This appears to have resulted in the poor liberation of chromite from secondary alteration minerals talc, serpentine, amphibole and chlorite that are naturally floatable minerals. The association of poorly liberated chromite with naturally floatable secondary alteration minerals particularly talc is known to result in the flotation of chromite (Ekmekçi et al., 2003).

The composition of chromite investigated in this project was defined by two distinctive groups. The first group was present in all three ore types and characterised by chromite with $Cr/Fe^{2+}>1$. The second group was present only in the UG2 ore affect by IRUP intrusion and was characterised by chromite with $Cr/Fe^{2+}<1$ (see discussion in Section 6.3). These compositions resulted from two different processes, that is primary crystallisation of the magma ($Cr/Fe^{2+}>1$) and post-magmatic modification due to IRUP intrusion ($Cr/Fe^{2+}<1$). The postmagmatic IRUP intrusion was hypothetised to contribute in changing the flotation behaviour of chromite from the UG2 ore affected by IURP intrusion. In Section 5.5.2, MLA analysis on the different compositional groups showed that floatable chromite from the UG2 ore affected by IRUP had a similar composition to the two other ore types. It was therefore concluded that the floatable chromite from the UG2 ore affected by IRUP intrusion was only composed of chromite from the $Cr/Fe^{2+}>1$ composition. Therefore, the compositional changes of chromite trigered by IRUP intrusion was found not to have any impact on the floatation behaviour of chromite.

6.4.3 Floatable Chromite

Investigation of a selected fraction size (38-75µm) by MLA showed that chromite mostly floated in the UG2 ore affected by IRUP intrusion and less in the UG2 normal and pothole reef (Fig. 5.7). The other two reef types only showed minor flotation of chromite that reported to the concentrate mostly through entrainment. Liberation analysis showed that chromite was well liberated in all three ore types. For the normal reef ore only 7% was not liberated while for the pothole reef and the IRUP affected reef ores these values were 8% and 11% not liberated respectively (Section 5.5.3.1). However, based on the flotation performance, it seems that the mineral association with the 7%, 8% and 11% of chromite not liberated is very different. In the normal and pothole reef ores, the lack of alteration minerals, means that the chromite is associated primarily with orthopyroxene and plagioclase, neither of which are naturally floatable (Becker *et al*., 2009). In contrast, the UG2 main seam ore affected by IRUP intrusion has a much higher proportion of alteration minerals (See Section 6.2) and MLA characterisation indicates that the mineral association with the floatable chromite for this ore is dominated by the secondary alteration minerals serpentine, chlorite, amphibole and talc (see Fig. 5.9). These minerals are known to be naturally floatable, particularly talc (Brough, 2008).

In fig 5.9 talc does not appear to be a dominant phase. However, of these alteration minerals talc is the best known for rendering hydrophilic minerals, hydrophobic and therefore floatable. One possible explanation for the apparent lack of talc observation, is the interaction of the SEM resolution with the way in which talc occurs in alteration assemblages. Talc is known to occur along rims and fractures as orthopyxene breaks down, this result in composite particles of orthopyroxene-talc (Becker *et al*., 2009). Very fine rims of talc, not picked up by SEM, can still make a mineral float. An example of the ability of talc to render hydrophilic mineral hydrophobic is given by in Becker *et al*. (2009). This suggests that if the IRUP ore were to be processed it would be imperative to properly characterise the alteration mineral assemblage which makes up the IRUP affected ore as this alteration assemblage has a profound effect on the way in which the IRUP ore behaves during mineral processing, ie in a flotation cell.

This can be explained by the resolution of automated SEM instruments which are governed by the size of the electron beam and its interaction volume and as a result could be characterise by poor detection of the finer talc particle (5 µm) (Gottlieb *et al*., 2000). These fine talc particles as well as fine particles of other secondary minerals (serpentine, chlorite and amphibole) that show greater association with chromite in the UG2 ore affected by IRUP intrusion could account for flotation of the seemingly free chromite.

6.5 Implications

UG2 ore affected by IRUP intrusion in platinum mining activities usually represents unmined regions. If mined these regions present both advantages and disadvantages with respect to the beneficiation of the UG2 ore. The UG2 ore affected by IRUP intrusion as already characterised above represents a UG2 ore that has deeply weakened by alteration triggered by the intrusion of the IRUP. The grinding process of such an ore concomitantly with the UG2 reef conventional ore can result in the over-grinding of this softer UG2 ore because the soft IRUP affected ore will disaggregate and become finer faster than the conventional UG2 ore. Although this over-grinding of the ore will result in good liberation of the valuable minerals (PGMs), the over-grinding process could lead to the grinding of the valuable mineral to finer particles that may poorly attach to bubbles in the pulp and consequently be lost to the tailings. The over-grinding of the UG2 ore affected by IRUP intrusion can also result in the production of finer chromite (formation of slime) that could easily be entrained by water and result in the dilution of the PGM grade. In addition, the use of standard depressant addition for normal reef ore when processing the UG2 ore affected by IRUP, means insufficient depressant is added to depress floatable gangue associated with UG2 ore affected by IRUP intrusion. This is because UG2 affected by IRUP as presented in section 6.2 is characterised by a great amount of associated naturally floated gangue. On the contrary, an addition of high depressant dosage to depress the great amount of floatable gangue association of the UG2 ore affected by IRUP can result in depressing more PGM carriers in the form of middlings. One of the consequences of the depression of middlings by high depressant dosage addition could be the reduction in PGM grade.

If the UG2 ore affected by IRUP intrusion were to be mined and processed, it should be done separately from the normal reef ore. The UG2 ore affected by IRUP intrusion which is a softer ore as presented in section 6.4.1, can be ground faster, resulting in a greater throughput than the other two ores due to its faster milling time (i.e. can get more IRUP ore through the mill in the same time interval as the two other ore types). One of the practicability parts of this process could take in account keeping this ore separate from the normal ore and stockpile it to a point where it can be efficiently processed. The second option of processing this ore could be together with the two other ore types. In that case the practicability of this would have to be studied properly in order to adjust milling time and reagent dosage to accommodate the combined ore. Treating these ores concomitantly without studying the parameters of its feasibility will result in a waste of energy which is a problem of concern in South Africa, given the South Africa's current energy crisis.

Chapter 7: CONCLUSION AND RECOMMENDATIONS

7.1 Conclusion

The principal goal of this study was to investigate the mineralogical characteristics and flotation performances of the UG2 main seam chromitite layer in a "normal reef" environment, in a UG2 reef affected by pothole formation environment and in a UG2 reef affected by IRUP intrusion environment. This was done for the purpose of examining any relationship between the mineralogical characteristics and flotation performance of chromite in these three environments.

From this study, the following conclusions can be made:

- Of the three environments studied, the UG2 normal reef and UG2 reef affected by pothole formation presented similar textural features, principally characterised by sub-equant anhedral fined-grained chromite, with minor intercumulate orthopyroxene and plagioclase. Chromite grains in the pothole formation environment locally demonstrated unusual irregular shapes, the origin of which was outside the scope of this project. The UG2 reef affected by IRUP intrusion was characterised by postcumulate textures dominated by highly fractured to brecciated grains and annealed polygonal grains with secondary silicates such as talc and serpentine present in the interstices between the chromite grains.
- Compositionally, the "UG2 normal reef" and the UG2 reef affected by pothole formation showed similar compositions comprising chromite ($Cr/Fe^{2+}>1$), whereas the UG2 affected by IRUP intrusion is characterised by two trends of compositions, one trend similar to the chromite from normal and the pothole reefs and a second trend that is Fe-Ti-rich and classifies as a magnetite ($Cr/Fe^{2+}<1$) transitional to

ulvöspinel composition. This second composition is associated with the roughly bottom 3 cm of the UG2 main seam near the contact with the footwall.

- The UG2 reef affected by IRUP intrusion was characterised by the shortest milling time and is the softest ore type, whereas the UG2 normal reef with the longest milling time is the hardest ore type. However, in comparison to the UG2 IRUP ore type, the UG2 normal and potholed reef ores have similar grinding behaviour. The main distinctive features potentially influencing the milling time in the UG2 affected by IRUP intrusion ore is the presence of annealed fractured grains, compositional changes in those grains and/or the highly altered aspect of this ore type. All these changes are linked to the emplacement of the IRUP.
- The UG2 normal reef ore and UG2 affected by pothole formation reef ore showed small amounts of floatable chromite due to minor attachment to silicates and alteration products found in those ores. In contrast, the UG2 affected by IRUP intrusion ore type is characterised by the highest amount of floated chromite. This was principally due to the attachment of chromite grains to a higher proportion of naturally floatable gangue that resulted from the alteration of primary pyroxenes to serpentine, talc and amphibole due to IRUP intrusion.

7.2 RECOMMENDATIONS

In the light of this study, the following recommendations can be made.

- The conclusions reached by this study are relevant to the sample materials tested and characterised only because of the limitations in the sample size investigated. Given the possibility that the 13kg of sample materials used for each triplicate is considered for representivity (Gy, 1978), it is highly recommended that further work from Waterval Shaft is conducted with representative samples of more appropriate masses to confirm these findings.
- With respect to the unusual nature of potholes and IRUP at Waterval, further studies should be undertaken to effectively characterise the nature of these features and

understand their relationships with mineralised reefs particularly the UG2 main seam

- It would be of good interests to characterise the mineralogical modifications that occur on PGMs subsequent to IRUP emplacements.

- Characterise the flotation properties of other gangue minerals resulting from the breakdown of orthopyroxene due to IRUP intrusion, particularly serpentine, chlorite, amphibole and serpentine and understand their effects on mineral beneficiation of the UG2 ore.

- An extensive process mineralogy studies done on the UG2 main seam and perhaps on the UG2 leader ores, to further investigate the variability of flotation performances, in terms of grinding and flotation performance, of this/these mineralised reef(s) as they approach pothole and IRUP areas.

Reference

Ballhaus, C.G. (1988): Potholes of the Merensky Reef at Brakspruit Shaft, Rustenburg Platinum Mines: Primary Disturbances in the Magmatic Stratigraphy. *Economic Geology*. Vol 83, pp. 1140-1158.

Barnes, S.-J., Maier, W. D. & Ashwal, L. D. (2004): Platinum-group-element distribution in the Main Zone and Upper Zone of the Bushveld Complex, South Africa. Chemical Geology 208, 293–317.

Baum, W., Lotter, N.O. and Whittaker, P.J. (2006): Process Mineralogy - A new generation for ore characterisation and plant optimization. Paper presented at *SME Annual Meeting*, Colorado.

Becker, M., Mainza, A.N., Powell, M.S., Bradshaw, D.J. and Knopjes, B. (2008): Quantifying the influence of classification with the 3 product cyclone on liberation and recovery of PGMs in UG2 ore. *Minerals Engineering*. 21, 549-558.

Becker, M., Harris, P.J., Wise, J.G. and Bradshaw, D.J. (2009): Mineralogical characterization of naturally floatable gangue in the Merensky reef of floatation. *International Journal of Mineral Processing*. pp. 1-35.

Bradshaw, D.J., Harris, P.J. and O'Connor, C.T. (2005): The effect of collectors and their interaction with depressants on the behavior of the froth phase in flotation. Presented at Centenary of Flotation Symposium, Brisbane, Australia.

Brough C. (2008). An investigation into the process mineralogy of the Merensky Reef at Northam Platinum Limited. MSc thesis, University of Cape Town.

Buntin, T.J., Grandstaff, D.E., Ulmer, G.C. and Gold, D.P. (1985): A pilot study of geochemical and redox relationships between potholes and adjacent normal Merensky reef of the Bushveld Complex. *Economic Geology.* Vol. 80, pp. 975-987.

Cameron, E.N. and Glover E.D. (1973): Unusual Titanian-Chromian Spinels from the Eastern Bushveld Complex. *American Mineralogist*, Vol. 58, pp. 172-188.

Cameron, E.N. (1977): Chromite in the central sector of the Eastern Bushveld Complex, South Africa. *American Mineral*. 62, 1082-1096.

Cawthorn, R.G. (1999): The platinum and palladium resources of the Bushveld Complex. *South African Journal of Science*, 95, pp. 481-489.

Cawthorn, R.G., Eales, H.V., Walraven, F., Uken, R. and Watkeys, M.K. (2006): The Bushveld Complex. *In*: Johnson, M.R., Anhaeusser, C.R. and Thomas, R.J. (Eds) The Geology of South Africa, pp. 261-281.

Cawthorn, R.G. and Barry, S.D. (1992): The Role of intercumulus residua in the formation of the pegmatoid association with the UG2 chromitite, Bushveld Complex. *Australian Journal of earth Sciences.* Vol. 39, pp. 263-276.

Cawthorn, R.G. and Walraven, F. (1998): Emplacement and crystallisation time for the Bushveld Complex. *Journal of Petrology*. Vol. 39, pp. 1669-1687.

Creelman, R.A. and Ward, C.R. (1996): A scanning electron microscope method for automated, quantitative analysis of mineral matter in coal. *International Journal of Coal Geology.* Vol. 30, pp. 249-269.

Crockett, R.N. (1969): The Geological significance of the margin of the Bushveld Basin in Botswana with particular reference to the Lobatse and Ramaotswa areas. Trans. *Geol. Soc. S. Afr*., 74: 211-235.

Deer, W.A., Howie, R.A. and Zussman, J. (1992): An introduction to the rock forming minerals, 2nd Edition.

Fragomeni, D., Hoffman, M., Kelly, A., Yu, S. and Lotter, N.O. (2006): FLOTATION MINI PILOT PLANT EXPERIENCE AT FALCONBRIDGE LIMITED. Paper presented at a conference, Sudbury.

Droop, G.T.R. (1987): A general equation for estimating Fe^{3+} concentrations in ferromagnesian silicates and oxides from microprobe analyses, using stoichiometric criteria. *Mineralogical Society,* Vol. 51, pp. 431-5

du Plessis, C.P. and Walraven, F. (1989): The tectonic setting of the Bushveld Complex in Southern Africa, Part 1. Structural deformation and distribution. *Technophysics*, Vol. 179, pp. 305-319.

Eales, H.V. (2001): A first introduction to the geology of the Bushveld Complex and those aspects of South African geology that relate to it. *The Council of Geosciences*. Vol. 2, pp. 38-39.

Eales, H.V. and Cawthorn, R.G. (1996): The Bushveld Complex. In: Cawthorn, R.G., (Eds), *Layered intrusions*. *Development in Petrology*. Vol. 15, pp. 181–229.

Eales, H.V. and Reynolds, I.M. (1986): Cryptic Variation within Chromitite of the Upper critical Zone, Northwestern Bushveld Complex. *Economic Geology*. Vol. 81, pp. 1056-1066.

Ekmekçi, Z., Bradshaw, D.J., Allison, S.A. and Harris, P.J. (2003): Effect of frother type on the flotation behaviour of chromite in the UG2 ore. *Minerals Engineering.* V.16, pp. 941-949.

Engelbrecht, J.P. (1985): The chromite of the Bushveld Complex in the Nietverdiend Area. *Economic Geology*. Vol. 80, pp. 896-910.

Engelbrecht, J.A. and Woodburn, E.T. (1975). The effect of froth height, aeration rate and gas precipitation on flotation. *J. S. Afr. Inst. Min. Metall*., 10, 125–132.

Fandrich, R., Gu, Y., Burrows D. and Moeller, K. (2007): Modern SEM-based mineral liberation analysis. *Inter. J. Miner process*. 84, 310-320.

Gallios, G.P., Deliyanni, E.A., Peleka, E.N. and Matis, K.A. (2007): Flotation of chromite and serpentine. *Separation and purification technology*. Vol. 55, pp. 232-237.

Godel, B., Barnes, S.J. and Maier, W.D. (2007): Platinum-Group Elements in Sulphide Minerals, Platinum-Group Minerals, and Whole-Rocks of the Merensky Reef (Bushveld Complex, South Africa): Implications for the Formation of the Reef. *Journal of Petrology.* Vol. 48, No. 8, pp. 1569-1604.

Goldstein, J. I., Newbury, D. E., Echlin, P., Joy, D. C., Lyman, C. E., Lifshin, E., Sawyer, L. and Michael, J. R. (2003): Scanning Electron Microscopy and X-Ray Microanalysis. 3rd ed, pp. 416-451.

Gottlieb, P., Wiilkie, G., Sutherland, D., Ho-Tun, E., Suthers, S., Perera, A., Jenkins, B., Spencer, S., Butcher A.R. and Rayner, J. (2000): Using quantitative electron microscopy for process mineralogy applications. *JOM 52*, 24-27

Gu, Y. (2003): Automated Scanning Electron Microscope Based Mineral Liberation Analysis. *Journal of Minerals and Materials Characterisation and Engineering.*

Gu, F. and Wills, B.A. (1988): Chromite Mineralogy and Processing. *Mineral Engineering*. Vol. 1, No. 3, pp. 235-240.

Gy, P.M., 1978. Sampling of Particulate Materials – Theory and Practice.

Hatton, C.J. and von Gruenewaldt, G. (1987): The geological setting and petrogenesis of the Bushveld chromite layers. In: Stowe, C.W. (ed.) Evolution of Chromium ore fields. New York: Van Nostrand Reinhold Co., 109-143.

Henley, K.J. (1983): Ore-Dressing Mineralogy – A Review of Techniques, Applications and Recent Developments. Spec. Publ. *Geol. Soc. S. Afri*., 7, pp175-200.

Hey, P.V. (1999): The effects of weathering on the UG2 Chromitite reef of the Bushveld Complex, with special reference to the platinum-group minerals. *South African Journal of Geology.* Vol. 102; No. 3, pp. 251-260.

Holwell, D. A., Boyce, A. J. and McDonald, I. (2007): Sulfur Isotope Variations within the Platreef Ni-Cu-PGE Deposit: Genetic Implications for the Origin of Sulfide Mineralization. *Economic Geology*. v. 102; No. 6; p. 1091-1110.

Hulbert, L.J and Von Gruenewaldt, G. (1985): Textural and Compositional Features of Chromite in the Lower and Critical Zones of the Bushveld Complex South of Potgietersrus. *Economic Geology.* Vol. 80, pp. 872-895.

Hunter, D.R. (1973a): The Bushveld Complex: a review. *Econ. Geol. Res. Unit.,* Univ. Witwatersrand, Info. Circ., 79, pp. 11.

Hunter, D.R. (1975): The regional geological setting of the Bushveld Complex (An adjunct to the provisional tectonic map of the Bushveld Complex). *Econ. Geol*. *Res. Unit*., Univ. Witwatersrand, 18pp

Hunter, D.R. (1976): Some Enigmas of the Bushveld Complex. *Econ. Geol*., 71: 229-248.

Irvine, T.N. (1965): Chromian Spinel as a Petrogenetic Indicator Part 1. Theory. *Canadian Journal of Earth Sciences*. Vol. 2, pp. 648-672.

Jansen, H. (1982): The Geology of the Waterberg basin in the Transvaal, Republic of South Africa. Mem. *Geol. Surv. S. Afr*., 71, pp. 98.

Kinloch, E.D. and Peyerl, W. (1990): Platinum-Group Minerals in Various Rock Types of the Merensky Reef: Genetic Implications. *Economic Geology*. Vol. 85, pp. 537-555.

Lastra, R. (2007): Seven practical application cases of liberation analysis. *Int*. *J. Miner. Process.,* 84. 337-347.

Lee, C.A. (1981): Post deposition structures in the Bushveld Complex mafic sequence. *J. Geol. Soc*. (Lond) 138: 327-341.

Li, C., Ripley, E.M., Merino, E. and Maier W.D. (2004): Replacement of base metal sulfides by actinolite, epidote, calcite, and magnetite in the UG2 and Merensky reef of the Bushveld Complex, South Africa. *Economic Geology.* Vol. 99; No. 1, pp. 173-184.

Lotter, N.O., Whittaker, P.J. Komos, L. Stckling, J.S. and Wikie, G.J. (2002): The Development of Process Mineralogy at Falconbridge Ltd., and application to the Raglan Mill, *CIM Bulletin*, Vol. 95, No. 1066, pp. 85-92.

Lumpkin, G.R. (2001): Crystal chemistry and durability of the spinel structure type in natural systems. *Progress in nuclear energy.* vol. 38, No. 3-4, pp. 447-454.

MacGregor, D. and Charles, H.S. (1963): The use of chrome spinels in petrographic studies of ultramafic intrusion. *Geological Survey of Canada in the Canadian Mineralogist*.

Mailula, T.D., Bradshaw, D.J. and Harris, P.J. (2003): The effect of copper sulphate addition on the recovery of chromite in the flotation of UG2 ore. *Journal of the South African institute of Mining and Metallurgy*. V.103. No. 2, pp. 143-146.

Mainza, A., Powell, M.S. and. Knopjes, B. (2005): A comparison of different cyclons in addressing the challenges in the classification of the dual density UG2 platinum ore. *The Journal of the South African Institute of Mining and Metallurgy*. Vol. 105, pp. 431-348.

McKenzie, A. (1996). The presence of spinel during matte smelting. *Proc.Trends in Base Metal Smelting and refining, Johannesburg.*

McLaren, C.H. and De Villiers, J.P.R. (1982): The platinum group chemistry and mineralogy of the UG-2 chromitite layer of the Bushveld Complex. *Econ. Geol*. Vol. 77, pp. 1348-1366.

Merkle, R.K.W. (1988): The effects of metasomatising fluids on the PGE-content of the UG1 chromitite layer. In *Geo-Platinum* 87 (Prichard, H.M., Potts, P.J., Bowles, J.F.W. and Cribb, S.J., eds.) Elsvier, London, U.K. (359).

Mondal, S. K. and Mathez, E. A. (2007): Origin of the UG2 chromite layer, Bushveld Complex. *Journal of petrology*. Vol.48. No. 3, pp. 495-510.

Neethling, S.J. and Cilliers, J.J. (2001): Simulation of the effect of froth washing on flotation performance. *Chem. Eng. Sci*. 56, pp. 6303-6311.

Neethling, S.J. and Cilliers, J.J. (2002): The entrainment of gangue into a flotation froth. *Int. J. Miner. Process.* Vol. 64, pp. 123-134.

Nel, E., Valenta, M. and Naude, N. (2005): Influence of open circuit regrinding milling on UG2 ore composition and mineralogy at Impala's UG2 concentrator. *Mineral Engineering*. Vol. 18, pp. 785-790.

Oosthuysen, M. (2008): personal communication, Waterval Mine, Geology department.

Penberthy, C. J., Oosthuyzen, E. J and Merkle, R. K. W. (2000): The recovery of platinum-group elements from the UG-2 chromitite, Bushveld Complex – a mineralogical perspective. *Mineralogy and Petrology.* Vol. 68, No. 1-3, pp. 213-222.

Pouchou, J.L. and Pichoir, F. (1991): Electron Probe Quantitation, K.F.J. Heinrich and D.E. Newbury Eds. (Plenum Press, New York,) p. 31.

Reid, D.L. and Basson, I.J. (2002): Iron ultramafic pegmatite replacement bodies within the Upper Critical Zone, Rustenburg Layered Suite, Northam Platinum Mine, South Africa. *Mineralogical Magazine*. Vol.66 (6), pp. 895-914.

Roach, T.A., Roeder, P.L. and Hulbert, L.J. (1998): Composition of Chromite in the Upper Chromitite, Muskox Layered Intrusion, Northwest Territories. *The Canadian Mineralogist*. Vol. 36, pp. 117-135.

Rule, C.M. and Anyimadu, A.K. (2007): Flotation cell technology and circuit design-an Anglo Platinum perspective. *The Journal of the Southern African Institute of Mining and Metallurgy*. Vol. 107, pp 615-622.

SACS (SOUTH AFRICAN COMMITTEE FOR STRATIGRAPHY). (1980): Stratigraphy of South Africa, South West Africa/Namibia and the Republics of Bophutswana, Transkei and Venda. *Handbook of the Geological Survey of South Africa 8*.

Savassi, O.N. (2005): A compartment model for mass transfer inside a conventional flotation cell. *International Journal of Mineral Processing.* Vol.77, pp. 65-79.

Savassi, O.N., Alexander, D.J., Franzidis, J.P and Manlapig, E.V. (1998): An ampirical model for entrainment in industrial flotation plant. *Mineral Engineering*. Vol. 11, No. 3, pp. 243-256.

Schouwstra, R.P., Kinloch, E.D. and Lee, C.A. (2000): A Short Geological Review of the Bushveld Complex. *Platinum Metal Review*, Vol. 44, (1), pp. 33-39.

Scoon, R.N. and Eales, H. (2002): Unusual Fe-Ti-Cr spinels from discordant bodies of iron-rich ultramafic pegmatite at the Amandebult Platinum mine, northwestern Bushveld Complex. *Mineralogical Magazine.* Vol. 66, No. 6, pp. 857-879.

Smith, D.S., Basson, I.J. and Reid D.L. (2003): Normal reef subfacies of the Merensky Reef at Northam Platinum Mine, Zwartklip Facies, Western Bushveld Complex, South Africa. *The Canadian Mineralogist.* Vol. 42, pp. 243-260.

Tavares, L.M. and das Neves, P.B. (2008): Microstructure of quarry rocks and relationships to particle breakage and crushing. *International Journal of Mineral Processing.* Vol.87, pp. 28-41.

Ulusoy, U. and Yokeler, M. (2005): Correlation of the surface roughness of some industrial minerals with their wettability parameters. *Chemical Engineering and Processing.* Vol. 44, Issue 5, pp. 555-563.

Valenta, M. (2007): Balancing the reagent suite to optimize grade and recovery. *Mineral Engeering*. Vol. 20, pp. 979-985.

van Schoor, M. (2005): The application of in-mine electrical resistance tomography (ERT) for mapping potholes and other disruptive features ahead of mining. *The journal of The South African Institute of mining and metallurgy*. Vol. 105, pp. 447-452.

Vermaak, C.F. and Von Gruenewaldt, G. (1986): Introduction to the Bushveld Complex. In: Anhaeusser, C.R. and Maske, S. (Eds) *Mineral Deposits of Southern Africa*. 2, Geol. Soc. S. Afr., pp. 1021-1029.

Viljoen, M.J and Hieber, R. (1986): The Rustenburg Section of the Rustenburg Platinum Mines Limited, With reference to the Meresky Reef. *In.* Anhaeusser, C.R and Maske, S. eds. *Mineral deposits of Southern Africa,* Vols. I and II, pp. 1107-1134. Geol. Soc. S. Afr., Johannesburg.

Viljoen, M.J. and Scoon, R.N. (1985): The distribution and main geologic features of discordant bodies of iron-rich ultramafic pegmatite in the Bushveld Complex. *Economic Geology*; Vol. 80, no. 4, p. 1109-1128.

Viring, R.G, and Cowell, M.W. (1999): The Merensky Reef on Northam Platinum Limited. *S. Afr. J. Geol*. 102: 192-208.

Voordrouw, R., Gutzmer, J. and Beukes, N.J. (2009): Intrusive origin for the Upper Group (UG1, UG2) stratiform chromitite seams in the Dwars River area, Bushveld Complex, South Africa. *Miner Petrol.*

Wagner, P.A. (1929): The platinum deposits and mines of South Africa: Edinburgh, Oliver and Boyd.

Walraven, F., Amstrong, R.A. and Kruger, F.J. (1990): A chronostratigraphic framework for north-central Kaapvaal craton, the Bushveld Complex and the Vredofort structure: *Tectono-physics*, Vol. 171, pp.23-48.

Wesseldijk, M.A., Reuter, Bradshaw, D.J. and Harris, P.J. (1999): The Flotation Behaviour of Chromite with Respect to the Beneficiation of the UG2 Ore. *Mineral Engineering*, V.12. No. 10, pp. 1177-1184.

White, J.A. (1994): The Potgieterus prospect-geology and exploration history. In: Anhaeusser, C.R. (Ed), Proceedings XVth CMMI congress. *The South African Institute Mining and Metallurgy Johannesburg*, 173-181.

Wiese, J. (2009): Investigating depressant behaviour on the flotation of selected Merensky ores. MSc thesis, University of Cape Town.

Wiese J.G., Harris P.J., Bradshaw D.J. (2005): The influence of the reagent suite on the flotation of ores from the Merensky Reef. *Minerals Engineering* 18: 189-198.

Wills, B.A. (1988): Mineral Processing Technology. An Introduction to the Practical Aspects of Ore Treatment and Mineral Recovery. 4th Edition, pp. 1-50.

Wills B.A. and Napier-Munn, T.J. (2006). Will's Mineral Processing Technology: An introduction to the practical aspects of ore treatment and mineral recovery. Elsevier: Amsterdam.

Yamazaki, D., Yoshino, T., Matsuzaki, T., Katsura, T and Yoneda, A. (2009): Texture of (Mg, Fe) SiO_3 perovskite and ferro-periclase aggregate: Implications for rheology of the lower mantle. *Physics of the Earth and Planetary Interiors,* Vol. 174, pp. 138-144.

Yekeler, M., Ulusoy, U. And Hiçylmaz, C. (2004): Effect of particle shape and roughness of talc mineral ground by different mills on the wettability and floatability. *Powder Technology*. Vol. 140, pp.68-78.

Sample No	Reef Type	Location	Stratigraphic Position	Grain size	Percentage Mineralogy							Description	Alteration	Annealing	Grain size distribution
					Opx	Plag	Chr	Cpx	Serp	Bt	Qtz				
WNR1	UG2 Normal Reef	Upper Contact	UG2 Hangingwall Norite	Fine to medium	70-80	10-15	≤1	≤1	0	0	0	Equigranular texture in which orthopyroxene is the cumulate phase and plagioclase the main interstitial phase. Chromite and biotite are absent or are in very minor proportions	Absent	Absent	Heterogeneous
			UG2 Main Seam	Fine	5-7	10-15	65-75	0	0	0	0	Granular texture in which fine grained chromite is the cumulate phase. Large annealed chromite grains are rarely seen. Patches of orthopyroxene are noticeable by their yellow bronish color	Absent	Very little	Heterogeneous
WNR2	UG2 Normal Reef	Middle Section	UG2 Main Seam	Fine	5-7	10-15	65-75	0	0	0	0	Chromite shows variable grain sizes. Annealing is rarely seen, but if present characterizes areas of darker and coaser grains than the unannealed areas	Absent	Very little	Heterogeneous
WNR3	UG2 Normal Reef	Bottom Contact	UG2 Main Seam	Fine	5-7	15-20	70-80	0	0	0	0	UG2 middle seam principally composed of cumulate chromite with of a granular texture. Plagioclase represents the interstial phase. Orthopyroxene is seen as brown spots on the sample	Absent	Mildly present	Heterogeneous
			Pegmatoidal Footwall Norite	Medium to coarse	70-80	10-15	≤1	≤2	0	≤2	0	Yellow-brown randomly distributed orthopyroxene represents the main phase of this sample. Plagioclase is the second most important phase, It is localized in the interspace between orthopyroxene. Accessory chromite, biotite and clinopyroxene are present but hard to indentify.	Present	Absent	Heterogeneous
WNR4	UG2 Normal Reef	Upper Contact	UG2 Hangingwall Norite	Fine to medium	75-85	10-15	≤1	≤1	0	0	0	Equigranular hangingwall norite characterized by the abundance presence of the orthopyroxene phase and secondary plagioclase. Chromite and biotite seem to be absent	Absent	Absent	Heterogeneous
			UG2 Main Seam	Fine	4-6	10-15	75-85	0	0	0	0	Granular texture mainly composed of fine grained chromite interspaced by plagioclase. Orthopyroxene is noticeable on this sample by its characteristic yollow brownish color.	Absent	Absent	Heterogeneous
WNR5	UG2 Normal Reef	Middle Section	UG2 Main Seam	Fine	5-7	10-15	65-75	0	0	0	0	Fine grained chromite is the overall aspect of this sample. It is granular and annealing is hardly noticed. Plagioclase occupies spaces between chromite grains.	Absent	Absent	Heterogeneous
WNR6	UG2 Normal Reef	Bottom Contact	UG2 Main Seam	Fine to medium	5-7	12-17	70-80	0	0	0	0	UG2 Main Seam bottom part in sharp but sinous contact with its footwall. This part is dominated by cumulus chromite with of a grnular texture. Feldspar represents the interstial phase. Orthopyroxene is seen as brown spots on the sample	Absent	Absent	Heterogeneous
			Pegmatoidal Footwall Norite	Fine	70-80	10-15	≤1	≤3	0	0	0	Pegmatoidal feldspatic pyroxenite (norite) footwall composed of corase grained orthopyroxe and plagioclase . Chromite can be seen as inclusions and at the boundary of these two principal mineral phases.	Absent	Absent	Heterogeneous
WNR7	UG2 Normal Reef	Upper Contact	UG2 Hangingwall Norite	Fine to medium	60-70	10-15	≤1	≤1	0	0	0	Fine to medium grained haningwall norite with orthopyroxene representing the main cumulate phase followed by plagioclase which the second main phase. Chromite and biotite are almost absent on this spmale.	Absent	Absent	Heterogeneous
			UG2 Main Seam	Fine	3-5	10-15	70-80	0	0	0	0	Fine grained granular UG2 main seam in sharp contact with its hangingwall feldspatic pyroxenite (norite).	Absent	Absent	Heterogeneous
WNR8	UG2 Normal Reef	Middle Section	UG2 Main Seam	Fine	3-5	10-15	70-80	0	0	0	0	Granular middle section of the UG2 chromitite Main Seam. This part of the section is also an illustaration of the variation in grain size distribution. This is shown by the coloring variation from dark to dark grey zones.	Absent	Absent	Heterogeneous
WNR9	UG2 Normal Reef	Bottom Contact	UG2 Main Seam	Fine to medium	5-7	10-15	65-75	0	0	0	0	UG2 Main Seam bottom part principally composed of cumulate chromite of a grnular texture. Feldspar represents the interstial phase and the second most important mineral phase. Accessory orthopyroxene is seen as eyellow brownish spots on the sample.	Absent	Present	Heterogeneous
			Pegmatoidal Footwall Norite	Medium to coarse	60-70	15-25	≤1	≤3	0	≤1	0	Pegmatoidal footwall norite mainly composed of more than yellow brown orthopyroxene, plagioclase. Chromite, biotite and clinopyroxene are accessory phases.	Present	Absent	Heterogeneous
WP1	UG2 potholed reef	Top Contact	UG2 Hangingwall Norite	Fine to medium	65-75	15-20	≤1	0	0	0	0	This hangingwall norite is characterized by a granular texture in which orthopyroxene is dominant over plagioclase. Despite its tiny proportion, chromite is the only accessory phase observable among the two dominant phases of this sample.	Absent	Absent	Heterogeneous
			UG2 Main Seam	Fine	5-7	10-15	70-80	0	0	0	0	This chromitite rock type sample is dominated like its name says by chromite grains. The latter are mainly fine. Small annealed areas with slighly coraser grains of darker color are present. The overall bulk gives a granular texture.	Absent	Almost absent	Heterogeneous
WP2	UG2 potholed reef	Middle Section	UG2 Main Seam	Fine	≤3	10-15	75-85	0	0	0	0	Granular texture mainly composed of fine grained chromite cemented together by plagioclase which fill in interspaces between chromite grains. Orthopyroxene is noticeable by the presence of yollow brownish color spots.	Absent	Absent	Heterogeneous
WP3	UG2 Potholed Reef	Bottom Contact	UG2 Main Seam	Fine to medium	≤4	10-15	75-85	0	0	0	0	Close to the contact region, the granular UG2 main seam shows a coarser texture in which annelling is also better expressed compare to the middle and upper section	Absent	Present	Heterogeneous
			Pegmatoidal Footwall Norite	Medium to coarse	75-90	7-10	≤1	≤2	0	≤1	0	UG2 Pegmatoidal footwall in which biotite is observed. Chromite is present at the boundary of the two principal phases orthopyroxene and plagioclase. But it is also seen as inclusion in these latter. These inclusions are better seen in plagioclase due to their constrating colors	Present	Absent	Heterogeneous
WP4	UG2 Potholed Reef	Top Contact	UG2 Hangingwall Norite	Fine to medium	60-70	20-25	≤1	0	0	0	0	This hangingwall rock displays a granular texture which consists predominently of orthopyroxene and plagioclase	Absent	Absent	Heterogeneous
			UG2 Main Seam	Fine	≤7	20-25	60-70	0	0	0	0	Granular texture mainly composed of fine grained chromite interspaced by plagioclase. The yellow brownish color characterizes the presence of orthopyroxene.	Absent	Almost absent	Heterogeneous
WP5	UG2 Potholed Reef	Middle Section	UG2 Main Seam	Fine	≤5	10-15	75-85	0	0	0	0	Granular UG2 chromitite main seam. This part of the main seam section is another illustration of the variation in grain size distribution. This is shown by the variation in color from dark to dark grey areas.	Absent	Little	Heterogeneous
WP6	UG2 Potholed Reef	Bottom Contact	UG2 Main Seam	Fine	≤5	10-15	75-85	0	0	0	0	This is a medium grained granular UG2 main seam sample composed principally chromite grains. These chromite grains show a slightly friable aspect.	Absent	Absent	Heterogeneous
			Pegmatoidal Footwall Norite	Coarse	75-90	7-10	≤1	≤2	0	≤1	0	Very coarse grained pegmatoidal feldspatic pyroxenite (norite) footwall composed mainly of corase grained orthopyroxe and plagioclase. Chromite and biotite are randomly distributed and represent accessory phases	Present	Absent	Heterogeneous

Sample No	Reef Type	Location	Stratigraphic Position	Grain size	Percentage Mineralogy							Description	Alteration	Annealing	Grain size distribution
					Opx	Plag	Chr	Cpx	Serp	Bt	Qtz				
WP7	UG2 Potholed Reef	Top Contact	UG2 Hangingwall Norite	Fine to medium	60-70	20-25	≤1	≤2	0	0	0	Hangingwall norite characterized by a granular texture. The main components of this sample are orthopyroxene and plagioclase. Plagioclase seems to represent the matrix to the pyroxene. Chromite and other common minerals are almost absent at this position.	Absent	Absent	Heterogeneous
			UG2 Main Seam	Fine	75-90	7-10	≤1	≤2	0	0	0	Chromite is present with fine variable grain sizes. These ones, hardly form small annealed zones with slighly coraser grains and darker color. The overall bulk gives a granular texture.	Absent	Absent	Heterogeneous
WP8	UG2 Potholed Reef	Middle Section	UG2 Main Seam	Fine	≤4	10-15	75-85	0	0	0	0	UG2 chromitite main seam showing a granular texture. This part illustrats also the random grain size distribution. This is shown by the variation in color from dark to dark grey zones.	Absent	Little	Heterogeneous
WP9	UG2 Potholed Reef	Bottom Contact	UG2 Main Seam	Fine to medium	5-7	15-20	75-85	0	0	0	0	UG2 main seam bottom part principally composed of cumulate chromite of a grnular texture.Feldspar represents the interstial phase. pyroxene is seen as brown spot on the sample.	Absent	Present	Heterogeneous
			Pegmatoidal Footwall Norite	Medium to coarse	65-75	10-20	≤1	≤3	0	≤2	0	This pegmatoidal footwall norite is compositionally dominated by yellow brown coarse grained orthopyroxene and coarse grained plagioclase, accessory chromite, biotite and clinopyroxene are present at tiny proportions.	Present	Absent	Heterogeneous
WI1	UG2 with IRUP	Top Contact	UG2 Hangingwall Norite	Medium	70-80	15-20	≤0.5	≤1	0	0	0	Equigranular feldspatic pyroxenite hangingwall with a dark colour, it is principally composed of altered orthopyroxene and plagioclase. chromite is hardly seen above the contact boundary.	Present	Absent	Heterogeneous
			UG2 Main Seam	Fine to medium	≤2	7	≥85	0	0	0	0	This sample shows a dark shiny granular appearance and is in sharp contact with the hangingwall norite. Chromite grains at this contact are finer than those bellow the contact zone despite the presence of some coarser grains which are in minute proportions.	Absent	Present	Heterogeneous
WI2	UG2 Reef with IRUP	Middle Section	UG2 Main Seam	Fine to medium	≤1	7	≥85	0	0	0	0	This sample like the one decsribed just above shows a dark shiny granular appearance. Chromite grains at this location are of equal sizes to the one just above. The dark appearance is related to the reduced in plagioclase proportion.	Absent	Present	Heterogeneous
WI3	UG2 Reef with IRUP	Bottom Contact	UG2 Main Seam	Medium	≤1	≤5	80-90	0	0	0	0	The size of chromite grains at this location is clearly coarser than what was described some 30 to 40 cm above this stratigraphic position. Coarser annealed grains are also well represented.	Absent	Present	Heterogeneous
			Quartzo-feldspatic Pegmatoidal Footwall	Medium to coarse	~0	60-70	≤1	0	1	3-5	20-30	The transitional contact between the UG2 main seam and its footwall is marked by an important concentration in coarse grained micas. Two principal minerals pahses are present: Plagioclase and quartz. Accessory chromite is disseminated in feldspar but not in quartz.	Present	Absent	Heterogeneous
WI4	UG2 Reef with IRUP	Top Contact	UG2 Hangingwall Norite	Fine to medium	70-80	15-20	≤0.5	≤1	0	0	0	Equigranular feldspatic pyroxenite (norite) hangingwall identical in various aspects to its predecesseur hangingwall in the IRUP reef type environment.	Present	Absent	Heterogeneous
			UG2 Main Seam	Fine	~0	5-10	≥85	0	0	0	0	UG2 sample of composed of fine grained chromite of a dark shiny granular appearance. These grains display a disparity in density repartion already observed on other samples. The alteration process is portrayed by the presence of serpentine on the sample.	Present	Little	Heterogeneous
WI5	UG2 Reef with IRUP	Middle Section	UG2 Main Seam	Fine	≤3	7-12	75-85	0	≤1	0	0	Despite the presence of some medium sizes chromite grains, this UG2 main seam middle section sample mostly exhibits a fine grained texture. Some veins of serpentine and plagioclase run in different directions.	Present	Little	Heterogeneous
WI6	UG2 Reef with IRUP	Bottom Contact	UG2 Main Seam	Medium	≤3	10-15	70-80	0	≤1	0	0	This sample represents the bottom contact between the UG2 main seam and its quartzo-feldspatic pegmatoidal footwall. It is marqued by the presence of medium grained chromite dominating over the fine and minute corase grained. This assemblage gives a granular texture appearance.	Present	Present	Heterogeneous
			Quartzo-feldspatic Pegmatoidal Footwall	Very coarse	~0	60-70	≤1	0	0.01	2-3	20-30	The pegmatoidal footwall mainly composed of coarse grained plagioclase and quartz shows coarse grained biotite principally distributed along the boundary between the UG2 main seam and its footwall. The soapy habit of serpentine is still present in this footwall.	Present	Absent	Heterogeneous
WI7	UG2 affected by an IRUP intrusion	Top Contact	UG2 Hangingwall Norite	Medium	2-3	60-70	10-15	≤1	≤1	1-2	0	This sample is a medium equigranular feldspatic pyroxenite hangingwall. It is separated from the UG2 main seam by a sharp contact. Biotite can be observed on this sample. Few mm wide irregular fractures in whichplagioclase has crystallized can also be observed.	Present	Absent	Heterogeneous
			UG2 Main Seam	Fine to medium	≤3	10-15	70-80	0	0	0	0	The top band of the UG2 main seam on this sample exhibits a medium grained-size in comparison to the top part of the second band few centimeter bellow it. Despite the presence of few scattered medium sized grains, the second band is in majority composed of fine grains and presents almost similar characteristics to the previous top contact (W.I.1).	Present	Absent	Heterogeneous
WI8	UG2 affected by an IRUP intrusion	Middle Section	UG2 Main Seam	Fine to medium	0	10-15	≥1	0	0	1-2	0	This is the replica of the sample described just above. Indeed, it chairs common features with the second band of the UG2 main seam except for the absence of the alteration aspect.	Absent	Absent	Heterogeneous
WI9	UG2 affected by an IRUP intrusion	Bottom Contact	UG2 Main Seam	Medium	0	~4	60-70	0	≤1	1-2	0.01	This sample dominated by the medium sized chromite grains. In the contrarily of other samples, this one does not show the normal stratigraphic relationship, but exhibits a disrupted aspect in which the coarse grainplagioclase and quartz have recrystallized not only below the UG2 main seam but also above it in the form of a big vein.	Present	Present	Heterogeneous
			Quartzo-feldspatic Pegmatoidal Footwall	Very coarse	0	60-70	≤1	0	≤1	1-2	20-30	This hand specimen displays like its predecessors a metasomatic effect which has transformed the footwall into a very coarse grained quartzo-feldspatic pegmatoidal footwall. Accessory chromite and biotite are randomly scatered in this footwall.	Absent	Absent	Heterogeneous

Block No.	1b	1b	1b	1b	1b	1b	1b	1b	1b	1b
Raw Analysis	1.00	2.00	3.00	4.00	5.00	6.00	7.00	8.00	9.00	10.00
Cr2O3	44.10	44.67	45.01	44.81	45.07	45.30	45.01	45.83	45.56	45.45
Al2O3	15.62	15.73	15.81	15.68	15.92	15.60	16.14	15.91	16.06	16.11
TiO2	0.97	1.06	1.11	0.98	1.03	1.08	0.98	0.96	1.02	1.01
FeO	28.61	28.74	28.76	28.89	28.79	28.87	29.10	29.37	29.46	29.01
MgO	8.44	8.48	8.49	8.75	8.47	8.58	8.50	8.57	8.68	8.67
MnO	0.66	0.66	0.72	0.70	0.55	0.60	0.43	0.66	0.66	0.63
NiO	0.22	0.18	0.15	0.19	0.21	0.14	0.15	0.18	0.15	0.14
Total	98.61	99.52	100.05	100.01	100.03	100.17	100.31	101.47	101.59	101.02
MnO corrected	0.48	0.49	0.54	0.52	0.37	0.42	0.25	0.48	0.48	0.45
Total	98.43	99.34	99.87	99.83	99.85	99.99	100.13	101.29	101.41	100.84
Corrected Analysis										
Cr2O3	44.10	44.67	45.01	44.81	45.07	45.30	45.01	45.83	45.56	45.45
Al2O3	15.62	15.73	15.81	15.68	15.92	15.60	16.14	15.91	16.06	16.11
TiO2	0.97	1.06	1.11	0.98	1.03	1.08	0.98	0.96	1.02	1.01
FeO	21.62	21.96	22.15	21.62	22.22	22.12	22.44	22.41	22.37	22.23
Fe2O3	7.77	7.53	7.35	8.09	7.30	7.50	7.41	7.73	7.88	7.53
MgO	8.44	8.48	8.49	8.75	8.47	8.58	8.50	8.57	8.68	8.67
MnO	0.48	0.49	0.54	0.52	0.37	0.42	0.25	0.48	0.48	0.45
NiO	0.22	0.18	0.15	0.19	0.21	0.14	0.15	0.18	0.18	0.15
Total	99.21	100.09	100.60	100.64	100.58	100.74	100.87	102.06	102.22	101.60
	Formula units based on 32 oxygens and Fe2+/Fe3+ assuming full site occupancy									
Cr	9.19	9.22	9.25	9.20	9.26	9.30	9.21	9.29	9.21	9.24
Al	4.85	4.84	4.84	4.80	4.88	4.78	4.93	4.81	4.84	4.88
Ti	0.19	0.21	0.22	0.19	0.20	0.21	0.19	0.19	0.20	0.20
Fe3+	1.54	1.48	1.44	1.58	1.43	1.47	1.44	1.49	1.52	1.46
Fe2+	4.77	4.80	4.81	4.69	4.83	4.80	4.86	4.81	4.79	4.78
Mg	3.31	3.30	3.29	3.39	3.28	3.32	3.28	3.28	3.31	3.32
Mn	0.11	0.11	0.12	0.11	0.08	0.09	0.05	0.10	0.10	0.10
Ni	0.05	0.04	0.03	0.04	0.04	0.03	0.03	0.04	0.04	0.03
Total	24.00	24.00	24.00	24.00	24.00	24.00	24.00	24.00	24.00	24.00
100Mg/Mg+Fe2+	34.45	34.23	34.03	35.67	33.79	34.66	33.52	34.06	34.36	34.38
100Cr/Cr+Al	65.44	65.57	65.62	65.71	65.50	66.07	65.16	65.89	65.54	65.42
100Fe3+/Cr+Al+Fe3+	9.89	9.53	9.26	10.14	9.17	9.43	9.26	9.57	9.73	9.35
Cr	0.87	0.88	0.89	0.88	0.89	0.89	0.89	0.90	0.90	0.90
Al	0.46	0.46	0.47	0.46	0.47	0.46	0.47	0.47	0.47	0.47
Ti	0.02	0.03	0.03	0.02	0.03	0.03	0.02	0.02	0.03	0.03
Fe	0.40	0.40	0.40	0.40	0.40	0.40	0.41	0.41	0.41	0.40
Mg	0.21	0.21	0.21	0.22	0.21	0.21	0.21	0.21	0.22	0.22
Mn	0.01	0.01	0.01	0.01	0.01	0.01	0.00	0.01	0.01	0.01
Ni	0.00	0.00	0.00	0.00	0.00	0.00	0.00	0.00	0.00	0.00
Total	1.97	1.99	2.00	2.00	2.00	2.00	2.01	2.03	2.03	2.02
No of Ions										
Cr	9.42	9.45	9.47	9.43	9.48	9.52	9.43	9.52	9.44	9.46
Al	4.97	4.96	4.96	4.92	4.99	4.89	5.04	4.93	4.96	5.00
Ti	0.20	0.21	0.22	0.20	0.21	0.22	0.20	0.19	0.20	0.20
Fe	6.46	6.43	6.40	6.44	6.40	6.42	6.45	6.45	6.46	6.39
Mg	3.40	3.38	3.36	3.47	3.36	3.40	3.36	3.36	3.39	3.40
Mn	0.11	0.11	0.12	0.12	0.08	0.09	0.06	0.11	0.11	0.10
Ni	0.05	0.04	0.03	0.04	0.04	0.03	0.03	0.04	0.04	0.03
Total	24.61	24.58	24.57	24.62	24.56	24.58	24.57	24.59	24.60	24.57
Fe Corrected on 32 O										
Fe3+	1.58	1.52	1.47	1.62	1.46	1.50	1.48	1.53	1.55	1.49
Fe2+	4.89	4.91	4.93	4.82	4.94	4.92	4.97	4.92	4.90	4.89

Block No.	2b	2b	2b	2b	2b	2b	2b	2b	2b	2b
Raw Analysis	11.00	12.00	13.00	14.00	15.00	16.00	17.00	18.00	19.00	20.00
Cr2O3	44.45	44.26	44.49	44.21	44.09	44.76	44.91	45.20	44.98	45.02
Al2O3	15.47	15.45	15.57	15.86	15.68	15.15	15.75	15.39	15.43	15.56
TiO2	1.15	1.09	1.05	1.06	1.01	1.12	0.79	0.88	1.01	0.93
FeO	28.79	28.76	28.84	28.85	28.94	28.76	28.22	28.91	28.78	28.98
MgO	8.58	8.53	8.76	8.59	8.42	8.63	8.67	8.71	8.51	8.46
MnO	0.57	0.70	0.47	0.68	0.67	0.57	0.64	0.62	0.50	0.59
NiO	0.21	0.29	0.11	0.15	0.26	0.19	0.17	0.15	0.26	0.25
Total	99.23	99.09	99.27	99.40	99.06	99.18	99.15	99.86	99.46	99.78
MnO corrected	0.40	0.53	0.29	0.50	0.49	0.39	0.46	0.44	0.32	0.41
Total	99.05	98.91	99.10	99.22	98.88	99.00	98.97	99.68	99.28	99.60
Corrected Analysis										
Cr2O3	44.45	44.26	44.49	44.21	44.09	44.76	44.91	45.20	44.98	45.02
Al2O3	15.47	15.45	15.57	15.86	15.68	15.15	15.75	15.39	15.43	15.56
TiO2	1.15	1.09	1.05	1.06	1.01	1.12	0.79	0.88	1.01	0.93
FeO	21.87	21.66	21.60	21.84	21.86	21.65	21.34	21.61	21.97	21.95
Fe2O3	7.69	7.90	8.04	7.79	7.87	7.90	7.64	8.12	7.57	7.81
MgO	8.58	8.53	8.76	8.59	8.42	8.63	8.67	8.71	8.51	8.46
MnO	0.40	0.53	0.29	0.50	0.49	0.39	0.46	0.44	0.32	0.41
NiO	0.14	0.21	0.29	0.11	0.15	0.26	0.19	0.17	0.15	0.26
Total	99.75	99.62	100.08	99.96	99.56	99.85	99.76	100.52	99.92	100.40
	Formula units based on 32 oxygens and Fe2+/Fe3+ assuming full site occupancy									
Cr	9.21	9.19	9.18	9.13	9.15	9.28	9.29	9.30	9.31	9.28
Al	4.78	4.78	4.79	4.88	4.86	4.68	4.86	4.72	4.76	4.78
Ti	0.23	0.22	0.21	0.21	0.20	0.22	0.16	0.17	0.20	0.18
Fe3+	1.52	1.56	1.58	1.53	1.55	1.56	1.50	1.59	1.49	1.53
Fe2+	4.79	4.76	4.71	4.77	4.80	4.75	4.67	4.70	4.81	4.79
Mg	3.35	3.34	3.41	3.34	3.30	3.37	3.38	3.38	3.32	3.29
Mn	0.09	0.12	0.06	0.11	0.11	0.09	0.10	0.10	0.07	0.09
Ni	0.03	0.04	0.06	0.02	0.03	0.05	0.04	0.04	0.03	0.05
Total	24.00	24.00	24.00	24.00	24.00	24.00	24.00	24.00	24.00	24.00
100Mg/Mg+Fe2+	35.01	34.99	35.85	34.63	34.12	35.76	35.49	35.84	34.69	34.36
100Cr/Cr+Al	65.83	65.77	65.71	65.15	65.34	66.45	65.67	66.32	66.16	65.99
100Fe3+/Cr+Al+Fe3+	9.79	10.05	10.16	9.85	9.99	10.05	9.61	10.18	9.59	9.83
Cr	0.88	0.87	0.88	0.87	0.87	0.88	0.89	0.89	0.89	0.89
Al	0.46	0.45	0.46	0.47	0.46	0.45	0.46	0.45	0.45	0.46
Ti	0.03	0.03	0.03	0.03	0.03	0.03	0.02	0.02	0.03	0.02
Fe	0.40	0.40	0.40	0.40	0.40	0.40	0.39	0.40	0.40	0.40
Mg	0.21	0.21	0.22	0.21	0.21	0.21	0.22	0.22	0.21	0.21
Mn	0.01	0.01	0.00	0.01	0.01	0.01	0.01	0.01	0.00	0.01
Ni	0.00	0.00	0.00	0.00	0.00	0.00	0.00	0.00	0.00	0.00
Total	1.98	1.98	1.99	1.99	1.98	1.98	1.99	1.99	1.98	1.99
No of Ions										
Cr	9.44	9.42	9.42	9.36	9.39	9.52	9.52	9.54	9.54	9.51
Al	4.90	4.90	4.91	5.01	4.98	4.80	4.98	4.85	4.88	4.90
Ti	0.23	0.22	0.21	0.21	0.20	0.23	0.16	0.18	0.20	0.19
Fe	6.47	6.48	6.46	6.46	6.52	6.47	6.33	6.46	6.46	6.48
Mg	3.44	3.42	3.50	3.43	3.38	3.46	3.46	3.47	3.40	3.37
Mn	0.09	0.12	0.07	0.11	0.11	0.09	0.10	0.10	0.07	0.09
Ni	0.03	0.05	0.06	0.02	0.03	0.06	0.04	0.04	0.03	0.06
Total	24.60	24.62	24.62	24.60	24.61	24.62	24.59	24.63	24.59	24.60
Fe Corrected on 32 O										
Fe3+	1.56	1.60	1.62	1.57	1.59	1.60	1.54	1.63	1.53	1.57
Fe2+	4.91	4.88	4.84	4.89	4.92	4.87	4.79	4.83	4.93	4.91

Block No.	3b	3b	3b	3b	3b	3b	3b	3b	3b	3b
Raw Analysis	21.00	22.00	23.00	24.00	25.00	26.00	27.00	28.00	29.00	30.00
Cr2O3	42.89	44.65	44.25	44.38	43.07	44.31	43.42	43.80	44.11	42.75
Al2O3	13.85	15.86	15.70	15.48	15.45	15.25	15.14	15.40	15.31	12.83
TiO2	1.84	1.05	1.03	1.01	1.02	1.06	1.02	0.99	0.97	1.94
FeO	33.63	30.87	30.72	30.77	30.05	30.98	30.34	30.33	30.64	34.13
MgO	8.03	8.47	8.49	8.53	8.27	8.50	8.43	8.41	8.48	7.68
MnO	0.65	0.53	0.75	0.69	0.68	0.78	0.53	0.60	0.68	0.52
NiO	0.39	0.13	0.12	0.15	0.16	0.16	0.19	0.25	0.23	0.30
Total	101.27	101.57	101.05	101.00	98.69	101.05	99.06	99.76	100.41	100.16
MnO corrected	0.48	0.35	0.57	0.51	0.50	0.60	0.35	0.42	0.51	0.35
Total	101.10	101.39	100.87	100.82	98.52	100.87	98.89	99.59	100.24	99.99
Corrected Analysis										
Cr2O3	42.89	44.65	44.25	44.38	43.07	44.31	43.42	43.80	44.11	42.75
Al2O3	13.85	15.86	15.70	15.48	15.45	15.25	15.14	15.40	15.31	12.83
TiO2	1.84	1.05	1.03	1.01	1.02	1.06	1.02	0.99	0.97	1.94
FeO	23.77	22.75	22.48	22.41	22.04	22.38	22.02	22.18	22.16	24.06
Fe2O3	10.96	9.02	9.15	9.28	8.90	9.55	9.24	9.06	9.42	11.18
MgO	8.03	8.47	8.49	8.53	8.27	8.50	8.43	8.41	8.48	7.68
MnO	0.48	0.35	0.57	0.51	0.50	0.60	0.35	0.42	0.51	0.35
NiO	0.25	0.39	0.13	0.12	0.15	0.16	0.16	0.19	0.25	0.23
Total	102.06	102.55	101.80	101.72	99.40	101.82	99.79	100.44	101.20	101.03
	Formula units based on 32 oxygens and Fe2+/Fe3+ assuming full site occupancy									
Cr	8.82	9.03	9.01	9.05	8.98	9.04	9.02	9.04	9.04	8.93
Al	4.25	4.78	4.77	4.71	4.80	4.64	4.69	4.74	4.68	4.00
Ti	0.36	0.20	0.20	0.20	0.20	0.21	0.20	0.19	0.19	0.39
Fe3+	2.14	1.74	1.77	1.80	1.77	1.85	1.83	1.78	1.84	2.22
Fe2+	5.17	4.87	4.84	4.83	4.86	4.83	4.84	4.84	4.81	5.32
Mg	3.11	3.23	3.26	3.28	3.25	3.27	3.30	3.27	3.28	3.02
Mn	0.10	0.08	0.12	0.11	0.11	0.13	0.08	0.09	0.11	0.08
Ni	0.05	0.08	0.03	0.02	0.03	0.03	0.03	0.04	0.05	0.05
Total	24.00	24.00	24.00	24.00	24.00	24.00	24.00	24.00	24.00	24.00
100Mg/Mg+Fe2+	33.04	33.47	33.91	34.37	33.62	34.53	34.65	34.13	34.53	32.48
100Cr/Cr+Al	67.50	65.37	65.40	65.79	65.15	66.08	65.79	65.61	65.89	69.08
100Fe3+/Cr+Al+Fe3+	14.10	11.16	11.41	11.58	11.36	11.94	11.76	11.44	11.81	14.67
Cr	0.85	0.88	0.87	0.88	0.85	0.87	0.86	0.86	0.87	0.84
Al	0.41	0.47	0.46	0.46	0.45	0.45	0.45	0.45	0.45	0.38
Ti	0.05	0.03	0.03	0.03	0.03	0.03	0.03	0.02	0.02	0.05
Fe	0.47	0.43	0.43	0.43	0.42	0.43	0.42	0.42	0.43	0.47
Mg	0.20	0.21	0.21	0.21	0.21	0.21	0.21	0.21	0.21	0.19
Mn	0.01	0.00	0.01	0.01	0.01	0.01	0.00	0.01	0.01	0.00
Ni	0.00	0.01	0.00	0.00	0.00	0.00	0.00	0.00	0.00	0.00
Total	1.98	2.02	2.01	2.00	1.96	2.00	1.97	1.98	1.99	1.94
No of Ions										
Cr	9.13	9.29	9.27	9.32	9.24	9.32	9.30	9.31	9.32	9.26
Al	4.40	4.92	4.91	4.85	4.94	4.78	4.83	4.88	4.82	4.15
Ti	0.37	0.21	0.21	0.20	0.21	0.21	0.21	0.20	0.20	0.40
Fe	7.58	6.79	6.81	6.83	6.82	6.89	6.87	6.82	6.85	7.82
Mg	3.22	3.32	3.35	3.38	3.34	3.37	3.40	3.37	3.38	3.14
Mn	0.11	0.08	0.13	0.11	0.12	0.13	0.08	0.10	0.11	0.08
Ni	0.05	0.08	0.03	0.03	0.03	0.03	0.04	0.04	0.05	0.05
Total	24.86	24.69	24.70	24.72	24.70	24.74	24.73	24.71	24.73	24.90
Fe Corrected on 32 O										
Fe3+	2.22	1.78	1.83	1.86	1.82	1.91	1.88	1.83	1.89	2.31
Fe2+	5.35	5.01	4.98	4.98	5.00	4.98	4.99	4.99	4.95	5.51

Block No.	4a	4a	4a	4a	4a	4a	4a	4a	4a	4a	5a	5a
Raw Analysis	31.00	32.00	33.00	34.00	35.00	36.00	37.00	38.00	39.00	40.00	41.00	42.00
Cr2O3	44.34	45.23	45.27	45.37	44.71	44.93	45.02	44.29	44.71	44.39	44.53	44.05
Al2O3	15.79	15.74	15.63	16.46	15.98	16.11	16.51	16.39	16.03	16.05	16.75	17.01
TiO2	1.04	1.00	0.97	0.85	1.00	0.98	0.82	0.96	1.03	1.09	1.02	0.91
FeO	28.61	29.03	28.83	28.53	28.92	29.01	28.73	28.79	28.53	28.55	28.63	28.31
MgO	8.77	8.95	8.85	9.04	8.80	9.04	8.95	8.96	9.07	9.09	9.18	8.98
MnO	0.68	0.73	0.56	0.51	0.62	0.75	0.47	0.45	0.63	0.72	0.74	0.56
NiO	0.16	0.14	0.18	0.25	0.24	0.10	0.17	0.08	0.13	0.17	0.20	0.21
Total	99.38	100.83	100.28	101.01	100.27	100.91	100.67	99.91	100.13	100.06	101.05	100.02
MnO corrected	0.50	0.55	0.38	0.33	0.44	0.57	0.29	0.27	0.45	0.55	0.56	0.38
Total	99.21	100.65	100.10	100.82	100.09	100.73	100.49	99.73	99.95	99.88	100.87	99.84
Corrected Analysis												
Cr2O3	44.34	45.23	45.27	45.37	44.71	44.93	45.02	44.29	44.71	44.39	44.53	44.05
Al2O3	15.79	15.74	15.63	16.46	15.98	16.11	16.51	16.39	16.03	16.05	16.75	17.01
TiO2	1.04	1.00	0.97	0.85	1.00	0.98	0.82	0.96	1.03	1.09	1.02	0.91
FeO	21.41	21.62	21.70	21.64	21.72	21.49	21.78	21.65	21.42	21.29	21.46	21.51
Fe2O3	8.00	8.24	7.92	7.65	8.01	8.36	7.73	7.94	7.91	8.07	7.98	7.56
MgO	8.77	8.95	8.85	9.04	8.80	9.04	8.95	8.96	9.07	9.09	9.18	8.98
MnO	0.50	0.55	0.38	0.33	0.44	0.57	0.29	0.27	0.45	0.55	0.56	0.38
NiO	0.30	0.16	0.14	0.18	0.25	0.24	0.10	0.17	0.08	0.13	0.17	0.20
Total	100.15	101.49	100.85	101.52	100.89	101.72	101.19	100.62	100.69	100.65	101.64	100.60
	Formula units based on 32 oxygens and Fe2+/Fe3+ assuming full site occupancy											
Cr	9.13	9.20	9.27	9.19	9.14	9.10	9.15	9.05	9.14	9.07	8.99	8.98
Al	4.85	4.77	4.77	4.97	4.87	4.87	5.00	4.99	4.88	4.89	5.05	5.17
Ti	0.20	0.19	0.19	0.16	0.19	0.19	0.16	0.19	0.20	0.21	0.20	0.18
Fe3+	1.57	1.60	1.54	1.48	1.56	1.61	1.49	1.54	1.54	1.57	1.53	1.47
Fe2+	4.67	4.65	4.70	4.64	4.70	4.60	4.68	4.68	4.63	4.60	4.58	4.64
Mg	3.40	3.43	3.42	3.45	3.39	3.45	3.43	3.45	3.50	3.50	3.49	3.45
Mn	0.11	0.12	0.08	0.07	0.10	0.12	0.06	0.06	0.10	0.12	0.12	0.08
Ni	0.06	0.03	0.03	0.04	0.05	0.05	0.02	0.04	0.02	0.03	0.03	0.04
Total	24.00	24.00	24.00	24.00	24.00	24.00	24.00	24.00	24.00	24.00	24.00	24.00
100Mg/Mg+Fe2+	35.78	36.42	36.05	35.94	35.44	36.47	35.41	35.66	36.74	36.87	36.29	35.17
100Cr/Cr+Al	65.31	65.83	66.01	64.90	65.23	65.17	64.64	64.44	65.16	64.96	64.06	63.46
100Fe3+/Cr+Al+Fe3+	10.08	10.24	9.91	9.44	10.01	10.35	9.55	9.90	9.88	10.11	9.85	9.39
Cr	0.88	0.89	0.89	0.90	0.88	0.89	0.89	0.87	0.88	0.88	0.88	0.87
Al	0.46	0.46	0.46	0.48	0.47	0.47	0.49	0.48	0.47	0.47	0.49	0.50
Ti	0.03	0.03	0.02	0.02	0.03	0.02	0.02	0.02	0.03	0.03	0.03	0.02
Fe	0.40	0.40	0.40	0.40	0.40	0.40	0.40	0.40	0.40	0.40	0.40	0.39
Mg	0.22	0.22	0.22	0.22	0.22	0.22	0.22	0.22	0.23	0.23	0.23	0.22
Mn	0.01	0.01	0.01	0.00	0.01	0.01	0.00	0.00	0.01	0.01	0.01	0.01
Ni	0.00	0.00	0.00	0.00	0.00	0.00	0.00	0.00	0.00	0.00	0.00	0.00
Total	1.99	2.02	2.01	2.03	2.01	2.02	2.02	2.01	2.01	2.01	2.03	2.02
No of Ions												
Cr	9.37	9.44	9.50	9.41	9.37	9.34	9.37	9.28	9.37	9.31	9.22	9.19
Al	4.98	4.90	4.89	5.09	5.00	4.99	5.13	5.12	5.01	5.02	5.17	5.29
Ti	0.21	0.20	0.19	0.17	0.20	0.19	0.16	0.19	0.21	0.22	0.20	0.18
Fe	6.39	6.41	6.40	6.26	6.42	6.38	6.33	6.38	6.32	6.33	6.27	6.25
Mg	3.49	3.52	3.50	3.54	3.48	3.55	3.51	3.54	3.58	3.59	3.58	3.53
Mn	0.11	0.12	0.09	0.07	0.10	0.13	0.06	0.06	0.10	0.12	0.12	0.09
Ni	0.07	0.03	0.03	0.04	0.05	0.05	0.02	0.04	0.02	0.03	0.04	0.04
Total	24.62	24.63	24.61	24.58	24.61	24.64	24.59	24.61	24.61	24.62	24.60	24.58
Fe Corrected on 32 O												
Fe3+	1.61	1.64	1.58	1.51	1.60	1.65	1.53	1.58	1.58	1.61	1.57	1.50
Fe2+	4.79	4.77	4.82	4.75	4.82	4.73	4.80	4.80	4.75	4.72	4.70	4.75

Block No.	5a	5a	5a	5a	5a	5a	5a	5a	6b	6b
Raw Analysis	43.00	44.00	45.00	46.00	47.00	48.00	49.00	50.00	51.00	52.00
Cr2O3	44.33	44.12	44.31	44.29	45.00	44.07	44.08	44.39	43.62	43.66
Al2O3	16.75	16.29	16.69	16.36	15.93	15.97	15.71	16.04	16.43	16.26
TiO2	0.98	0.98	1.01	0.85	1.06	1.06	1.03	0.95	0.92	1.00
FeO	28.60	28.65	28.49	28.57	29.21	28.19	28.67	28.58	28.15	28.19
MgO	8.97	9.06	8.89	9.05	8.97	8.75	8.79	8.84	8.91	8.84
MnO	0.57	0.60	0.62	0.74	0.69	0.70	0.66	0.59	0.65	0.68
NiO	0.14	0.29	0.20	0.24	0.17	0.30	0.15	0.08	0.21	0.12
Total	100.33	99.99	100.21	100.08	101.02	99.04	99.09	99.47	98.89	98.75
MnO corrected	0.39	0.43	0.44	0.56	0.51	0.53	0.48	0.41	0.48	0.50
Total	100.15	99.81	100.03	99.90	100.84	98.86	98.91	99.29	98.71	98.57
Corrected Analysis										
Cr2O3	44.33	44.12	44.31	44.29	45.00	44.07	44.08	44.39	43.62	43.66
Al2O3	16.75	16.29	16.69	16.36	15.93	15.97	15.71	16.04	16.43	16.26
TiO2	0.98	0.98	1.01	0.85	1.06	1.06	1.03	0.95	0.92	1.00
FeO	21.66	21.34	21.64	21.12	21.72	21.36	21.30	21.49	21.17	21.19
Fe2O3	7.70	8.12	7.62	8.28	8.33	7.59	8.19	7.88	7.76	7.78
MgO	8.97	9.06	8.89	9.05	8.97	8.75	8.79	8.84	8.91	8.84
MnO	0.39	0.43	0.44	0.56	0.51	0.53	0.48	0.41	0.48	0.50
NiO	0.21	0.14	0.29	0.20	0.24	0.17	0.30	0.15	0.08	0.21
Total	100.99	100.47	100.88	100.70	101.74	99.49	99.87	100.15	99.37	99.44
	Formula units based on 32 oxygens and Fe2+/Fe3+ assuming full site occupancy									
Cr	9.01	9.03	9.03	9.04	9.12	9.12	9.10	9.13	9.01	9.02
Al	5.08	4.97	5.07	4.98	4.82	4.93	4.84	4.92	5.06	5.01
Ti	0.19	0.19	0.20	0.16	0.20	0.21	0.20	0.19	0.18	0.20
Fe3+	1.49	1.58	1.48	1.61	1.61	1.49	1.61	1.54	1.53	1.53
Fe2+	4.66	4.62	4.66	4.56	4.66	4.68	4.65	4.68	4.63	4.63
Mg	3.44	3.49	3.41	3.48	3.43	3.41	3.42	3.43	3.47	3.45
Mn	0.08	0.09	0.10	0.12	0.11	0.12	0.11	0.09	0.11	0.11
Ni	0.04	0.03	0.06	0.04	0.05	0.04	0.06	0.03	0.02	0.04
Total	24.00	24.00	24.00	24.00	24.00	24.00	24.00	24.00	24.00	24.00
100Mg/Mg+Fe2+	35.31	36.42	35.06	36.51	36.19	35.54	36.04	35.72	35.80	35.72
100Cr/Cr+Al	63.96	64.50	64.04	64.48	65.45	64.92	65.30	64.99	64.03	64.29
100Fe3+/Cr+Al+Fe3+	9.57	10.16	9.49	10.29	10.34	9.62	10.35	9.90	9.78	9.83
Cr	0.87	0.87	0.87	0.87	0.89	0.87	0.87	0.88	0.86	0.86
Al	0.49	0.48	0.49	0.48	0.47	0.47	0.46	0.47	0.48	0.48
Ti	0.02	0.02	0.03	0.02	0.03	0.03	0.03	0.02	0.02	0.03
Fe	0.40	0.40	0.40	0.40	0.41	0.39	0.40	0.40	0.39	0.39
Mg	0.22	0.22	0.22	0.22	0.22	0.22	0.22	0.22	0.22	0.22
Mn	0.01	0.01	0.01	0.01	0.01	0.01	0.01	0.01	0.01	0.01
Ni	0.00	0.00	0.00	0.00	0.00	0.00	0.00	0.00	0.00	0.00
Total	2.02	2.01	2.02	2.01	2.02	1.99	1.99	2.00	1.99	1.99
No of Ions										
Cr	9.23	9.26	9.25	9.28	9.37	9.35	9.35	9.36	9.24	9.25
Al	5.20	5.10	5.19	5.11	4.94	5.05	4.97	5.04	5.19	5.14
Ti	0.19	0.20	0.20	0.17	0.21	0.21	0.21	0.19	0.18	0.20
Fe	6.30	6.36	6.29	6.33	6.43	6.32	6.43	6.38	6.31	6.32
Mg	3.52	3.58	3.49	3.57	3.52	3.50	3.51	3.51	3.56	3.53
Mn	0.09	0.10	0.10	0.13	0.11	0.12	0.11	0.09	0.11	0.11
Ni	0.04	0.03	0.06	0.04	0.05	0.04	0.06	0.03	0.02	0.04
Total	24.59	24.62	24.58	24.64	24.64	24.59	24.64	24.61	24.60	24.60
Fe Corrected on 32 O										
Fe3+	1.53	1.62	1.51	1.65	1.65	1.53	1.65	1.58	1.56	1.57
Fe2+	4.77	4.74	4.78	4.68	4.78	4.79	4.78	4.79	4.74	4.75

Block No.	6b	6b	6b	6b	6b	6b	6b	6b	7c	7c
Raw Analysis	53.00	54.00	55.00	56.00	57.00	58.00	59.00	60.00	61.00	62.00
Cr2O3	43.25	43.54	43.31	43.29	43.76	43.96	42.97	43.22	44.59	44.50
Al2O3	16.54	16.37	16.57	17.01	17.18	17.70	17.04	17.10	15.87	15.91
TiO2	1.01	0.95	0.85	0.91	1.01	0.93	0.94	0.87	0.96	0.96
FeO	28.12	28.18	28.19	27.54	28.41	28.51	27.95	28.06	28.80	28.73
MgO	8.97	8.98	9.07	9.17	9.33	9.25	9.03	9.07	8.69	8.45
MnO	0.60	0.55	0.62	0.50	0.70	0.55	0.68	0.47	0.67	0.64
NiO	0.31	0.21	0.25	0.22	0.18	0.18	0.19	0.18	0.14	0.18
Total	98.80	98.77	98.87	98.64	100.56	101.08	98.80	98.98	99.72	99.36
MnO corrected	0.42	0.37	0.44	0.33	0.53	0.38	0.51	0.30	0.49	0.46
Total	98.63	98.60	98.70	98.46	100.39	100.90	98.63	98.80	99.54	99.18
Corrected Analysis										
Cr2O3	43.25	43.54	43.31	43.29	43.76	43.96	42.97	43.22	44.59	44.50
Al2O3	16.54	16.37	16.57	17.01	17.18	17.70	17.04	17.10	15.87	15.91
TiO2	1.01	0.95	0.85	0.91	1.01	0.93	0.94	0.87	0.96	0.96
FeO	21.15	21.01	20.83	20.79	21.15	21.60	20.97	21.12	21.67	21.96
Fe2O3	7.75	7.97	8.18	7.50	8.07	7.69	7.75	7.71	7.93	7.52
MgO	8.97	8.98	9.07	9.17	9.33	9.25	9.03	9.07	8.69	8.45
MnO	0.42	0.37	0.44	0.33	0.53	0.38	0.51	0.30	0.49	0.46
NiO	0.12	0.31	0.21	0.25	0.22	0.18	0.18	0.19	0.18	0.14
Total	99.21	99.49	99.48	99.25	101.24	101.68	99.40	99.58	100.39	99.89
	Formula units based on 32 oxygens and Fe2+/Fe3+ assuming full site occupancy									
Cr	8.94	8.99	8.93	8.92	8.84	8.84	8.85	8.88	9.17	9.20
Al	5.10	5.04	5.09	5.22	5.18	5.30	5.23	5.24	4.87	4.91
Ti	0.20	0.19	0.17	0.18	0.19	0.18	0.18	0.17	0.19	0.19
Fe3+	1.52	1.57	1.60	1.47	1.55	1.47	1.52	1.51	1.55	1.48
Fe2+	4.63	4.59	4.54	4.53	4.52	4.59	4.57	4.59	4.71	4.80
Mg	3.49	3.49	3.53	3.56	3.55	3.50	3.51	3.51	3.37	3.29
Mn	0.09	0.08	0.10	0.07	0.11	0.08	0.11	0.07	0.11	0.10
Ni	0.03	0.06	0.04	0.05	0.05	0.04	0.04	0.04	0.04	0.03
Total	24.00	24.00	24.00	24.00	24.00	24.00	24.00	24.00	24.00	24.00
100Mg/Mg+Fe2+	35.93	36.29	36.59	36.50	36.64	35.39	35.78	35.75	35.16	33.91
100Cr/Cr+Al	63.68	64.08	63.67	63.06	63.08	62.49	62.85	62.89	65.33	65.22
100Fe3+/Cr+Al+Fe3+	9.79	10.04	10.27	9.42	9.97	9.42	9.74	9.65	9.95	9.50
Cr	0.85	0.86	0.85	0.85	0.86	0.87	0.85	0.85	0.88	0.88
Al	0.49	0.48	0.49	0.50	0.51	0.52	0.50	0.50	0.47	0.47
Ti	0.03	0.02	0.02	0.02	0.03	0.02	0.02	0.02	0.02	0.02
Fe	0.39	0.39	0.39	0.38	0.40	0.40	0.39	0.39	0.40	0.40
Mg	0.22	0.22	0.23	0.23	0.23	0.23	0.22	0.23	0.22	0.21
Mn	0.01	0.01	0.01	0.00	0.01	0.01	0.01	0.00	0.01	0.01
Ni	0.00	0.00	0.00	0.00	0.00	0.00	0.00	0.00	0.00	0.00
Total	1.99	1.99	1.99	2.00	2.03	2.05	2.00	2.00	2.00	1.99
No of Ions										
Cr	9.16	9.22	9.16	9.13	9.07	9.05	9.07	9.10	9.40	9.42
Al	5.23	5.17	5.23	5.35	5.31	5.43	5.36	5.37	4.99	5.02
Ti	0.20	0.19	0.17	0.18	0.20	0.18	0.19	0.17	0.19	0.19
Fe	6.30	6.31	6.31	6.14	6.23	6.21	6.24	6.25	6.42	6.44
Mg	3.58	3.58	3.62	3.65	3.64	3.59	3.59	3.60	3.45	3.37
Mn	0.10	0.08	0.10	0.07	0.12	0.08	0.12	0.07	0.11	0.10
Ni	0.03	0.07	0.05	0.05	0.05	0.04	0.04	0.04	0.04	0.03
Total	24.60	24.62	24.63	24.58	24.61	24.58	24.60	24.59	24.61	24.58
Fe Corrected on 32 O										
Fe3+	1.56	1.61	1.65	1.51	1.59	1.51	1.56	1.55	1.59	1.52
Fe2+	4.74	4.70	4.66	4.64	4.64	4.70	4.68	4.70	4.83	4.92

Block No.	7c	7c	7c	7c	7c	7c	7c	7c	8a	8a
Raw Analysis	63.00	64.00	65.00	66.00	67.00	68.00	69.00	70.00	71.00	72.00
Cr2O3	44.75	44.46	44.54	44.17	43.99	43.80	43.83	44.55	43.61	42.20
Al2O3	15.42	16.18	15.83	15.68	15.89	15.93	15.65	15.42	16.37	17.05
TiO2	0.99	1.04	0.82	0.99	0.96	1.00	0.99	1.03	1.20	0.99
FeO	28.97	28.40	28.71	28.62	28.95	28.63	28.88	29.19	28.09	28.76
MgO	8.46	8.72	8.78	8.75	8.74	8.71	8.71	8.76	9.26	9.49
MnO	0.66	0.71	0.56	0.61	0.75	0.68	0.78	0.54	0.52	0.69
NiO	0.30	0.21	0.16	0.11	0.28	0.22	0.17	0.24	0.13	0.18
Total	99.54	99.72	99.40	98.94	99.55	98.97	99.01	99.74	99.17	99.37
MnO corrected	0.48	0.53	0.38	0.43	0.57	0.50	0.60	0.36	0.35	0.52
Total	99.36	99.54	99.23	98.76	99.38	98.79	98.83	99.56	99.00	99.20
Corrected Analysis										
Cr2O3	44.75	44.46	44.54	44.17	43.99	43.80	43.83	44.55	43.61	42.20
Al2O3	15.42	16.18	15.83	15.68	15.89	15.93	15.65	15.42	16.37	17.05
TiO2	0.99	1.04	0.82	0.99	0.96	1.00	0.99	1.03	1.20	0.99
FeO	21.88	21.58	21.39	21.41	21.49	21.34	21.28	21.69	21.02	20.61
Fe2O3	7.88	7.58	8.13	8.01	8.29	8.10	8.44	8.34	7.86	9.05
MgO	8.46	8.72	8.78	8.75	8.74	8.71	8.71	8.76	9.26	9.49
MnO	0.48	0.53	0.38	0.43	0.57	0.50	0.60	0.36	0.35	0.52
NiO	0.18	0.30	0.21	0.16	0.11	0.28	0.22	0.17	0.24	0.13
Total	100.02	100.40	100.08	99.62	100.04	99.66	99.72	100.33	99.90	100.05
	Formula units based on 32 oxygens and Fe2+/Fe3+ assuming full site occupancy									
Cr	9.26	9.13	9.18	9.15	9.07	9.06	9.07	9.18	8.95	8.61
Al	4.76	4.95	4.86	4.84	4.89	4.91	4.83	4.74	5.01	5.19
Ti	0.19	0.20	0.16	0.20	0.19	0.20	0.20	0.20	0.23	0.19
Fe3+	1.55	1.48	1.59	1.58	1.63	1.59	1.66	1.63	1.54	1.76
Fe2+	4.79	4.68	4.66	4.69	4.69	4.67	4.66	4.73	4.56	4.45
Mg	3.30	3.37	3.41	3.42	3.40	3.40	3.40	3.40	3.58	3.65
Mn	0.11	0.12	0.08	0.10	0.13	0.11	0.13	0.08	0.08	0.11
Ni	0.04	0.06	0.04	0.03	0.02	0.06	0.05	0.04	0.05	0.03
Total	24.00	24.00	24.00	24.00	24.00	24.00	24.00	24.00	24.00	24.00
100Mg/Mg+Fe2+	34.55	35.01	35.81	35.83	35.47	35.46	35.83	35.95	37.41	37.87
100Cr/Cr+Al	66.06	64.82	65.36	65.38	64.98	64.84	65.26	65.95	64.12	62.40
100Fe3+/Cr+Al+Fe3+	9.97	9.52	10.20	10.15	10.44	10.25	10.68	10.51	9.91	11.30
Cr	0.88	0.88	0.88	0.87	0.87	0.86	0.86	0.88	0.86	0.83
Al	0.45	0.48	0.47	0.46	0.47	0.47	0.46	0.45	0.48	0.50
Ti	0.02	0.03	0.02	0.02	0.02	0.02	0.02	0.03	0.03	0.02
Fe	0.40	0.40	0.40	0.40	0.40	0.40	0.40	0.41	0.39	0.40
Mg	0.21	0.22	0.22	0.22	0.22	0.22	0.22	0.22	0.23	0.24
Mn	0.01	0.01	0.01	0.01	0.01	0.01	0.01	0.01	0.00	0.01
Ni	0.00	0.00	0.00	0.00	0.00	0.00	0.00	0.00	0.00	0.00
Total	1.98	2.00	1.99	1.98	1.99	1.98	1.98	1.99	2.00	2.00
No of Ions										
Cr	9.50	9.35	9.42	9.38	9.31	9.30	9.32	9.42	9.18	8.87
Al	4.88	5.07	4.99	4.97	5.02	5.04	4.96	4.87	5.13	5.34
Ti	0.20	0.21	0.16	0.20	0.19	0.20	0.20	0.21	0.24	0.20
Fe	6.50	6.32	6.42	6.43	6.48	6.43	6.50	6.53	6.25	6.39
Mg	3.38	3.46	3.50	3.50	3.49	3.49	3.49	3.49	3.67	3.76
Mn	0.11	0.12	0.09	0.10	0.13	0.11	0.14	0.08	0.08	0.12
Ni	0.04	0.07	0.04	0.04	0.02	0.06	0.05	0.04	0.05	0.03
Total	24.61	24.58	24.63	24.62	24.64	24.63	24.66	24.65	24.61	24.70
Fe Corrected on 32 O										
Fe3+	1.59	1.52	1.64	1.62	1.67	1.64	1.71	1.68	1.57	1.81
Fe2+	4.91	4.80	4.79	4.81	4.81	4.79	4.79	4.85	4.68	4.58

Block No.	8a	8a	8a	8a	8a	8a	8a	8a	9c	9c
Raw Analysis	73.00	74.00	75.00	76.00	77.00	78.00	79.00	80.00	81.00	82.00
Cr2O3	44.01	44.02	43.97	43.11	43.55	42.99	43.71	44.19	41.23	40.50
Al2O3	16.81	16.81	17.22	16.69	16.56	16.83	17.07	16.89	11.44	11.17
TiO2	1.07	1.03	1.03	0.98	0.99	0.99	1.06	1.14	2.37	2.27
FeO	28.56	28.49	28.45	28.00	28.00	27.98	28.35	28.44	37.71	37.18
MgO	9.32	9.28	9.62	9.25	9.14	9.36	9.44	9.43	7.30	7.15
MnO	0.58	0.62	0.56	0.65	0.63	0.60	0.73	0.73	0.66	0.55
NiO	0.21	0.09	0.18	0.23	0.15	0.15	0.15	0.09	0.13	0.10
Total	100.56	100.32	101.03	98.91	99.01	98.89	100.51	100.91	100.84	98.91
MnO corrected	0.40	0.45	0.39	0.47	0.45	0.43	0.55	0.56	0.50	0.39
Total	100.38	100.15	100.85	98.74	98.84	98.72	100.33	100.74	100.68	98.75
Corrected Analysis										
Cr2O3	44.01	44.02	43.97	43.11	43.55	42.99	43.71	44.19	41.23	40.50
Al2O3	16.81	16.81	17.22	16.69	16.56	16.83	17.07	16.89	11.44	11.17
TiO2	1.07	1.03	1.03	0.98	0.99	0.99	1.06	1.14	2.37	2.27
FeO	21.29	21.23	21.10	20.70	20.88	20.66	21.02	21.21	25.29	24.86
Fe2O3	8.08	8.07	8.17	8.12	7.91	8.13	8.15	8.03	13.80	13.68
MgO	9.32	9.28	9.62	9.25	9.14	9.36	9.44	9.43	7.30	7.15
MnO	0.40	0.45	0.39	0.47	0.45	0.43	0.55	0.56	0.50	0.39
NiO	0.18	0.21	0.09	0.18	0.23	0.15	0.15	0.15	0.09	0.13
Total	101.17	101.07	101.58	99.50	99.71	99.53	101.15	101.60	102.02	100.15
	Formula units based on 32 oxygens and Fe2+/Fe3+ assuming full site occupancy									
Cr	8.91	8.92	8.84	8.87	8.95	8.83	8.84	8.91	8.62	8.63
Al	5.08	5.08	5.16	5.12	5.08	5.15	5.15	5.08	3.57	3.55
Ti	0.21	0.20	0.20	0.19	0.19	0.19	0.20	0.22	0.47	0.46
Fe3+	1.56	1.56	1.56	1.59	1.55	1.59	1.57	1.54	2.75	2.77
Fe2+	4.56	4.55	4.49	4.50	4.54	4.49	4.50	4.52	5.59	5.60
Mg	3.56	3.55	3.65	3.59	3.54	3.62	3.60	3.58	2.88	2.87
Mn	0.09	0.10	0.08	0.10	0.10	0.09	0.12	0.12	0.11	0.09
Ni	0.04	0.04	0.02	0.04	0.05	0.03	0.03	0.03	0.02	0.03
Total	24.00	24.00	24.00	24.00	24.00	24.00	24.00	24.00	24.00	24.00
100Mg/Mg+Fe2+	36.94	36.80	37.79	37.28	36.83	37.57	37.33	37.35	31.40	31.39
100Cr/Cr+Al	63.72	63.72	63.13	63.39	63.81	63.14	63.20	63.70	70.73	70.86
100Fe3+/Cr+Al+Fe3+	10.02	10.01	10.04	10.21	9.93	10.21	10.08	9.93	18.39	18.56
Cr	0.87	0.87	0.87	0.85	0.86	0.85	0.86	0.87	0.81	0.80
Al	0.49	0.49	0.51	0.49	0.49	0.50	0.50	0.50	0.34	0.33
Ti	0.03	0.03	0.03	0.02	0.02	0.02	0.03	0.03	0.06	0.06
Fe	0.40	0.40	0.40	0.39	0.39	0.39	0.39	0.40	0.52	0.52
Mg	0.23	0.23	0.24	0.23	0.23	0.23	0.23	0.23	0.18	0.18
Mn	0.01	0.01	0.01	0.01	0.01	0.01	0.01	0.01	0.01	0.01
Ni	0.00	0.00	0.00	0.00	0.00	0.00	0.00	0.00	0.00	0.00
Total	2.03	2.02	2.04	1.99	2.00	2.00	2.03	2.04	1.92	1.89
No of Ions										
Cr	9.14	9.15	9.07	9.10	9.18	9.06	9.06	9.13	9.02	9.04
Al	5.21	5.21	5.30	5.25	5.20	5.29	5.28	5.20	3.73	3.72
Ti	0.21	0.20	0.20	0.20	0.20	0.20	0.21	0.22	0.49	0.48
Fe	6.28	6.27	6.21	6.25	6.24	6.24	6.22	6.22	8.73	8.78
Mg	3.65	3.64	3.74	3.68	3.63	3.72	3.69	3.68	3.01	3.01
Mn	0.09	0.10	0.09	0.11	0.10	0.10	0.12	0.12	0.12	0.09
Ni	0.04	0.04	0.02	0.04	0.05	0.03	0.03	0.03	0.02	0.03
Total	24.61	24.61	24.62	24.63	24.61	24.63	24.62	24.61	25.13	25.14
Fe Corrected on 32 O										
Fe3+	1.60	1.60	1.60	1.63	1.59	1.63	1.61	1.58	2.88	2.91
Fe2+	4.68	4.67	4.60	4.62	4.66	4.60	4.61	4.64	5.86	5.87

Block No.	9c	9c	9c	9c	9c	9c	9c	9c
Raw Analysis	83.00	84.00	85.00	86.00	87.00	88.00	89.00	90.00
Cr2O3	41.10	39.63	39.92	41.34	41.24	41.47	41.52	41.12
Al2O3	11.36	11.31	11.65	10.85	11.70	11.12	11.50	11.32
TiO2	2.13	2.22	2.01	1.90	1.88	2.13	1.85	2.38
FeO	36.32	38.03	37.66	38.14	36.48	36.70	36.40	36.40
MgO	7.15	6.87	7.01	6.35	6.95	6.76	6.99	7.11
MnO	0.72	0.61	0.66	0.57	0.65	0.69	0.51	0.67
NiO	0.17	0.24	0.22	0.14	0.24	0.19	0.24	0.36
Total	98.95	98.91	99.14	99.28	99.13	99.06	99.01	99.34
MnO corrected	0.56	0.45	0.50	0.40	0.48	0.53	0.34	0.50
Total	98.78	98.75	98.98	99.11	98.96	98.90	98.84	99.18
Corrected Analysis								
Cr2O3	41.10	39.63	39.92	41.34	41.24	41.47	41.52	41.12
Al2O3	11.36	11.31	11.65	10.85	11.70	11.12	11.50	11.32
TiO2	2.13	2.22	2.01	1.90	1.88	2.13	1.85	2.38
FeO	24.55	25.21	24.83	25.76	24.76	25.06	24.70	24.83
Fe2O3	13.08	14.25	14.26	13.76	13.02	12.94	13.00	12.85
MgO	7.15	6.87	7.01	6.35	6.95	6.76	6.99	7.11
MnO	0.56	0.45	0.50	0.40	0.48	0.53	0.34	0.50
NiO	0.10	0.17	0.24	0.22	0.14	0.24	0.19	0.24
Total	100.03	100.10	100.43	100.57	100.17	100.25	100.09	100.35
	Formula units based on 32 oxygens and Fe2+/Fe3+ assuming full site occupancy							
Cr	8.76	8.46	8.48	8.84	8.77	8.85	8.84	8.74
Al	3.61	3.60	3.69	3.46	3.71	3.54	3.65	3.59
Ti	0.43	0.45	0.41	0.39	0.38	0.43	0.37	0.48
Fe3+	2.65	2.89	2.88	2.80	2.64	2.63	2.64	2.60
Fe2+	5.53	5.69	5.58	5.82	5.57	5.66	5.57	5.58
Mg	2.87	2.76	2.81	2.56	2.79	2.72	2.81	2.85
Mn	0.13	0.10	0.11	0.09	0.11	0.12	0.08	0.11
Ni	0.02	0.04	0.05	0.05	0.03	0.05	0.04	0.05
Total	24.00	24.00	24.00	24.00	24.00	24.00	24.00	24.00
100Mg/Mg+Fe2+	31.40	29.74	30.30	27.55	30.00	29.59	30.45	31.04
100Cr/Cr+Al	70.81	70.14	69.68	71.87	70.27	71.43	70.78	70.89
100Fe3+/Cr+Al+Fe3+	17.66	19.36	19.16	18.55	17.44	17.50	17.42	17.42
Cr	0.81	0.78	0.79	0.82	0.81	0.82	0.82	0.81
Al	0.33	0.33	0.34	0.32	0.34	0.33	0.34	0.33
Ti	0.05	0.06	0.05	0.05	0.05	0.05	0.05	0.06
Fe	0.51	0.53	0.52	0.53	0.51	0.51	0.51	0.51
Mg	0.18	0.17	0.17	0.16	0.17	0.17	0.17	0.18
Mn	0.01	0.01	0.01	0.01	0.01	0.01	0.00	0.01
Ni	0.00	0.00	0.00	0.00	0.00	0.00	0.00	0.00
Total	1.89	1.88	1.89	1.88	1.89	1.89	1.89	1.90
No of Ions								
Cr	9.15	8.88	8.90	9.26	9.17	9.25	9.24	9.12
Al	3.77	3.78	3.87	3.63	3.88	3.70	3.82	3.75
Ti	0.45	0.47	0.43	0.40	0.40	0.45	0.39	0.50
Fe	8.56	9.02	8.88	9.04	8.58	8.66	8.57	8.54
Mg	3.00	2.90	2.95	2.68	2.91	2.84	2.93	2.97
Mn	0.13	0.11	0.12	0.10	0.11	0.13	0.08	0.12
Ni	0.02	0.04	0.05	0.05	0.03	0.05	0.04	0.05
Total	25.09	25.20	25.19	25.15	25.08	25.08	25.08	25.06
Fe Corrected on 32 O								
Fe3+	2.77	3.04	3.03	2.93	2.75	2.75	2.75	2.71
Fe2+	5.78	5.98	5.85	6.10	5.82	5.91	5.82	5.83

Block No.	1c	1c	1c	1c	1c	1c	1c	1c	1c
Raw Analysis	1	2	3	4	5	6	7	8	9
Cr2O3	43.89	43.24	43.50	43.77	42.53	42.75	43.14	43.15	43.20
Al2O3	16.20	16.06	15.86	16.12	16.82	16.43	16.63	16.20	16.89
TiO2	1.28	1.32	1.29	1.14	1.08	1.13	1.17	1.15	1.17
FeO	29.86	29.18	29.50	28.99	28.77	28.69	29.06	28.59	29.08
MgO	8.89	8.52	8.41	8.74	8.74	8.54	8.65	8.72	8.81
MnO	0.56	0.63	0.59	0.54	0.71	0.61	0.57	0.69	0.82
NiO	0.26	0.22	0.26	0.24	0.25	0.16	0.15	0.14	0.16
Total	100.95	99.16	99.41	99.54	98.90	98.31	99.36	98.64	100.13
MnO corrected	0.39	0.46	0.42	0.36	0.54	0.44	0.39	0.51	0.64
Total	100.78	98.99	99.23	99.36	98.73	98.14	99.19	98.46	99.96
Corrected Analysis									
Cr2O3	43.89	43.24	43.50	43.77	42.53	42.75	43.14	43.15	43.20
Al2O3	16.20	16.06	15.86	16.12	16.82	16.43	16.63	16.20	16.89
TiO2	1.28	1.32	1.29	1.14	1.08	1.13	1.17	1.15	1.17
FeO	22.16	22.09	22.29	21.80	21.47	21.74	22.03	21.49	21.84
Fe2O3	8.56	7.88	8.01	7.99	8.11	7.73	7.81	7.89	8.05
MgO	8.89	8.52	8.41	8.74	8.74	8.54	8.65	8.72	8.81
MnO	0.39	0.46	0.42	0.36	0.54	0.44	0.39	0.51	0.64
NiO	0.26	0.22	0.26	0.24	0.25	0.16	0.15	0.14	0.14
Total	101.63	99.78	100.04	100.16	99.54	98.91	99.97	99.25	100.75
	Formula units based on 32 oxygens and Fe2+/Fe3+ assuming full site occupancy								
Cr	8.90	8.94	8.99	9.00	8.77	8.89	8.87	8.94	8.81
Al	4.90	4.95	4.89	4.94	5.17	5.10	5.10	5.01	5.14
Ti	0.25	0.26	0.25	0.22	0.21	0.22	0.23	0.23	0.23
Fe3+	1.65	1.55	1.58	1.56	1.59	1.53	1.53	1.56	1.56
Fe2+	4.75	4.83	4.87	4.74	4.68	4.78	4.79	4.71	4.71
Mg	3.40	3.32	3.27	3.39	3.40	3.35	3.35	3.41	3.39
Mn	0.08	0.10	0.09	0.08	0.12	0.10	0.09	0.11	0.14
Ni	0.05	0.05	0.05	0.05	0.05	0.03	0.03	0.03	0.03
Total	24.00	24.00	24.00	24.00	24.00	24.00	24.00	24.00	24.00
100Mg/Mg+Fe2+	35.21	33.94	33.54	34.97	34.48	33.89	33.89	35.08	34.41
100Cr/Cr+Al	64.49	64.36	64.78	64.56	62.90	63.56	63.50	64.11	63.17
100Fe3+/Cr+Al+Fe3+	10.70	10.04	10.20	10.08	10.25	9.86	9.86	10.04	10.07
Cr	0.87	0.85	0.86	0.86	0.84	0.84	0.85	0.85	0.85
Al	0.48	0.47	0.47	0.47	0.49	0.48	0.49	0.48	0.50
Ti	0.03	0.03	0.03	0.03	0.03	0.03	0.03	0.03	0.03
Fe	0.42	0.41	0.41	0.40	0.40	0.40	0.40	0.40	0.40
Mg	0.22	0.21	0.21	0.22	0.22	0.21	0.21	0.22	0.22
Mn	0.01	0.01	0.01	0.01	0.01	0.01	0.01	0.01	0.01
Ni	0.00	0.00	0.00	0.00	0.00	0.00	0.00	0.00	0.00
Total	2.02	1.99	1.99	2.00	1.99	1.97	2.00	1.98	2.01
No of Ions									
Cr	9.15	9.17	9.22	9.24	9.00	9.11	9.10	9.17	9.03
Al	5.04	5.08	5.01	5.07	5.31	5.22	5.23	5.13	5.27
Ti	0.25	0.27	0.26	0.23	0.22	0.23	0.23	0.23	0.23
Fe	6.58	6.54	6.62	6.47	6.44	6.47	6.48	6.43	6.43
Mg	3.49	3.40	3.36	3.48	3.49	3.43	3.44	3.50	3.47
Mn	0.09	0.10	0.09	0.08	0.12	0.10	0.09	0.12	0.14
Ni	0.05	0.05	0.06	0.05	0.05	0.04	0.03	0.03	0.03
Total	24.65	24.61	24.62	24.62	24.63	24.60	24.60	24.61	24.62
Fe Corrected on 32 O									
Fe3+	1.70	1.59	1.62	1.60	1.63	1.57	1.57	1.60	1.60
Fe2+	4.88	4.95	5.00	4.87	4.81	4.90	4.92	4.83	4.83

Block No.	1c	2c	2c	2c	2c	2c	2c	2c	2c
Raw Analysis	10	11	12	13	14	15	16	17	18
Cr2O3	43.28	43.23	43.38	43.90	44.06	43.82	43.60	43.81	43.76
Al2O3	17.59	16.82	16.59	16.86	16.74	16.55	16.91	17.10	16.69
TiO2	1.11	0.95	1.10	1.13	1.17	1.08	1.05	0.92	1.15
FeO	29.18	28.16	28.53	29.05	28.75	28.73	28.39	28.30	28.38
MgO	8.85	8.95	9.04	9.23	9.06	9.05	9.11	9.22	9.00
MnO	0.62	0.63	0.62	0.67	0.65	0.54	0.70	0.64	0.66
NiO	0.13	0.26	0.21	0.20	0.30	0.14	0.29	0.26	0.22
Total	100.76	99.01	99.47	101.03	100.72	99.92	100.05	100.24	99.85
MnO corrected	0.44	0.45	0.45	0.50	0.47	0.36	0.52	0.47	0.48
Total	100.58	98.83	99.30	100.85	100.55	99.74	99.87	100.07	99.68
Corrected Analysis									
Cr2O3	43.28	43.23	43.38	43.90	44.06	43.82	43.60	43.81	43.76
Al2O3	17.59	16.82	16.59	16.86	16.74	16.55	16.91	17.10	16.69
TiO2	1.11	0.95	1.10	1.13	1.17	1.08	1.05	0.92	1.15
FeO	22.22	21.21	21.26	21.55	21.70	21.45	21.31	21.11	21.47
Fe2O3	7.73	7.73	8.08	8.33	7.83	8.08	7.87	7.99	7.68
MgO	8.85	8.95	9.04	9.23	9.06	9.05	9.11	9.22	9.00
MnO	0.44	0.45	0.45	0.50	0.47	0.36	0.52	0.47	0.48
NiO	0.16	0.13	0.26	0.21	0.20	0.30	0.14	0.29	0.26
Total	101.39	99.47	100.16	101.70	101.23	100.70	100.52	100.90	100.49
	Formula units based on 32 oxygens and Fe2+/Fe3+ assuming full site occupancy								
Cr	8.75	8.90	8.89	8.85	8.94	8.94	8.89	8.89	8.94
Al	5.30	5.17	5.07	5.07	5.06	5.03	5.14	5.17	5.08
Ti	0.21	0.19	0.21	0.22	0.23	0.21	0.20	0.18	0.22
Fe3+	1.49	1.52	1.58	1.60	1.51	1.57	1.53	1.54	1.49
Fe2+	4.75	4.62	4.61	4.60	4.66	4.63	4.60	4.53	4.64
Mg	3.37	3.48	3.49	3.51	3.46	3.48	3.50	3.52	3.46
Mn	0.10	0.10	0.10	0.11	0.10	0.08	0.11	0.10	0.11
Ni	0.03	0.03	0.05	0.04	0.04	0.06	0.03	0.06	0.05
Total	24.00	24.00	24.00	24.00	24.00	24.00	24.00	24.00	24.00
100Mg/Mg+Fe2+	33.54	35.51	36.10	36.30	35.64	36.02	35.98	36.33	35.63
100Cr/Cr+Al	62.26	63.27	63.68	63.59	63.83	63.97	63.36	63.22	63.74
100Fe3+/Cr+Al+Fe3+	9.58	9.73	10.15	10.31	9.75	10.10	9.82	9.89	9.63
Cr	0.85	0.85	0.86	0.87	0.87	0.86	0.86	0.86	0.86
Al	0.52	0.50	0.49	0.50	0.49	0.49	0.50	0.50	0.49
Ti	0.03	0.02	0.03	0.03	0.03	0.03	0.03	0.02	0.03
Fe	0.41	0.39	0.40	0.40	0.40	0.40	0.40	0.39	0.39
Mg	0.22	0.22	0.22	0.23	0.22	0.22	0.23	0.23	0.22
Mn	0.01	0.01	0.01	0.01	0.01	0.01	0.01	0.01	0.01
Ni	0.00	0.00	0.00	0.00	0.00	0.00	0.00	0.00	0.00
Total	2.03	1.99	2.00	2.03	2.03	2.01	2.01	2.02	2.01
No of Ions									
Cr	8.96	9.13	9.12	9.09	9.16	9.17	9.11	9.12	9.16
Al	5.43	5.30	5.20	5.20	5.19	5.16	5.27	5.30	5.21
Ti	0.22	0.19	0.22	0.22	0.23	0.22	0.21	0.18	0.23
Fe	6.39	6.29	6.34	6.36	6.32	6.36	6.28	6.23	6.28
Mg	3.45	3.56	3.58	3.60	3.55	3.57	3.59	3.61	3.55
Mn	0.10	0.10	0.10	0.11	0.11	0.08	0.12	0.10	0.11
Ni	0.03	0.03	0.06	0.04	0.04	0.06	0.03	0.06	0.05
Total	24.59	24.60	24.62	24.63	24.60	24.62	24.60	24.61	24.59
Fe Corrected on 32 O									
Fe3+	1.52	1.55	1.62	1.64	1.55	1.61	1.57	1.58	1.53
Fe2+	4.87	4.74	4.73	4.72	4.77	4.75	4.71	4.65	4.75

Block No.	2c	2c	3c	3c	3c	3c	3c	3c	3c
Raw Analysis	19	20	21	22	23	24	25	26	27
Cr2O3	42.97	43.59	43.78	43.83	43.75	43.99	43.83	43.31	44.33
Al2O3	16.88	16.33	16.87	16.96	16.92	16.68	16.79	16.87	17.12
TiO2	1.03	1.12	0.77	0.94	1.00	0.97	0.91	0.91	0.88
FeO	28.44	28.38	28.00	27.58	27.68	27.37	27.41	27.62	28.17
MgO	9.13	9.02	9.56	9.44	9.52	9.34	9.33	9.49	9.68
MnO	0.65	0.70	0.55	0.49	0.63	0.57	0.53	0.53	0.57
NiO	0.31	0.18	0.28	0.18	0.14	0.18	0.25	0.19	0.12
Total	99.41	99.32	99.82	99.42	99.63	99.11	99.06	98.93	100.87
MnO corrected	0.47	0.53	0.37	0.31	0.45	0.40	0.36	0.35	0.39
Total	99.24	99.15	99.64	99.24	99.45	98.93	98.88	98.75	100.69
Corrected Analysis									
Cr2O3	42.97	43.59	43.78	43.83	43.75	43.99	43.83	43.31	44.33
Al2O3	16.88	16.33	16.87	16.96	16.92	16.68	16.79	16.87	17.12
TiO2	1.03	1.12	0.77	0.94	1.00	0.97	0.91	0.91	0.88
FeO	21.07	21.13	20.46	20.67	20.60	20.69	20.65	20.39	20.76
Fe2O3	8.19	8.06	8.39	7.68	7.86	7.42	7.51	8.03	8.24
MgO	9.13	9.02	9.56	9.44	9.52	9.34	9.33	9.49	9.68
MnO	0.47	0.53	0.37	0.31	0.45	0.40	0.36	0.35	0.39
NiO	0.22	0.31	0.18	0.28	0.18	0.14	0.18	0.25	0.19
Total	99.97	100.08	100.38	100.11	100.29	99.64	99.57	99.62	101.59
	Formula units based on 32 oxygens and Fe2+/Fe3+ assuming full site occupancy								
Cr	8.80	8.95	8.91	8.94	8.91	9.03	9.00	8.88	8.91
Al	5.16	5.00	5.12	5.16	5.14	5.11	5.14	5.16	5.13
Ti	0.20	0.22	0.15	0.18	0.19	0.19	0.18	0.18	0.17
Fe3+	1.60	1.58	1.62	1.49	1.52	1.45	1.47	1.57	1.58
Fe2+	4.57	4.59	4.41	4.46	4.44	4.49	4.49	4.42	4.42
Mg	3.53	3.49	3.67	3.63	3.66	3.61	3.61	3.67	3.67
Mn	0.10	0.12	0.08	0.07	0.10	0.09	0.08	0.08	0.08
Ni	0.04	0.06	0.04	0.06	0.04	0.03	0.04	0.05	0.04
Total	24.00	24.00	24.00	24.00	24.00	24.00	24.00	24.00	24.00
100Mg/Mg+Fe2+	36.27	36.43	38.50	37.72	38.18	37.65	37.52	38.30	38.44
100Cr/Cr+Al	63.06	64.16	63.51	63.41	63.43	63.88	63.64	63.25	63.46
100Fe3+/Cr+Al+Fe3+	10.27	10.15	10.38	9.57	9.79	9.30	9.40	10.05	10.09
Cr	0.85	0.86	0.86	0.86	0.86	0.87	0.87	0.85	0.87
Al	0.50	0.48	0.50	0.50	0.50	0.49	0.49	0.50	0.50
Ti	0.03	0.03	0.02	0.02	0.03	0.02	0.02	0.02	0.02
Fe	0.40	0.40	0.39	0.38	0.39	0.38	0.38	0.38	0.39
Mg	0.23	0.22	0.24	0.23	0.24	0.23	0.23	0.24	0.24
Mn	0.01	0.01	0.01	0.00	0.01	0.01	0.01	0.00	0.01
Ni	0.00	0.00	0.00	0.00	0.00	0.00	0.00	0.00	0.00
Total	2.00	2.00	2.01	2.01	2.02	2.00	2.00	2.00	2.04
No of Ions									
Cr	9.03	9.18	9.15	9.16	9.13	9.24	9.22	9.11	9.14
Al	5.29	5.13	5.26	5.29	5.27	5.23	5.26	5.29	5.27
Ti	0.21	0.22	0.15	0.19	0.20	0.19	0.18	0.18	0.17
Fe	6.33	6.32	6.19	6.10	6.11	6.08	6.10	6.14	6.15
Mg	3.62	3.58	3.77	3.72	3.75	3.70	3.70	3.76	3.77
Mn	0.11	0.12	0.08	0.07	0.10	0.09	0.08	0.08	0.09
Ni	0.05	0.07	0.04	0.06	0.04	0.03	0.04	0.05	0.04
Total	24.63	24.62	24.64	24.59	24.60	24.57	24.58	24.62	24.62
Fe Corrected on 32 O									
Fe3+	1.64	1.62	1.67	1.53	1.56	1.48	1.50	1.61	1.62
Fe2+	4.69	4.71	4.52	4.57	4.55	4.60	4.59	4.53	4.53

Block No.	3c	3c	3c	4b	4b	4b	4b	4b	4b
Raw Analysis	28	29	30	31	32	33	34	35	36
Cr2O3	44.20	44.17	44.00	43.88	43.05	43.49	44.40	43.55	44.98
Al2O3	17.13	17.03	17.15	17.74	18.44	17.33	17.07	17.75	17.33
TiO2	0.87	0.96	0.92	0.88	0.92	0.81	0.88	0.83	0.79
FeO	27.91	27.72	27.84	28.54	28.24	28.39	28.60	28.56	28.25
MgO	9.53	9.33	9.25	9.11	9.46	8.87	8.72	9.09	9.17
MnO	0.57	0.65	0.62	0.55	0.72	0.73	0.47	0.60	0.66
NiO	0.24	0.19	0.27	0.19	0.14	0.18	0.28	0.21	0.20
Total	100.44	100.04	100.05	100.87	100.96	99.79	100.42	100.61	101.37
MnO corrected	0.40	0.47	0.44	0.37	0.55	0.55	0.29	0.43	0.48
Total	100.26	99.87	99.88	100.70	100.78	99.61	100.24	100.43	101.19
Corrected Analysis									
Cr2O3	44.20	44.17	44.00	43.88	43.05	43.49	44.40	43.55	44.98
Al2O3	17.13	17.03	17.15	17.74	18.44	17.33	17.07	17.75	17.33
TiO2	0.87	0.96	0.92	0.88	0.92	0.81	0.88	0.83	0.79
FeO	20.83	20.92	21.06	21.65	21.19	21.45	22.07	21.48	21.48
Fe2O3	7.86	7.56	7.54	7.65	7.83	7.71	7.25	7.86	7.51
MgO	9.53	9.33	9.25	9.11	9.46	8.87	8.72	9.09	9.17
MnO	0.40	0.47	0.44	0.37	0.55	0.55	0.29	0.43	0.48
NiO	0.12	0.24	0.19	0.27	0.19	0.14	0.18	0.28	0.21
Total	100.93	100.67	100.56	101.54	101.62	100.34	100.86	101.29	101.96
	Formula units based on 32 oxygens and Fe2+/Fe3+ assuming full site occupancy								
Cr	8.94	8.97	8.95	8.84	8.62	8.88	9.04	8.79	9.04
Al	5.17	5.16	5.20	5.33	5.50	5.27	5.18	5.34	5.19
Ti	0.17	0.18	0.18	0.17	0.18	0.16	0.17	0.16	0.15
Fe3+	1.51	1.46	1.46	1.47	1.49	1.50	1.41	1.51	1.44
Fe2+	4.46	4.50	4.53	4.61	4.49	4.63	4.75	4.59	4.57
Mg	3.63	3.57	3.55	3.46	3.57	3.41	3.35	3.46	3.47
Mn	0.09	0.10	0.10	0.08	0.12	0.12	0.06	0.09	0.10
Ni	0.02	0.05	0.04	0.05	0.04	0.03	0.04	0.06	0.04
Total	24.00	24.00	24.00	24.00	24.00	24.00	24.00	24.00	24.00
100Mg/Mg+Fe2+	37.74	37.00	36.45	34.79	35.72	34.47	33.70	34.84	35.58
100Cr/Cr+Al	63.37	63.49	63.24	62.39	61.02	62.73	63.56	62.19	63.51
100Fe3+/Cr+Al+Fe3+	9.69	9.38	9.35	9.39	9.56	9.58	9.00	9.66	9.17
Cr	0.87	0.87	0.87	0.87	0.85	0.86	0.88	0.86	0.89
Al	0.50	0.50	0.50	0.52	0.54	0.51	0.50	0.52	0.51
Ti	0.02	0.02	0.02	0.02	0.02	0.02	0.02	0.02	0.02
Fe	0.39	0.39	0.39	0.40	0.39	0.40	0.40	0.40	0.39
Mg	0.24	0.23	0.23	0.23	0.23	0.22	0.22	0.23	0.23
Mn	0.01	0.01	0.01	0.01	0.01	0.01	0.00	0.01	0.01
Ni	0.00	0.00	0.00	0.00	0.00	0.00	0.00	0.00	0.00
Total	2.03	2.02	2.02	2.04	2.05	2.01	2.02	2.04	2.05
No of Ions									
Cr	9.17	9.19	9.16	9.05	8.83	9.09	9.25	9.01	9.25
Al	5.30	5.28	5.33	5.45	5.64	5.40	5.30	5.48	5.31
Ti	0.17	0.19	0.18	0.17	0.18	0.16	0.17	0.16	0.15
Fe	6.12	6.10	6.13	6.23	6.13	6.28	6.30	6.25	6.14
Mg	3.72	3.66	3.63	3.54	3.66	3.50	3.43	3.55	3.55
Mn	0.09	0.10	0.10	0.08	0.12	0.12	0.07	0.10	0.11
Ni	0.03	0.05	0.04	0.06	0.04	0.03	0.04	0.06	0.04
Total	24.60	24.58	24.57	24.58	24.59	24.59	24.55	24.59	24.56
Fe Corrected on 32 O									
Fe3+	1.55	1.50	1.49	1.50	1.53	1.54	1.44	1.55	1.47
Fe2+	4.57	4.60	4.64	4.72	4.60	4.75	4.86	4.70	4.67

Block No.	4b	4b	4b	4b	5a	5a	5a	5a	5a
Raw Analysis	37	38	39	40	41	42	43	44	45
Cr2O3	44.07	44.28	43.84	43.76	43.29	43.16	44.09	43.94	43.95
Al2O3	17.50	17.26	17.45	17.54	17.89	17.11	17.30	17.48	17.71
TiO2	0.87	0.79	0.86	0.77	0.89	0.89	0.88	0.90	0.92
FeO	28.31	28.29	28.24	28.23	27.49	27.86	28.54	28.40	28.67
MgO	9.30	9.45	9.23	9.15	9.13	9.10	9.38	9.23	9.17
MnO	0.61	0.66	0.62	0.80	0.77	0.52	0.78	0.68	0.60
NiO	0.25	0.20	0.21	0.12	0.07	0.13	0.15	0.13	0.20
Total	100.91	100.93	100.43	100.36	99.53	98.77	101.11	100.77	101.21
MnO corrected	0.44	0.49	0.44	0.62	0.59	0.35	0.60	0.51	0.43
Total	100.73	100.76	100.26	100.19	99.35	98.59	100.93	100.60	101.04
Corrected Analysis									
Cr2O3	44.07	44.28	43.84	43.76	43.29	43.16	44.09	43.94	43.95
Al2O3	17.50	17.26	17.45	17.54	17.89	17.11	17.30	17.48	17.71
TiO2	0.87	0.79	0.86	0.77	0.89	0.89	0.88	0.90	0.92
FeO	21.29	20.91	21.25	21.13	21.10	21.06	21.15	21.37	21.73
Fe2O3	7.80	8.20	7.78	7.90	7.10	7.55	8.21	7.81	7.72
MgO	9.30	9.45	9.23	9.15	9.13	9.10	9.38	9.23	9.17
MnO	0.44	0.49	0.44	0.62	0.59	0.35	0.60	0.51	0.43
NiO	0.20	0.25	0.20	0.21	0.12	0.07	0.13	0.15	0.13
Total	101.46	101.63	101.03	101.06	100.11	99.30	101.74	101.39	101.75
	Formula units based on 32 oxygens and Fe2+/Fe3+ assuming full site occupancy								
Cr	8.88	8.91	8.87	8.85	8.81	8.88	8.87	8.86	8.83
Al	5.26	5.18	5.26	5.29	5.43	5.25	5.19	5.26	5.31
Ti	0.17	0.15	0.17	0.15	0.17	0.17	0.17	0.17	0.18
Fe3+	1.50	1.57	1.50	1.52	1.38	1.48	1.57	1.50	1.48
Fe2+	4.54	4.45	4.55	4.52	4.55	4.59	4.50	4.56	4.62
Mg	3.53	3.59	3.52	3.49	3.50	3.53	3.55	3.51	3.47
Mn	0.09	0.10	0.10	0.13	0.13	0.08	0.13	0.11	0.09
Ni	0.04	0.05	0.04	0.04	0.02	0.02	0.03	0.03	0.03
Total	24.00	24.00	24.00	24.00	24.00	24.00	24.00	24.00	24.00
100Mg/Mg+Fe2+	36.05	37.24	35.86	35.55	35.10	35.90	36.69	35.75	35.00
100Cr/Cr+Al	62.80	63.24	62.76	62.60	61.87	62.85	63.08	62.76	62.46
100Fe3+/Cr+Al+Fe3+	9.57	10.03	9.58	9.71	8.81	9.48	10.06	9.60	9.45
Cr	0.87	0.87	0.87	0.86	0.85	0.85	0.87	0.87	0.87
Al	0.52	0.51	0.51	0.52	0.53	0.50	0.51	0.51	0.52
Ti	0.02	0.02	0.02	0.02	0.02	0.02	0.02	0.02	0.02
Fe	0.39	0.39	0.39	0.39	0.38	0.39	0.40	0.40	0.40
Mg	0.23	0.23	0.23	0.23	0.23	0.23	0.23	0.23	0.23
Mn	0.01	0.01	0.01	0.01	0.01	0.00	0.01	0.01	0.01
Ni	0.00	0.00	0.00	0.00	0.00	0.00	0.00	0.00	0.00
Total	2.04	2.04	2.03	2.03	2.02	2.00	2.04	2.04	2.05
No of Ions									
Cr	9.10	9.14	9.09	9.07	9.01	9.10	9.09	9.08	9.04
Al	5.39	5.31	5.39	5.42	5.56	5.38	5.32	5.39	5.44
Ti	0.17	0.16	0.17	0.15	0.18	0.18	0.17	0.18	0.18
Fe	6.18	6.18	6.19	6.19	6.06	6.21	6.23	6.21	6.24
Mg	3.62	3.68	3.61	3.58	3.58	3.62	3.65	3.60	3.56
Mn	0.10	0.11	0.10	0.14	0.13	0.08	0.13	0.11	0.09
Ni	0.04	0.05	0.04	0.04	0.03	0.02	0.03	0.03	0.03
Total	24.59	24.62	24.59	24.60	24.54	24.58	24.62	24.59	24.58
Fe Corrected on 32 O									
Fe3+	1.53	1.61	1.53	1.56	1.41	1.52	1.61	1.54	1.51
Fe2+	4.65	4.57	4.66	4.63	4.65	4.70	4.62	4.67	4.73

Block No.	5a	5a	5a	5a	5a	6b	6b	6b	6b
Raw Analysis	46	47	48	49	50	51	52	53	54
Cr2O3	43.78	44.31	43.72	44.17	43.53	45.39	45.57	45.42	45.04
Al2O3	17.36	17.27	17.41	17.31	17.34	16.03	16.26	16.27	16.25
TiO2	0.85	0.94	0.94	0.82	0.95	1.00	1.00	1.02	1.07
FeO	28.36	28.38	28.43	28.04	28.60	29.47	29.13	29.13	29.24
MgO	9.39	9.41	9.24	9.22	9.18	8.64	8.77	8.71	8.55
MnO	0.53	0.58	0.67	0.50	0.50	0.60	0.55	0.66	0.70
NiO	0.25	0.29	0.23	0.05	0.15	0.19	0.24	0.24	0.32
Total	100.51	101.16	100.64	100.11	100.25	101.33	101.52	101.44	101.18
MnO corrected	0.36	0.40	0.49	0.33	0.32	0.42	0.37	0.48	0.52
Total	100.33	100.98	100.46	99.94	100.07	101.15	101.34	101.26	101.00
Corrected Analysis									
Cr2O3	43.78	44.31	43.72	44.17	43.53	45.39	45.57	45.42	45.04
Al2O3	17.36	17.27	17.41	17.31	17.34	16.03	16.26	16.27	16.25
TiO2	0.85	0.94	0.94	0.82	0.95	1.00	1.00	1.02	1.07
FeO	21.08	21.23	21.25	21.23	21.55	22.39	22.28	22.22	22.37
Fe2O3	8.08	7.94	7.98	7.57	7.83	7.88	7.61	7.67	7.63
MgO	9.39	9.41	9.24	9.22	9.18	8.64	8.77	8.71	8.55
MnO	0.36	0.40	0.49	0.33	0.32	0.42	0.37	0.48	0.52
NiO	0.20	0.25	0.29	0.23	0.05	0.15	0.19	0.24	0.24
Total	101.09	101.74	101.32	100.87	100.75	101.90	102.05	102.03	101.68
	Formula units based on 32 oxygens and Fe2+/Fe3+ assuming full site occupancy								
Cr	8.85	8.91	8.83	8.95	8.84	9.21	9.21	9.19	9.15
Al	5.23	5.18	5.24	5.23	5.25	4.85	4.90	4.91	4.92
Ti	0.16	0.18	0.18	0.16	0.18	0.19	0.19	0.20	0.21
Fe3+	1.55	1.52	1.53	1.46	1.51	1.52	1.46	1.48	1.48
Fe2+	4.51	4.51	4.54	4.55	4.63	4.80	4.77	4.76	4.81
Mg	3.58	3.57	3.52	3.52	3.51	3.31	3.34	3.32	3.27
Mn	0.08	0.09	0.11	0.07	0.07	0.09	0.08	0.10	0.11
Ni	0.04	0.05	0.06	0.05	0.01	0.03	0.04	0.05	0.05
Total	24.00	24.00	24.00	24.00	24.00	24.00	24.00	24.00	24.00
100Mg/Mg+Fe2+	36.71	36.79	35.94	35.99	35.57	34.25	34.57	34.37	33.63
100Cr/Cr+Al	62.83	63.25	62.74	63.12	62.74	65.51	65.27	65.18	65.01
100Fe3+/Cr+Al+Fe3+	9.94	9.74	9.83	9.33	9.70	9.76	9.40	9.49	9.49
Cr	0.86	0.87	0.86	0.87	0.86	0.90	0.90	0.90	0.89
Al	0.51	0.51	0.51	0.51	0.51	0.47	0.48	0.48	0.48
Ti	0.02	0.02	0.02	0.02	0.02	0.03	0.03	0.03	0.03
Fe	0.39	0.39	0.40	0.39	0.40	0.41	0.41	0.41	0.41
Mg	0.23	0.23	0.23	0.23	0.23	0.21	0.22	0.22	0.21
Mn	0.01	0.01	0.01	0.00	0.00	0.01	0.01	0.01	0.01
Ni	0.00	0.00	0.00	0.00	0.00	0.00	0.00	0.00	0.00
Total	2.03	2.04	2.03	2.03	2.02	2.03	2.03	2.03	2.02
No of Ions									
Cr	9.07	9.13	9.05	9.17	9.05	9.44	9.43	9.41	9.37
Al	5.37	5.31	5.37	5.36	5.38	4.97	5.02	5.03	5.04
Ti	0.17	0.18	0.18	0.16	0.19	0.20	0.20	0.20	0.21
Fe	6.22	6.19	6.22	6.16	6.29	6.48	6.38	6.38	6.44
Mg	3.67	3.65	3.60	3.61	3.60	3.39	3.42	3.40	3.35
Mn	0.08	0.09	0.11	0.07	0.07	0.09	0.08	0.11	0.12
Ni	0.04	0.05	0.06	0.05	0.01	0.03	0.04	0.05	0.05
Total	24.61	24.60	24.60	24.57	24.60	24.60	24.58	24.58	24.58
Fe Corrected on 32 O									
Fe3+	1.59	1.56	1.57	1.50	1.55	1.56	1.50	1.51	1.51
Fe2+	4.62	4.63	4.65	4.66	4.74	4.92	4.88	4.87	4.92

Block No.	6b	6b	6b	6b	6b	6b	7c	7c	7c
Raw Analysis	55	56	57	58	59	60	61	62	63
Cr2O3	43.47	45.22	44.95	44.74	44.91	44.48	43.75	43.78	44.10
Al2O3	16.72	15.70	15.64	16.01	16.26	15.95	15.93	15.90	15.95
TiO2	1.03	1.03	1.20	1.05	1.12	1.32	1.20	1.07	1.17
FeO	28.29	29.10	29.53	29.46	29.22	29.70	29.21	29.87	29.84
MgO	8.76	8.45	8.57	8.66	8.60	8.54	8.41	8.56	8.55
MnO	0.74	0.71	0.54	0.64	0.52	0.64	0.70	0.75	0.54
NiO	0.14	0.27	0.19	0.24	0.21	0.18	0.11	0.14	0.10
Total	99.15	100.49	100.60	100.79	100.84	100.82	99.30	100.07	100.23
MnO corrected	0.57	0.53	0.36	0.46	0.34	0.47	0.52	0.57	0.37
Total	98.98	100.31	100.42	100.62	100.66	100.64	99.13	99.89	100.06
Corrected Analysis									
Cr2O3	43.47	45.22	44.95	44.74	44.91	44.48	43.75	43.78	44.10
Al2O3	16.72	15.70	15.64	16.01	16.26	15.95	15.93	15.90	15.95
TiO2	1.03	1.03	1.20	1.05	1.12	1.32	1.20	1.07	1.17
FeO	21.39	22.24	22.38	22.17	22.44	22.57	22.17	22.10	22.44
Fe2O3	7.66	7.62	7.94	8.10	7.54	7.92	7.83	8.63	8.22
MgO	8.76	8.45	8.57	8.66	8.60	8.54	8.41	8.56	8.55
MnO	0.57	0.53	0.36	0.46	0.34	0.47	0.52	0.57	0.37
NiO	0.32	0.14	0.27	0.19	0.24	0.21	0.18	0.11	0.14
Total	99.92	100.94	101.30	101.38	101.44	101.46	99.99	100.73	100.92
	Formula units based on 32 oxygens and Fe2+/Fe3+ assuming full site occupancy								
Cr	8.94	9.27	9.19	9.12	9.14	9.06	9.04	8.98	9.03
Al	5.12	4.80	4.76	4.86	4.93	4.85	4.91	4.87	4.87
Ti	0.20	0.20	0.23	0.20	0.22	0.26	0.23	0.21	0.23
Fe3+	1.50	1.49	1.55	1.57	1.46	1.54	1.54	1.69	1.60
Fe2+	4.65	4.82	4.84	4.78	4.83	4.87	4.85	4.80	4.86
Mg	3.39	3.27	3.30	3.33	3.30	3.28	3.27	3.31	3.30
Mn	0.12	0.12	0.08	0.10	0.07	0.10	0.12	0.13	0.08
Ni	0.07	0.03	0.06	0.04	0.05	0.04	0.04	0.02	0.03
Total	24.00	24.00	24.00	24.00	24.00	24.00	24.00	24.00	24.00
100Mg/Mg+Fe2+	34.73	33.93	34.37	34.48	33.78	33.79	33.56	34.26	33.91
100Cr/Cr+Al	63.55	65.88	65.85	65.21	64.94	65.15	64.81	64.87	64.96
100Fe3+/Cr+Al+Fe3+	9.64	9.56	9.97	10.11	9.40	9.95	9.95	10.85	10.34
Cr	0.86	0.89	0.89	0.88	0.89	0.88	0.86	0.86	0.87
Al	0.49	0.46	0.46	0.47	0.48	0.47	0.47	0.47	0.47
Ti	0.03	0.03	0.03	0.03	0.03	0.03	0.03	0.03	0.03
Fe	0.39	0.40	0.41	0.41	0.41	0.41	0.41	0.42	0.42
Mg	0.22	0.21	0.21	0.21	0.21	0.21	0.21	0.21	0.21
Mn	0.01	0.01	0.01	0.01	0.00	0.01	0.01	0.01	0.01
Ni	0.00	0.00	0.00	0.00	0.00	0.00	0.00	0.00	0.00
Total	2.00	2.00	2.01	2.01	2.02	2.01	1.99	2.00	2.00
No of Ions									
Cr	9.16	9.50	9.42	9.35	9.36	9.29	9.27	9.23	9.27
Al	5.25	4.92	4.89	4.99	5.05	4.97	5.03	5.00	5.00
Ti	0.21	0.21	0.24	0.21	0.22	0.26	0.24	0.22	0.23
Fe	6.30	6.47	6.54	6.51	6.44	6.57	6.55	6.66	6.63
Mg	3.48	3.35	3.38	3.41	3.38	3.37	3.36	3.40	3.39
Mn	0.13	0.12	0.08	0.10	0.08	0.10	0.12	0.13	0.08
Ni	0.07	0.03	0.06	0.04	0.05	0.04	0.04	0.02	0.03
Total	24.59	24.59	24.61	24.62	24.57	24.61	24.61	24.67	24.63
Fe Corrected on 32 O									
Fe3+	1.54	1.52	1.58	1.61	1.49	1.58	1.58	1.73	1.64
Fe2+	4.77	4.94	4.96	4.90	4.95	4.99	4.97	4.93	4.99

Block No.	7c	7c	7c	7c	7c	7c	7c	8b	8b
Raw Analysis	64	65	66	67	68	69	70	71	72
Cr2O3	44.67	44.63	43.75	43.43	43.62	43.70	44.60	44.43	42.62
Al2O3	16.07	15.43	16.09	16.25	16.57	16.16	15.83	17.36	16.59
TiO2	1.17	1.20	1.18	1.21	1.04	1.08	1.00	1.09	1.01
FeO	29.79	29.78	29.81	29.88	29.10	29.17	28.57	28.76	28.50
MgO	8.67	8.25	8.58	8.53	8.62	8.70	8.41	9.12	8.74
MnO	0.67	0.49	0.68	0.60	0.75	0.58	0.68	0.51	0.59
NiO	0.21	0.15	0.30	0.17	0.11	0.16	0.10	0.19	0.17
Total	101.25	99.93	100.40	100.06	99.80	99.54	99.20	101.46	98.21
MnO corrected	0.49	0.31	0.51	0.43	0.57	0.40	0.51	0.33	0.42
Total	101.07	99.75	100.22	99.89	99.62	99.36	99.02	101.28	98.04
Corrected Analysis									
Cr2O3	44.67	44.63	43.75	43.43	43.62	43.70	44.60	44.43	42.62
Al2O3	16.07	15.43	16.09	16.25	16.57	16.16	15.83	17.36	16.59
TiO2	1.17	1.20	1.18	1.21	1.04	1.08	1.00	1.09	1.01
FeO	22.46	22.70	22.27	22.32	21.92	21.90	21.94	22.08	21.34
Fe2O3	8.15	7.87	8.38	8.40	7.97	8.08	7.37	7.42	7.96
MgO	8.67	8.25	8.58	8.53	8.62	8.70	8.41	9.12	8.74
MnO	0.49	0.31	0.51	0.43	0.57	0.40	0.51	0.33	0.42
NiO	0.10	0.21	0.15	0.30	0.17	0.11	0.16	0.10	0.19
Total	101.77	100.60	100.91	100.86	100.48	100.12	99.81	101.94	98.86
	Formula units based on 32 oxygens and Fe2+/Fe3+ assuming full site occupancy								
Cr	9.07	9.20	8.95	8.89	8.94	8.99	9.23	8.93	8.85
Al	4.86	4.74	4.91	4.96	5.06	4.96	4.89	5.20	5.14
Ti	0.23	0.23	0.23	0.24	0.20	0.21	0.20	0.21	0.20
Fe3+	1.57	1.54	1.63	1.64	1.55	1.58	1.45	1.42	1.57
Fe2+	4.82	4.95	4.82	4.83	4.75	4.77	4.80	4.69	4.69
Mg	3.32	3.21	3.31	3.29	3.33	3.37	3.28	3.46	3.42
Mn	0.11	0.07	0.11	0.09	0.13	0.09	0.11	0.07	0.09
Ni	0.02	0.04	0.03	0.06	0.04	0.02	0.03	0.02	0.04
Total	24.00	24.00	24.00	24.00	24.00	24.00	24.00	24.00	24.00
100Mg/Mg+Fe2+	34.25	33.09	34.00	33.60	33.92	34.68	33.86	34.91	34.81
100Cr/Cr+Al	65.09	65.99	64.58	64.19	63.84	64.46	65.39	63.18	63.27
100Fe3+/Cr+Al+Fe3+	10.15	9.97	10.53	10.57	10.00	10.18	9.33	9.13	10.11
Cr	0.88	0.88	0.86	0.86	0.86	0.86	0.88	0.88	0.84
Al	0.47	0.45	0.47	0.48	0.49	0.48	0.47	0.51	0.49
Ti	0.03	0.03	0.03	0.03	0.03	0.03	0.03	0.03	0.03
Fe	0.41	0.41	0.41	0.42	0.40	0.41	0.40	0.40	0.40
Mg	0.22	0.20	0.21	0.21	0.21	0.22	0.21	0.23	0.22
Mn	0.01	0.00	0.01	0.01	0.01	0.01	0.01	0.00	0.01
Ni	0.00	0.00	0.00	0.00	0.00	0.00	0.00	0.00	0.00
Total	2.02	1.99	2.00	2.00	2.00	1.99	1.99	2.05	1.98
No of Ions									
Cr	9.30	9.44	9.19	9.13	9.17	9.23	9.45	9.14	9.08
Al	4.99	4.86	5.04	5.09	5.19	5.09	5.00	5.32	5.27
Ti	0.23	0.24	0.24	0.24	0.21	0.22	0.20	0.21	0.20
Fe	6.56	6.66	6.63	6.64	6.47	6.52	6.41	6.26	6.42
Mg	3.40	3.29	3.40	3.38	3.41	3.46	3.36	3.54	3.51
Mn	0.11	0.07	0.11	0.10	0.13	0.09	0.11	0.07	0.10
Ni	0.02	0.05	0.03	0.06	0.04	0.02	0.03	0.02	0.04
Total	24.62	24.61	24.65	24.65	24.61	24.62	24.57	24.56	24.62
Fe Corrected on 32 O									
Fe3+	1.61	1.58	1.68	1.68	1.59	1.62	1.49	1.45	1.61
Fe2+	4.95	5.08	4.95	4.96	4.87	4.89	4.92	4.80	4.81

Block No.	8b	8b	8b	8b	8b	8b	8b	8b	9b
Raw Analysis	73	74	75	76	77	78	79	80	81
Cr2O3	42.61	42.85	43.46	43.14	43.08	42.77	42.73	42.83	44.59
Al2O3	16.24	16.28	16.46	16.52	16.41	16.70	16.26	15.83	16.57
TiO2	1.14	0.95	0.99	1.01	0.98	1.10	1.22	1.12	1.03
FeO	28.26	28.30	28.28	28.53	28.25	28.81	28.72	28.70	28.54
MgO	8.63	8.57	8.71	8.77	8.66	8.66	8.55	8.41	8.85
MnO	0.64	0.59	0.66	0.68	0.66	0.55	0.47	0.69	0.64
NiO	0.26	0.21	0.11	0.28	0.18	0.16	0.16	0.22	0.22
Total	97.78	97.75	98.66	98.93	98.22	98.75	98.11	97.81	100.46
MnO corrected	0.47	0.42	0.49	0.50	0.49	0.38	0.30	0.52	0.46
Total	97.61	97.58	98.48	98.75	98.04	98.57	97.93	97.64	100.28
Corrected Analysis									
Cr2O3	42.61	42.85	43.46	43.14	43.08	42.77	42.73	42.83	44.59
Al2O3	16.24	16.28	16.46	16.52	16.41	16.70	16.26	15.83	16.57
TiO2	1.14	0.95	0.99	1.01	0.98	1.10	1.22	1.12	1.03
FeO	21.33	21.27	21.40	21.42	21.25	21.76	21.84	21.58	21.78
Fe2O3	7.70	7.81	7.65	7.90	7.78	7.83	7.65	7.91	7.51
MgO	8.63	8.57	8.71	8.77	8.66	8.66	8.55	8.41	8.85
MnO	0.47	0.42	0.49	0.50	0.49	0.38	0.30	0.52	0.46
NiO	0.17	0.26	0.21	0.11	0.28	0.18	0.16	0.16	0.22
Total	98.28	98.41	99.35	99.37	98.93	99.37	98.71	98.37	101.03
	Formula units based on 32 oxygens and Fe2+/Fe3+ assuming full site occupancy								
Cr	8.91	8.96	8.99	8.92	8.95	8.84	8.91	8.98	9.08
Al	5.06	5.07	5.08	5.09	5.09	5.15	5.05	4.95	5.03
Ti	0.23	0.19	0.19	0.20	0.19	0.22	0.24	0.22	0.20
Fe3+	1.53	1.55	1.51	1.55	1.54	1.54	1.52	1.58	1.46
Fe2+	4.72	4.70	4.68	4.69	4.67	4.76	4.82	4.79	4.69
Mg	3.40	3.38	3.40	3.42	3.39	3.38	3.36	3.33	3.40
Mn	0.11	0.09	0.11	0.11	0.11	0.08	0.07	0.12	0.10
Ni	0.04	0.06	0.04	0.02	0.06	0.04	0.03	0.03	0.05
Total	24.00	24.00	24.00	24.00	24.00	24.00	24.00	24.00	24.00
100Mg/Mg+Fe2+	34.77	34.54	34.79	34.96	34.77	34.08	34.05	34.15	34.94
100Cr/Cr+Al	63.77	63.84	63.90	63.65	63.77	63.19	63.80	64.47	64.34
100Fe3+/Cr+Al+Fe3+	9.88	9.97	9.67	9.99	9.88	9.92	9.80	10.18	9.35
Cr	0.84	0.85	0.86	0.85	0.85	0.84	0.84	0.85	0.88
Al	0.48	0.48	0.48	0.49	0.48	0.49	0.48	0.47	0.49
Ti	0.03	0.02	0.02	0.03	0.02	0.03	0.03	0.03	0.03
Fe	0.39	0.39	0.39	0.40	0.39	0.40	0.40	0.40	0.40
Mg	0.21	0.21	0.22	0.22	0.21	0.21	0.21	0.21	0.22
Mn	0.01	0.01	0.01	0.01	0.01	0.01	0.00	0.01	0.01
Ni	0.00	0.00	0.00	0.00	0.00	0.00	0.00	0.00	0.00
Total	1.96	1.96	1.99	1.99	1.98	1.99	1.97	1.96	2.02
No of Ions									
Cr	9.14	9.18	9.21	9.14	9.18	9.06	9.13	9.22	9.29
Al	5.19	5.20	5.20	5.22	5.21	5.28	5.18	5.08	5.15
Ti	0.23	0.19	0.20	0.20	0.20	0.22	0.25	0.23	0.21
Fe	6.41	6.42	6.34	6.40	6.37	6.46	6.49	6.53	6.29
Mg	3.49	3.46	3.48	3.51	3.48	3.46	3.45	3.41	3.48
Mn	0.11	0.10	0.11	0.11	0.11	0.09	0.07	0.12	0.10
Ni	0.04	0.06	0.05	0.02	0.06	0.04	0.04	0.03	0.05
Total	24.60	24.61	24.59	24.61	24.61	24.61	24.60	24.62	24.57
Fe Corrected on 32 O									
Fe3+	1.57	1.59	1.54	1.59	1.58	1.58	1.56	1.62	1.49
Fe2+	4.84	4.82	4.80	4.80	4.79	4.88	4.94	4.91	4.80

Block No.	9b	9b	9b	9b	9b	9b	9b	9b	9b
Raw Analysis	82	83	84	85	86	87	88	89	90
Cr2O3	44.10	43.88	43.55	43.62	43.91	43.54	43.95	43.89	43.72
Al2O3	16.60	16.63	17.62	16.02	16.50	16.67	16.22	16.08	16.32
TiO2	1.03	0.96	0.84	1.06	1.11	1.12	1.04	1.13	1.09
FeO	28.72	27.90	27.68	28.62	28.28	28.24	28.65	28.54	28.60
MgO	9.07	9.03	9.15	8.96	9.13	9.21	8.97	9.00	9.00
MnO	0.54	0.66	0.62	0.60	0.68	0.69	0.73	0.69	0.56
NiO	0.24	0.19	0.21	0.24	0.18	0.13	0.24	0.21	0.14
Total	100.30	99.26	99.66	99.12	99.77	99.60	99.80	99.54	99.43
MnO corrected	0.37	0.49	0.44	0.43	0.50	0.52	0.55	0.51	0.38
Total	100.12	99.08	99.48	98.95	99.60	99.43	99.63	99.37	99.26
Corrected Analysis									
Cr2O3	44.10	43.88	43.55	43.62	43.91	43.54	43.95	43.89	43.72
Al2O3	16.60	16.63	17.62	16.02	16.50	16.67	16.22	16.08	16.32
TiO2	1.03	0.96	0.84	1.06	1.11	1.12	1.04	1.13	1.09
FeO	21.52	21.05	21.09	21.22	21.19	21.10	21.35	21.25	21.39
Fe2O3	8.00	7.61	7.32	8.22	7.88	7.94	8.12	8.10	8.02
MgO	9.07	9.03	9.15	8.96	9.13	9.21	8.97	9.00	9.00
MnO	0.37	0.49	0.44	0.43	0.50	0.52	0.55	0.51	0.38
NiO	0.22	0.24	0.19	0.21	0.24	0.18	0.13	0.24	0.21
Total	100.91	99.89	100.20	99.74	100.44	100.27	100.33	100.20	100.13
	Formula units based on 32 oxygens and Fe2+/Fe3+ assuming full site occupancy								
Cr	8.97	9.01	8.87	9.00	8.97	8.90	9.01	9.01	8.97
Al	5.04	5.09	5.35	4.93	5.03	5.08	4.96	4.92	4.99
Ti	0.20	0.19	0.16	0.21	0.21	0.22	0.20	0.22	0.21
Fe3+	1.55	1.49	1.42	1.61	1.53	1.54	1.58	1.58	1.57
Fe2+	4.63	4.57	4.55	4.63	4.58	4.56	4.63	4.62	4.64
Mg	3.48	3.49	3.51	3.48	3.52	3.55	3.47	3.48	3.48
Mn	0.08	0.11	0.10	0.09	0.11	0.11	0.12	0.11	0.08
Ni	0.05	0.05	0.04	0.04	0.05	0.04	0.03	0.05	0.04
Total	24.00	24.00	24.00	24.00	24.00	24.00	24.00	24.00	24.00
100Mg/Mg+Fe2+	35.98	36.16	35.50	36.43	36.59	36.78	36.16	36.51	36.13
100Cr/Cr+Al	64.05	63.89	62.37	64.61	64.09	63.66	64.50	64.67	64.25
100Fe3+/Cr+Al+Fe3+	9.96	9.54	9.08	10.39	9.87	9.95	10.19	10.20	10.08
Cr	0.87	0.87	0.86	0.86	0.87	0.86	0.87	0.87	0.86
Al	0.49	0.49	0.52	0.47	0.49	0.49	0.48	0.47	0.48
Ti	0.03	0.02	0.02	0.03	0.03	0.03	0.03	0.03	0.03
Fe	0.40	0.39	0.39	0.40	0.39	0.39	0.40	0.40	0.40
Mg	0.22	0.22	0.23	0.22	0.23	0.23	0.22	0.22	0.22
Mn	0.01	0.01	0.01	0.01	0.01	0.01	0.01	0.01	0.01
Ni	0.00	0.00	0.00	0.00	0.00	0.00	0.00	0.00	0.00
Total	2.02	2.00	2.02	1.99	2.01	2.01	2.00	2.00	2.00
No of Ions									
Cr	9.20	9.23	9.08	9.24	9.20	9.12	9.24	9.25	9.20
Al	5.17	5.22	5.48	5.06	5.15	5.21	5.09	5.05	5.12
Ti	0.21	0.19	0.17	0.21	0.22	0.22	0.21	0.23	0.22
Fe	6.34	6.21	6.10	6.41	6.27	6.26	6.38	6.36	6.37
Mg	3.57	3.58	3.60	3.58	3.60	3.64	3.56	3.57	3.57
Mn	0.08	0.11	0.10	0.10	0.11	0.12	0.12	0.12	0.09
Ni	0.05	0.05	0.04	0.04	0.05	0.04	0.03	0.05	0.05
Total	24.61	24.59	24.56	24.64	24.60	24.61	24.63	24.62	24.62
Fe Corrected on 32 O									
Fe3+	1.59	1.52	1.45	1.66	1.57	1.58	1.63	1.62	1.61
Fe2+	4.75	4.68	4.65	4.75	4.70	4.68	4.75	4.74	4.76

Block No.	1c	1c	1c	1c	1c	1c	1c	1c	1c	1c	2a	2a
Raw Analysis	1	2	3	4	5	6	7	8	9	10	11	12
Cr2O3	43.68	43.81	43.94	43.41	44.68	45.30	44.61	44.31	44.60	44.37	45.44	45.86
Al2O3	18.88	18.18	18.35	18.78	17.21	16.35	17.02	18.20	17.92	18.30	17.98	18.27
TiO2	1.00	1.07	1.08	1.02	1.18	1.03	1.10	1.19	1.15	1.15	0.94	0.93
FeO	28.57	28.51	28.91	28.93	28.86	28.81	29.13	28.11	28.00	26.89	26.89	27.03
MgO	7.99	7.81	7.97	7.80	7.72	7.40	7.58	8.10	7.94	8.19	7.79	7.90
MnO	0.55	0.49	0.51	0.54	0.62	0.57	0.60	0.48	0.61	0.61	0.59	0.67
NiO	0.15	0.16	0.14	0.11	0.12	0.11	0.18	0.12	0.08	0.07	0.19	0.22
Total	100.82	100.02	100.90	100.59	100.39	99.56	100.22	100.50	100.29	99.59	99.83	100.87
MnO corrected	0.37	0.31	0.33	0.36	0.44	0.39	0.42	0.31	0.43	0.43	0.41	0.49
Total	100.64	99.84	100.72	100.42	100.21	99.38	100.04	100.33	100.11	99.41	99.65	100.69
Corrected Analysis												
Cr2O3	43.68	43.81	43.94	43.41	44.68	45.30	44.61	44.31	44.60	44.37	45.44	45.86
Al2O3	18.88	18.18	18.35	18.78	17.21	16.35	17.02	18.20	17.92	18.30	17.98	18.27
TiO2	1.00	1.07	1.08	1.02	1.18	1.03	1.10	1.19	1.15	1.15	0.94	0.93
FeO	23.61	23.62	23.71	23.87	23.74	23.76	23.79	23.48	23.45	22.91	23.33	23.37
Fe2O3	5.52	5.43	5.78	5.63	5.69	5.61	5.94	5.15	5.05	4.43	3.96	4.07
MgO	7.99	7.81	7.97	7.80	7.72	7.40	7.58	8.10	7.94	8.19	7.79	7.90
MnO	0.37	0.31	0.33	0.36	0.44	0.39	0.42	0.31	0.43	0.43	0.41	0.49
NiO	0.15	0.16	0.14	0.11	0.12	0.11	0.18	0.12	0.12	0.08	0.07	0.19
Total	101.19	100.39	101.30	100.98	100.78	99.94	100.64	100.84	100.66	99.86	99.93	101.07
Formula units based on 32 oxygens and Fe2+/Fe3+ assuming full site occupancy												
Cr	8.84	8.96	8.90	8.81	9.15	9.40	9.17	9.01	9.10	9.09	9.34	9.31
Al	5.70	5.55	5.54	5.69	5.26	5.06	5.22	5.52	5.45	5.59	5.51	5.53
Ti	0.19	0.21	0.21	0.20	0.23	0.20	0.21	0.23	0.22	0.22	0.18	0.18
Fe3+	1.06	1.06	1.11	1.09	1.11	1.11	1.16	1.00	0.98	0.86	0.78	0.79
Fe2+	5.05	5.11	5.08	5.13	5.15	5.22	5.17	5.05	5.06	4.96	5.07	5.02
Mg	3.05	3.01	3.05	2.99	2.98	2.90	2.94	3.11	3.06	3.16	3.02	3.02
Mn	0.08	0.07	0.07	0.08	0.10	0.09	0.09	0.07	0.09	0.10	0.09	0.11
Ni	0.03	0.03	0.03	0.02	0.02	0.02	0.04	0.02	0.02	0.02	0.02	0.04
Total	24.00	24.00	24.00	24.00	24.00	24.00	24.00	24.00	24.00	24.00	24.00	24.00
100Mg/Mg+Fe2+	28.34	28.25	28.66	27.62	28.68	28.17	28.25	29.39	29.05	29.97	28.51	28.65
100Cr/Cr+Al	60.81	61.77	61.62	60.78	63.52	65.01	63.73	62.02	62.53	61.91	62.89	62.73
100Fe3+/Cr+Al+Fe3+	6.81	6.79	7.16	6.98	7.15	7.12	7.48	6.42	6.32	5.56	4.96	5.03
Cr	0.86	0.86	0.87	0.86	0.88	0.89	0.88	0.87	0.88	0.88	0.90	0.90
Al	0.56	0.53	0.54	0.55	0.51	0.48	0.50	0.54	0.53	0.54	0.53	0.54
Ti	0.03	0.03	0.03	0.03	0.03	0.03	0.03	0.03	0.03	0.03	0.02	0.02
Fe	0.40	0.40	0.40	0.40	0.40	0.40	0.41	0.39	0.39	0.37	0.37	0.38
Mg	0.20	0.19	0.20	0.19	0.19	0.18	0.19	0.20	0.20	0.20	0.19	0.20
Mn	0.01	0.00	0.00	0.01	0.01	0.01	0.01	0.00	0.01	0.01	0.01	0.01
Ni	0.00	0.00	0.00	0.00	0.00	0.00	0.00	0.00	0.00	0.00	0.00	0.00
Total	2.05	2.02	2.04	2.04	2.02	1.99	2.01	2.04	2.03	2.03	2.02	2.05
No of Ions												
Cr	8.99	9.12	9.06	8.97	9.32	9.57	9.34	9.15	9.25	9.21	9.45	9.43
Al	5.79	5.64	5.64	5.79	5.35	5.15	5.32	5.61	5.54	5.67	5.58	5.60
Ti	0.20	0.21	0.21	0.20	0.23	0.21	0.22	0.23	0.23	0.23	0.19	0.18
Fe	6.22	6.28	6.31	6.32	6.37	6.44	6.45	6.14	6.14	5.91	5.92	5.88
Mg	3.10	3.06	3.10	3.04	3.04	2.95	2.99	3.16	3.10	3.21	3.05	3.06
Mn	0.08	0.07	0.07	0.08	0.10	0.09	0.09	0.07	0.10	0.10	0.09	0.11
Ni	0.03	0.03	0.03	0.02	0.03	0.02	0.04	0.02	0.02	0.02	0.02	0.04
Total	24.41	24.41	24.43	24.42	24.43	24.43	24.45	24.39	24.38	24.33	24.30	24.30
Fe Corrected on 32 O												
Fe3+	1.08	1.08	1.13	1.11	1.13	1.13	1.18	1.01	1.00	0.88	0.78	0.80
Fe2+	5.14	5.20	5.17	5.22	5.24	5.31	5.27	5.13	5.14	5.03	5.13	5.08

Bloc	2a	2a	2a	2a	2a	2a	2a	2a	3a	3a	3a	3a	3a	3a
Raw	13	14	15	16	17	18	19	20	21	22	23	24	25	26
Cr2C	45.56	46.18	46.22	45.31	45.62	46.66	46.18	45.82	20.46	22.03	23.80	25.96	25.01	33.62
Al2C	18.51	17.93	17.97	18.55	18.21	17.70	17.74	18.04	3.99	3.94	5.13	5.72	5.26	9.57
TiO2	0.90	0.91	0.96	0.93	0.94	0.87	0.86	0.87	9.37	8.93	8.09	7.67	9.97	3.22
FeO	26.95	26.74	26.74	26.51	27.01	27.11	26.82	26.99	64.97	64.02	61.79	59.31	58.75	52.08
MgC	7.97	8.03	8.09	8.29	8.12	7.93	7.94	7.90	0.13	0.23	0.18	0.16	0.16	1.26
MnC	0.63	0.56	0.60	0.64	0.55	0.48	0.70	0.58	1.06	1.13	1.15	1.25	1.13	0.59
NiO	0.21	0.20	0.21	0.16	0.26	0.21	0.26	0.24	0.13	0.05	0.03	0.07	0.02	0.02
Total	100.73	100.55	100.77	100.38	100.69	100.96	100.51	100.45	100.10	100.34	100.17	100.13	100.31	100.37
MnC	0.45	0.38	0.41	0.45	0.36	0.29	0.52	0.40	0.97	1.04	1.05	1.14	1.03	0.46
Total	100.55	100.37	100.58	100.19	100.51	100.77	100.32	100.26	100.02	100.25	100.07	100.02	100.21	100.24
Cor														
Cr2C	45.56	46.18	46.22	45.31	45.62	46.66	46.18	45.82	20.46	22.03	23.80	25.96	25.01	33.62
Al2C	18.51	17.93	17.97	18.55	18.21	17.70	17.74	18.04	3.99	3.94	5.13	5.72	5.26	9.57
TiO2	0.90	0.91	0.96	0.93	0.94	0.87	0.86	0.87	9.37	8.93	8.09	7.67	9.97	3.22
FeO	23.24	23.10	23.10	22.71	23.13	23.37	23.00	23.18	42.53	41.99	41.16	40.42	42.15	35.62
Fe2C	4.11	4.04	4.04	4.22	4.31	4.16	4.24	4.23	24.94	24.49	22.93	20.99	18.45	18.30
MgC	7.97	8.03	8.09	8.29	8.12	7.93	7.94	7.90	0.13	0.23	0.18	0.16	0.16	1.26
MnC	0.45	0.38	0.41	0.45	0.36	0.29	0.52	0.40	0.97	1.04	1.05	1.14	1.03	0.46
NiO	0.22	0.21	0.20	0.21	0.16	0.26	0.21	0.26	0.24	0.13	0.05	0.03	0.07	0.02
Total	100.97	100.79	100.98	100.67	100.84	101.24	100.69	100.71	102.63	102.78	102.40	102.08	102.11	102.07
Form oxyge assun occur														
Cr	9.25	9.41	9.39	9.20	9.27	9.48	9.43	9.34	4.65	5.00	5.39	5.87	5.66	7.41
Al	5.60	5.45	5.44	5.61	5.52	5.36	5.40	5.49	1.35	1.33	1.73	1.93	1.78	3.14
Ti	0.17	0.18	0.19	0.18	0.18	0.17	0.17	0.17	2.03	1.93	1.74	1.65	2.15	0.67
Fe3+	0.79	0.78	0.78	0.82	0.83	0.80	0.82	0.82	5.40	5.29	4.94	4.52	3.98	3.84
Fe2+	4.99	4.98	4.97	4.88	4.97	5.02	4.97	5.00	10.23	10.07	9.85	9.67	10.10	8.30
Mg	3.05	3.08	3.10	3.17	3.11	3.04	3.06	3.04	0.06	0.10	0.08	0.07	0.07	0.52
Mn	0.10	0.08	0.09	0.10	0.08	0.06	0.11	0.09	0.24	0.25	0.25	0.28	0.25	0.11
Ni	0.05	0.04	0.04	0.04	0.03	0.05	0.04	0.05	0.06	0.03	0.01	0.01	0.02	0.00
Total	24.00	24.00	24.00	24.00	24.00	24.00	24.00	24.00	24.00	24.00	24.00	24.00	24.00	24.00
100M	28.80	29.56	29.76	30.24	29.64	29.24	29.47	28.96	0.50	0.86	0.67	0.58	0.59	4.59
100C	62.28	63.33	63.30	62.10	62.69	63.87	63.57	63.00	77.47	78.93	75.68	75.28	76.11	70.20
100F	5.08	5.01	5.01	5.22	5.34	5.14	5.27	5.25	47.34	45.51	40.97	36.68	34.83	26.67
Cr	0.90	0.91	0.91	0.89	0.90	0.92	0.91	0.90	0.40	0.43	0.47	0.51	0.49	0.66
Al	0.54	0.53	0.53	0.55	0.54	0.52	0.52	0.53	0.12	0.12	0.15	0.17	0.15	0.28
Ti	0.02	0.02	0.02	0.02	0.02	0.02	0.02	0.02	0.23	0.22	0.20	0.19	0.25	0.08
Fe	0.38	0.37	0.37	0.37	0.38	0.38	0.37	0.38	0.90	0.89	0.86	0.83	0.82	0.72
Mg	0.20	0.20	0.20	0.21	0.20	0.20	0.20	0.20	0.00	0.01	0.00	0.00	0.00	0.03
Mn	0.01	0.01	0.01	0.01	0.01	0.00	0.01	0.01	0.01	0.01	0.01	0.02	0.01	0.01
Ni	0.00	0.00	0.00	0.00	0.00	0.00	0.00	0.00	0.00	0.00	0.00	0.00	0.00	0.00
Total	2.05	2.04	2.05	2.05	2.04	2.04	2.04	2.04	1.68	1.69	1.70	1.72	1.74	1.79
No o														
Cr	9.36	9.52	9.51	9.32	9.40	9.61	9.55	9.47	5.13	5.50	5.88	6.36	6.07	7.91
Al	5.67	5.52	5.51	5.69	5.59	5.43	5.47	5.56	1.49	1.47	1.89	2.09	1.90	3.36
Ti	0.18	0.18	0.19	0.18	0.18	0.17	0.17	0.17	2.23	2.12	1.90	1.79	2.30	0.72
Fe	5.86	5.83	5.82	5.77	5.88	5.90	5.87	5.90	17.22	16.90	16.16	15.37	15.08	12.97
Mg	3.09	3.12	3.14	3.21	3.15	3.08	3.10	3.08	0.06	0.11	0.08	0.07	0.08	0.56
Mn	0.10	0.08	0.09	0.10	0.08	0.06	0.11	0.09	0.26	0.28	0.28	0.30	0.27	0.12
Ni	0.05	0.04	0.04	0.04	0.03	0.05	0.04	0.06	0.06	0.03	0.01	0.01	0.02	0.00
Total	24.31	24.30	24.30	24.31	24.32	24.31	24.32	24.32	26.46	26.40	26.21	25.99	25.71	25.64
Fe C														
Fe3+	0.80	0.79	0.79	0.83	0.85	0.82	0.84	0.83	5.95	5.81	5.40	4.90	4.26	4.10
Fe2+	5.05	5.04	5.03	4.94	5.04	5.09	5.03	5.07	11.28	11.08	10.76	10.48	10.82	8.87

Bloc	3a	3a	3a	3a	4a	4a	4a	4a	4a	4a	4a	4a	4a	4a
Raw	27	28	29	30	31	32	33	34	35	36	37	38	39	40
Cr2C	34.11	34.86	35.16	34.97	46.78	46.81	46.36	47.07	46.56	46.78	46.60	46.90	46.36	46.40
Al2C	9.97	10.31	10.48	10.50	14.27	14.59	14.65	14.42	14.59	14.96	14.50	14.03	14.39	14.65
TiO2	3.06	2.90	2.69	2.78	2.11	2.17	2.15	2.18	2.02	1.94	1.98	1.89	2.03	1.97
FeO	51.35	50.47	49.69	50.26	29.80	29.96	29.74	29.67	29.41	29.27	29.49	29.60	29.86	28.85
MgC	1.45	1.68	1.74	1.40	6.59	6.77	6.84	6.66	6.80	6.89	6.82	6.75	6.77	7.02
MnC	0.65	0.63	0.57	0.66	0.58	0.56	0.65	0.54	0.59	0.65	0.59	0.53	0.58	0.66
NiO	0.03	0.16	0.04	0.10	0.26	0.17	0.10	0.26	0.18	0.26	0.21	0.13	0.11	0.04
Total	100.61	101.01	100.37	100.67	100.39	101.02	100.49	100.81	100.17	100.76	100.19	99.82	100.10	99.58
MnC	0.51	0.49	0.43	0.52	0.39	0.37	0.46	0.35	0.40	0.46	0.40	0.34	0.40	0.48
Total	100.48	100.87	100.23	100.53	100.20	100.84	100.30	100.62	99.98	100.57	100.00	99.63	99.92	99.40
Cor														
Cr2C	34.11	34.86	35.16	34.97	46.78	46.81	46.36	47.07	46.56	46.78	46.60	46.90	46.36	46.40
Al2C	9.97	10.31	10.48	10.50	14.27	14.59	14.65	14.42	14.59	14.96	14.50	14.03	14.39	14.65
TiO2	3.06	2.90	2.69	2.78	2.11	2.17	2.15	2.18	2.02	1.94	1.98	1.89	2.03	1.97
FeO	35.21	34.78	34.30	34.96	25.81	25.79	25.49	25.95	25.30	25.30	25.22	25.19	25.44	24.80
Fe2C	17.93	17.44	17.10	17.00	4.44	4.63	4.72	4.14	4.58	4.42	4.75	4.90	4.92	4.49
MgC	1.45	1.68	1.74	1.40	6.59	6.77	6.84	6.66	6.80	6.89	6.82	6.75	6.77	7.02
MnC	0.51	0.49	0.43	0.52	0.39	0.37	0.46	0.35	0.40	0.46	0.40	0.34	0.40	0.48
NiO	0.02	0.03	0.16	0.04	0.10	0.26	0.17	0.10	0.26	0.18	0.26	0.21	0.13	0.11
Total	102.26	102.48	102.06	102.18	100.48	101.39	100.84	100.87	100.52	100.93	100.53	100.20	100.43	99.92
Form oxyge assun occur														
Cr	7.48	7.60	7.68	7.65	9.80	9.71	9.65	9.82	9.73	9.71	9.74	9.85	9.70	9.73
Al	3.26	3.35	3.42	3.43	4.46	4.51	4.55	4.49	4.55	4.63	4.52	4.40	4.49	4.58
Ti	0.64	0.60	0.56	0.58	0.42	0.43	0.43	0.43	0.40	0.38	0.39	0.38	0.40	0.39
Fe3+	3.74	3.62	3.56	3.54	0.88	0.91	0.93	0.82	0.91	0.87	0.94	0.98	0.98	0.90
Fe2+	8.16	8.02	7.93	8.09	5.72	5.66	5.61	5.72	5.59	5.56	5.57	5.60	5.63	5.50
Mg	0.60	0.69	0.72	0.58	2.60	2.65	2.69	2.62	2.68	2.70	2.69	2.67	2.67	2.77
Mn	0.12	0.12	0.10	0.12	0.09	0.08	0.10	0.08	0.09	0.10	0.09	0.08	0.09	0.11
Ni	0.00	0.01	0.04	0.01	0.02	0.05	0.04	0.02	0.06	0.04	0.06	0.05	0.03	0.02
Total	24.00	24.00	24.00	24.00	24.00	24.00	24.00	24.00	24.00	24.00	24.00	24.00	24.00	24.00
100M	5.24	6.06	6.30	5.00	25.58	26.03	26.42	25.64	26.44	26.47	26.63	26.74	26.38	27.53
100C	69.64	69.39	69.23	69.08	68.74	68.27	67.98	68.64	68.15	67.70	68.30	69.15	68.36	67.99
100F	25.84	24.83	24.27	24.23	5.84	6.04	6.18	5.43	5.99	5.74	6.21	6.44	6.46	5.90
Cr	0.67	0.69	0.69	0.69	0.92	0.92	0.91	0.93	0.92	0.92	0.92	0.93	0.91	0.92
Al	0.29	0.30	0.31	0.31	0.42	0.43	0.43	0.42	0.43	0.44	0.43	0.41	0.42	0.43
Ti	0.08	0.07	0.07	0.07	0.05	0.05	0.05	0.05	0.05	0.05	0.05	0.05	0.05	0.05
Fe	0.71	0.70	0.69	0.70	0.41	0.42	0.41	0.41	0.41	0.41	0.41	0.41	0.42	0.40
Mg	0.04	0.04	0.04	0.03	0.16	0.17	0.17	0.17	0.17	0.17	0.17	0.17	0.17	0.17
Mn	0.01	0.01	0.01	0.01	0.01	0.01	0.01	0.00	0.01	0.01	0.01	0.00	0.01	0.01
Ni	0.00	0.00	0.00	0.00	0.00	0.00	0.00	0.00	0.00	0.00	0.00	0.00	0.00	0.00
Total	1.80	1.82	1.81	1.81	1.98	2.00	1.99	1.99	1.99	2.00	1.98	1.97	1.98	1.98
No o														
Cr	7.97	8.08	8.17	8.13	9.94	9.85	9.80	9.95	9.87	9.85	9.88	10.01	9.86	9.87
Al	3.48	3.57	3.63	3.64	4.52	4.58	4.62	4.54	4.61	4.70	4.59	4.47	4.56	4.65
Ti	0.68	0.64	0.59	0.62	0.43	0.43	0.43	0.44	0.41	0.39	0.40	0.38	0.41	0.40
Fe	12.70	12.38	12.21	12.36	6.70	6.67	6.65	6.63	6.60	6.52	6.62	6.68	6.72	6.49
Mg	0.64	0.73	0.76	0.61	2.64	2.69	2.73	2.65	2.72	2.74	2.73	2.72	2.71	2.81
Mn	0.13	0.12	0.11	0.13	0.09	0.08	0.10	0.08	0.09	0.10	0.09	0.08	0.09	0.11
Ni	0.00	0.01	0.04	0.01	0.02	0.06	0.04	0.02	0.06	0.04	0.06	0.05	0.03	0.02
Total	25.60	25.54	25.51	25.50	24.34	24.35	24.36	24.32	24.35	24.34	24.36	24.38	24.38	24.35
Fe C														
Fe3+	3.99	3.85	3.78	3.76	0.90	0.93	0.95	0.83	0.92	0.89	0.96	1.00	1.00	0.91
Fe2+	8.71	8.53	8.43	8.60	5.80	5.74	5.70	5.80	5.67	5.64	5.66	5.69	5.72	5.58

Bloc	5a	5a	5a	5a	5a	5a	5a	5a	5a	5a	6c	6c	6c	6c
Raw	41	42	43	44	45	46	47	48	49	50	51	52	53	54
Cr2C	46.47	45.97	46.34	46.14	46.37	46.22	45.70	46.20	45.85	46.06	20.46	21.34	20.78	19.82
Al2C	17.08	17.07	17.24	17.04	16.94	17.45	17.03	16.76	16.80	16.97	4.88	5.55	5.34	4.31
TiO2	1.04	1.03	1.08	1.00	1.04	0.19	0.99	0.93	0.99	1.05	12.07	8.86	8.06	9.92
FeO	27.36	27.22	27.22	27.47	27.27	28.15	28.24	27.34	28.09	27.75	59.27	62.52	63.73	63.40
MgC	7.89	7.63	7.69	7.85	7.70	7.28	7.24	7.61	7.14	7.43	0.10	0.44	0.28	0.20
MnC	0.67	0.68	0.52	0.58	0.76	0.60	0.55	0.61	0.69	0.71	1.14	0.90	1.02	1.23
NiO	0.17	0.08	0.15	0.18	0.10	0.19	0.16	0.24	0.16	0.25	0.11	0.06	0.01	0.03
Total	100.68	99.69	100.24	100.25	100.19	100.09	99.92	99.68	99.71	100.21	98.01	99.66	99.22	98.90
MnC	0.49	0.50	0.34	0.40	0.58	0.41	0.37	0.42	0.50	0.52	1.06	0.81	0.94	1.15
Total	100.49	99.50	100.05	100.07	100.00	99.90	99.74	99.50	99.53	100.03	97.93	99.57	99.13	98.82
Cor														
Cr2C	46.47	45.97	46.34	46.14	46.37	46.22	45.70	46.20	45.85	46.06	20.46	21.34	20.78	19.82
Al2C	17.08	17.07	17.24	17.04	16.94	17.45	17.03	16.76	16.80	16.97	4.88	5.55	5.34	4.31
TiO2	1.04	1.03	1.08	1.00	1.04	0.19	0.99	0.93	0.99	1.05	12.07	8.86	8.06	9.92
FeO	23.37	23.36	23.71	23.27	23.30	23.46	24.08	23.30	23.98	23.77	43.12	41.61	41.27	42.30
Fe2C	4.43	4.29	3.90	4.66	4.41	5.21	4.62	4.49	4.57	4.42	17.95	23.24	24.96	23.44
MgC	7.89	7.63	7.69	7.85	7.70	7.28	7.24	7.61	7.14	7.43	0.10	0.44	0.28	0.20
MnC	0.49	0.50	0.34	0.40	0.58	0.41	0.37	0.42	0.50	0.52	1.06	0.81	0.94	1.15
NiO	0.04	0.17	0.08	0.15	0.18	0.10	0.19	0.16	0.24	0.16	0.25	0.11	0.06	0.01
Total	100.80	100.02	100.38	100.50	100.53	100.33	100.23	99.86	100.07	100.38	99.87	101.95	101.68	101.15
Form oxyge assun occur														
Cr	9.51	9.49	9.52	9.47	9.53	9.52	9.44	9.56	9.50	9.49	4.74	4.83	4.73	4.56
Al	5.21	5.25	5.28	5.21	5.19	5.36	5.25	5.17	5.19	5.21	1.69	1.87	1.81	1.48
Ti	0.20	0.20	0.21	0.20	0.20	0.04	0.19	0.18	0.20	0.21	2.66	1.91	1.75	2.17
Fe3+	0.86	0.84	0.76	0.91	0.86	1.02	0.91	0.88	0.90	0.87	3.96	5.01	5.41	5.13
Fe2+	5.06	5.10	5.15	5.05	5.06	5.11	5.26	5.10	5.26	5.18	10.58	9.97	9.94	10.29
Mg	3.04	2.97	2.98	3.04	2.98	2.83	2.82	2.97	2.79	2.89	0.04	0.19	0.12	0.09
Mn	0.11	0.11	0.07	0.09	0.13	0.09	0.08	0.09	0.11	0.12	0.26	0.20	0.23	0.28
Ni	0.01	0.04	0.02	0.03	0.04	0.02	0.04	0.03	0.05	0.03	0.06	0.03	0.01	0.00
Total	24.00	24.00	24.00	24.00	24.00	24.00	24.00	24.00	24.00	24.00	24.00	24.00	24.00	24.00
100M	29.62	28.66	28.53	29.58	29.10	27.00	26.84	28.88	26.68	27.77	0.34	1.59	1.00	0.75
100C	64.60	64.36	64.32	64.49	64.73	63.97	64.27	64.90	64.67	64.54	73.77	72.07	72.29	75.50
100F	5.54	5.40	4.90	5.84	5.54	6.43	5.83	5.66	5.78	5.57	38.12	42.77	45.25	45.95
Cr	0.92	0.91	0.91	0.91	0.92	0.91	0.90	0.91	0.90	0.91	0.40	0.42	0.41	0.39
Al	0.50	0.50	0.51	0.50	0.50	0.51	0.50	0.49	0.49	0.50	0.14	0.16	0.16	0.13
Ti	0.03	0.03	0.03	0.03	0.03	0.00	0.02	0.02	0.02	0.03	0.30	0.22	0.20	0.25
Fe	0.38	0.38	0.38	0.38	0.38	0.39	0.39	0.38	0.39	0.39	0.82	0.87	0.89	0.88
Mg	0.20	0.19	0.19	0.19	0.19	0.18	0.18	0.19	0.18	0.18	0.00	0.01	0.01	0.01
Mn	0.01	0.01	0.00	0.01	0.01	0.01	0.01	0.01	0.01	0.01	0.01	0.01	0.01	0.02
Ni	0.00	0.00	0.00	0.00	0.00	0.00	0.00	0.00	0.00	0.00	0.00	0.00	0.00	0.00
Total	2.03	2.01	2.02	2.02	2.02	2.01	2.01	2.01	2.00	2.01	1.69	1.70	1.68	1.67
No o														
Cr	9.64	9.62	9.64	9.61	9.66	9.68	9.58	9.70	9.64	9.63	5.08	5.28	5.22	5.00
Al	5.28	5.33	5.35	5.29	5.26	5.45	5.32	5.25	5.27	5.29	1.81	2.05	2.00	1.62
Ti	0.21	0.20	0.21	0.20	0.21	0.04	0.20	0.19	0.20	0.21	2.85	2.09	1.92	2.38
Fe	6.00	6.02	5.99	6.05	6.01	6.24	6.26	6.07	6.25	6.13	15.58	16.38	16.93	16.91
Mg	3.08	3.01	3.01	3.08	3.03	2.88	2.86	3.01	2.83	2.93	0.04	0.21	0.13	0.10
Mn	0.11	0.11	0.08	0.09	0.13	0.09	0.08	0.09	0.11	0.12	0.28	0.22	0.25	0.31
Ni	0.01	0.04	0.02	0.03	0.04	0.02	0.04	0.03	0.05	0.03	0.06	0.03	0.02	0.00
Total	24.33	24.32	24.29	24.35	24.33	24.40	24.35	24.34	24.35	24.33	25.70	26.25	26.47	26.31
Fe C														
Fe3+	0.88	0.85	0.77	0.92	0.88	1.04	0.92	0.90	0.91	0.88	4.24	5.48	5.97	5.63
Fe2+	5.13	5.17	5.22	5.13	5.13	5.20	5.34	5.17	5.33	5.25	11.33	10.90	10.96	11.28

Bloc	6c	6c	6c	6c	6c	6c	7a	7a	7a	7a	7a	7a	7a	7a
Raw	55	56	57	58	59	60	61	62	63	64	65	66	67	68
Cr2C	19.72	25.70	27.30	28.49	29.40	30.38	43.71	44.11	43.93	43.35	43.97	44.24	44.24	43.85
Al2C	4.66	6.86	7.59	8.18	8.58	9.12	17.68	17.64	17.55	18.43	17.53	17.33	17.27	17.69
TiO2	8.37	7.57	7.45	6.58	5.72	5.38	1.22	1.18	1.17	1.19	1.11	1.28	1.18	1.22
FeO	65.58	58.19	56.41	55.45	55.32	53.95	30.34	30.09	29.52	29.29	29.74	29.88	29.53	29.48
MgC	0.10	0.72	0.70	0.66	0.75	0.78	6.13	6.45	6.62	6.71	6.41	6.48	6.59	6.72
MnC	0.97	0.64	0.81	0.55	0.67	0.65	0.64	0.45	0.68	0.66	0.41	0.54	0.67	0.48
NiO	0.11	0.03	0.16	0.02	0.03	0.00	0.17	0.12	0.10	0.12	0.14	0.16	0.12	0.11
Total	99.51	99.70	100.42	99.93	100.46	100.26	99.88	100.03	99.56	99.74	99.31	99.90	99.60	99.54
MnC	0.89	0.54	0.70	0.43	0.55	0.52	0.46	0.27	0.50	0.48	0.24	0.36	0.49	0.30
Total	99.43	99.60	100.31	99.82	100.34	100.14	99.70	99.85	99.38	99.57	99.14	99.72	99.43	99.36
Corr														
Cr2C	19.72	25.70	27.30	28.49	29.40	30.38	43.71	44.11	43.93	43.35	43.97	44.24	44.24	43.85
Al2C	4.66	6.86	7.59	8.18	8.58	9.12	17.68	17.64	17.55	18.43	17.53	17.33	17.27	17.69
TiO2	8.37	7.57	7.45	6.58	5.72	5.38	1.22	1.18	1.17	1.19	1.11	1.28	1.18	1.22
FeO	42.11	39.94	39.76	39.13	38.50	38.05	26.12	25.74	25.12	25.21	25.55	25.61	25.12	25.22
Fe2C	26.08	20.28	18.51	18.13	18.69	17.67	4.69	4.83	4.89	4.53	4.66	4.75	4.89	4.73
MgC	0.10	0.72	0.70	0.66	0.75	0.78	6.13	6.45	6.62	6.71	6.41	6.48	6.59	6.72
MnC	0.89	0.54	0.70	0.43	0.55	0.52	0.46	0.27	0.50	0.48	0.24	0.36	0.49	0.30
NiO	0.03	0.11	0.03	0.16	0.02	0.03	0.00	0.17	0.12	0.10	0.12	0.14	0.16	0.12
Total	101.97	101.71	102.03	101.78	102.21	101.94	100.00	100.39	99.89	100.00	99.59	100.18	99.96	99.84
Form oxyge assun occur														
Cr	4.50	5.78	6.10	6.36	6.52	6.74	9.09	9.13	9.12	8.95	9.17	9.18	9.20	9.10
Al	1.59	2.30	2.53	2.72	2.84	3.02	5.48	5.44	5.43	5.67	5.45	5.36	5.35	5.47
Ti	1.82	1.62	1.58	1.40	1.21	1.14	0.24	0.23	0.23	0.23	0.22	0.25	0.23	0.24
Fe3+	5.67	4.34	3.93	3.85	3.95	3.73	0.93	0.95	0.97	0.89	0.92	0.94	0.97	0.93
Fe2+	10.16	9.50	9.39	9.24	9.04	8.93	5.75	5.64	5.52	5.51	5.64	5.62	5.52	5.54
Mg	0.04	0.30	0.29	0.28	0.31	0.33	2.40	2.52	2.59	2.61	2.52	2.53	2.58	2.63
Mn	0.22	0.13	0.17	0.10	0.13	0.12	0.10	0.06	0.11	0.11	0.05	0.08	0.11	0.07
Ni	0.01	0.02	0.01	0.04	0.00	0.01	0.00	0.04	0.02	0.02	0.03	0.03	0.03	0.02
Total	24.00	24.00	24.00	24.00	24.00	24.00	24.00	24.00	24.00	24.00	24.00	24.00	24.00	24.00
100N	0.38	2.58	2.46	2.32	2.65	2.73	21.39	22.71	23.66	23.34	22.71	23.07	23.75	23.87
100C	73.94	71.53	70.68	70.01	69.69	69.08	62.37	62.64	62.67	61.21	62.71	63.12	63.20	62.43
100F	48.22	34.96	31.33	29.79	29.67	27.66	5.99	6.13	6.22	5.73	5.95	6.06	6.24	6.02
Cr	0.39	0.51	0.54	0.56	0.58	0.60	0.86	0.87	0.87	0.86	0.87	0.87	0.87	0.87
Al	0.14	0.20	0.22	0.24	0.25	0.27	0.52	0.52	0.52	0.54	0.52	0.51	0.51	0.52
Ti	0.21	0.19	0.19	0.16	0.14	0.13	0.03	0.03	0.03	0.03	0.03	0.03	0.03	0.03
Fe	0.91	0.81	0.79	0.77	0.77	0.75	0.42	0.42	0.41	0.41	0.41	0.42	0.41	0.41
Mg	0.00	0.02	0.02	0.02	0.02	0.02	0.15	0.16	0.16	0.17	0.16	0.16	0.16	0.17
Mn	0.01	0.01	0.01	0.01	0.01	0.01	0.01	0.00	0.01	0.01	0.00	0.01	0.01	0.00
Ni	0.00	0.00	0.00	0.00	0.00	0.00	0.00	0.00	0.00	0.00	0.00	0.00	0.00	0.00
Total	1.66	1.74	1.76	1.76	1.77	1.78	1.99	2.00	2.00	2.01	1.99	2.00	1.99	2.00
No o														
Cr	4.99	6.23	6.52	6.80	6.98	7.18	9.23	9.27	9.26	9.08	9.31	9.32	9.34	9.23
Al	1.76	2.48	2.71	2.91	3.04	3.22	5.57	5.53	5.52	5.76	5.53	5.44	5.44	5.56
Ti	2.01	1.75	1.69	1.49	1.29	1.21	0.24	0.24	0.23	0.24	0.22	0.26	0.24	0.24
Fe	17.55	14.94	14.26	14.00	13.90	13.49	6.78	6.69	6.59	6.49	6.66	6.66	6.59	6.57
Mg	0.05	0.33	0.31	0.30	0.34	0.35	2.44	2.55	2.63	2.65	2.56	2.57	2.62	2.67
Mn	0.24	0.14	0.18	0.11	0.14	0.13	0.10	0.06	0.11	0.11	0.05	0.08	0.11	0.07
Ni	0.01	0.03	0.01	0.04	0.00	0.01	0.00	0.04	0.02	0.02	0.03	0.03	0.03	0.02
Total	26.61	25.90	25.69	25.65	25.70	25.59	24.36	24.37	24.37	24.34	24.36	24.36	24.37	24.36
Fe C														
Fe3+	6.28	4.68	4.21	4.12	4.23	3.98	0.94	0.97	0.98	0.90	0.94	0.95	0.98	0.95
Fe2+	11.27	10.25	10.05	9.88	9.67	9.52	5.83	5.72	5.60	5.59	5.72	5.71	5.61	5.62

Bloc	7a	7a	8c	8c	8c	8c	8c	8c	8c	8c	8c	8c	9c	9c
Raw	69	70	71	72	73	74	75	76	77	78	79	80	81	82
Cr2C	44.46	43.96	44.17	43.20	43.99	44.33	44.68	44.00	43.18	43.42	44.81	44.65	19.41	19.32
Al2C	17.67	17.602	18.21	18.12	17.95	17.51	17.36	17.98	18.41	18.06	17.88	17.16	5.67	5.71
TiO2	1.23	1.16	0.95	0.99	0.93	0.93	0.93	0.96	1.01	0.89	0.90	0.92	10.83	11.42
FeO	29.83	29.42	28.55	29.21	29.26	28.99	28.86	28.77	28.92	28.87	28.71	28.81	59.95	61.35
MgC	6.78	6.59	6.74	6.54	6.72	6.48	6.43	6.62	6.97	6.78	6.50	6.62	0.39	0.34
MnC	0.45	0.65	0.56	0.54	0.68	0.51	0.55	0.49	0.47	0.56	0.49	0.59	0.80	0.77
NiO	0.18	0.12	0.22	0.06	0.10	0.24	0.21	0.13	0.16	0.21	0.12	0.19	0.05	0.00
Total	100.60	99.50	99.40	98.66	99.63	98.99	99.02	98.96	99.13	98.79	99.42	98.94	97.09	98.90
MnC	0.27	0.47	0.38	0.37	0.51	0.33	0.38	0.31	0.29	0.38	0.31	0.42	0.72	0.69
Total	100.42	99.32	99.22	98.49	99.46	98.81	98.84	98.78	98.95	98.62	99.24	98.76	97.01	98.82
Cor														
Cr2C	44.46	43.96	44.17	43.20	43.99	44.33	44.68	44.00	43.18	43.42	44.81	44.65	19.41	19.32
Al2C	17.67	17.60	18.21	18.12	17.95	17.51	17.36	17.98	18.41	18.06	17.88	17.16	5.67	5.71
TiO2	1.23	1.16	0.95	0.99	0.93	0.93	0.93	0.96	1.01	0.89	0.90	0.92	10.83	11.42
FeO	25.48	25.11	24.84	24.95	24.87	25.04	24.98	24.89	24.61	24.51	25.15	24.68	42.10	43.42
Fe2C	4.83	4.79	4.12	4.73	4.88	4.40	4.30	4.31	4.80	4.85	3.95	4.58	19.83	19.92
MgC	6.78	6.59	6.74	6.54	6.72	6.48	6.43	6.62	6.97	6.78	6.50	6.62	0.39	0.34
MnC	0.27	0.47	0.38	0.37	0.51	0.33	0.38	0.31	0.29	0.38	0.31	0.42	0.72	0.69
NiO	0.11	0.18	0.12	0.22	0.06	0.10	0.24	0.21	0.13	0.16	0.21	0.12	0.19	0.05
Total	100.83	99.86	99.53	99.12	99.90	99.12	99.30	99.29	99.40	99.06	99.72	99.15	99.14	100.87
Form oxyge assun occur														
Cr	9.14	9.13	9.17	9.01	9.11	9.28	9.35	9.17	8.95	9.05	9.31	9.35	4.51	4.41
Al	5.42	5.45	5.63	5.64	5.54	5.46	5.41	5.59	5.69	5.62	5.54	5.36	1.96	1.94
Ti	0.24	0.23	0.19	0.20	0.18	0.18	0.19	0.19	0.20	0.18	0.18	0.18	2.39	2.48
Fe3+	0.94	0.95	0.81	0.94	0.96	0.88	0.86	0.86	0.95	0.96	0.78	0.91	4.39	4.33
Fe2+	5.54	5.52	5.45	5.51	5.45	5.54	5.53	5.49	5.40	5.41	5.53	5.47	10.35	10.50
Mg	2.63	2.58	2.64	2.57	2.62	2.56	2.53	2.60	2.72	2.66	2.55	2.61	0.17	0.15
Mn	0.06	0.10	0.08	0.08	0.11	0.07	0.08	0.07	0.07	0.09	0.07	0.09	0.18	0.17
Ni	0.02	0.04	0.02	0.05	0.01	0.02	0.05	0.04	0.03	0.03	0.04	0.03	0.04	0.01
Total	24.00	24.00	24.00	24.00	24.00	24.00	24.00	24.00	24.00	24.00	24.00	24.00	24.00	24.00
100N	23.98	23.54	23.78	23.07	23.85	23.23	23.17	23.50	24.58	24.18	23.02	24.12	1.38	1.19
100C	62.78	62.61	61.93	61.52	62.18	62.93	63.32	62.14	61.14	61.71	62.69	63.56	69.66	69.43
100F	6.09	6.09	5.21	6.03	6.16	5.61	5.49	5.48	6.07	6.16	5.00	5.84	40.38	40.53
Cr	0.88	0.87	0.87	0.85	0.87	0.87	0.88	0.87	0.85	0.86	0.88	0.88	0.38	0.38
Al	0.52	0.52	0.54	0.53	0.53	0.52	0.51	0.53	0.54	0.53	0.53	0.51	0.17	0.17
Ti	0.03	0.03	0.02	0.02	0.02	0.02	0.02	0.02	0.03	0.02	0.02	0.02	0.27	0.29
Fe	0.42	0.41	0.40	0.41	0.41	0.40	0.40	0.40	0.40	0.40	0.40	0.40	0.83	0.85
Mg	0.17	0.16	0.17	0.16	0.17	0.16	0.16	0.16	0.17	0.17	0.16	0.16	0.01	0.01
Mn	0.00	0.01	0.01	0.01	0.01	0.00	0.01	0.00	0.00	0.01	0.00	0.01	0.01	0.01
Ni	0.00	0.00	0.00	0.00	0.00	0.00	0.00	0.00	0.00	0.00	0.00	0.00	0.00	0.00
Total	2.02	2.00	2.00	1.99	2.00	1.98	1.99	1.99	2.00	1.99	2.00	1.98	1.68	1.71
No o														
Cr	9.28	9.27	9.29	9.15	9.25	9.41	9.47	9.29	9.09	9.19	9.43	9.49	4.87	4.76
Al	5.50	5.54	5.71	5.72	5.63	5.54	5.49	5.66	5.78	5.70	5.61	5.44	2.12	2.10
Ti	0.24	0.23	0.19	0.20	0.19	0.19	0.19	0.19	0.20	0.18	0.18	0.19	2.58	2.68
Fe	6.59	6.56	6.35	6.55	6.51	6.51	6.47	6.43	6.44	6.47	6.39	6.47	15.91	16.00
Mg	2.67	2.62	2.67	2.61	2.66	2.59	2.57	2.64	2.77	2.71	2.58	2.65	0.18	0.16
Mn	0.06	0.11	0.09	0.08	0.11	0.08	0.09	0.07	0.07	0.09	0.07	0.09	0.19	0.18
Ni	0.02	0.04	0.03	0.05	0.01	0.02	0.05	0.05	0.03	0.04	0.04	0.03	0.05	0.01
Total	24.37	24.37	24.31	24.36	24.37	24.34	24.33	24.33	24.37	24.37	24.30	24.35	25.92	25.89
Fe C														
Fe3+	0.96	0.96	0.82	0.95	0.98	0.89	0.87	0.87	0.96	0.98	0.79	0.93	4.74	4.68
Fe2+	5.63	5.60	5.52	5.59	5.54	5.62	5.60	5.56	5.48	5.49	5.60	5.55	11.18	11.32

Block No.	1c	1c	1c	1c	1c	1c	1c	1c	1c	1c
Raw Analysis	1	2	3	4	5	6	7	8	9	10
Cr2O3	43.68	43.81	43.94	43.41	44.68	45.30	44.61	44.31	44.60	44.37
Al2O3	18.88	18.18	18.35	18.78	17.21	16.35	17.02	18.20	17.92	18.30
TiO2	1.00	1.07	1.08	1.02	1.18	1.03	1.10	1.19	1.15	1.15
FeO	28.57	28.51	28.91	28.93	28.86	28.81	29.13	28.11	28.00	26.89
MgO	7.99	7.81	7.97	7.80	7.72	7.40	7.58	8.10	7.94	8.19
MnO	0.55	0.49	0.51	0.54	0.62	0.57	0.60	0.48	0.61	0.61
NiO	0.15	0.16	0.14	0.11	0.12	0.11	0.18	0.12	0.08	0.07
Total	100.82	100.02	100.90	100.59	100.39	99.56	100.22	100.50	100.29	99.59
MnO corrected	0.37	0.31	0.33	0.36	0.44	0.39	0.42	0.31	0.43	0.43
Total	100.64	99.84	100.72	100.42	100.21	99.38	100.04	100.33	100.11	99.41
Corrected Analysis										
Cr2O3	43.68	43.81	43.94	43.41	44.68	45.30	44.61	44.31	44.60	44.37
Al2O3	18.88	18.18	18.35	18.78	17.21	16.35	17.02	18.20	17.92	18.30
TiO2	1.00	1.07	1.08	1.02	1.18	1.03	1.10	1.19	1.15	1.15
FeO	23.61	23.62	23.71	23.87	23.74	23.76	23.79	23.48	23.45	22.91
Fe2O3	5.52	5.43	5.78	5.63	5.69	5.61	5.94	5.15	5.05	4.43
MgO	7.99	7.81	7.97	7.80	7.72	7.40	7.58	8.10	7.94	8.19
MnO	0.37	0.31	0.33	0.36	0.44	0.39	0.42	0.31	0.43	0.43
NiO	0.15	0.16	0.14	0.11	0.12	0.11	0.18	0.12	0.12	0.08
Total	101.19	100.39	101.30	100.98	100.78	99.94	100.64	100.84	100.66	99.86
	Formula units based on 32 oxygens and Fe2+/Fe3+ assuming full site occupancy									
Cr	8.84	8.96	8.90	8.81	9.15	9.40	9.17	9.01	9.10	9.09
Al	5.70	5.55	5.54	5.69	5.26	5.06	5.22	5.52	5.45	5.59
Ti	0.19	0.21	0.21	0.20	0.23	0.20	0.21	0.23	0.22	0.22
Fe3+	1.06	1.06	1.11	1.09	1.11	1.11	1.16	1.00	0.98	0.86
Fe2+	5.05	5.11	5.08	5.13	5.15	5.22	5.17	5.05	5.06	4.96
Mg	3.05	3.01	3.05	2.99	2.98	2.90	2.94	3.11	3.06	3.16
Mn	0.08	0.07	0.07	0.08	0.10	0.09	0.09	0.07	0.09	0.10
Ni	0.03	0.03	0.03	0.02	0.02	0.02	0.04	0.02	0.02	0.02
Total	24.00	24.00	24.00	24.00	24.00	24.00	24.00	24.00	24.00	24.00
100Mg/Mg+Fe2+	28.34	28.25	28.66	27.62	28.68	28.17	28.25	29.39	29.05	29.97
100Cr/Cr+Al	60.81	61.77	61.62	60.78	63.52	65.01	63.73	62.02	62.53	61.91
100Fe3+/Cr+Al+Fe3+	6.81	6.79	7.16	6.98	7.15	7.12	7.48	6.42	6.32	5.56
Cr	0.86	0.86	0.87	0.86	0.88	0.89	0.88	0.87	0.88	0.88
Al	0.56	0.53	0.54	0.55	0.51	0.48	0.50	0.54	0.53	0.54
Ti	0.03	0.03	0.03	0.03	0.03	0.03	0.03	0.03	0.03	0.03
Fe	0.40	0.40	0.40	0.40	0.40	0.40	0.41	0.39	0.39	0.37
Mg	0.20	0.19	0.20	0.19	0.19	0.18	0.19	0.20	0.20	0.20
Mn	0.01	0.00	0.00	0.01	0.01	0.01	0.01	0.00	0.01	0.01
Ni	0.00	0.00	0.00	0.00	0.00	0.00	0.00	0.00	0.00	0.00
Total	2.05	2.02	2.04	2.04	2.02	1.99	2.01	2.04	2.03	2.03
No of Ions										
Cr	8.99	9.12	9.06	8.97	9.32	9.57	9.34	9.15	9.25	9.21
Al	5.79	5.64	5.64	5.79	5.35	5.15	5.32	5.61	5.54	5.67
Ti	0.20	0.21	0.21	0.20	0.23	0.21	0.22	0.23	0.23	0.23
Fe	6.22	6.28	6.31	6.32	6.37	6.44	6.45	6.14	6.14	5.91
Mg	3.10	3.06	3.10	3.04	3.04	2.95	2.99	3.16	3.10	3.21
Mn	0.08	0.07	0.07	0.08	0.10	0.09	0.09	0.07	0.10	0.10
Ni	0.03	0.03	0.03	0.02	0.03	0.02	0.04	0.02	0.02	0.02
Total	24.41	24.41	24.43	24.42	24.43	24.43	24.45	24.39	24.38	24.33
Fe Corrected on 32 O										
Fe3+	1.08	1.08	1.13	1.11	1.13	1.13	1.18	1.01	1.00	0.88
Fe2+	5.14	5.20	5.17	5.22	5.24	5.31	5.27	5.13	5.14	5.03

Block No.	2a	2a	2a	2a	2a	2a	2a	2a	2a	2a
Raw Analysis	11	12	13	14	15	16	17	18	19	20
Cr2O3	45.44	45.86	45.56	46.18	46.22	45.31	45.62	46.66	46.18	45.82
Al2O3	17.98	18.27	18.51	17.93	17.97	18.55	18.21	17.70	17.74	18.04
TiO2	0.94	0.93	0.90	0.91	0.96	0.93	0.94	0.87	0.86	0.87
FeO	26.89	27.03	26.95	26.74	26.74	26.51	27.01	27.11	26.82	26.99
MgO	7.79	7.90	7.97	8.03	8.09	8.29	8.12	7.93	7.94	7.90
MnO	0.59	0.67	0.63	0.56	0.60	0.64	0.55	0.48	0.70	0.58
NiO	0.19	0.22	0.21	0.20	0.21	0.16	0.26	0.21	0.26	0.24
Total	99.83	100.87	100.73	100.55	100.77	100.38	100.69	100.96	100.51	100.45
MnO corrected	0.41	0.49	0.45	0.38	0.41	0.45	0.36	0.29	0.52	0.40
Total	99.65	100.69	100.55	100.37	100.58	100.19	100.51	100.77	100.32	100.26
Corrected Analysis										
Cr2O3	45.44	45.86	45.56	46.18	46.22	45.31	45.62	46.66	46.18	45.82
Al2O3	17.98	18.27	18.51	17.93	17.97	18.55	18.21	17.70	17.74	18.04
TiO2	0.94	0.93	0.90	0.91	0.96	0.93	0.94	0.87	0.86	0.87
FeO	23.33	23.37	23.24	23.10	23.10	22.71	23.13	23.37	23.00	23.18
Fe2O3	3.96	4.07	4.11	4.04	4.04	4.22	4.31	4.16	4.24	4.23
MgO	7.79	7.90	7.97	8.03	8.09	8.29	8.12	7.93	7.94	7.90
MnO	0.41	0.49	0.45	0.38	0.41	0.45	0.36	0.29	0.52	0.40
NiO	0.07	0.19	0.22	0.21	0.20	0.21	0.16	0.26	0.21	0.26
Total	99.93	101.07	100.97	100.79	100.98	100.67	100.84	101.24	100.69	100.71
	Formula units based on 32 oxygens and Fe2+/Fe3+ assuming full site occupancy									
Cr	9.34	9.31	9.25	9.41	9.39	9.20	9.27	9.48	9.43	9.34
Al	5.51	5.53	5.60	5.45	5.44	5.61	5.52	5.36	5.40	5.49
Ti	0.18	0.18	0.17	0.18	0.19	0.18	0.18	0.17	0.17	0.17
Fe3+	0.78	0.79	0.79	0.78	0.78	0.82	0.83	0.80	0.82	0.82
Fe2+	5.07	5.02	4.99	4.98	4.97	4.88	4.97	5.02	4.97	5.00
Mg	3.02	3.02	3.05	3.08	3.10	3.17	3.11	3.04	3.06	3.04
Mn	0.09	0.11	0.10	0.08	0.09	0.10	0.08	0.06	0.11	0.09
Ni	0.02	0.04	0.05	0.04	0.04	0.04	0.03	0.05	0.04	0.05
Total	24.00	24.00	24.00	24.00	24.00	24.00	24.00	24.00	24.00	24.00
100Mg/Mg+Fe2+	28.51	28.65	28.80	29.56	29.76	30.24	29.64	29.24	29.47	28.96
100Cr/Cr+Al	62.89	62.73	62.28	63.33	63.30	62.10	62.69	63.87	63.57	63.00
100Fe3+/Cr+Al+Fe3+	4.96	5.03	5.08	5.01	5.01	5.22	5.34	5.14	5.27	5.25
Cr	0.90	0.90	0.90	0.91	0.91	0.89	0.90	0.92	0.91	0.90
Al	0.53	0.54	0.54	0.53	0.53	0.55	0.54	0.52	0.52	0.53
Ti	0.02	0.02	0.02	0.02	0.02	0.02	0.02	0.02	0.02	0.02
Fe	0.37	0.38	0.38	0.37	0.37	0.37	0.38	0.38	0.37	0.38
Mg	0.19	0.20	0.20	0.20	0.20	0.21	0.20	0.20	0.20	0.20
Mn	0.01	0.01	0.01	0.01	0.01	0.01	0.01	0.00	0.01	0.01
Ni	0.00	0.00	0.00	0.00	0.00	0.00	0.00	0.00	0.00	0.00
Total	2.02	2.05	2.05	2.04	2.05	2.05	2.04	2.04	2.04	2.04
No of Ions										
Cr	9.45	9.43	9.36	9.52	9.51	9.32	9.40	9.61	9.55	9.47
Al	5.58	5.60	5.67	5.52	5.51	5.69	5.59	5.43	5.47	5.56
Ti	0.19	0.18	0.18	0.18	0.19	0.18	0.18	0.17	0.17	0.17
Fe	5.92	5.88	5.86	5.83	5.82	5.77	5.88	5.90	5.87	5.90
Mg	3.05	3.06	3.09	3.12	3.14	3.21	3.15	3.08	3.10	3.08
Mn	0.09	0.11	0.10	0.08	0.09	0.10	0.08	0.06	0.11	0.09
Ni	0.02	0.04	0.05	0.04	0.04	0.04	0.03	0.05	0.04	0.06
Total	24.30	24.30	24.31	24.30	24.30	24.31	24.32	24.31	24.32	24.32
Fe Corrected on 32 O										
Fe3+	0.78	0.80	0.80	0.79	0.79	0.83	0.85	0.82	0.84	0.83
Fe2+	5.13	5.08	5.05	5.04	5.03	4.94	5.04	5.09	5.03	5.07

Block No.	3a	3a	3a	3a	3a	3a	3a	3a	3a	3a
Raw Analysis	21	22	23	24	25	26	27	28	29	30
Cr2O3	20.46	22.03	23.80	25.96	25.01	33.62	34.11	34.86	35.16	34.97
Al2O3	3.99	3.94	5.13	5.72	5.26	9.57	9.97	10.31	10.48	10.50
TiO2	9.37	8.93	8.09	7.67	9.97	3.22	3.06	2.90	2.69	2.78
FeO	64.97	64.02	61.79	59.31	58.75	52.08	51.35	50.47	49.69	50.26
MgO	0.13	0.23	0.18	0.16	0.16	1.26	1.45	1.68	1.74	1.40
MnO	1.06	1.13	1.15	1.25	1.13	0.59	0.65	0.63	0.57	0.66
NiO	0.13	0.05	0.03	0.07	0.02	0.02	0.03	0.16	0.04	0.10
Total	100.10	100.34	100.17	100.13	100.31	100.37	100.61	101.01	100.37	100.67
MnO corrected	0.97	1.04	1.05	1.14	1.03	0.46	0.51	0.49	0.43	0.52
Total	100.02	100.25	100.07	100.02	100.21	100.24	100.48	100.87	100.23	100.53
Corrected Analysis										
Cr2O3	20.46	22.03	23.80	25.96	25.01	33.62	34.11	34.86	35.16	34.97
Al2O3	3.99	3.94	5.13	5.72	5.26	9.57	9.97	10.31	10.48	10.50
TiO2	9.37	8.93	8.09	7.67	9.97	3.22	3.06	2.90	2.69	2.78
FeO	42.53	41.99	41.16	40.42	42.15	35.62	35.21	34.78	34.30	34.96
Fe2O3	24.94	24.49	22.93	20.99	18.45	18.30	17.93	17.44	17.10	17.00
MgO	0.13	0.23	0.18	0.16	0.16	1.26	1.45	1.68	1.74	1.40
MnO	0.97	1.04	1.05	1.14	1.03	0.46	0.51	0.49	0.43	0.52
NiO	0.24	0.13	0.05	0.03	0.07	0.02	0.02	0.03	0.16	0.04
Total	102.63	102.78	102.40	102.08	102.11	102.07	102.26	102.48	102.06	102.18
	Formula units based on 32 oxygens and Fe2+/Fe3+ assuming full site occupancy									
Cr	4.65	5.00	5.39	5.87	5.66	7.41	7.48	7.60	7.68	7.65
Al	1.35	1.33	1.73	1.93	1.78	3.14	3.26	3.35	3.42	3.43
Ti	2.03	1.93	1.74	1.65	2.15	0.67	0.64	0.60	0.56	0.58
Fe3+	5.40	5.29	4.94	4.52	3.98	3.84	3.74	3.62	3.56	3.54
Fe2+	10.23	10.07	9.85	9.67	10.10	8.30	8.16	8.02	7.93	8.09
Mg	0.06	0.10	0.08	0.07	0.07	0.52	0.60	0.69	0.72	0.58
Mn	0.24	0.25	0.25	0.28	0.25	0.11	0.12	0.12	0.10	0.12
Ni	0.06	0.03	0.01	0.01	0.02	0.00	0.00	0.01	0.04	0.01
Total	24.00	24.00	24.00	24.00	24.00	24.00	24.00	24.00	24.00	24.00
100Mg/Mg+Fe2+	0.50	0.86	0.67	0.58	0.59	4.59	5.24	6.06	6.30	5.00
100Cr/Cr+Al	77.47	78.93	75.68	75.28	76.11	70.20	69.64	69.39	69.23	69.08
100Fe3+/Cr+Al+Fe3+	47.34	45.51	40.97	36.68	34.83	26.67	25.84	24.83	24.27	24.23
Cr	0.40	0.43	0.47	0.51	0.49	0.66	0.67	0.69	0.69	0.69
Al	0.12	0.12	0.15	0.17	0.15	0.28	0.29	0.30	0.31	0.31
Ti	0.23	0.22	0.20	0.19	0.25	0.08	0.08	0.07	0.07	0.07
Fe	0.90	0.89	0.86	0.83	0.82	0.72	0.71	0.70	0.69	0.70
Mg	0.00	0.01	0.00	0.00	0.00	0.03	0.04	0.04	0.04	0.03
Mn	0.01	0.01	0.01	0.02	0.01	0.01	0.01	0.01	0.01	0.01
Ni	0.00	0.00	0.00	0.00	0.00	0.00	0.00	0.00	0.00	0.00
Total	1.68	1.69	1.70	1.72	1.74	1.79	1.80	1.82	1.81	1.81
No of Ions										
Cr	5.13	5.50	5.88	6.36	6.07	7.91	7.97	8.08	8.17	8.13
Al	1.49	1.47	1.89	2.09	1.90	3.36	3.48	3.57	3.63	3.64
Ti	2.23	2.12	1.90	1.79	2.30	0.72	0.68	0.64	0.59	0.62
Fe	17.22	16.90	16.16	15.37	15.08	12.97	12.70	12.38	12.21	12.36
Mg	0.06	0.11	0.08	0.07	0.08	0.56	0.64	0.73	0.76	0.61
Mn	0.26	0.28	0.28	0.30	0.27	0.12	0.13	0.12	0.11	0.13
Ni	0.06	0.03	0.01	0.01	0.02	0.00	0.00	0.01	0.04	0.01
Total	26.46	26.40	26.21	25.99	25.71	25.64	25.60	25.54	25.51	25.50
Fe Corrected on 32 O										
Fe3+	5.95	5.81	5.40	4.90	4.26	4.10	3.99	3.85	3.78	3.76
Fe2+	11.28	11.08	10.76	10.48	10.82	8.87	8.71	8.53	8.43	8.60

Block No.	4a	4a	4a	4a	4a	4a	4a	4a	4a	4a
Raw Analysis	31	32	33	34	35	36	37	38	39	40
Cr2O3	46.78	46.81	46.36	47.07	46.56	46.78	46.60	46.90	46.36	46.40
Al2O3	14.27	14.59	14.65	14.42	14.59	14.96	14.50	14.03	14.39	14.65
TiO2	2.11	2.17	2.15	2.18	2.02	1.94	1.98	1.89	2.03	1.97
FeO	29.80	29.96	29.74	29.67	29.41	29.27	29.49	29.60	29.86	28.85
MgO	6.59	6.77	6.84	6.66	6.80	6.89	6.82	6.75	6.77	7.02
MnO	0.58	0.56	0.65	0.54	0.59	0.65	0.59	0.53	0.58	0.66
NiO	0.26	0.17	0.10	0.26	0.18	0.26	0.21	0.13	0.11	0.04
Total	100.39	101.02	100.49	100.81	100.17	100.76	100.19	99.82	100.10	99.58
MnO corrected	0.39	0.37	0.46	0.35	0.40	0.46	0.40	0.34	0.40	0.48
Total	100.20	100.84	100.30	100.62	99.98	100.57	100.00	99.63	99.92	99.40
Corrected Analysis										
Cr2O3	46.78	46.81	46.36	47.07	46.56	46.78	46.60	46.90	46.36	46.40
Al2O3	14.27	14.59	14.65	14.42	14.59	14.96	14.50	14.03	14.39	14.65
TiO2	2.11	2.17	2.15	2.18	2.02	1.94	1.98	1.89	2.03	1.97
FeO	25.81	25.79	25.49	25.95	25.30	25.30	25.22	25.19	25.44	24.80
Fe2O3	4.44	4.63	4.72	4.14	4.58	4.42	4.75	4.90	4.92	4.49
MgO	6.59	6.77	6.84	6.66	6.80	6.89	6.82	6.75	6.77	7.02
MnO	0.39	0.37	0.46	0.35	0.40	0.46	0.40	0.34	0.40	0.48
NiO	0.10	0.26	0.17	0.10	0.26	0.18	0.26	0.21	0.13	0.11
Total	100.48	101.39	100.84	100.87	100.52	100.93	100.53	100.20	100.43	99.92
	Formula units based on 32 oxygens and Fe2+/Fe3+ assuming full site occupancy									
Cr	9.80	9.71	9.65	9.82	9.73	9.71	9.74	9.85	9.70	9.73
Al	4.46	4.51	4.55	4.49	4.55	4.63	4.52	4.40	4.49	4.58
Ti	0.42	0.43	0.43	0.43	0.40	0.38	0.39	0.38	0.40	0.39
Fe3+	0.88	0.91	0.93	0.82	0.91	0.87	0.94	0.98	0.98	0.90
Fe2+	5.72	5.66	5.61	5.72	5.59	5.56	5.57	5.60	5.63	5.50
Mg	2.60	2.65	2.69	2.62	2.68	2.70	2.69	2.67	2.67	2.77
Mn	0.09	0.08	0.10	0.08	0.09	0.10	0.09	0.08	0.09	0.11
Ni	0.02	0.05	0.04	0.02	0.06	0.04	0.06	0.05	0.03	0.02
Total	24.00	24.00	24.00	24.00	24.00	24.00	24.00	24.00	24.00	24.00
100Mg/Mg+Fe2+	25.58	26.03	26.42	25.64	26.44	26.47	26.63	26.74	26.38	27.53
100Cr/Cr+Al	68.74	68.27	67.98	68.64	68.15	67.70	68.30	69.15	68.36	67.99
100Fe3+/Cr+Al+Fe3+	5.84	6.04	6.18	5.43	5.99	5.74	6.21	6.44	6.46	5.90
Cr	0.92	0.92	0.91	0.93	0.92	0.92	0.92	0.93	0.91	0.92
Al	0.42	0.43	0.43	0.42	0.43	0.44	0.43	0.41	0.42	0.43
Ti	0.05	0.05	0.05	0.05	0.05	0.05	0.05	0.05	0.05	0.05
Fe	0.41	0.42	0.41	0.41	0.41	0.41	0.41	0.41	0.42	0.40
Mg	0.16	0.17	0.17	0.17	0.17	0.17	0.17	0.17	0.17	0.17
Mn	0.01	0.01	0.01	0.00	0.01	0.01	0.01	0.00	0.01	0.01
Ni	0.00	0.00	0.00	0.00	0.00	0.00	0.00	0.00	0.00	0.00
Total	1.98	2.00	1.99	1.99	1.99	2.00	1.98	1.97	1.98	1.98
No of Ions										
Cr	9.94	9.85	9.80	9.95	9.87	9.85	9.88	10.01	9.86	9.87
Al	4.52	4.58	4.62	4.54	4.61	4.70	4.59	4.47	4.56	4.65
Ti	0.43	0.43	0.43	0.44	0.41	0.39	0.40	0.38	0.41	0.40
Fe	6.70	6.67	6.65	6.63	6.60	6.52	6.62	6.68	6.72	6.49
Mg	2.64	2.69	2.73	2.65	2.72	2.74	2.73	2.72	2.71	2.81
Mn	0.09	0.08	0.10	0.08	0.09	0.10	0.09	0.08	0.09	0.11
Ni	0.02	0.06	0.04	0.02	0.06	0.04	0.06	0.05	0.03	0.02
Total	24.34	24.35	24.36	24.32	24.35	24.34	24.36	24.38	24.38	24.35
Fe Corrected on 32 O										
Fe3+	0.90	0.93	0.95	0.83	0.92	0.89	0.96	1.00	1.00	0.91
Fe2+	5.80	5.74	5.70	5.80	5.67	5.64	5.66	5.69	5.72	5.58

Block No.	6c	6c	6c	6c	6c	6c	6c	6c	6c	6c
Raw Analysis	51	52	53	54	55	56	57	58	59	60
Cr2O3	20.46	21.34	20.78	19.82	19.72	25.70	27.30	28.49	29.40	30.38
Al2O3	4.88	5.55	5.34	4.31	4.66	6.86	7.59	8.18	8.58	9.12
TiO2	12.07	8.86	8.06	9.92	8.37	7.57	7.45	6.58	5.72	5.38
FeO	59.27	62.52	63.73	63.40	65.58	58.19	56.41	55.45	55.32	53.95
MgO	0.10	0.44	0.28	0.20	0.10	0.72	0.70	0.66	0.75	0.78
MnO	1.14	0.90	1.02	1.23	0.97	0.64	0.81	0.55	0.67	0.65
NiO	0.11	0.06	0.01	0.03	0.11	0.03	0.16	0.02	0.03	0.00
Total	98.01	99.66	99.22	98.90	99.51	99.70	100.42	99.93	100.46	100.26
MnO corrected	1.06	0.81	0.94	1.15	0.89	0.54	0.70	0.43	0.55	0.52
Total	97.93	99.57	99.13	98.82	99.43	99.60	100.31	99.82	100.34	100.14
Corrected Analysis										
Cr2O3	20.46	21.34	20.78	19.82	19.72	25.70	27.30	28.49	29.40	30.38
Al2O3	4.88	5.55	5.34	4.31	4.66	6.86	7.59	8.18	8.58	9.12
TiO2	12.07	8.86	8.06	9.92	8.37	7.57	7.45	6.58	5.72	5.38
FeO	43.12	41.61	41.27	42.30	42.11	39.94	39.76	39.13	38.50	38.05
Fe2O3	17.95	23.24	24.96	23.44	26.08	20.28	18.51	18.13	18.69	17.67
MgO	0.10	0.44	0.28	0.20	0.10	0.72	0.70	0.66	0.75	0.78
MnO	1.06	0.81	0.94	1.15	0.89	0.54	0.70	0.43	0.55	0.52
NiO	0.25	0.11	0.06	0.01	0.03	0.11	0.03	0.16	0.02	0.03
Total	99.87	101.95	101.68	101.15	101.97	101.71	102.03	101.78	102.21	101.94
	Formula units based on 32 oxygens and Fe2+/Fe3+ assuming full site occupancy									
Cr	4.74	4.83	4.73	4.56	4.50	5.78	6.10	6.36	6.52	6.74
Al	1.69	1.87	1.81	1.48	1.59	2.30	2.53	2.72	2.84	3.02
Ti	2.66	1.91	1.75	2.17	1.82	1.62	1.58	1.40	1.21	1.14
Fe3+	3.96	5.01	5.41	5.13	5.67	4.34	3.93	3.85	3.95	3.73
Fe2+	10.58	9.97	9.94	10.29	10.16	9.50	9.39	9.24	9.04	8.93
Mg	0.04	0.19	0.12	0.09	0.04	0.30	0.29	0.28	0.31	0.33
Mn	0.26	0.20	0.23	0.28	0.22	0.13	0.17	0.10	0.13	0.12
Ni	0.06	0.03	0.01	0.00	0.01	0.02	0.01	0.04	0.00	0.01
Total	24.00	24.00	24.00	24.00	24.00	24.00	24.00	24.00	24.00	24.00
100Mg/Mg+Fe2+	0.34	1.59	1.00	0.75	0.38	2.58	2.46	2.32	2.65	2.73
100Cr/Cr+Al	73.77	72.07	72.29	75.50	73.94	71.53	70.68	70.01	69.69	69.08
100Fe3+/Cr+Al+Fe3+	38.12	42.77	45.25	45.95	48.22	34.96	31.33	29.79	29.67	27.66
Cr	0.40	0.42	0.41	0.39	0.39	0.51	0.54	0.56	0.58	0.60
Al	0.14	0.16	0.16	0.13	0.14	0.20	0.22	0.24	0.25	0.27
Ti	0.30	0.22	0.20	0.25	0.21	0.19	0.19	0.16	0.14	0.13
Fe	0.82	0.87	0.89	0.88	0.91	0.81	0.79	0.77	0.77	0.75
Mg	0.00	0.01	0.01	0.01	0.00	0.02	0.02	0.02	0.02	0.02
Mn	0.01	0.01	0.01	0.02	0.01	0.01	0.01	0.01	0.01	0.01
Ni	0.00	0.00	0.00	0.00	0.00	0.00	0.00	0.00	0.00	0.00
Total	1.69	1.70	1.68	1.67	1.66	1.74	1.76	1.76	1.77	1.78
No of Ions										
Cr	5.08	5.28	5.22	5.00	4.99	6.23	6.52	6.80	6.98	7.18
Al	1.81	2.05	2.00	1.62	1.76	2.48	2.71	2.91	3.04	3.22
Ti	2.85	2.09	1.92	2.38	2.01	1.75	1.69	1.49	1.29	1.21
Fe	15.58	16.38	16.93	16.91	17.55	14.94	14.26	14.00	13.90	13.49
Mg	0.04	0.21	0.13	0.10	0.05	0.33	0.31	0.30	0.34	0.35
Mn	0.28	0.22	0.25	0.31	0.24	0.14	0.18	0.11	0.14	0.13
Ni	0.06	0.03	0.02	0.00	0.01	0.03	0.01	0.04	0.00	0.01
Total	25.70	26.25	26.47	26.31	26.61	25.90	25.69	25.65	25.70	25.59
Fe Corrected on 32 O										
Fe3+	4.24	5.48	5.97	5.63	6.28	4.68	4.21	4.12	4.23	3.98
Fe2+	11.33	10.90	10.96	11.28	11.27	10.25	10.05	9.88	9.67	9.52

Bloc	9c	9c	9c	9c	9c	9c	9c	9c
Raw	83	84	85	86	87	88	89	90
Cr2C	18.93	18.64	18.17	16.60	16.36	11.50	9.53	13.77
Al2C	5.54	5.46	5.43	5.12	5.04	4.55	4.70	4.69
TiO2	11.29	11.54	11.88	11.99	12.37	12.18	13.15	13.46
FeO	61.71	61.78	62.25	63.01	63.39	68.64	69.01	64.92
MgC	0.00	0.21	0.09	0.10	0.13	0.05	0.18	0.21
MnC	0.93	0.77	0.78	1.19	0.75	0.61	0.60	0.64
NiO	0.07	0.05	0.06	0.04	0.03	0.07	0.06	0.07
Total	98.47	98.45	98.67	98.06	98.05	97.60	97.21	97.75
MnC	0.86	0.70	0.71	1.13	0.68	0.57	0.56	0.58
Total	98.39	98.38	98.60	97.99	97.99	97.55	97.18	97.69
Cor								
Cr2C	18.93	18.64	18.17	16.60	16.36	11.50	9.53	13.77
Al2C	5.54	5.46	5.43	5.12	5.04	4.55	4.70	4.69
TiO2	11.29	11.54	11.88	11.99	12.37	12.18	13.15	13.46
FeO	43.55	43.58	44.12	43.77	44.45	45.35	45.88	45.38
Fe2C	20.18	20.23	20.15	21.39	21.05	25.88	25.70	21.72
MgC	0.00	0.21	0.09	0.10	0.13	0.05	0.18	0.21
MnC	0.86	0.70	0.71	1.13	0.68	0.57	0.56	0.58
NiO	0.00	0.07	0.05	0.06	0.04	0.03	0.07	0.06
Total	100.34	100.43	100.60	100.16	100.11	100.10	99.77	99.86
Form								
oxyge								
assun								
occur								
Cr	4.36	4.29	4.18	3.84	3.79	2.67	2.22	3.20
Al	1.90	1.87	1.86	1.77	1.74	1.58	1.63	1.62
Ti	2.47	2.53	2.60	2.64	2.72	2.69	2.91	2.97
Fe3+	4.43	4.43	4.41	4.71	4.64	5.73	5.70	4.80
Fe2+	10.62	10.60	10.73	10.71	10.88	11.16	11.30	11.15
Mg	0.00	0.09	0.04	0.04	0.06	0.02	0.08	0.09
Mn	0.21	0.17	0.17	0.28	0.17	0.14	0.14	0.15
Ni	0.00	0.02	0.01	0.01	0.01	0.01	0.02	0.01
Total	24.00	24.00	24.00	24.00	24.00	24.00	24.00	24.00
100M	0.01	0.73	0.31	0.36	0.46	0.16	0.60	0.70
100C	69.62	69.59	69.16	68.48	68.54	62.90	57.62	66.31
100F	41.40	41.82	42.21	45.65	45.64	57.40	59.67	49.90
Cr	0.37	0.37	0.36	0.33	0.32	0.23	0.19	0.27
Al	0.16	0.16	0.16	0.15	0.15	0.13	0.14	0.14
Ti	0.28	0.29	0.30	0.30	0.31	0.30	0.33	0.34
Fe	0.86	0.86	0.87	0.88	0.88	0.96	0.96	0.90
Mg	0.00	0.01	0.00	0.00	0.00	0.00	0.00	0.01
Mn	0.01	0.01	0.01	0.02	0.01	0.01	0.01	0.01
Ni	0.00	0.00	0.00	0.00	0.00	0.00	0.00	0.00
Total	1.69	1.69	1.70	1.67	1.68	1.63	1.63	1.66
No o								
Cr	4.72	4.63	4.51	4.17	4.11	2.97	2.46	3.48
Al	2.06	2.03	2.01	1.92	1.89	1.75	1.81	1.77
Ti	2.67	2.73	2.81	2.87	2.96	2.99	3.23	3.24
Fe	16.26	16.25	16.36	16.76	16.84	18.75	18.87	17.37
Mg	0.00	0.10	0.04	0.05	0.06	0.02	0.09	0.10
Mn	0.23	0.19	0.19	0.30	0.18	0.16	0.15	0.16
Ni	0.00	0.02	0.01	0.02	0.01	0.01	0.02	0.01
Total	25.94	25.94	25.93	26.09	26.05	26.65	26.63	26.14
Fe C								
Fe3+	4.78	4.79	4.76	5.12	5.03	6.36	6.32	5.23
Fe2+	11.48	11.46	11.59	11.64	11.81	12.39	12.54	12.14

Block No.	7a	7a	7a	7a	7a	7a	7a	7a	7a	7a
Raw Analysis	61	62	63	64	65	66	67	68	69	70
Cr2O3	43.71	44.11	43.93	43.35	43.97	44.24	44.24	43.85	44.46	43.96
Al2O3	17.68	17.64	17.55	18.43	17.53	17.33	17.27	17.69	17.67	17.602
TiO2	1.22	1.18	1.17	1.19	1.11	1.28	1.18	1.22	1.23	1.16
FeO	30.34	30.09	29.52	29.29	29.74	29.88	29.53	29.48	29.83	29.42
MgO	6.13	6.45	6.62	6.71	6.41	6.48	6.59	6.72	6.78	6.59
MnO	0.64	0.45	0.68	0.66	0.41	0.54	0.67	0.48	0.45	0.65
NiO	0.17	0.12	0.10	0.12	0.14	0.16	0.12	0.11	0.18	0.12
Total	99.88	100.03	99.56	99.74	99.31	99.90	99.60	99.54	100.60	99.50
MnO corrected	0.46	0.27	0.50	0.48	0.24	0.36	0.49	0.30	0.27	0.47
Total	99.70	99.85	99.38	99.57	99.14	99.72	99.43	99.36	100.42	99.32
Corrected Analysis										
Cr2O3	43.71	44.11	43.93	43.35	43.97	44.24	44.24	43.85	44.46	43.96
Al2O3	17.68	17.64	17.55	18.43	17.53	17.33	17.27	17.69	17.67	17.60
TiO2	1.22	1.18	1.17	1.19	1.11	1.28	1.18	1.22	1.23	1.16
FeO	26.12	25.74	25.12	25.21	25.55	25.61	25.12	25.22	25.48	25.11
Fe2O3	4.69	4.83	4.89	4.53	4.66	4.75	4.89	4.73	4.83	4.79
MgO	6.13	6.45	6.62	6.71	6.41	6.48	6.59	6.72	6.78	6.59
MnO	0.46	0.27	0.50	0.48	0.24	0.36	0.49	0.30	0.27	0.47
NiO	0.00	0.17	0.12	0.10	0.12	0.14	0.16	0.12	0.11	0.18
Total	100.00	100.39	99.89	100.00	99.59	100.18	99.96	99.84	100.83	99.86

Formula units based on 32 oxygens and Fe2+/Fe3+ assuming full site occupancy

Cr	9.09	9.13	9.12	8.95	9.17	9.18	9.20	9.10	9.14	9.13
Al	5.48	5.44	5.43	5.67	5.45	5.36	5.35	5.47	5.42	5.45
Ti	0.24	0.23	0.23	0.23	0.22	0.25	0.23	0.24	0.24	0.23
Fe3+	0.93	0.95	0.97	0.89	0.92	0.94	0.97	0.93	0.94	0.95
Fe2+	5.75	5.64	5.52	5.51	5.64	5.62	5.52	5.54	5.54	5.52
Mg	2.40	2.52	2.59	2.61	2.52	2.53	2.58	2.63	2.63	2.58
Mn	0.10	0.06	0.11	0.11	0.05	0.08	0.11	0.07	0.06	0.10
Ni	0.00	0.04	0.02	0.02	0.03	0.03	0.03	0.02	0.02	0.04
Total	24.00	24.00	24.00	24.00	24.00	24.00	24.00	24.00	24.00	24.00
100Mg/Mg+Fe2+	21.39	22.71	23.66	23.34	22.71	23.07	23.75	23.87	23.98	23.54
100Cr/Cr+Al	62.37	62.64	62.67	61.21	62.71	63.12	63.20	62.43	62.78	62.61
100Fe3+/Cr+Al+Fe3+	5.99	6.13	6.22	5.73	5.95	6.06	6.24	6.02	6.09	6.09
Cr	0.86	0.87	0.87	0.86	0.87	0.87	0.87	0.87	0.88	0.87
Al	0.52	0.52	0.52	0.54	0.52	0.51	0.51	0.52	0.52	0.52
Ti	0.03	0.03	0.03	0.03	0.03	0.03	0.03	0.03	0.03	0.03
Fe	0.42	0.42	0.41	0.41	0.41	0.42	0.41	0.41	0.42	0.41
Mg	0.15	0.16	0.16	0.17	0.16	0.16	0.16	0.17	0.17	0.16
Mn	0.01	0.00	0.01	0.01	0.00	0.01	0.01	0.00	0.00	0.01
Ni	0.00	0.00	0.00	0.00	0.00	0.00	0.00	0.00	0.00	0.00
Total	1.99	2.00	2.00	2.01	1.99	2.00	1.99	2.00	2.02	2.00
No of Ions										
Cr	9.23	9.27	9.26	9.08	9.31	9.32	9.34	9.23	9.28	9.27
Al	5.57	5.53	5.52	5.76	5.53	5.44	5.44	5.56	5.50	5.54
Ti	0.24	0.24	0.23	0.24	0.22	0.26	0.24	0.24	0.24	0.23
Fe	6.78	6.69	6.59	6.49	6.66	6.66	6.59	6.57	6.59	6.56
Mg	2.44	2.55	2.63	2.65	2.56	2.57	2.62	2.67	2.67	2.62
Mn	0.10	0.06	0.11	0.11	0.05	0.08	0.11	0.07	0.06	0.11
Ni	0.00	0.04	0.02	0.02	0.03	0.03	0.03	0.02	0.02	0.04
Total	24.36	24.37	24.37	24.34	24.36	24.36	24.37	24.36	24.37	24.37
Fe Corrected on 32 O										
Fe3+	0.94	0.97	0.98	0.90	0.94	0.95	0.98	0.95	0.96	0.96
Fe2+	5.83	5.72	5.60	5.59	5.72	5.71	5.61	5.62	5.63	5.60

Block No.	8c	8c	8c	8c	8c	8c	8c	8c	8c	8c
Raw Analysis	71	72	73	74	75	76	77	78	79	80
Cr2O3	44.17	43.20	43.99	44.33	44.68	44.00	43.18	43.42	44.81	44.65
Al2O3	18.21	18.12	17.95	17.51	17.36	17.98	18.41	18.06	17.88	17.16
TiO2	0.95	0.99	0.93	0.93	0.93	0.96	1.01	0.89	0.90	0.92
FeO	28.55	29.21	29.26	28.99	28.86	28.77	28.92	28.87	28.71	28.81
MgO	6.74	6.54	6.72	6.48	6.43	6.62	6.97	6.78	6.50	6.62
MnO	0.56	0.54	0.68	0.51	0.55	0.49	0.47	0.56	0.49	0.59
NiO	0.22	0.06	0.10	0.24	0.21	0.13	0.16	0.21	0.12	0.19
Total	99.40	98.66	99.63	98.99	99.02	98.96	99.13	98.79	99.42	98.94
MnO corrected	0.38	0.37	0.51	0.33	0.38	0.31	0.29	0.38	0.31	0.42
Total	99.22	98.49	99.46	98.81	98.84	98.78	98.95	98.62	99.24	98.76
Corrected Analysis										
Cr2O3	44.17	43.20	43.99	44.33	44.68	44.00	43.18	43.42	44.81	44.65
Al2O3	18.21	18.12	17.95	17.51	17.36	17.98	18.41	18.06	17.88	17.16
TiO2	0.95	0.99	0.93	0.93	0.93	0.96	1.01	0.89	0.90	0.92
FeO	24.84	24.95	24.87	25.04	24.98	24.89	24.61	24.51	25.15	24.68
Fe2O3	4.12	4.73	4.88	4.40	4.30	4.31	4.80	4.85	3.95	4.58
MgO	6.74	6.54	6.72	6.48	6.43	6.62	6.97	6.78	6.50	6.62
MnO	0.38	0.37	0.51	0.33	0.38	0.31	0.29	0.38	0.31	0.42
NiO	0.12	0.22	0.06	0.10	0.24	0.21	0.13	0.16	0.21	0.12
Total	99.53	99.12	99.90	99.12	99.30	99.29	99.40	99.06	99.72	99.15
	Formula units based on 32 oxygens and Fe2+/Fe3+ assuming full site occupancy									
Cr	9.17	9.01	9.11	9.28	9.35	9.17	8.95	9.05	9.31	9.35
Al	5.63	5.64	5.54	5.46	5.41	5.59	5.69	5.62	5.54	5.36
Ti	0.19	0.20	0.18	0.18	0.19	0.19	0.20	0.18	0.18	0.18
Fe3+	0.81	0.94	0.96	0.88	0.86	0.86	0.95	0.96	0.78	0.91
Fe2+	5.45	5.51	5.45	5.54	5.53	5.49	5.40	5.41	5.53	5.47
Mg	2.64	2.57	2.62	2.56	2.53	2.60	2.72	2.66	2.55	2.61
Mn	0.08	0.08	0.11	0.07	0.08	0.07	0.07	0.09	0.07	0.09
Ni	0.02	0.05	0.01	0.02	0.05	0.04	0.03	0.03	0.04	0.03
Total	24.00	24.00	24.00	24.00	24.00	24.00	24.00	24.00	24.00	24.00
100Mg/Mg+Fe2+	23.78	23.07	23.85	23.23	23.17	23.50	24.58	24.18	23.02	24.12
100Cr/Cr+Al	61.93	61.52	62.18	62.93	63.32	62.14	61.14	61.71	62.69	63.56
100Fe3+/Cr+Al+Fe3+	5.21	6.03	6.16	5.61	5.49	5.48	6.07	6.16	5.00	5.84
Cr	0.87	0.85	0.87	0.87	0.88	0.87	0.85	0.86	0.88	0.88
Al	0.54	0.53	0.53	0.52	0.51	0.53	0.54	0.53	0.53	0.51
Ti	0.02	0.02	0.02	0.02	0.02	0.02	0.03	0.02	0.02	0.02
Fe	0.40	0.41	0.41	0.40	0.40	0.40	0.40	0.40	0.40	0.40
Mg	0.17	0.16	0.17	0.16	0.16	0.16	0.17	0.17	0.16	0.16
Mn	0.01	0.01	0.01	0.00	0.01	0.00	0.00	0.01	0.00	0.01
Ni	0.00	0.00	0.00	0.00	0.00	0.00	0.00	0.00	0.00	0.00
Total	2.00	1.99	2.00	1.98	1.99	1.99	2.00	1.99	2.00	1.98
No of Ions										
Cr	9.29	9.15	9.25	9.41	9.47	9.29	9.09	9.19	9.43	9.49
Al	5.71	5.72	5.63	5.54	5.49	5.66	5.78	5.70	5.61	5.44
Ti	0.19	0.20	0.19	0.19	0.19	0.19	0.20	0.18	0.18	0.19
Fe	6.35	6.55	6.51	6.51	6.47	6.43	6.44	6.47	6.39	6.47
Mg	2.67	2.61	2.66	2.59	2.57	2.64	2.77	2.71	2.58	2.65
Mn	0.09	0.08	0.11	0.08	0.09	0.07	0.07	0.09	0.07	0.09
Ni	0.03	0.05	0.01	0.02	0.05	0.05	0.03	0.04	0.04	0.03
Total	24.31	24.36	24.37	24.34	24.33	24.33	24.37	24.37	24.30	24.35
Fe Corrected on 32 O										
Fe3+	0.82	0.95	0.98	0.89	0.87	0.87	0.96	0.98	0.79	0.93
Fe2+	5.52	5.59	5.54	5.62	5.60	5.56	5.48	5.49	5.60	5.55

Block No.	9c	9c	9c	9c	9c	9c	9c	9c	9c	9c
Raw Analysis	81	82	83	84	85	86	87	88	89	90
Cr2O3	19.41	19.32	18.93	18.64	18.17	16.60	16.36	11.50	9.53	13.77
Al2O3	5.67	5.71	5.54	5.46	5.43	5.12	5.04	4.55	4.70	4.69
TiO2	10.83	11.42	11.29	11.54	11.88	11.99	12.37	12.18	13.15	13.46
FeO	59.95	61.35	61.71	61.78	62.25	63.01	63.39	68.64	69.01	64.92
MgO	0.39	0.34	0.00	0.21	0.09	0.10	0.13	0.05	0.18	0.21
MnO	0.80	0.77	0.93	0.77	0.78	1.19	0.75	0.61	0.60	0.64
NiO	0.05	0.00	0.07	0.05	0.06	0.04	0.03	0.07	0.06	0.07
Total	97.09	98.90	98.47	98.45	98.67	98.06	98.05	97.60	97.21	97.75
MnO corrected	0.72	0.69	0.86	0.70	0.71	1.13	0.68	0.57	0.56	0.58
Total	97.01	98.82	98.39	98.38	98.60	97.99	97.99	97.55	97.18	97.69
Corrected Analysis										
Cr2O3	19.41	19.32	18.93	18.64	18.17	16.60	16.36	11.50	9.53	13.77
Al2O3	5.67	5.71	5.54	5.46	5.43	5.12	5.04	4.55	4.70	4.69
TiO2	10.83	11.42	11.29	11.54	11.88	11.99	12.37	12.18	13.15	13.46
FeO	42.10	43.42	43.55	43.58	44.12	43.77	44.45	45.35	45.88	45.38
Fe2O3	19.83	19.92	20.18	20.23	20.15	21.39	21.05	25.88	25.70	21.72
MgO	0.39	0.34	0.00	0.21	0.09	0.10	0.13	0.05	0.18	0.21
MnO	0.72	0.69	0.86	0.70	0.71	1.13	0.68	0.57	0.56	0.58
NiO	0.19	0.05	0.00	0.07	0.05	0.06	0.04	0.03	0.07	0.06
Total	99.14	100.87	100.34	100.43	100.60	100.16	100.11	100.10	99.77	99.86
	Formula units based on 32 oxygens and Fe2+/Fe3+ assuming full site occupancy									
Cr	4.51	4.41	4.36	4.29	4.18	3.84	3.79	2.67	2.22	3.20
Al	1.96	1.94	1.90	1.87	1.86	1.77	1.74	1.58	1.63	1.62
Ti	2.39	2.48	2.47	2.53	2.60	2.64	2.72	2.69	2.91	2.97
Fe3+	4.39	4.33	4.43	4.43	4.41	4.71	4.64	5.73	5.70	4.80
Fe2+	10.35	10.50	10.62	10.60	10.73	10.71	10.88	11.16	11.30	11.15
Mg	0.17	0.15	0.00	0.09	0.04	0.04	0.06	0.02	0.08	0.09
Mn	0.18	0.17	0.21	0.17	0.17	0.28	0.17	0.14	0.14	0.15
Ni	0.04	0.01	0.00	0.02	0.01	0.01	0.01	0.01	0.02	0.01
Total	24.00	24.00	24.00	24.00	24.00	24.00	24.00	24.00	24.00	24.00
100Mg/Mg+Fe2+	1.38	1.19	0.01	0.73	0.31	0.36	0.46	0.16	0.60	0.70
100Cr/Cr+Al	69.66	69.43	69.62	69.59	69.16	68.48	68.54	62.90	57.62	66.31
100Fe3+/Cr+Al+Fe3+	40.38	40.53	41.40	41.82	42.21	45.65	45.64	57.40	59.67	49.90
Cr	0.38	0.38	0.37	0.37	0.36	0.33	0.32	0.23	0.19	0.27
Al	0.17	0.17	0.16	0.16	0.16	0.15	0.15	0.13	0.14	0.14
Ti	0.27	0.29	0.28	0.29	0.30	0.30	0.31	0.30	0.33	0.34
Fe	0.83	0.85	0.86	0.86	0.87	0.88	0.88	0.96	0.96	0.90
Mg	0.01	0.01	0.00	0.01	0.00	0.00	0.00	0.00	0.00	0.01
Mn	0.01	0.01	0.01	0.01	0.01	0.02	0.01	0.01	0.01	0.01
Ni	0.00	0.00	0.00	0.00	0.00	0.00	0.00	0.00	0.00	0.00
Total	1.68	1.71	1.69	1.69	1.70	1.67	1.68	1.63	1.63	1.66
No of Ions										
Cr	4.87	4.76	4.72	4.63	4.51	4.17	4.11	2.97	2.46	3.48
Al	2.12	2.10	2.06	2.03	2.01	1.92	1.89	1.75	1.81	1.77
Ti	2.58	2.68	2.67	2.73	2.81	2.87	2.96	2.99	3.23	3.24
Fe	15.91	16.00	16.26	16.25	16.36	16.76	16.84	18.75	18.87	17.37
Mg	0.18	0.16	0.00	0.10	0.04	0.05	0.06	0.02	0.09	0.10
Mn	0.19	0.18	0.23	0.19	0.19	0.30	0.18	0.16	0.15	0.16
Ni	0.05	0.01	0.00	0.02	0.01	0.02	0.01	0.01	0.02	0.01
Total	25.92	25.89	25.94	25.94	25.93	26.09	26.05	26.65	26.63	26.14
Fe Corrected on 32 O										
Fe3+	4.74	4.68	4.78	4.79	4.76	5.12	5.03	6.36	6.32	5.23
Fe2+	11.18	11.32	11.48	11.46	11.59	11.64	11.81	12.39	12.54	12.14

Appendix C1- UG2 normal reef

Normal Reef Blank foats

Float no.	Reagents	Samples	Time, min	Mass Pull, g	Water recovery	Cum Mass, g	Cum Water, g	Ave cum Mass, g	Std dev	Std error
c		C1	3.0000	7.1500	143.6900	7.1500	143.6900	7.8600	1.0370	0.7332
		C2	5.0000	5.5300	193.6500	12.6800	337.3400	13.0133	1.2342	0.8727
	Dow 250 (40g/t)	C3	9.0000	5.0500	192.8900	17.7300	530.2300	17.9267	1.3458	0.9516
1.0000	SIBX (100g/t)	C4	15.0000	3.7500	151.2300	21.4800	681.4600	21.7700	0.8911	0.6301
		Feed		17.7200						
		T1		1182.6800						
		T2		24.9100						
		T3		25.2100						
		Cc +Tt Mass Bal								

Float no.	Reagents	Samples	Time, min	Mass Pull, g	Water recovery	Cum Mass, g	Cum Water, g
		C1	3.0000	9.0500	164.9600	9.0500	164.9600
		C2	5.0000	5.3300	196.8100	14.3800	361.7700
	Dow 250 (40g/t)	C3	9.0000	4.9800	187.9600	19.3600	549.7300
2.0000	SIBX (100g/t)	C4	15.0000	3.4100	145.4400	22.7700	695.1700
		Feed		19.3200			
		T1		1176.8400			
		T2		28.9500			
		T3		28.4900			

Float no.	Reagents	Samples	Time, min	Mass Pull, g	Water recovery	Cum Mass, g	Cum Water, g
		C1	3.0000	7.3800	165.7700	7.3800	165.7700
		C2	5.0000	4.6000	155.3200	11.9800	321.0900
	Dow 250 (40g/t)	C3	9.0000	4.7100	173.7800	16.6900	494.8700
3.0000	SIBX (100g/t)	C4	15.0000	4.3700	173.6600	21.0600	668.5300
		Feed		19.8200			
		T1		1188.5600			
		T2		25.1900			
		T3		25.2700			

Normal Reef Floats with depressant

Float no.	Reagents	Samples	Time, min	Mass Pull, g	Water recovery	Cum Mass, g	Cum Water, g	Ave cum Mass, g	Std dev	Std error
		C1	5.0000	3.8500	145.0100	3.8500	145.0100	3.5667	0.2902	0.2052
		C2	7.0000	2.1300	78.6000	5.9800	223.6100	5.3533	0.6250	0.4419
	Dow 250 (40g/t)	C3	11.0000	1.3400	44.0700	7.3200	267.6800	7.2733	0.0404	0.0286
4.0000	SIBX (100g/t)	C4	17.0000	2.9100	130.4100	10.2300	398.0900	10.0900	0.1400	0.0990
	Sty 504 (400g/t)	Feed		23.2000						
		T1		1183.7200						
		T2		24.6600						
		T3		25.3600						
		Cc +Tt Mass Bal								

Float no.	Reagents	Samples	Time, min	Mass Pull, g	Water recovery	Cum Mass, g	Cum Water, g
		C1	5.0000	3.2700	134.6500	3.2700	134.6500
		C2	7.0000	1.4600	62.6200	4.7300	197.2700
	Dow 250 (40g/t)	C3	11.0000	2.5200	104.7900	7.2500	302.0600
5.0000	SIBX (100g/t)	C4	17.0000	2.7000	118.0200	9.9500	420.0800
	Sty 504 (400g/t)	Feed		25.9200			
		T1		1198.1200			
		T2		26.0300			
		T3		25.2600			

Float no.	Reagents	Samples	Time, min	Mass Pull, g	Water recovery	Cum Mass, g	Cum Water, g
		C1	5.0000	3.5800	139.4700	3.5800	139.4700
		C2	7.0000	1.7700	64.8700	5.3500	204.3400
	Dow 250 (40g/t)	C3	11.0000	1.9000	79.7000	7.2500	284.0400
6.0000	SIBX (100g/t)	C4	17.0000	2.8400	120.4600	10.0900	404.5000
	Sty 504 (400g/t)	Feed		22.4600			
		T1		1203.8600			
		T2		24.2900			
		T3		22.8100			

Appendix C2- UG2 potholed reef

Pothole Blank floats

Float no.	Reagents	Samples	Time, min	Mass Pull, g	Water recovery	Cum Mass, g	Cum Water, g	Ave cum Mass, g	Std dev	Std error
		C1	3.0000	9.0700	175.4700	9.0700	175.4700	11.4033	7.2196	5.1050
		C2	5.0000	7.9200	208.2800	16.9900	383.7500	19.5467	2.2183	1.5685
	Dow 250 (40g/t)	C3	9.0000	7.2300	210.8400	24.2200	594.5900	26.1400	1.6704	1.1812
7.0000	SIBX (100g/t)	C4	15.0000	5.2200	181.4100	29.4400	776.0000	30.8033	1.1951	0.8451
	Sty 504 (400g/t)	Feed		25.2500						
		T1		1172.8800						
		T2		24.5500						
		T3		24.2900						
		Cc +Tt								
		Mass Bal								

Float no.	Reagents	Samples	Time, min	Mass Pull, g	Water recovery	Cum Mass, g	Cum Water, g
		C1	3.0000	13.1400	220.4900	13.1400	220.4900
		C2	5.0000	7.8200	222.2900	20.9600	442.7800
	Dow 250 (40g/t)	C3	9.0000	5.9800	187.1500	26.9400	629.9300
8.0000	SIBX (100g/t)	C4	15.0000	4.3600	162.7500	31.3000	792.6800
	Sty 504 (400g/t)	Feed		27.1100			
		T1		1174.1300			
		T2		24.9100			
		T3		26.1800			

Float no.	Reagents	Samples	Time, min	Mass Pull, g	Water recovery	Cum Mass, g	Cum Water, g
		C1	3.0000	12.0000	199.4700	12.0000	199.4700
		C2	5.0000	8.6900	229.0900	20.6900	428.5600
	Dow 250 (40g/t)	C3	9.0000	6.5700	218.6200	27.2600	647.1800
9.0000	SIBX (100g/t)	C4	15.0000	4.4100	172.3300	31.6700	819.5100
	Sty 504 (400g/t)	Feed		26.4200			
		T1		1172.4400			
		T2		26.5600			
		T3		26.5500			

Pothole floats with depressant

Float no.	Reagents	Samples	Time, min	Mass Pull, g	Water recovery	Cum Mass, g	Cum Water, g	Ave cum Mass, g	Std dev	Std error
		C1	5.0000	6.8000	165.9300	6.8000	165.9300	7.1100	0.3151	0.2228
		C2	7.0000	3.3000	120.2800	10.1000	286.2100	10.2400	0.1572	0.1111
	Dow 250 (40g/t)	C3	11.0000	3.6600	153.4500	13.7600	439.6600	13.7867	0.0379	0.0268
10.0000	SIBX (100g/t)	C4	17.0000	3.5400	159.1000	17.3000	598.7600	17.5300	0.3812	0.2695
	Sty 504 (400g/t)	Feed		29.3600						
		T1		1185.1500						
		T2		28.9300						
		T3		28.2500						
		Cc +Tt								
		Mass Bal								

Float no.	Reagents	Samples	Time, min	Mass Pull, g	Water recovery	Cum Mass, g	Cum Water, g
		C1	5.0000	7.4300	159.8200	7.4300	159.8200
		C2	7.0000	2.9800	91.5600	10.4100	251.3800
	Dow 250 (40g/t)	C3	11.0000	3.4200	129.7700	13.8300	381.1500
11.0000	SIBX (100g/t)	C4	17.0000	4.1400	182.1200	17.9700	563.2700
	Sty 504 (400g/t)	Feed		27.5100			
		T1		1179.7600			
		T2		29.3300			
		T3		27.7300			

Float no.	Reagents	Samples	Time, min	Mass Pull, g	Water recovery	Cum Mass, g	Cum Water, g
		C1	5.0000	7.1000	139.0600	7.1000	139.0600
		C2	7.0000	3.1100	100.5200	10.2100	239.5800
	Dow 250 (40g/t)	C3	11.0000	3.5600	133.0200	13.7700	372.6000
12.0000	SIBX (100g/t)	C4	17.0000	3.5500	167.3800	17.3200	539.9800
	Sty 504 (400g/t)	Feed		26.1000			
		T1		1193.2200			
		T2		27.0600			
		T3		23.7300			

Appendix C3- UG2 IRUP reef

IRUP blank floats

Float no.	Reagents	Samples	Time, min	Mass Pull, g	Water recovery	Cum Mass, g	Cum Water, g	Ave cum Mass, g	Std dev	Std error
		C1	3.0000	21.9400	163.0400	21.9400	163.0400	20.8133	1.0964	0.7753
		C2	5.0000	15.7100	146.4000	37.6500	309.4400	35.2200	2.5930	1.8336
	Dow 250 (40g/t)	C3	9.0000	11.4000	122.7600	49.0500	432.2000	47.2967	2.4011	1.6978
13.0000	SIBX (100g/t)	C4	15.0000	9.7700	142.5400	58.8200	574.7400	50.5533	2.8252	1.9977
	Sty 504 (400g/t)	Feed		28.1100						
		T1		1143.8700						
		T2		29.1000						
		T3		27.4100						
		Cc +Tt Mass Bal								

Float no.	Reagents	Samples	Time, min	Mass Pull, g	Water recovery	Cum Mass, g	Cum Water, g
		C1	3.0000	19.7500	141.9100	19.7500	141.9100
		C2	5.0000	12.7400	94.4000	32.4900	236.3100
	Dow 250 (40g/t)	C3	9.0000	12.0700	171.9200	44.5600	408.2300
14.0000	SIBX (100g/t)	C4	15.0000	8.9900	145.9300	53.5500	554.1600
	Sty 504 (400g/t)	Feed		27.5300			
		T1		1145.7700			
		T2		27.6900			
		T3		25.7400			

Float no.	Reagents	Samples	Time, min	Mass Pull, g	Water recovery	Cum Mass, g	Cum Water, g
		C1	3.0000	20.7500	151.1000	20.7500	151.1000
		C2	5.0000	14.7700	130.1100	35.5200	281.2100
	Dow 250 (40g/t)	C3	9.0000	12.7600	148.8100	48.2800	430.0200
14.0000	SIBX (100g/t)	C4	15.0000	9.6700	155.7900	57.9500	585.8100
	Sty 504 (400g/t)	Feed		28.6700			
		T1		1148.1400			
		T2		26.6400			
		T3		26.0100			

IRUP floats with depressant

Float no.	Reagents	Samples	Time, min	Mass Pull, g	Water recovery	Cum Mass, g	Cum Water, g	Ave cum Mass, g	Std dev	Std error
		C1	5.0000	2.3500	117.0600	2.3500	117.0600	2.4167	0.2566	0.1814
		C2	7.0000	1.3800	57.4800	3.7300	174.5400	3.7800	0.2193	0.1551
	Dow 250 (40g/t)	C3	11.0000	2.5800	119.8900	6.3100	294.4300	5.9667	0.3400	0.2405
16.0000	SIBX (100g/t)	C4	17.0000	2.5300	130.4500	8.8400	424.8800	8.3700	0.4204	0.2972
	Sty 504 (400g/t)	Feed		26.1500						
		T1		1195.1400						
		T2		27.3300						
		T3		29.3700						
		Cc +Tt Mass Bal								

Float no.	Reagents	Samples	Time, min	Mass Pull, g	Water recovery	Cum Mass, g	Cum Water, g
		C1	5.0000	2.2000	117.6600	2.2000	117.6600
		C2	7.0000	1.3900	71.2400	3.5900	188.9000
	Dow 250 (40g/t)	C3	11.0000	2.0400	100.7300	5.6300	289.6300
17.0000	SIBX (100g/t)	C4	17.0000	2.4000	111.7600	8.0300	401.3900
	Sty 504 (400g/t)	Feed		28.5000			
		T1		1193.0600			
		T2		28.7100			
		T3		28.1700			

Float no.	Reagents	Samples	Time, min	Mass Pull, g	Water recovery	Cum Mass, g	Cum Water, g
		C1	5.0000	2.7000	119.5800	2.7000	119.5800
		C2	7.0000	1.3200	66.7300	4.0200	186.3100
	Dow 250 (40g/t)	C3	11.0000	1.9400	97.8500	5.9600	284.1600
18.0000	SIBX (100g/t)	C4	17.0000	2.2800	122.6000	8.2400	406.7600
	Sty 504 (400g/t)	Feed		25.6200			
		T1		1190.8100			
		T2		28.7000			
		T3		27.8500			

Appendix D: Chemical assay

ELEMENTS	Al	Ca	Co	Cr	Cu	Fe	Mg	Mn	Ni	Pb	Si	Ti	V	Zn
UNITS	%	%	ppm	ppm	ppm	%	%	ppm	ppm	ppm	%	%	ppm	ppm
DETECTION	0.02	0.2	20	50	20	0.01	0.01	20	20	50	0.1	0.01	50	20
METHOD	D/OES	D/OES	D/OES	D/OES	D/OES	D/OES	D/OES	D/OES	D/OES	D/OES	D/OES	D/OES	D/OES	D/OES
COMMENTS: 1418.0/0813928 (03/12/2008) CLIENT O/N: Serge Opoubou-Lando 1/1														
SAMPLE NUMBERS														
Normal Reef C1 blank float	7.66	3.4	385	101821	5257	11	7.12	1083	12217	X	13.6	0.36	671	283
Normal Reef C2 blank float	7.83	3.9	208	85042	1356	9.26	8.75	1117	5498	X	16.7	0.31	568	229
Normal Reef C3 blank float	8.22	3.9	158	93581	741	9.64	8.56	1172	3234	X	16.4	0.32	617	283
Normal Reef C4 blank float	8.28	3.8	137	98989	519	9.87	8.26	1182	2603	X	15.7	0.32	654	269
Normal Reef Feed 1	9.11	1.8	230	221645	73	17.34	5.93	1513	1375	X	6	0.47	1446	625
Normal Reef T2 blank float	9.4	1.8	235	236694	X	18.04	6.06	1569	1328	X	5.9	0.49	1535	610
Normal Reef T3 blank flot	9.33	1.8	232	233412	X	17.93	6.01	1560	1318	X	5.9	0.49	1513	597
Normal Reef Cl float + Sty 504	8.84	3.2	493	143893	7167	14.71	5.76	1226	17097	X	10.6	0.41	947	365
Normal Reef C2 float + Sty 505	8.7	3.8	570	119881	11529	13.82	6.02	1181	20909	X	12.4	0.36	779	336
Normal Reef C3 float + Sty 506	9.35	4	339	126031	4548	12.49	6.32	1238	9986	X	13.3	0.35	833	342
Normal Reef C4 float + Sty 507	8.72	3.8	183	119263	2100	11.63	6.04	1174	6255	X	12.5	0.31	878	335
Normal Reef Feed 2	8.89	1.6	138	219851	47	17.73	5.81	1505	1448	X	5.7	0.45	1632	667
Normal Reef T2 float + Sty 504	8.98	1.6	140	225598	X	18.04	5.85	1537	1356	X	5.5	0.46	1671	657
Normal Reef T3 float + Sty 504	8.87	1.7	138	223823	X	17.94	5.84	1526	1360	X	5.6	0.45	1639	677
Pothole C1 blank float	5.47	2.7	783	66789	29138	16.19	6.64	794	45633	63	12.2	0.18	535	183
Pothole C2 blank float	6.81	3.2	203	84509	5178	11.01	9.4	1138	11740	X	16.4	0.23	700	212
Pothole C3 blank float	7.09	3.3	120	90278	2888	10.66	9.08	1179	5419	X	15.9	0.23	721	247
Pothole C4 blank float	7.6	3.3	108	104706	2028	11.4	8.78	1267	4120	X	15.3	0.26	831	302
Pothole feed1	8.94	1.7	226	224584	363	17.49	6.05	1518	1711	X	6.1	0.4	1607	582
Pothole T2 float	8.94	1.6	228	229660	69	17.81	6.05	1556	1283	X	5.6	0.41	1680	629
Pothole T3 flot	8.79	1.6	214	228430	67	17.44	5.87	1517	1251	X	5.5	0.4	1651	634
Pothole C1 float + Sty 504	6.03	2.7	1160	85251	43542	21.04	3.36	790	63485	70	7.7	0.19	611	281
Pothole C2 float + Sty 504	7.91	3.8	668	102783	18673	15.45	4.54	1027	39948	66	11	0.24	746	279
Pothole C3 float + Sty 504	9.28	4.4	354	115654	8175	13.28	5.23	1162	18682	76	13	0.28	832	309
Pothole C4 float + Sty 504	9.43	4.4	229	119113	5079	12.56	5.32	1190	9626	X	13	0.28	868	313
Pothole Feed2	9.33	1.8	235	232156	369	18.14	6.3	1577	1765	X	6.3	0.41	1663	588
Pothole T2 float + Sty 504	9.32	1.7	227	234293	97	18.17	6.3	1593	1302	X	5.9	0.42	1703	617
Pothole T3 float + Sty 504	9.11	1.7	226	226817	93	17.61	6.15	1550	1279	X	6.1	0.4	1647	604
IRUP C1 blank float	4.22	2	235	104626	1881	12.07	11.16	1033	3422	129	16.4	0.29	737	429
IRUP C2 blank float	4.59	2	198	116276	419	12.51	10.7	1113	2474	86	15.2	0.31	826	429
IRUP C3 blank float	5.2	2	193	134059	252	13.9	10.1	1293	2053	X	13.6	0.37	951	666
IRUP C4 blank float	5.65	1.9	192	152822	198	15.12	9.2	1450	1939	X	11.8	0.43	1066	596
IRUP Feed	8.05	0.9	261	258518	29	21.46	5.32	1868	1382	X	3	0.7	1827	864
IRUP T2 blank float	8.1	0.9	260	262436	X	21.6	5	1880	1288	X	2.4	0.72	1844	852
IRUP T3 blank float	8.08	0.8	250	258066	X	21.4	4.88	1866	1270	X	2.2	0.71	1817	821
IRUP C1 float + Sty 504	6.19	1.4	695	173835	9617	19.73	6.45	1766	11125	336	6.6	0.6	1268	752
IRUP C2 float + Sty 504	5.94	1.5	857	163795	6826	19.36	6.85	1802	14217	796	7.5	0.62	1218	715
IRUP C3 float + Sty 504	6.06	1.5	582	163778	3003	18.65	7.22	1856	9137	390	8	0.66	1233	719
IRUP C4 float + Sty 504	5.84	1.6	394	156033	1626	17.47	7.52	1824	5783	96	8.7	0.66	1181	773
IRUP T2 float + Sty 504	7.91	0.9	249	256415	X	21.06	5.17	1844	1325	X	2.9	0.7	1796	857
IRUP T3 float + Sty 504	7.82	0.9	245	246700	X	20.7	5.13	1802	1294	X	2.8	0.68	1751	816
CHECKS														
Normal Reef C1 blank float	7.52	3.5	395	99082	5323	11.09	7.03	1044	12945	X	13.7	0.35	673	302
Pothole T3 flot	8.7	1.6	218	219036	63	17.28	5.87	1466	1223	X	5.6	0.39	1587	630
IRUP T3 float + Sty 504	7.75	0.9	247	249043	X	20.72	5.06	1807	1282	X	2.7	0.68	1755	846
STANDARDS														
MPL-2	4.37	0.8	234	1335	1926	2.48	0.82	1758	1808	1981	33.7	0.02	161	1327
SARM5	2.11	2	104	24059	X	8.81	15.04	1634	575	X	24.5	0.11	266	124
AMIS0010	7.19	2.1	1040	151650	755	14.39	7.41	5214	1151	X	11.1	0.36	1091	437
SARM72	7.89	1.4	217	204856	366	17.42	6.71	1507	1728	X	6.6	0.41	1408	562
BLANKS														
Control Blank	X	X	X	X	X	0.03	X	X	X	X	X	X	X	X
Control Blank	X	X	X	74	X	0.01	X	X	X	X	X	X	X	33
Acid Blank	X	X	X	X	X	X	X	X	X	X	X	X	X	X

Appendix E1 - Normal Reef

Reef type	Metal	Slope	Water rec (g)	Metal new mass (g)	Metal actual mass (g)	Floted mass (g)
UG2 Normal Reef	Al	0.0022	158.1400	0.3479	0.6021	0.2542
			340.0667	0.7481	1.0056	0.2575
			524.9433	1.1549	1.4095	0.2546
			681.7200	1.4998	1.7277	0.2279
	Cr	0.0030	158.1400	0.4744	0.8003	0.3259
			340.0667	1.0202	1.2386	0.2184
			524.9433	1.5748	1.6564	0.0816
			681.7200	2.0452	1.9832	0.0620
	Mg	0.0015	158.1400	0.2372	0.5596	0.3224
			340.0667	0.5101	1.0105	0.5004
			524.9433	0.7874	1.4311	0.6437
			681.7200	1.0226	1.7486	0.7260
	Ca	0.0009	158.1400	0.1423	0.2672	0.1249
			340.0667	0.3061	0.4682	0.1621
			524.9433	0.4724	0.6598	0.1874
			681.7200	0.6135	0.8059	0.1924
	Si	0.0030	158.1400	0.4744	1.0690	0.5946
			340.0667	1.0202	1.9296	0.9094
			524.9433	1.5748	2.7354	1.1606
			681.7200	2.0452	3.3388	1.2936
	Fe	0.0030	158.1400	0.4744	0.8646	0.3902
			340.0667	1.0202	1.3418	0.3216
			524.9433	1.5748	1.8154	0.2406
			681.7200	2.0452	2.1948	0.1496
	Ti	0.0030	158.1400	0.4744	0.8646	0.3902
			340.0667	1.0202	1.3418	0.3216
			524.9433	1.5748	1.8154	0.2406
			681.7200	2.0452	2.1948	0.1496

Appendix E2 - Pothole Reef

Reef type	Metal	Slope	Water rec (g)	Metal new mass (g)	Metal actual mass (g)	Floted mass (g)
UG2 Potholed Reef	Al	0.0023	198.4767	0.4565	0.6238	0.1673
			418.3633	0.9622	1.1783	0.2161
			623.9000	1.4350	1.6458	0.2108
			796.0633	1.8309	2.0020	0.1711
	Cr	0.0029	198.4767	0.5756	0.7616	0.1860
			418.3633	1.2133	1.4498	0.2365
			623.9000	1.8093	2.0450	0.2357
			796.0633	2.3086	2.5333	0.2247
	Mg	0.0015	198.4767	0.2977	0.7572	0.4595
			418.3633	0.6275	1.5227	0.8952
			623.9000	0.9359	2.1213	1.1855
			796.0633	1.1941	2.5308	1.3367
	Ca	0.0011	198.4767	0.2183	0.3079	0.0896
			418.3633	0.4602	0.5685	0.1083
			623.9000	0.6863	0.7861	0.0998
			796.0633	0.8757	0.9399	0.0642
	Si	0.0031	198.4767	0.6153	1.3912	0.7759
			418.3633	1.2969	2.7267	1.4298
			623.9000	1.9341	3.7751	1.8410
			796.0633	2.4678	4.4885	2.0207
	Fe	0.0034	198.4767	0.6748	1.8462	1.1714
			418.3633	1.4224	2.7428	1.3204
			623.9000	2.1213	3.4456	1.3243
			796.0633	2.7066	3.9773	1.2707
	Ti	0.0034	198.4767	0.6748	1.8462	1.1714
			418.3633	1.4224	2.7428	1.3204
			623.9000	2.1213	3.4456	1.3243
			796.0633	2.7066	3.9773	1.2707

Appendix E3 - IRUP Reef

Reef type	Metal	Slope	Water rec (g)	Metal new mass (g)	Metal actual mass (g)	Floted mass (g)
UG2 IRUP Reef	Al	0.0012	152.0167	0.1824	0.8783	0.6959
			275.6533	0.3308	1.5396	1.2088
			423.4833	0.5082	2.1676	1.6594
			571.5700	0.6859	2.7030	2.0171
	Cr	0.0033	152.0167	0.5017	2.1776	1.6759
			275.6533	0.9097	3.8528	2.9431
			423.4833	1.3975	5.4718	4.0743
			571.5700	1.8862	6.9200	5.0338
	Mg	0.0015	152.0167	0.2280	2.3228	2.0948
			275.6533	0.4135	3.8643	3.4508
			423.4833	0.6352	5.0840	4.4488
			571.5700	0.8574	5.9559	5.0985
	Ca	0.0003	152.0167	0.0456	0.4163	0.3707
			275.6533	0.0827	0.7044	0.6217
			423.4833	0.1270	0.9459	0.8189
			571.5700	0.1715	1.1260	0.9545
	Si	0.0017	152.0167	0.2584	3.4134	3.1550
			275.6533	0.4686	5.6032	5.1346
			423.4833	0.7199	7.2456	6.5257
			571.5700	0.9717	8.3639	7.3922
	Fe	0.0037	152.0167	0.5625	2.5122	1.9497
			275.6533	1.0199	4.3144	3.2945
			423.4833	1.5669	5.9931	4.4262
			571.5700	2.1148	7.4260	5.3112
	Ti	0.0037	152.0167	0.5625	2.5122	1.9497
			275.6533	1.0199	4.3144	3.2945
			423.4833	1.5669	5.9931	4.4262
			571.5700	2.1148	7.4260	5.3112

Appendix F: Modal Mineralogies

Appendix F1.1: Normal reef

Mineral	Wt%	Area%	Area (micron)	Particle Count	Grain Count
AgNiBiTe	0	0	0	3	3
AgTe	0	0	0	0	0
AgSi	0.03	0.08	0	967	1074
Al	0	0.01	0	9	9
Anorthite	31.73	34.93	0	39401	42068
Apatite	0.08	0.08	0	108	110
Au	0	0	0	1	1
AuAg	0	0	0	30	30
AuBiPdTe	0	0	0	0	0
Augite	0.25	0.24	0	1819	2133
BiNi	0	0	0	3	3
Calcite	0.02	0.02	0	95	102
CaTiZrO	0	0	0	21	22
Chalcopyrite	2.55	1.85	0	16220	27327
Chlorite	4.98	5.04	0	10901	13665
Chromite	3.7	2.5	0	4399	4743
Cl	0.01	0.02	0	17	17
ClSiO	0.11	0.34	0	4998	7570
CrCaFeNiAlSiO	0.01	0.02	0	153	177
CrFeNiSiO	0.01	0.02	0	112	127
CuCrFeS	0	0	0	41	49
CuNi	0	0	0	0	0
CuZn	0	0	0	5	5
Dolomite	0.01	0.01	0	58	61
Enstatite	17.02	15.67	0	19804	21691
Epidote	16.96	15.17	0	26421	35493
Fe	0	0	0	9	13
FeAlSiO	0.02	0.05	0	632	911
FeCaSO	0	0	0	33	42
FeCo	0	0	0	1	2
FeNiAsS	0	0	0	208	221
FeNiCuS	0.01	0.02	0	970	2046
FeO	0.02	0.05	0	301	407
FeSi	0.01	0.04	0	171	176
Galena	0.06	0.02	0	2720	4115
Ilmenite	0	0	0	4	4
Orthoclase	0.18	0.22	0	620	670
MgO	0	0	0	1	1
Ni	0	0	0	0	0
NiAs	0	0	0	0	0
NiFe	0	0	0	1	1
NiP	0	0	0	1	2
NiS	0.01	0.03	0	426	540
PbTe	0	0	0	0	0

PdBiFeTe	0	0	0	67	71
PdBiTe	0	0	0	7	7
PdFeAs	0	0	0	31	36
PdNiS	0	0	0	15	17
PdPtFeNiS	0	0	0	136	142
PdSb	0	0	0	0	0
Pentlandite	4.93	3.01	0	13401	24406
Phlogopite	1.74	1.85	0	2633	2687
PtAs	0	0	0	0	0
PtFe	0	0	0	45	72
PtFeAsSeS	0	0	0	980	1279
PtFeCuS	0	0	0	6	8
PtFeSnS	0	0	0	77	81
PtIrRhAsS	0	0	0	1	2
PtNiFeS	0	0	0	4	4
PtPdBiTe	0	0.01	0	743	865
PtPdNiS	0	0.01	0	209	227
PtRhAsS	0	0	0	0	0
PtRhCuS	0	0	0	119	144
PtRhFeNiS	0.01	0.02	0	1695	2757
PtS	0	0	0	202	226
PtSb	0	0	0	40	43
PtTeBi	0.01	0.02	0	377	430
PtTeBiFeCuS	0.02	0.05	0	3597	6587
Pyrite	0	0	0	356	516
Pyrrhotite	1.75	1.16	0	5950	18073
Quartz	2.05	2.35	0	3996	5181
RuS	0	0	0	217	247
Rutile	0.25	0.18	0	489	496
Serpentine	8.34	11.03	0	15441	17885
Si	0.02	0.07	0	463	501
Sphalerite	0	0	0	10	18
Sphene	0.03	0.03	0	457	491
Talc	1.46	1.59	0	3944	4663
Tremolite	0.96	0.98	0	4502	5696
UPb	0	0	0	60	60
UTiSiO	0	0.01	0	152	175
Wollastonite	0.38	0.41	0	1647	1889
Zn	0	0.01	0	49	49
ZrO	0	0	0	15	16
Unknown	0.09	0.27	0	8580	16095
Invalid	0.16	0.47	0	2598	3610
Total	100	100	0	101462	281383

Appendix F1.2: Potholed reef

Mineral	Wt%	Area%	Area (micron)	Particle Count	Grain Count
AgNiBiTe	0	0	0	2	2
AgTe	0	0	0	0	0
AgSi	0.02	0.04	0	873	978
Al	0	0.01	0	17	17
Anorthite	22.03	23.99	0	51815	55158
Apatite	0.03	0.03	0	86	88
Au	0	0	0	2	2
AuAg	0.01	0.02	0	93	94
AuBiPdTe	0	0	0	21	21
Augite	0.18	0.17	0	1267	1410
BiNi	0	0	0	0	0
Calcite	0.01	0.01	0	86	96
CaTiZrO	0	0	0	22	23
Chalcopyrite	8.69	6.34	0	36212	64377
Chlorite	1.37	1.37	0	5252	6413
Chromite	2.42	1.62	0	5608	6192
Cl	0	0.01	0	58	59
ClSiO	2.02	4.61	0	22072	24749
CrCaFeNiAlSiO	0	0.01	0	219	261
CrFeNiSiO	0	0.01	0	239	279
CuCrFeS	0	0	0	210	247
CuNi	0	0	0	0	0
CuZn	0	0	0	2	2
Dolomite	0.01	0.01	0	25	25
Enstatite	17.89	16.49	0	26940	28229
Epidote	10.22	9.12	0	32993	44756
Fe	0	0	0	19	31
FeAlSiO	0.01	0.02	0	517	682
FeCaSO	0	0	0	88	105
FeCo	0	0	0	0	0
FeNiAsS	0	0	0	183	189
FeNiCuS	0.02	0.05	0	2287	5422
FeO	0.01	0.04	0	553	857
FeSi	0	0.01	0	155	172
Galena	0.13	0.05	0	6419	10343
Ilmenite	0	0	0	10	10
Orthoclase	0.11	0.13	0	667	696
MgO	0	0	0	0	0
Ni	0	0	0	0	0
NiAs	0	0	0	0	0
NiFe	0	0	0	0	0
NiP	0	0	0	0	0
NiS	0	0	0	25	31

PbTe	0	0	0	0	0
PdBiFeTe	0	0	0	414	465
PdBiTe	0	0	0	21	21
PdFeAs	0	0	0	2	2
PdNiS	0	0	0	0	0
PdPtFeNiS	0	0	0	44	45
PdSb	0	0	0	0	0
Pentlandite	12.98	7.91	0	24633	43624
Phlogopite	1.09	1.16	0	3063	3103
PtAs	0	0	0	4	4
PtFe	0	0	0	14	15
PtFeAsSeS	0.01	0.02	0	3280	4764
PtFeCuS	0	0	0	3	3
PtFeSnS	0	0	0	46	51
PtIrRhAsS	0	0	0	0	0
PtNiFeS	0	0	0	1	1
PtPdBiTe	0.34	0.77	0	4641	5102
PtPdNiS	0	0.01	0	81	86
PtRhAsS	0	0	0	0	0
PtRhCuS	0	0	0	40	42
PtRhFeNiS	0.02	0.06	0	5912	11515
PtS	0	0	0	105	117
PtSb	0	0	0	59	61
PtTeBi	0.01	0.02	0	459	496
PtTeBiFeCuS	1.73	3.96	0	23978	39689
Pyrite	0.03	0.02	0	1274	2517
Pyrrhotite	8.54	5.71	0	11238	27304
Quartz	1.63	1.84	0	7066	9347
RuS	0	0	0	133	144
Rutile	0.04	0.03	0	196	203
Serpentine	3.79	4.91	0	10793	11726
Si	0.02	0.05	0	581	643
Sphalerite	0	0	0	0	0
Sphene	0.01	0.01	0	146	150
Talc	0.31	0.34	0	1417	1605
Tremolite	0.47	0.49	0	2180	2574
UPb	1.69	3.81	0	10494	10553
UTiSiO	0	0.01	0	96	107
Wollastonite	0.18	0.19	0	1909	2128
Zn	0	0	0	1	1
ZrO	0	0	0	29	29
Unknown	0.08	0.22	0	13510	24565
Invalid	1.85	4.28	0	15776	20255
Total	100	100	0	175083	475073

Appendinx F1.3: UG2 affected by IRUP

Mineral	Wt%	Area%	Area (micron)	Particle Count	Grain Count
AgNiBiTe	0	0	0	0	0
AgTe	0	0	0	0	0
AgSi	0.01	0.05	0	454	499
Al	0	0	0	4	4
Anorthite	0.11	0.13	0	189	204
Apatite	0.03	0.03	0	55	56
Au	0	0	0	0	0
AuAg	0	0	0	0	0
AuBiPdTe	0	0	0	0	0
Augite	4.25	4.35	0	5375	5624
BiNi	0	0	0	0	0
Calcite	0.81	0.98	0	1461	1606
CaTiZrO	0	0	0	2	2
Chalcopyrite	0.29	0.22	0	570	826
Chlorite	11.07	12.06	0	10505	10869
Chromite	27.32	19.93	0	24429	27552
Cl	0	0	0	9	9
ClSiO	0.03	0.09	0	860	1005
CrCaFeNiAlSiO	0.01	0.02	0	103	115
CrFeNiSiO	0.01	0.02	0	96	103
CuCrFeS	0	0	0	79	161
CuNi	0	0	0	0	0
CuZn	0	0	0	3	3
Dolomite	0.01	0.01	0	53	54
Enstatite	31.35	31.01	0	28880	31234
Epidote	0.05	0.04	0	165	193
Fe	0	0	0	6	19
FeAlSiO	0.04	0.13	0	201	227
FeCaSO	0	0	0	41	54
FeCo	0	0	0	0	0
FeNiAsS	0	0	0	8	9
FeNiCuS	0	0	0	72	162
FeO	0.01	0.02	0	118	140
FeSi	0.01	0.02	0	73	73
Galena	0.01	0	0	159	239
Ilmenite	0.07	0.05	0	52	55
Orthoclase	0	0	0	36	37
MgO	0	0	0	3	4
Ni	0	0	0	1	3
NiAs	0	0	0	0	0
NiFe	0	0	0	0	0
NiP	0	0	0	2	2

NiS	0	0	0	0	0
PbTe	0	0	0	1	1
PdBiFeTe	0	0	0	3	4
PdBiTe	0	0	0	0	0
PdFeAs	0	0	0	4	5
PdNiS	0	0	0	3	3
PdPtFeNiS	0	0	0	2	2
PdSb	0	0	0	16	19
Pentlandite	0.4	0.26	0	1826	2369
Phlogopite	0.01	0.01	0	45	45
PtAs	0	0	0	2	2
PtFe	0	0	0	14	14
PtFeAsSeS	0	0	0	93	138
PtFeCuS	0	0	0	0	0
PtFeSnS	0	0	0	2	2
PtIrRhAsS	0	0	0	2	2
PtNiFeS	0	0	0	0	0
PtPdBiTe	0	0	0	14	15
PtPdNiS	0	0	0	0	0
PtRhAsS	0	0	0	0	0
PtRhCuS	0	0	0	0	0
PtRhFeNiS	0	0	0	91	144
PtS	0	0	0	8	8
PtSb	0	0	0	14	14
PtTeBi	0	0	0	81	86
PtTeBiFeCuS	0	0.01	0	231	487
Pyrite	0	0	0	0	0
Pyrrhotite	0.31	0.22	0	211	255
Quartz	0.12	0.15	0	233	252
RuS	0	0	0	6	7
Rutile	0.02	0.01	0	22	24
Serpentine	11.53	16.34	0	15963	16926
Si	0.01	0.03	0	110	112
Sphalerite	0	0	0	1	1
Sphene	0.08	0.08	0	668	724
Talc	3.94	4.58	0	5114	5513
Tremolite	6.93	7.56	0	9726	11468
UPb	0	0	0	5	5
UTiSiO	0	0	0	29	35
Wollastonite	1.1	1.28	0	2091	2641
Zn	0	0	0	2	2
ZrO	0	0	0	0	0
Unknown	0.02	0.07	0	744	1037
Invalid	0.06	0.19	0	640	798
Total	100	100	0	84485	124303

Appendix F2: Mineral associations

Appendix F2.1: Normal reef

Mineral	Association with chromite
AgSi	0.01
Anorthite	1.21
Apatite	0
Augite	0.16
BiNi	0
Chalcopyrite	0.15
Chlorite	0.74
ClSiO	0.37
CrCaFeNiAlSiO	0.02
CrFeNiSiO	0.06
CuCrFeS	0.02
Dolomite	0.01
Enstatite	0.48
Epidote	1.47
Fe	0
FeAlSiO	0.01
FeNiCuS	0.01
FeO	0.01
Orthoclase	0.02
NiS	0.01
PdNiS	0.01
Pentlandite	0.26
Phlogopite	0.1
PtPdBiTe	0.01
PtRhCuS	0.01
PtRhFeNiS	0.01
Pyrite	0
Pyrrhotite	0.08
Quartz	0.1
RuS	0.02
Rutile	0.28
Serpentine	0.56
Si	0.01
Sphalerite	0
Talc	0.08
Tremolite	0.33
UTiSiO	0.01
Wollastonite	0.02
Unknown	0.13
Invalid	0.02
Free Surface	93.21

Appendix F2.2: Potholed reef

Mineral	Association with chromite
Anorthite	1.48
Apatite	0
Augite	0.2
Calcite	0
Chalcopyrite	0.41
Chlorite	0.32
ClSiO	0.57
CrCaFeNiAlSiO	0.02
CrFeNiSiO	0.03
CuCrFeS	0.11
Dolomite	0.01
Enstatite	0.76
Epidote	1.03
FeNiCuS	0.02
FeO	0.02
Galena	0.01
Orthoclase	0.03
PtTeBi	0.01
PtTeBiFeCuS	0.05
Pyrite	0
Pyrrhotite	0.22
Quartz	0.17
Rutile	0.01
Serpentine	0.36
Si	0.01
Sphalerite	0
Sphene	0.01
Talc	0.04
Tremolite	0.16
UPb	0.05
UTiSiO	0.01
Wollastonite	0.06
Unknown	0.18
Invalid	0.15
Free Surface	92.73

Appendix F2.3: UG2 affected by IRUP

Mineral	Association with chromite
AgSi	0.02
Anorthite	0.04
Apatite	0
Augite	0.46
Calcite	0.77
Chalcopyrite	0.1
Chlorite	0.74
ClSiO	0.18
CrCaFeNiAlSiO	0.02
CrFeNiSiO	0.02
CuCrFeS	0.04
Dolomite	0
Enstatite	3.61
Epidote	0.02
FeAlSiO	0.02
FeSi	0.01
Galena	0
Ilmenite	0.01
Orthoclase	0
Pentlandite	0.09
Phlogopite	0
Pyrite	0
Pyrrhotite	0.06
Quartz	0.04
Rutile	0
Serpentine	1.54
Si	0.01
Sphalerite	0
Sphene	0.02
Talc	0.46
Tremolite	1.37
Wollastonite	0.38
Unknown	0.11
Invalid	0.09
Free Surface	89.73